The role of Pref-1 in *in vitro* adipogenic differentiation of mesenchymal stromal/stem cells

By

Carina Corte-Real da Silva

12019527

Submitted in fulfilment of the requirements for the degree

Masters of Science (Medical Immunology)

In the Faculty of Health Sciences

Department of Immunology

University of Pretoria

2019

Supervisor: Dr Chrisna Durandt

Co-Supervisor: Prof Michael S. Pepper

Co-Supervisor: Dr Melvin A. Ambele

Contact information

Candidate

Name: Carina Corte-Real da Silva

Student nr.: 12019527

Department: Department of Immunology

Faculty of Health Sciences

University of Pretoria

Tel.: 082 446 2658

Email: carinacrdasilva@gmail.com

Supervisor

Name: Dr Chrisna Durandt

Department: Institute for Cellular and Molecular Medicine, Department of Immunology

Position: Senior Medical Scientist

Faculty of Health Sciences

University of Pretoria

Tel.: 012 319 2101

Email: chrisna.durandt@up.ac.za

Co-Supervisor 1

Name: Prof Michael S. Pepper

Department: Department of Immunology

Position: Director of the Institute for Cellular and Molecular Medicine

Faculty of Health Sciences

University of Pretoria

Tel.: 012 319 2190/79

Email: michael.pepper@up.ac.za

Co-Supervisor 2

Name: Dr Melvin A. Ambele

Department: Department of Oral Pathology and Oral Biology

Position: Senior Research Officer

Faculty of Health Sciences

University of Pretoria

Tel.: 012 319 2101

Email: melvin.ambele@up.ac.za

Head of Department

Name: Prof Pieter W.A. Meyer

Department: Department of Immunology

Faculty of Health Sciences

University of Pretoria

Tel.: 012 319 2624

Email: Pieter.meyer@up.ac.za

Declaration of Authenticity

I hereby declare the work herein contained to be my own, original work, and that any contributors are appropriately acknowledged. Furthermore, I declare that all source material is cited appropriately, and to my knowledge, neither I nor any declared contributors are aware of any plagiarism in the following work.

Contributor	Contribution
Ms C.C. da Silva	Laboratory work, data analysis and write up of dissertation
Dr C. Durandt	Conceptualization of project, project overview, assistance in laboratory, editing of dissertation
Dr M.A. Ambele	Project overview, editing of dissertation
Prof M.S. Pepper	Project overview, editing of dissertation
Mrs I. Janse van Rensburg	Collection of murine tissue
Mrs M van Heerden	Immunohistochemistry
Dr T. Kungoane	Assistance with interpretation of IHC images
Dr R. Anderson	Assistance with Western blots

I hereby submit the following title as my own work, and confirm that all contributors (if any) are listed in the above table.

Title of work:

The role of Pref-1 in *in vitro* adipogenic differentiation of mesenchymal stromal/stem cells

(MSc Dissertation)

Date: 30 April 2019

Name: Carina Corte-Real da Silva

Signature:

Abstract

Obesity is characterized by an excessive amount of body fat which can negatively affect health as it is a risk factor for various non-communicable diseases such as cardiovascular disease and diabetes, amongst others. A better understanding of the process of fat cell formation, a process known as adipogenesis, would aid in finding sustainable solutions to this growing global health challenge. The ability of human derived mesenchymal stromal/stem cells (hMSCs) to differentiate into adipocytes holds great promise to serve as an *in vitro* model to study human adipogenesis. It is known from the literature that hMSCs from different sources within the body may differ in their differentiation potential. It is well reported that human Wharton's jelly derived MSCs (hWJSCs) have reduced adipogenic differentiation capacity when compared to hMSCs isolated from adipose tissue. hMSCs isolated from adipose tissue are referred to as adipose-derived mesenchymal stromal/stem cells (hASCs). The poor adipogenic differentiation potential of hWJSCs has also been observed in our group. We also observed elevated pre-adipocyte factor 1 (Pref-1) mRNA levels in hWJSCs. The observed elevated Pref-1 mRNA levels in hWJSCs led to the hypothesis that this may be responsible for hWJSCs poor adipogenic differentiation capacity. Pref-1 is a transmembrane protein capable of being cleaved to give rise to a 50 kDa soluble protein which is thought to be an important adipogenic inhibitor by preventing cells from maturing into adipocytes thereby keeping them in a pre-adipocyte state. It was therefore important to confirm whether the elevated Pref-1 gene expression observed translated into higher levels of Pref-1 protein in hWJSCs when compared to hASCs. The aim of this study was to further investigate a previous observation in our group of elevated Pref-1 gene expression levels in hWJSCs undergoing adipogenesis. This will be done by examining the association between Pref-1 protein expression levels in hWJSCs and hASCs and their respective *in vitro* adipogenic differentiation potential. The cells were induced to undergo adipogenesis for a period of 21 days and monitored on days 0, 1, 3, 7, 14 and 21. During this time period, the adipogenic differentiation potential of the cells was assessed by means of flow cytometry (quantitative) and microscopy

(qualitative). The level of Pref-1 protein expression was investigated using various techniques which included flow cytometry, ELISA and western blot assays. Gene expression was determined by reverse transcription quantitative polymerase chain reaction (RT-qPCR). As previously determined, hWJSCs displayed poor adipogenic differentiation despite the upregulation of peroxisome proliferator activated receptor gamma (PPARγ). Flow cytometry data revealed hASCs to have greater levels of Pref-1 protein expression on the cell surface. We were unable to detect any Pref-1 protein in the cell culture supernatant collected at each time point using ELISA, but western blot data suggested that there may be more soluble Pref-1 protein in the cell culture supernatant obtained from hWJSCs. Gene expression data also revealed higher levels of Pref-1 mRNA in hWJSCs. However, the amount of Pref-1 protein detected was very low and no statistical significance could be determined between Pref-1 expression in hASCs versus hWJSCs in any of the assays. The *in vivo* data obtained by immunohistochemistry shows that both adipose tissue and umbilical cord express Pref-1 around blood vessels. The umbilical cord does however have additional Pref-1 staining that is not associated with blood vessels. The stromal cells in the Wharton's jelly displayed positive Pref-1 staining. How this finding correlates with the *in vitro* results obtained is unclear. Comparing the adipogenic differentiation potential of hWJSCs to hASCs did however allow for an interesting observation. hASCs were able to upregulate CD36 (a fatty acid translocase) during the adipogenic differentiation period, while this was not observed for hWJSCs. The low levels of Pref-1 protein expression combined with the upregulation of PPARγ in hWJSCs thus raises the question as to whether other regulatory elements, currently unknown, downstream of PPARγ, suppress the upregulation of end-stage adipogenic genes and consequently prevent the induced hWJSCs from acquiring the phenotypic characteristics associated with mature adipocytes.

Key words: MSCs; hASCs; adipose tissue; hWJSCs; Wharton's jelly; adipogenesis; Pref-1; differentiation

Dedication

Gostaria de dedicar esta dissertação com muito amor e carinho ao meu avô - Joaquim Pereira da Silva. Eu sei que o avô ficaria muito orgulhoso de mim.

I would like to dedicate this dissertation, with lots of love and affection, to my grandfather – Joaquim Pereira da Silva. I know that you would have been very proud.

Acknowledgements

I would like to thank Prof Michael Pepper (co-supervisor) for giving me the opportunity to complete my MSc degree at the Institute for Cellular and Molecular Medicine. It was a challenging yet enriching experience.

To my supervisor, Dr Chrisna Durandt, thank you for all the time and effort you invested in me. You were always prepared to help, even if it meant staying late, coming in on weekends and losing precious time with your four-legged children. It was a rough ride but you always made sure I remained positive and focused on my goal. I am also thankful to my co-supervisor, Dr Melvin Ambele, who always checked up on me when he could to ensure I retained a positive attitude.

As for my work colleagues, I couldn't have asked for a better group of people to work with. Candice Herd, Elize Wolmarans, Juanita Mellet, Candice Murdoch, Catherine Wickham and Mqondise Tshabalala, thank you for your support and friendship. You guys definitely made this journey a lot more interesting and memorable.

Lastly, I would also like to thank my parents, Carlos da Silva and Sandra da Silva, as well as my fiancé, Angelo Babbo. Thank you for always supporting me unconditionally throughout this long journey. You guys always stood by and listened to all my complaints and triumphs even when you had no idea what I was actually talking about. I would not have been able to do this without you guys.

Table of Contents

Table of Figures

List of Tables

Table of Equations

List of Abbreviations, Symbols and Units

A

7-AAD	7-Aminoactinomycin D
ADD1	Determination and differentiation factor 1
AdipoQ	Adiponectin
aP2	Adipocyte protein 2
APC	Allophycocyanin
APC/Cy7	Allophycocyanin /Cyanin7
ASC	Adipose derived mesenchymal stromal cells
AT	Adipose tissue

B

BAT	Brown adipose tissue
BM	Bone marrow
BMP	Bone morphogenic protein
BV421	Brilliant Violet™ 421

C

cAMP	Cyclic AMP
CB	Cord blood

CD	Cluster of differentiation
Cdc25c	Cell division cycle 25C phosphatase
C/EBP	CCAAT/enhancer-binding protein
cm^2	Square centimetres
CMG	Cdc45-MCM-GINS complex
CO_2	Carbon dioxide
C_q	Quantitative cycle
C_T	Threshold cycle

D

DAB	3,3'-diaminobenzidine
DLK1	Delta like homolog 1
DMEM	Dulbecco's modified Eagle's medium
DNA	Deoxyribonucleic acid
DNMT3B	DNA Methyltransferase 3 Beta
DOS	Delta and Osm11
DSL	Delta-Serrate-LAG-2

E

ECM	Extracellular matrix
EGF	Epidermal growth factor

ERG2	Early growth response protein 2
ERK	Extracellular signalling kinase

F	
FA1	Fetal antigen 1
FBS	Fetal bovine serum
FITC	Fluorescein isothiocyanate
FS	Forward scatter

G	
g	G-force / Centrifugal force
g	gram
GABRB3	Gamma-aminobutyric acid receptor subunit beta-3
gDNA	Genomic DNA
GLUT4	Glucose transporter type 4

H	
H&E	Hematoxylin and eosin
hASC	Human adipose derived mesenchymal stromal cells
HLA	Human leukocyte antigen
hMSC	Human derived mesenchymal stromal cells
HRP	Horse radish peroxidase

HSA	Human serum albumin
HSC	Haematopoietic stem cells
hWJSC	Human Wharton's jelly derived mesenchymal stromal cells

I

IBMX	3-isobutyl-1-methylxanthine
IGF-1	Insulin like growth factor-1
IND	Induced
iPS	Induced pluripotent stem cells
ISCT	International Society of Cellular Therapy

J

JNK	c-Jun amino-terminal kinases

K

kDa	Kilodalton
KLF	Krüppel-like factor
KO	Krome Orange

L

L	Litre
LDL	Low density lipoprotein
LEP	Leptin

Lin	Linear
LP	Long pass

M

M-phase	Mitotic phase
Meis1	Myeloid ecotropic insertion site 1
min	Minute
mL	Millilitre
MIQE	Minimum Information for Publication of Quantitative Real-Time PCR Experiments
mRNA	Messenger ribonucleic acid
MSC	Mesenchymal stromal cell
mW	milliwatt
Myf5	Myogenic factor 5

N

NA	Not applicable
NANOG	Nanog homeobox
ng	Nanogram
ng/µL	Nanogram/microliter
NI	Non-induced

nm	Nanometer
NRTC	No reverse transcriptase control
NTC	No template control

O_2	Oxygen
Oct4	Octamer-binding transcription factor 4

PBS	Phosphate buffered saline
PE	Phycoerythrin
PE/Cy7	Phycoerythrin/Cyanin7
PEPCK	Phosphoenolpyruvate carboxylase
PLIN	Perilipin
PMT	Photomultiplier tube
PPARG	Peroxisome proliferator-activated receptor gamma
PPIA	Peptidylprolyl Isomerase A
PRDM16	PR domain containing 16
Pref-1	Pre-adipocyte factor 1
PVDF	Polyvinylidene difluoride

	Q
qPCR	Quantitative polymerase chain reaction

	R
r^2	Correlation coefficient
RNA	Ribonucleic acid
RT	Reverse transcriptase
RT-qPCR	Real-time quantitative polymerase chain reaction
RXR	Retinoid-X-receptor

	S
S-phase	Synthesis phase
SCD1	Stearoyl-CoA desaturase-1
SEM	Standard error of the mean
sec	Seconds
Sox9	SRY (Sex Determining Region Y)-Box 9
SREBP-1	Sterol regulatory element-binding transcription factor
SS	Side scatter
STAT	Signal transducer and activator of transcription
STD	Standard

T

TACE	Tumour necrosis factor alpha converting enzyme
TBP	TATA binding protein
TNF-α	Tumour necrosis factor alpha

U

UC	Umbilical cord
UCP1	Uncoupling protein 1

V

v/v	Volume/volume
VDC	Vybrant® DyeCycle
v/w	Volume/weight

W

WAT	White adipose tissue
WOF	World Obesity Federation
WJSC	Wharton's Jelly derived mesenchymal stromal cells

Y

YWHAZ	Tyrosine 3-Monooxygenase/Tryptophan 5-Monooxygenase Activation Protein, Zeta

Other

>	Greater than

<	Less than
%	Percentage
~	Approximately
±	Plus-minus
^{0}C	Degrees Celsius
$^{0}C/s$	Degree Celcius per second
α	Alpha
β	Beta
γ	Gamma
δ	Delta
Δ	Delta
ε	Epsilon
ζ	Zeta
μg	Microgram
μL	Microliter
μm	Micrometre
μM	Micromolar
μg/mL	Microgram/millilitre

Chapter 1: Introduction

1.1 Introduction

Obesity is a health burden world-wide. According to statistics provided by the World Obesity Federation (WOF), approximately half of the adult South African population can be classified as obese (1). Obesity is characterized by an excessive amount of body fat that can negatively affect health through a number of non-communicable diseases (2, 3). A better understanding of adipogenesis, the process of fat cell formation, would aid in finding sustainable solutions to this global health challenge.

Currently, the majority of research studies focusing on adipogenesis are performed using murine 3T3-L1 cell lines and/or in murine experimental animal models (4-7). It is unclear whether results from these murine studies can be directly translated to the human setting. More studies using cells of human origin are therefore needed. The ability of human derived mesenchymal stromal/stem cells (hMSCs) to differentiate into adipocytes holds great promise to serve as an *in vitro* model to study adipogenesis. The focus area of this dissertation is therefore the study of adipogenic differentiation potential of hMSCs.

Mesenchymal stromal/stem cells (MSCs) reside in nearly all post-natal human tissues and organs (8). For the work performed in this study, adipose and umbilical cord tissues were the sources of choice for MSC isolation. These are two commonly utilized sources of MSCs as they are readily available and associated with minimal ethical concern (9, 10). Adipose tissue can be obtained as a medical waste product from patients undergoing liposuction or abdominoplasty procedures and umbilical cords can be obtained as a medical waste product after childbirth. Both these tissues can thus be collected with minimal ethical implications as long as the patients from whom the tissue is obtained give their written informed consent.

Human derived ASCs (hASCs) and human derived WJSCs (hWJSCs) are known to differ in their adipogenic differentiation potential. The hASCs are reported to have excellent adipogenic differentiation potential (10-12), while hWJSCs are reported to display poor adipogenic differentiation capacity (13-16). The underlying cause for

this difference has not yet been completely elucidated and requires further investigation. The reported differences in the adipogenic differentiation potential of these two cell types allow for a comparative *in* vitro model to identify molecular targets that differ between cells with good and poor adipogenic differentiation potential. Understanding the differences and similarities between these two models will provide insight into the potential mechanisms involved in regulating adipogenesis in these two cell types

In a recent study performed in our laboratory by Ms Karlien Kallmeyer (results unpublished), hASCs were compared to hWJSCs. It was found that both cells types adhere to the above listed criteria. In addition, she confirmed findings from other published studies that hWJSCs display poor adipogenic differentiation potential in comparison to hASCs. Analysis of hWJSC qPCR data revealed elevated levels of a gene known to be an inhibitor of adipogenesis, namely pre-adipocyte factor 1 (Pref-1). This observation along with what is known in literature about Pref-1 led to the hypothesis that the sustained expression of the *Pref-1* gene in hWJSCs may contribute to the poor adipogenic differentiation capacity observed.

1.2 Aim and Objectives

1.2.1 Aim

The aim of this project is to compare the adipogenic differentiation capacity of hWJSCs and hASCs as well as determine the level of Pref-1 expression in each cell type.

1.2.2 Objectives

The study objectives were:

(i)   Isolation and characterization of hMSCs from adipose tissue and Wharton's jelly;

(ii)   Qualitative and quantitative assessment of the adipogenic differentiation potential of these cells;

(iii)   Determine the level of Pref-1 protein and mRNA expression in these two cell types;

    (iv)   Investigate the *in vivo* expression level of this protein in adipose tissue and umbilical cord tissue samples.

1.3 Dissertation outline

The observations and results recorded in this study will be presented as follows in this dissertation: A brief overview of the relevant literature is summarized in Chapter 2. The isolation, expansion and characterization of the cells are described in Chapter 3. Chapter 4 describes the adipogenic differentiation potential of the cells. Assessment of Pref-1 protein and mRNA expression is presented and discussed in Chapter 5. And lastly, a synopsis of the main findings in this study is provided in Chapter 6.

1.4 References

1. Obesity prevalence worldwide - Adults: World Obesity Federation; [Available from: https://www.worldobesitydata.org/map/overview-adults.

2. Gadde KM, Martin CK, Berthoud HR, Heymsfield SB. Obesity: Pathophysiology and Management. J Am Coll Cardiol. 2018;71(1):69-84.

3. Gurevich-Panigrahi T, Panigrahi S, Wiechec E, Los M. Obesity: pathophysiology and clinical management. Curr Med Chem. 2009;16(4):506-21.

4. Boney CM, Fiedorek FT, Jr., Paul SR, Gruppuso PA. Regulation of preadipocyte factor-1 gene expression during 3T3-L1 cell differentiation. Endocrinology. 1996;137(7):2923-8.

5. Nueda ML, Gonzalez-Gomez MJ, Rodriguez-Cano MM, Monsalve EM, Diaz-Guerra MJM, Sanchez-Solana B, et al. DLK proteins modulate NOTCH signaling to influence a brown or white 3T3-L1 adipocyte fate. Sci Rep. 2018;8(1):16923.

6. Smas CM, Sul HS. Pref-1, a protein containing EGF-like repeats, inhibits adipocyte differentiation. Cell. 1993;73(4):725-34.

7. Gregoire FM, Smas CM, Sul HS. Understanding adipocyte differentiation. Physiol Rev. 1998;78(3):783-809.

8. Kobolak J, Dinnyes A, Memic A, Khademhosseini A, Mobasheri A. Mesenchymal stem cells: Identification, phenotypic characterization, biological

properties and potential for regenerative medicine through biomaterial micro-engineering of their niche. Methods. 2016;99(15):62-8.

9. Kobolak J, Dinnyes A, Memic A, Khademhosseini A, Mobasheri A. Mesenchymal stem cells: Identification, phenotypic characterization, biological properties and potential for regenerative medicine through biomaterial micro-engineering of their niche. Methods. 2015.

10. Orbay H, Tobita M, Mizuno H. Mesenchymal stem cells isolated from adipose and other tissues: basic biological properties and clinical applications. Stem Cells Int. 2012;2012:461718.

11. Karagianni M, Brinkmann I, Kinzebach S, Grassl M, Weiss C, Bugert P, et al. A comparative analysis of the adipogenic potential in human mesenchymal stromal cells from cord blood and other sources. Cytotherapy. 2013;15(1):76-88.

12. Xu L, Liu Y, Sun Y, Wang B, Xiong Y, Lin W, et al. Tissue source determines the differentiation potentials of mesenchymal stem cells: a comparative study of human mesenchymal stem cells from bone marrow and adipose tissue. Stem Cell Res Ther. 2017;8(1):275.

13. Bieback K, Brinkmann I. Mesenchymal stromal cells from human perinatal tissues: From biology to cell therapy. World J Stem Cells. 2010;2(4):81-92.

14. Wang HS, Hung SC, Peng ST, Huang CC, Wei HM, Guo YJ, et al. Mesenchymal stem cells in the Wharton's jelly of the human umbilical cord. Stem Cells. 2004;22(7):1330-7.

15. Fong CY, Subramanian A, Biswas A, Bongso A. Freezing of Fresh Wharton's Jelly From Human Umbilical Cords Yields High Post-Thaw Mesenchymal Stem Cell Numbers for Cell-Based Therapies. J Cell Biochem. 2016;117(4):815-27.

16. Ragni E, Vigano M, Parazzi V, Montemurro T, Montelatici E, Lavazza C, et al. Adipogenic potential in human mesenchymal stem cells strictly depends on adult or foetal tissue harvest. Int J Biochem Cell Biol. 2013;45(11):2456-66.

Chapter 2:   Literature Review

2.1 Obesity

Obesity is characterised by an excess amount of adipose tissue and results from hypertrophy (increase in the size of adipocytes (fat cells)) or hyperplasia (increase in the number of new adipocytes) (1, 2). Increased adipose tissue results in metabolic stress which in turn leads to an inflammatory response as well as increased fatty acid, triglyceride and LDL cholesterol levels. Obesity is associated with a number of co-morbidities (3). Common non-communicable diseases which are closely associated with obesity include diabetes mellitus, hypertension, cardiovascular disease and cancer (4, 5). Thus, with an increase in obesity there is also an increase in the number of people suffering from associated non-communicable diseases which results in an overburdened health care system (6). Obesity is becoming an increasing health burden world-wide and South Africa is no exception (4, 7). According to the 2016 data collected by the World Obesity Federation (WOF), 52% of adult South Africans are obese (Figure 2.1). This statistics is expected to increase to 60% percent by 2025 according to the WOF (8).
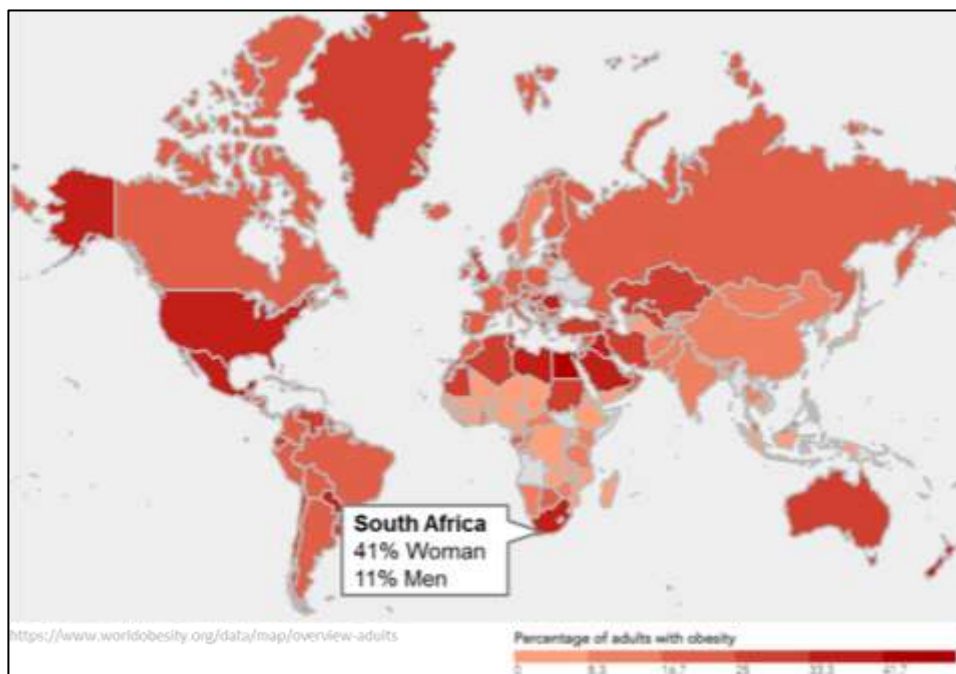
Figure 2.1: Obesity prevalence worldwide in adults. According to the 2016 statistics obtained from World Obesity, 41% of adult South African woman and 11% of adult South African males are obese. Image modified from: https://www.worldobesitydata.org/map/overview-adults.

A better understanding of fat cell formation and maturation, a process known as adipogenesis, could aid in finding sustainable solutions to this global health challenge (3, 9). The ability of human derived mesenchymal stromal/stem cells (hMSCs) to differentiate into adipocytes holds great promise as an *in vitro* model to study human adipogenesis (10, 11).

2.2 Stem Cells

Stem cells are undifferentiated, self-renewing cells which are capable of differentiating into more specialised cells (12, 13). These cells can be subdivided into sub-types based on their differentiation potential. Totipotent stem cells have the greatest differentiation capacity. During embryonic development, a whole organism is capable of arising from totipotent stem cells. An example would be a zygote or an early blastomere, which is capable of forming embryonic and extra-embryonic tissue (13). Once the zygote develops into a blastocyst, the inner cell mass is capable of forming all the cells of an organism except for extra embryonic tissue. The cells of the inner cell mass are thus known as pluripotent stem cells. These pluripotent stem cells can be harvested from the inner cell mass in which case they are referred to as embryonic stem cells, and their use in research is highly controversial (12, 13). In 1998 the first embryonic stem cells were isolated from a human blastocyst (14, 15). This raised major concerns in the public as it was viewed as destroying a potential human life. Another example of pluripotent stem cells would be induced pluripotent stem (iPS) cells. iPS cells are made from somatic cells which have been reprogrammed *in vitro* with the aid of retroviruses to induce the expression of octamer-binding transcription factor 4 (Oct4), sex determining region-Y box 2 (Sox2), c-Myc and Krüppel-like factor 4 (KLF4) or they can be created by somatic nuclear transfer (13, 16, 17). Multipotent stem cells are another type of stem cell which are able to differentiate into different, but a limited number of cell lineages (16). For example, haematopoietic stem cells (HSCs) are capable of producing all the cells which constitute the blood system. This includes cells of the lymphoid and myeloid lineage. However, lymphoid or myeloid progenitor cells are only capable of producing cells of that specific lineage and are therefore termed oligopotent. Oligopotent stem cells are only capable of differentiating into a restricted number of lineage-associated cell types. Lastly, stem cells can also be classified as unipotent,

which means they are only capable of differentiating into a single specific cell type (13).

Stem cells can also be categorised into broader categories such as embryonic-, adult- and iPS stem cells. Adult stem cells refer to stem cells that can be found in adult tissues/organs (12, 13). These cells were first identified in the bone marrow but can be found in a variety of organs such as adipose tissue, dental pulp, skin, peripheral blood, umbilical cord and cord blood, to name a few (18, 19). Their main function in the body is to maintain cell turnover by replacing damaged or lost cells as a result of injury or disease which may have occurred (12, 13). Well known examples of adult stem cells include HSCs and mesenchymal stromal/stem cells (MSCs).

2.2.1 Mesenchymal Stromal/Stem Cells

Mesenchymal Stromal/Stem Cells are multipotent adult stem cells that were first discovered in murine bone marrow (BM-MSCs) by Friedenstein and colleagues (20-22). Within organs, MSCs play an important role in cell replacement and regeneration and secretion of bioactive molecules, and are also thought to have an immune-modulatory role (19, 20). These stem cells are well known for their adipogenic, osteogenic and chondrogenic differentiation capacity (22, 23); they are however not restricted to differentiating into these three cell types. Since their discovery, MSCs have been shown to differentiate into many other cell types such as muscle, tendons and ligaments, neural cells, cardiomyocytes among others (19, 22).

As mentioned before, MSCs were originally isolated from bone marrow, but since then adipose tissue and the umbilical cord have gained popularity as attractive sources for MSC isolation (23-26). Bone marrow aspiration is painful (requiring anaesthesia) and invasive with only a small number of MSCs being obtained (0.001-0.01%). In addition, there is a decline in the number of MSCs present in the bone marrow with increasing age (20, 27). All these factors make bone marrow a less attractive source for isolating MSCs for most cell therapy applications. Adipose tissue on the other hand is considered a biological waste product from liposuction and abdominoplasty procedures and the umbilical cord is also considered a biological waste product after child birth (28-30). The use of adipose tissue and umbilical cord tissue are thus both associated with fewer ethical concerns and does

not require any additional invasive procedures other than the surgical procedures indicated. The number of MSCs that can be isolated from these sources is also greater when compared to the expected MSC yield from bone marrow (Table 2.1).

Tissue	Isolation efficiency	
1 mL bone marrow	100 – 1000 stem cells	(31)
1 g adipose tissue	5 000 stem cells	(31)
1 cm^2 umbilical cord	1000 – 5 000 stem cells	(32)

In this study, MSCs were isolated from adipose tissue and Wharton's Jelly (found within the umbilical cord). These MSCs are respectively referred to as adipose derived stromal cells (ASCs) and Wharton's Jelly derived stromal cells (WJSCs).

2.3 Adipose tissue

Adipose tissue is an endocrine organ comprising of terminally differentiated fat cells (adipocytes), pre-adipocytes/ASCs, fibroblasts, endothelial cells, nerve cells and immune cells which function together to maintain homeostasis within the tissue (Figure 2.2) (2, 34).
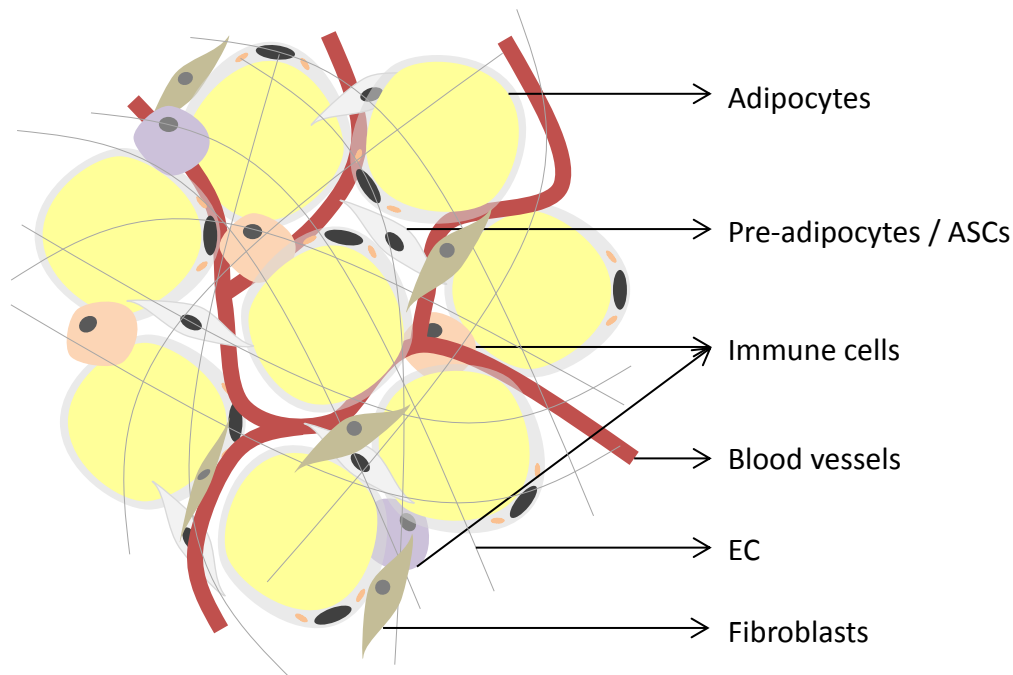
Figure 2.2: Schematic representation of adipose tissue. Adipose tissue is comprised of adipocytes, pre-adipocytes/ASCs, blood vessels, immune cells, fibroblast, nerve cells and ECM amongst others.

There are two types of adipose tissue in mammals: white and brown adipose tissue (35, 36) (Figure 2.3). White adipose tissue (WAT) is the main type of adipose tissue found throughout our bodies (35-37) (Figure 2.3 A). White adipose tissue can further be subdivided into visceral and subcutaneous adipose tissue. Visceral WAT is found around organs providing protection, while subcutaneous WAT is found directly under the skin providing insulation (36).
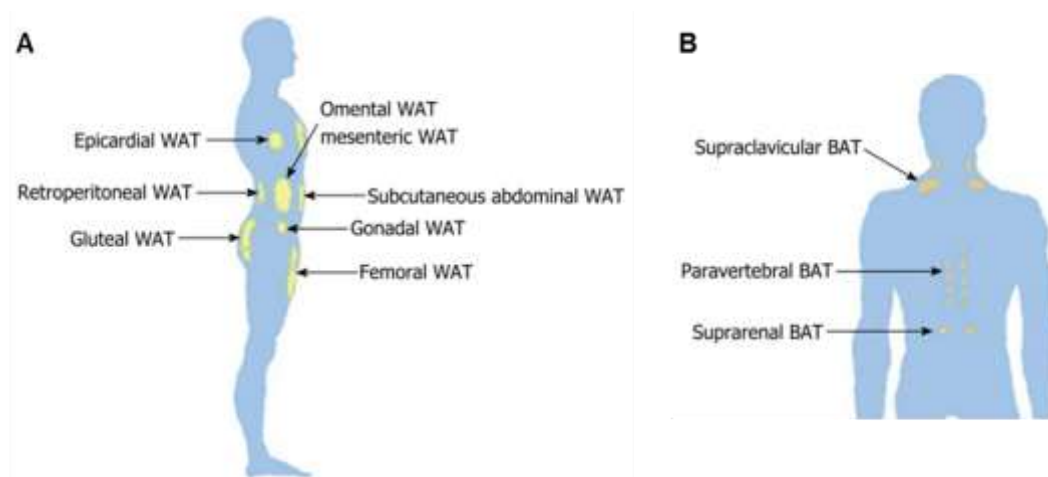
Figure 2.3: Distribution of WAT and BAT in adults. A. Location of WAT depots in adults. **B.** Location of BAT depots in adults. Image is from Park et al 2014 (36). WAT, white adipose tissue; BAT, brown adipose tissue.

White adipose tissue is mainly involved in energy storage but also plays a role in insulin signalling, glucose metabolism and lipid metabolism through the secretion of cytokines (35, 37, 38). Cytokines released by adipose tissue are also known as adipokines (Table 2.2).

Table 2.2: Adipokines secreted by WAT and their function

Adipokine	Function
Leptin	Suppresses appetite Insulin sensitizing Inhibition of lipogenesis Increases fatty acid oxidation Decreases hepatic gluconeogenesis Increases glycolysis
Adiponectin	Anti-inflammatory Insulin sensitizing Decrease hepatic gluconeogenesis Increases fatty acid oxidation
Resistin	Maintenance of fasting glycaemia Pro-inflammatory Increases gluconeogenesis Decreases glycolysis Insulin resistance
Apelin	Insulin sensitizing
Visfatin	Insulin sensitizing Increases insulin secretion Pro-inflammatory Glucose uptake by myocytes and adipocytes
Tumour necrosis factor alpha	Insulin resistance Inhibition of insulin secretion
Interleukin 6	Insulin resistance Inhibition of adipogenesis Increase hepatic gluconeogenesis Decrease visfatin and adiponectin secretion

Summarised from Kuryszko et al 2016 (38)

White adipose tissue stores energy in the form of triglycerides within lipid filled vacuoles in white adipocytes (39). Mature white adipocytes are characterised by a single large lipid droplet which occupies the majority of the cytosol and has few mitochondria (Figure 2.4). These cells originate from MSCs within adipose tissue (ASCs) that do not express myogenic factor 5 (Myf-5) (35, 36).

Unlike WAT, brown adipose tissue (BAT) is largely involved in energy expenditure and is a lot more scarce than WAT (1). Small regions of BAT can be found on the upper back and around the kidneys (Figure 2.3 B) (36). A unique feature of brown

adipocytes is the expression of uncoupling protein 1 (UCP1), a mitochondrial protein, which allows for BATs role in energy expenditure (40). During cold exposure, the sympathetic nervous system is stimulated and norepinephrine is released which results in BAT producing heat through non-shivering thermogenesis (35). In order to do so, fatty acids are released through lipolysis and are used by UCP1 for heat production (36, 41). Another difference between WAT and BAT adipose tissue is the morphology and origin of the resident adipocytes. Brown adipocytes are more ellipsoid in shape, mitochondria rich and contain multiple lipid droplets within the cytosol (35) (Figure 2.4). In contrast to white adipocytes, brown adipocytes arise from Myf5-expressing (Myf-5-positve) progenitor cells (MSCs).

A third type of adipocyte which shares features of both white and brown adipocytes but displays a unique gene expression signature has also been identified (42). These adipocytes are referred to as beige adipocytes and are found in WAT depots. Beige adipocytes are thought to originate from Myf-5 negative MSCs, just like white adipocytes, but are involved in energy expenditure and express UCP1, like brown adipocytes (36, 42). Morphologically, beige adipocytes are very similar to brown adipocytes displaying higher levels of mitochondria and multi-locullar lipids (35, 42, 43) (Figure 2.4). Beige adipocytes have also been described as an inducible adipocyte as they require external stimulation such as cold exposure, exercise, tissue injury or long term use of a peroxisome proliferator-activated receptor γ (PPARγ) agonist for their development/differentiation (40). The differentiation from white to beige is modulated by PRDM16 (PR domain containing 16), a transcription coregulatory factor which is involved in BAT development and regulates the expression of genes involved in thermogenesis (2, 35, 44).
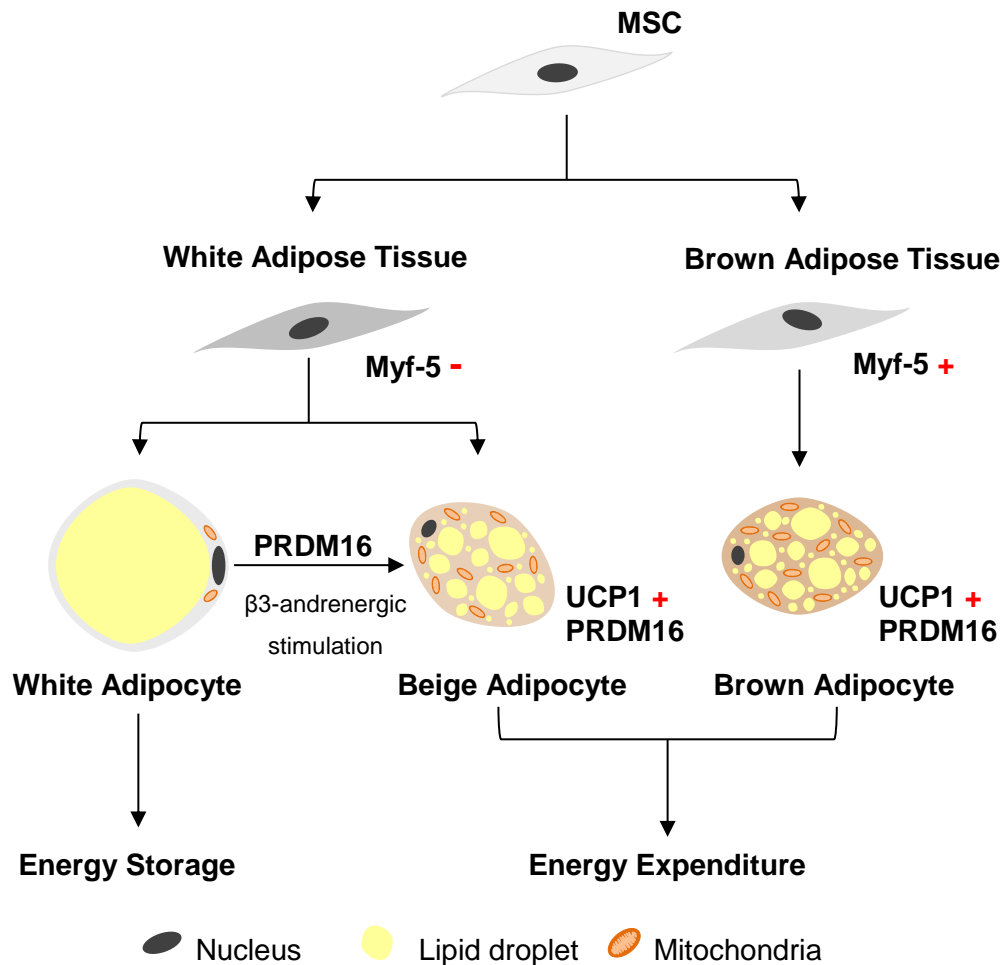
Figure 2.4: Origin of adipocytes. White and beige adipocytes arise from different precursor cells in their respective adipose tissue. White adipocytes are involved in energy storage and contain one unilocular lipid droplet which occupies the majority of the cytosol. Beige and brown adipocytes are involved in energy expenditure through UCP1. The expression of PRDM16 regulates the differentiation of white adipocytes into beige adipocytes. Image modified from Sarjeant and Stephens et al. 2012 (35). MSC, mesenchymal stromal/stem cell; Myf-5, myogenic factor 5; PRDM16, PR domain containing 16; UCP1, uncoupling protein 1.

2.3.1 Adipose derived Stromal/Stem Cells (ASCs)

Lipoaspirate or solid adipose tissue can be processed to yield a heterogeneous mixture of cells, known as the stromal vascular fraction (SVF), from which ASCs can be isolated (22, 45, 46). The SVF is comprised of a heterogeneous population of cells which includes ASCs, erythrocytes, endothelial cells, lymphocytes, fibroblasts, immune cells and others (Figure 2.2 and Table 2.3) (46). The proportion of different cells present in the SVF is difficult to estimate as these proportions may change from

sample to sample depending on the isolation technique used, the processing of the cells as well as the donor's health status (45). However, only 2% of the nucleated cells obtained from lipoaspirate are ASCs (28, 31).

Table 2.3: Composition of SVF as estimated by Bourin et al. 2013

Nucleated cells in SVF	% in SVF
HSCs and progenitor cells	<0.1
Granulocytes	10 – 15
Monocytes	5 – 15
Lymphocytes	10 – 15
Endothelial cells	10 – 20
Pericytes	3 – 5
Stromal cells	15 – 30

In 2001, Zuk and colleagues were the first to identify, describe and isolate ASCs from the SVF (47). Zuk and colleagues identified a population of cells which displayed tri-lineage differentiation capacity and expressed cell surface antigens that did not match that of HSCs i.e. CD29, CD44, CD71, CD90, and CD105 (28, 47). Later, the ISCT together with the International Federation for Adipose tissue (IFATS) published a set of criteria for the identification of ASCs specifically. In order for cells to be defined as ASCs, they need to adhere to a specific set of when cultured *in vitro* (46):

i.   Ability to adhere to plastic when cultured under standard conditions;

ii. Express a specific set of cell surface antigens. More than 90% of the cells are required to be positive for markers CD13, CD105, CD73 and CD90, while less than 2% of the cells should be positive for CD11b and CD45. In addition, CD36 could be included as a positive marker and CD106 as a negative marker in order to distinguish ASCs from bone marrow MSCs (BM-MSCs);

iii. Display tri-lineage differentiation potential i.e. the ability to differentiate into osteoblasts, adipocytes and chondrocytes *in vitro.*

2.4. Umbilical cord

The umbilical cord is between 40 and 60 cm in length, and its main function is to supply nutrition to the growing foetus (25). The umbilical cord is a simple structure comprised of an outer epithelial layer, Wharton's Jelly, the umbilical vein and the two umbilical arteries (Figure 2.5) (25, 29). Wharton's Jelly refers to mucoid connective tissue composed mainly of proteoglycans and different types of collagen which protects the umbilical vessels (25, 48, 49). No blood vessels, nerves or lymph vessels are present in Wharton's jelly tissue (25). WJSCs can be obtained from four sources within the umbilical cord which includes; (i) umbilical cord lining, (ii) sub-endothelial layer, (iii) perivascular zone and (iv) Wharton's jelly (48).
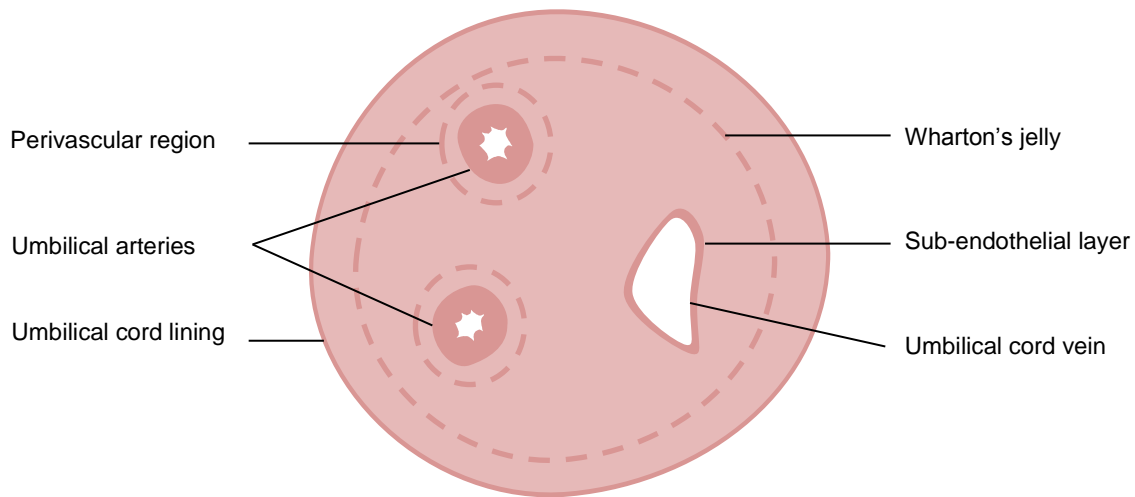
Figure 2.5: Schematic illustration of a cross section of an umbilical cord. Mesenchymal stromal cells can be obtained from the umbilical cord lining, perivascular region, sub-endothelial layer and Wharton's Jelly.

2.4.1 Wharton's Jelly derived Stromal Cells

Wharton's jelly derived MSCs were first isolated from Wharton's Jelly in 1991 by McElreavey and colleagues (50). Recently human derived WJSCs (hWJSCs) have gained popularity as a source of MSCs for therapeutic purposes. There are a number of clinical trials which have investigated the use of hWJSCs to treat various clinical indications, such as diabetes, haematological disorders, autoimmune disorders, cardiovascular, respiratory amongst many others (Figure 2.6) (25, 32).
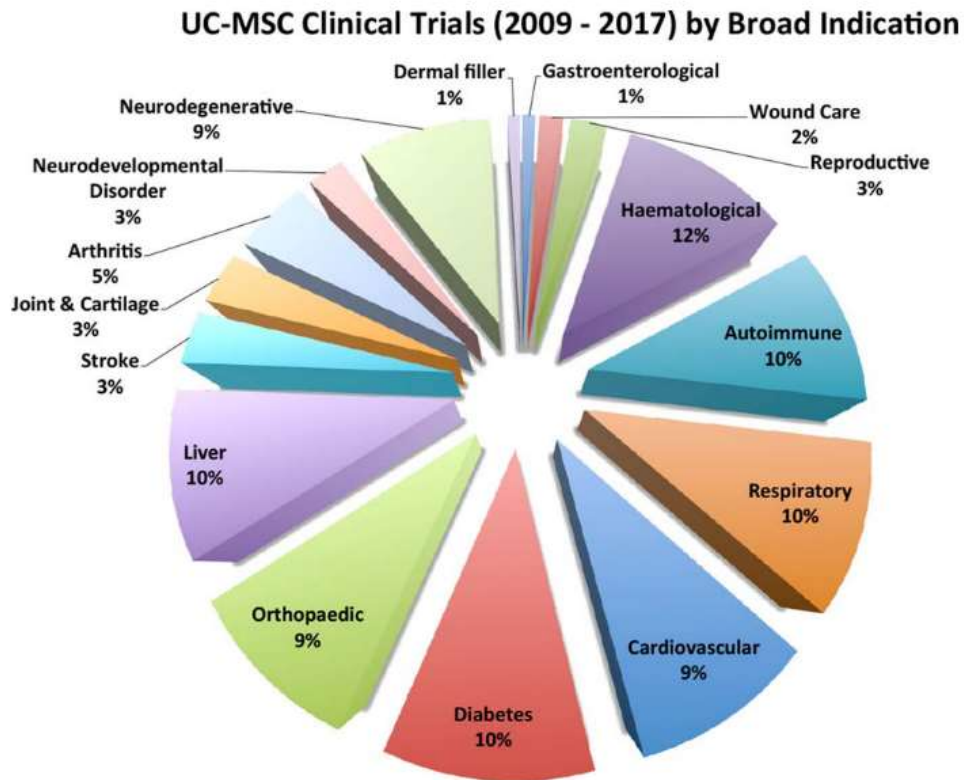
Figure 2.6: Pie chart illustrating the percentage of registered clinical trials using human umbilical cord MSCs as summarised by Davies et al. 2017. The data is based on results obtained from Clinicaltrials.gov and includes 109 clinical trials. Image is from Davies et al. 2017(25).

Some advantages of using hWJSCs include (i) high isolation efficiency (1 to 5 x10^4 cells/cm of umbilical cord); (ii) the fact that they are considered to be biological waste and thus there is minimal association with ethical or moral issues; and (iii) the cells are considered to be more primitive as they express a number of embryonic stem cell markers such as NANOG, DNMT3B and GABRB3 (25, 26, 28, 29, 32).

With regard to immunophenotype, hWJSCs have a similar phenotype to hASCs and adhere to the criteria set out by the ISCT. The hWJSCs have been shown to be positive for CD13, CD29, CD73, CD90, CD105, HLA-ABC and negative for CD45, CD133 and HLA-DR (29, 51). The positive markers occur at a frequency greater than 90% and the negative markers occur at a frequency below 1% (29).

2.5 Adipogenic differentiation capacity of hASCs and hWJSCs

Human derived ASCs and WJSCs have been shown to be similar in many aspects. Both cell types can easily be harvested with minimal ethical implications, display spindle morphology *in vitro*, have immunomodulatory properties, have low tumorigenicity and express similar cell surface markers (52, 53). They have however been shown to have different proliferation rates (hWJSCs have a higher proliferation rate), different cytokine secretion profiles and different differentiation capacities (52). Of interest to the present study is the adipogenic differentiation capacity of these two cell types.

The adipogenic differentiation capacity of hWJSCs has been described as being poor by a number of studies (18, 54-56) whereas hASCs have been shown to easily differentiate along the adipogenic lineage (23, 52). The reasons for this have not yet been properly elucidated. One study did however suggest that the environment in which the cells are found is capable of influencing their differentiation capacity (54). Pierdomenico and colleagues showed that hWJSCs which were obtained from diabetic mothers displayed a better adipogenic differentiation capacity in comparison to hWJSCs obtained from healthy donors (54). It has also been suggested that MSCs are capable of retaining methylation signatures from the tissues they were isolated from which could influence gene expression and ultimately differentiation capacity (23).

2.6 Adipogenesis

Adipogenesis is the complex, multi-step process by which precursor cells, such as MSCs, differentiate into mature adipocytes. This process can be broken down into three stages: (i) cell commitment, (ii) mitotic clonal expansion, and (iii) terminal differentiation (57, 58). Cell commitment involves the differentiation of MSCs into pre-adipocytes. During this stage the cells commit to undergo adipogenic differentiation (59, 60). During mitotic clonal expansion pre-adipocytes undergo two rounds of mitosis (57). Mitotic clonal expansion is an important step in adipogenesis as the unwinding of the DNA, an essential step during DNA replication, allows transcription factors to bind to the DNA and by so doing initiate a well-regulated

cascade of gene regulation events required for adipogenic differentiation (59). Last, during terminal differentiation end-stage adipogenesis-associated genes are upregulated allowing pre-adipocytes to acquire all the morphological, genetic and biochemical characteristics of mature adipocytes (59, 60).

In order to study adipogenesis *in vitro*, the cells are stimulated with an adipogenic differentiation cocktail. The components of the adipogenic cocktail include: (i) insulin, which is required for mitotic clonal expansion and aids in lipid accumulation (36, 60); (ii) dexamethasone, which is a glucocorticoid used to induce the expression of the main transcription factor, proliferator-activated receptor gamma (PPARγ), and downregulate a well-known inhibitor of adipogenesis, Pref-1; and (iii) 3-isobutyl-1methylxanthine (IBMX), which is a phosphodiesterase inhibitor is needed to activate another important set of transcription factors, CCAAT-enhancer-binding proteins (C/EBP) β and δ (discussed below) as well as increase cyclic AMP (cAMP) levels (36).

2.6.1 Transcriptional regulation of adipogenesis

Adipogenesis is regulated by several genes (Figure 2.7). The main positive regulator is PPARγ (61, 62). Other positive regulators include the C/EBP family of transcription factors, the Krüppel-like factor (KLF) family of transcription factors, sterol regulatory element binding protein-1 (SREBP-1), and signal transducer and activator of transcription (STAT) transcription factors (35, 62, 63). Some negative adipogenic regulators include Pref-1 (64-67), GATA and the Wnt (wingless/integrated) family of transcription factors (35).
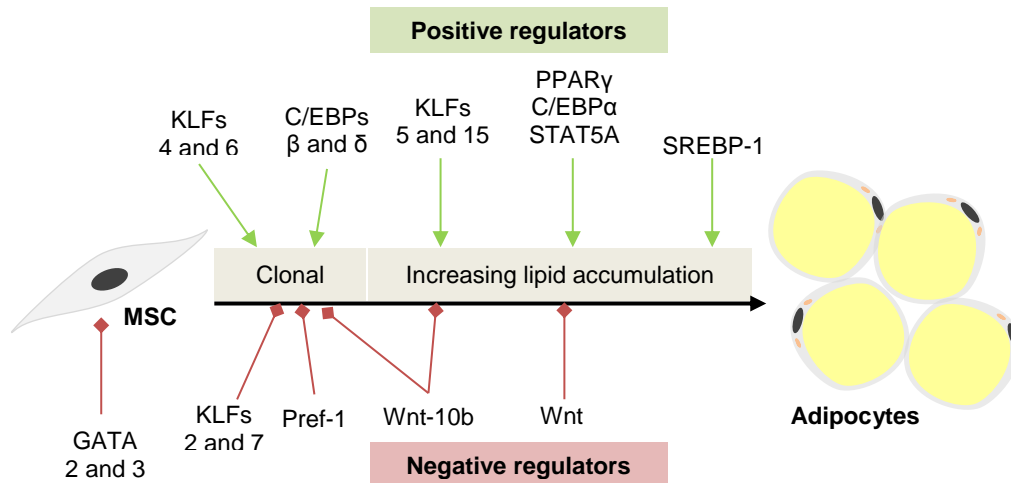
Figure 2.7: Positive and negative regulators of adipogenesis. Adipogenesis is tightly regulated by a number of transcription factors which are expressed at different stages during the adipogenic differentiation pathway. Image modified from Sarjeant and Stephens et al. 2012 (35). MSC, Mesenchymal stromal/stem cell; AP-1, activating protein-1; KLFs, Krüppel-like factors; C/EBP, CAAT-enhancer binding proteins; PPARγ, Peroxisome proliferator-activated receptor gamma; STAT, Signal transducer and activator of transcription; SREBP-1, sterol regulatory element binding protein 1; Pref-1, pre-adipocyte factor 1; Wnt, Wingless/Integrated protein.

The role of the above mentioned regulators of adipogenesis is discussed below. The main focus is however on Pref-1, which is the protein of interest for the study described herein.

2.6.1.1 Peroxisome proliferator-activated receptor gamma (PPARγ)

The PPARγ transcription factor is considered the main regulator of adipogenesis. It forms part of the nuclear receptor superfamily of ligand inducible transcription factors (68-70). Besides adipogenesis, PPARγ is also known to have a role in lipogenesis, energy homeostasis and insulin sensitivity (70, 71). There are two isoforms of the PPARγ transcription factor, namely PPARγ1 and PPARγ2 which arise through alternative promoter usage. The PPARγ1 isoform can be found in all cells, but PPARγ2 is restricted to adipose tissue and is considered a better transcription activator of adipogenesis (62, 71).

During adipogenesis, PPARγ expression is induced by dexamethasone *(in vitro)* and cAMP *(in vivo)* (2). The activation of PPARγ requires the formation of a heterodimer with another nuclear hormone receptor such as the retinoid-x-receptor (RXR) (70,

72). Once activated, PPARγ is able to bind to and activate the promoters of adipocyte specific genes such as fatty acid binding protein 4 (FABP4) [also known as adipocyte protein 2 (aP2)] which is an adipocyte selective fatty acid binding protein, as well as phosphoenolpyruvate carboxylase (PEPCK) which is involved in gluconeogenesis (62). PPARγ has become widely known as the master regulator of adipogenesis as many modulators of adipogenesis interfere with either its expression or activity (35, 73, 74). As a result PPARγ is often used a marker gene in studies investigating adipogenesis (22).

2.6.1.2 CCAAT enhancer binding proteins (C/EBPs)

The C/EBPs are a group of leucine zipper transcription factors that are involved in cell differentiation and function (75). There are a number of C/EBP isoforms, namely C/EBPα, C/EBPβ, C/EBPδ, C/EBPγ, C/EBPε and C/EBPζ which arise through alternative promoter usage (74, 76). In order to be functional these transcription factors are known to form homodimers or heterodimers with each other (60, 62). During adipogenic differentiation, C/EBPβ and C/EBPδ are the first to be expressed during early adipogenesis. *In vitro*, the expression of C/EBPβ and C/EBPδ are induced by IBMX and dexamethasone respectively (35, 36, 62, 74). These two C/EBPs are then responsible for *trans*-activating PPARγ and C/EBPα (62, 77). Once activated, C/EBPα is responsible for the transcription of a number of adipocyte specific genes such as aP2 (fatty acid binding protein), SCD1 (fatty acid metabolism), GLUT4 (glucose transporter), PEPCK (gluconeogenesis) and leptin (satiety hormone) (60).

Apart from activating PPARγ and C/EBPα, C/EBPβ is also thought to be involved in mitotic clonal expansion by acting on certain components of the CMG (Cdc45-MCM-GINS) complex as well as cell division cycle 25C phosphatase (Cdc25c) (77). The CMG complex is an enzyme that unwinds double stranded DNA at replication forks while Cdc25c is involved in entry into the S- and M-phases of the cell cycle (77, 78).

The remaining C/EBP proteins, C/EBPγ and C/EBPζ, are thought to play an inhibitory role in adipogenesis (62, 74). Their expression is suppressed during early stages of adipogenesis and increases again towards the end of the differentiation process (62). The most likely mechanism is through heterodimer formation with

C/EBPβ which results in its inactivation and subsequent inability to activate PPARγ and C/EBPα (74).

2.6.1.3 Sterol regulatory element binding protein-1 (SREBP-1)

The SREBPs are basic helix loop helix transcription factors (60, 62). Due to alternative promoter usage, there are three isoforms of SREBP: SREBP-1a, SREBP-1c and SREBP2. Within WAT, SREBP-1c is the dominant isoform (35). During adipogenesis SREBP-1c plays a role in regulating lipogenesis related genes such as lipoprotein lipase, fatty acid synthase as well as glycerol phosphate acyltransferase (60). It is also thought to increase PPARγ's transcriptional activity through the production of endogenous ligands for PPARγ (60, 62).

2.6.1.4 Krüppel-like factors

The KLFs form part of a zinc finger family of transcription factors which have been shown to play a role in a number of cellular differentiation processes as well as proliferation (35, 79). There are 17 mammalian KLFs of which 8 are known to be involved in adipogenesis. These include KLFs 4, 5, 6, 9 and 15 as promoters of adipogenesis while KLFs 2, 3 and 7 are suppressors of adipogenesis (2, 79). The functions of the respective KLFs are summarized in Table 2.4.

Table 2.4: Summary of the various Krüppel-like factors and their functions in adipogenesis

Krüppel-like factor	Expression & Function	Reference
POSITIVE REGULATORS		
KLF4	• Expressed very early upon adipogenic stimulation and consequently highly expressed in pre-adipocytes • Activate C/EBPβ together with early growth response protein 2 (ERG2) • Downregulated via a negative feedback loop	(79, 80)
KL5	• Expressed early in the adipogenic differentiation pathway • Expression is induced by C/EBPβ and C/EBPδ • Aids in inducing PPARγ2 expression	(79, 81)
KLF6	• Suppresses the expression of Pref-1, an inhibitor of adipogenesis, by binding to its promoter	(82)
KLF9	• Expression is induced later along the adipogenic differentiation pathway. • Involved in PPARγ2 transactivation along with C/EBPα.	(83)
KLF15	• Promotes adipocyte maturation and the expression of GLUT4	(79)
NEGATIVE REGULATORS		
KLF2	• Opposite effect to KLF6 • Capable of restoring Pref-1 expression which will result in the inhibition of adipogenesis	(84)
KLF3	• Supress C/EBPα	(79)
KLF7	• Decrease the expression of adipogenic genes such as PPARγ, C/EBPβ, FABP4 and adipsin	(79)

2.6.1.5 Signal transducer and activator of transcription (STAT) proteins

There are a number of STAT proteins - STAT1, STAT2, STAT3, STAT4, STAT5A, STAT5B and STAT6 (35). Of these, STAT3, STAT5A and STAT5B play a role during

adipogenesis. STAT3 is thought to promote C/EBPβ expression (85) whereas STAT5 proteins are thought to contribute to adipocyte development through induction of PPARγ expression (35, 86).

2.6.1.6 GATA transcription factors

The GATA transcription factors bind to specific (A/T)GATA(A/G) DNA sequences to regulate cellular proliferation and differentiation. There are 6 GATA transcription factors of which GATA-2 and GATA-3 play an inhibitory role during adipogenesis (35). These transcription factors suppress adipogenesis by binding to the promoter region of PPARγ, decreasing its activity (87). It has also been shown that GATA-2 and -3 are capable of forming complexes with C/EBPβ and C/EBPα which results in the suppression of adipogenesis by disrupting their activity (88).

2.6.1.7 Wnt signalling

There are a large number of proteins (>16) that belong to the Wnt family of glycoproteins. This family of proteins plays a role in cell fate determination, differentiation and proliferation through the frizzled receptor and low density lipoprotein-related protein 5/6 co-receptor (35, 76). Two Wnt proteins have been shown to be involved in adipogenesis – Wnt10 and Wnt5a. Both of these Wnt proteins act as inhibitors of adipogenesis by supressing the expression of PPARγ and C/EBPα (35).

2.6.1.8 Pre-adipocyte factor 1 (Pref-1)

Pre-adipocyte factor 1 (*Pref-1*) is a paternally imprinted gene located on the long arm of chromosome 14 (14q32.2) (89). Apart from the name *Pref-1*, the gene product is also known as pG2, fetal antigen 1 (FA1) and delta-like (dlk) protein.

In 1987, Helman and colleagues (90, 91) were investigating highly expressed genes in pheochromocytoma and found a gene product which they referred to as pG2. A year later, Fay and colleagues (92) found the Pref-1 protein in amniotic fluid which they referred to as FA1 since they suspected the protein to be of foetal origin. The name, dlk, was introduced in 1993 when Laborda and colleagues (93) were investigating small cell lung carcinoma. They found a protein, referred to it as dlk protein, thought to be part of the epidermal growth-factor like superfamily. However,

the first time that the Pref-1 was implicated in adipogenesis was in 1993 by Smas & Sul (94). The term "Pre-adipocyte Factor" was given due to the fact that the mRNA was highly expressed in the pre-adipocyte cell line 3T3-L1 but not in mature adipocytes. Since then, sequence alignments have however shown that FA1, dlk and Pref-1 are actually the product of the same gene with some post transcriptional modifications (95, 96).

The Pref-1 protein is a 385 amino acid protein belonging to the epidermal growth factor (EGF) like family of proteins and exhibits homology to the Notch/Delta/Serrata family of EGF-like proteins (94, 97-99). Pref-1 lacks the Delta-Serrate-LAG-2 (DSL) domain found in classical canonical Notch ligands, but it does possess Delta and OSM-11 (DOS) domains which are found in Notch ligands (100). The protein size ranges between 50 kDa and 60 kDa due to post translational modifications such as N-linked glycosylation (98).

Looking at its structure, Pref-1 is a transmembrane protein containing six EGF-like repeats within the extracellular domain, a juxtamembrane region, a transmembrane domain and a cytoplasmic domain (Figure 2.8) (66, 98, 99). Within its extracellular domain there are two cleavage sites, one in the juxtamembrane region and one near the fourth EGF-like repeat. Cleavage at the juxtamembrane region by tumour necrosis factor alpha converting enzyme (TACE) results in a full length, large soluble 50 kDa form of the protein while cleavage near the fourth EGF-like repeat results in a small soluble 25 kDa form of the protein (101, 102). Only the 50 kDa soluble form of the protein has been implicated as an inhibitor of adipogenesis (66, 99, 102, 103). The activity, function and role of the small soluble unit are currently unknown.

Due to alternative splicing, the Pref-1 protein can be found in four isoforms, Pref-1 A – D (Figure 2.8) (97). The Pref-1A form is the full length protein capable of producing both soluble products. The remaining forms (B-D) contain in-frame deletions in the extracellular domain. Nevertheless, despite the deletion, Pref-1 B is still capable of producing both soluble forms as the deletion does not affect either cleavage site (Figure 2.8). The remaining forms, Pref-1 C-D, are only capable of producing the small soluble form as the deletion removes the cleavage site within the juxtamembrane region (Figure 2.8) (98, 99).
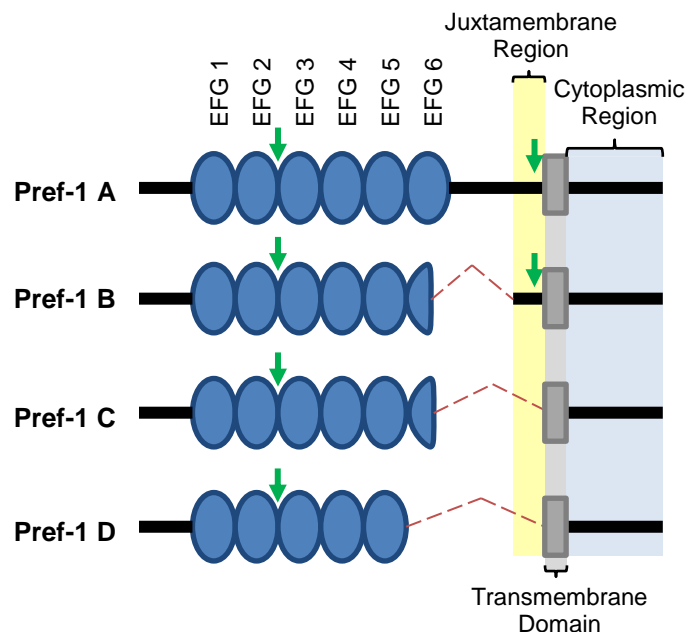
Figure 2.8: Structure of the different Pref-1 isoforms. The Pref-1 protein can be found in four isoforms (Pref-1 A, B, C and D) due to alternative splicing. Pref-1A is the full length protein while isoforms B-D contain in-frame deletions (98). The red dotted line indicates the missing sections due to the in-frame deletions. Green arrows indicate the cleavage sites for the generation of the soluble forms of the protein. Image adapted from Sul et al. 2009.

In vitro, Pref-1 expression has been shown to be regulated by IBMX and dexamethasone. During the differentiation process, IBMX increases Pref-1 levels (104) which are then subsequently downregulated by dexamethasone (105). The downregulation of Pref-1 is important as the sustained expression of this protein will inhibit adipogenesis (66, 98, 99).

2.6.1.8.1 Pref-1 mechanism of action

The exact mechanism by which Pref-1 is able to inhibit adipogenesis has not yet been fully elucidated. Two pathways have been implicated in Pref-1's mechanism of action, the mitogen activated protein kinases (MAPK) signalling pathway and the Notch signalling pathway.

2.6.1.8.1.1 Pref-1 and the MAPK Kinase (MEK)/ERK signalling pathway

The MAPKs play a role in cell differentiation and proliferation by transmitting extracellular signals received by cell surface receptors to transcription factors within the nucleus in order to affect/regulate the transcription of genes (106). Extracellular

signal-regulated kinase (ERK) 1, 2 and 5, c-Jun amino-terminal kinases (JNK) 1-3 and p38 kinases are phosphorylation induced, serine/threonine kinases which form part of the MAPK family of kinases (106, 107).

Pref-1 is thought to affect adipogenesis through the activation of ERK1/2 and MAPK/ERK (MEK)/ERK 1/2 (108). Kim and colleagues (2007) used Pref-1 null mouse embryo fibroblasts (MEF) to investigate Pref-1's mode of adipogenic inhibition (108). Their work showed that Pref-1 is capable of inducing the phosphorylation of ERK1/2 which ultimately affects the transcription of PPARγ2, inhibiting adipogenesis. The exact manner in which Pref-1 mediates ERK1/2 phosphorylation is however unknown. The authors (108) postulated that GATA-3 may be responsible for the PPARγ suppression observed based on work done by Tong *et al.* 2000 (87). This would suggest that the MAPK/ERK cascade potentially regulates adipogenesis through the adipogenic transcription factor, GATA-3, which when upregulated suppresses PPARγ activation and consequently adipogenesis. Based on these findings, Kim and colleagues (2007) suggested that Pref-1 mediated phosphorylation of ERK1/2 induces adipogenic transcription factors, such as GATA-3, which then through PPARγ suppression inhibits adipogenesis. Wang and colleagues (109) built on the above concept proposed by Kim and colleagues and implicate sex-determining region-Y box 9 (Sox9) in the inhibition pathway. Sox9, which is known for its role in chondrogenesis and osteogenesis, is known to be activated by the MEK/ERK pathway (98). Wang and colleagues showed that Sox9 is capable of inhibiting adipogenesis by binding to the promoter regions of C/EBPβ and C/EBPδ which in turn prevents the activation of PPARG and C/EBPα (109). As a result, adipogenesis is inhibited. These authors (98, 108, 109) thus propose the following mechanism of action: (i) Pref-1 mediates the phosphorylation and subsequent activation of the MEK/ERK pathway through an unknown interaction partner which in turn will (ii) upregulate the expression of Sox9 which (iii) will bind to the promoter regions of C/EBPβ and C/EBPδ resulting in the inhibition of adipogenesis (98, 108, 109).

In 2010, Wang and colleagues (110) identified fibronectin and the α5β1 integrin as the missing interaction partners in the above pathway. The authors (110) suggest that once Pref-1 is cleaved from the cell surface by TACE, the 50kDa soluble protein binds to the C-terminal of fibronectin. The Pref-1-fibronectin- α5β1integrin interaction is then thought to activate the MEK/ERK pathway which in turn will activate Sox9 and inhibit adipogenesis as described in Figure 2.9 (66, 110).
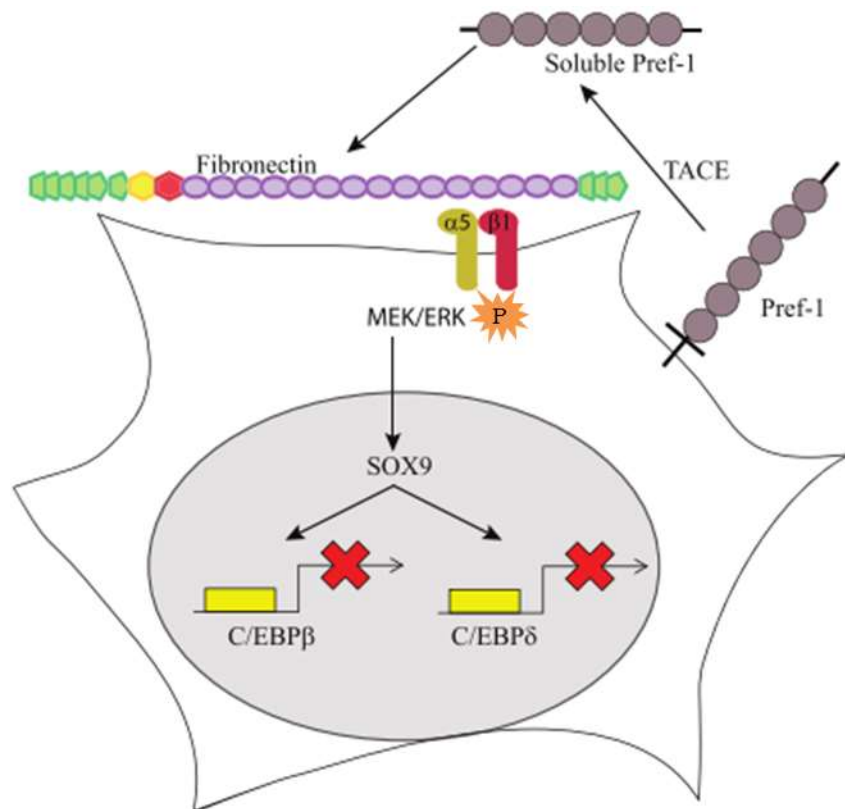
Figure 2.9: Pref-1 inhibition of adipogenesis through fibronectin, MEK/ERK and Sox9 interactions. Membrane bound Pref-1 is cleaved by TACE at the cell surface to generate a soluble 50 kDa biologically active form of the protein. The biologically active soluble form interacts with the C-terminal of fibronectin. The Pref-1-fibronectin-α5β1-integrin complex activates the MEK/ERK pathway which induces Sox9 expression. Sox9 inhibits adipogenesis through suppression of C/EBPβ and C/EBPδ. TACE, TNFα converting enzyme, MEK/ERK, MAPK/ERK kinase/extracellular signal regulated kinase; Sox9, sex determining region-Y box9; C/EBP, CAAT/enhancer-binding protein; P, Phosphorylation. Image was adapted from Hudak and Sul 2013 (66).

There is however controversy regarding the idea that Pref-1 mediates ERK1/2 phosphorylation. Work presented by Zhang and colleagues (111) demonstrated that Pref-1 expression impairs ERK1/2 phosphorylation through the downregulation of

insulin-like growth factor 1 (IGF-1). Work by Ruiz-Hidalgo and colleagues also demonstrated that there was no increase in ERK1/2 phosphorylation upon the induction of Pref-1 expression (112). The authors were however working with different cell types; Zhang and colleagues (111) worked on 3T3-L1 cells, Ruiz-Hidalgo and colleagues (112) worked on BALB/c 3T3 and Kim and colleagues (108) worked with MEFs.

Whether the results could have been influenced by the cell types used is unknown. This is an interesting concept as Nueda and colleagues (113) showed that Pref-1 can have both pro- and anti-adipogenic effects depending on the cell line used. The role of Pref-1 was investigated in two cell types: 3T3-L1 cells and C3H10T1/2. The C3H10T1/2 cells displayed a poor adipogenic differentiation capacity in comparison to the 3T3-L1 cells. However, the adipogenic capacity of the C3H10T1/2 cells was increased when Pref-1 levels were upregulated in the cells through transfection with Pref-1 cDNA constructs encoding the extracellular portion of the protein. The downregulation of Pref-1 was also investigated in the C3H10T1/2 cells and there was no effect on the cells poor adipogenic differentiation capacity. When the same experiments were repeated using 3T3-L1 cells, overexpression inhibited adipogenesis and downregulation enhanced adipogenesis.

2.6.1.8.1.2 Pref-1 and the Notch signalling pathway

This pathway is known to be responsible for a number of processes such as cell determination, differentiation and proliferation. There are five canonical NOTCH ligands which have been identified in humans – JAGGED1, JAGGED2 and Delta like (DLL) 1, 3 and 4 (114, 115). A typical feature of canonical Notch ligands is the presence of a Delta-Serrate-LAG-2 (DSL) domain. When Notch ligands interact with their respective receptors, the intracellular active domain of the Notch receptor is released and relocates to the cell nucleus where it will affect the expression of a number of transcription factors (114). Pref-1 lacks the DSL domain but contains a Delta and OSM-11 (DOS) domain which is common in non-canonical Notch ligands (115).

Previous work in *Drosophila melanogaster* and *Candida elegans* with regards to Pref-1 and Notch signalling rendered contradictory results with enhancing and

suppressing effects being demonstrated respectively (116, 117). Wang and colleagues (110) were unable to detect any interaction between Pref-1 and Notch and concluded that Notch was unnecessary for Pref-1 signalling. However, recent work by Nueda and colleagues (114) on the 3T3-L1 cell line suggests that Pref-1 interacts with all four Notch receptors i.e. Notch1, 2, 3 and 4. The authors conclude that Pref-1 is capable of inhibiting all four Notch receptors to varying degrees which will result in pro-adipogenic or anti-adipogenic Notch signalling (114).

2.4 Conclusion

Obesity is fast becoming a health burden world-wide (4, 7, 8). The increased levels of adipose tissue in obese patients are often associated with a number of non-communicable diseases (7). As a result, a large proportion of individuals spend a major period of their lives suffering from chronic illnesses which in turn result in overburdened healthcare systems. A better understanding of adipogenesis (the process of fat cell formation) is therefore needed in order to find sustainable solutions to this health challenge (3, 9).

The majority of the studies which look at adipogenesis are performed on murine 3T3-L1 cell lines and/or in murine experimental animal models (2, 44, 60). The ability of MSCs to differentiate into adipocytes holds great promise to serve as an *in vitro* model to study human adipogenesis. It is however unclear if the results from murine studies can be directly translated to the human setting and more studies using cells of human origin are therefore needed. This concern is highlighted in the contradiction in findings regarding the role of Pref-1 during adipocyte differentiation documented for studies making use of different murine cell lines (113). The main objective of this study was to develop a better understanding of the relationship between Pref-1 protein expression and adipocyte differentiation using cells of human origin. We also opted to investigate naturally expressed Pref-1 protein in contrast to using genetically modified cells that were modified to overexpress Pref-1.

2.5 References

1. Lynes MD, Tseng YH. Deciphering adipose tissue heterogeneity. Ann N Y Acad Sci. 2018;1411(1):5-20.

2. Kuri-Harcuch W, Velez-delValle C, Vazquez-Sandoval A, Hernandez-Mosqueira C, Fernandez-Sanchez V. A cellular perspective of adipogenesis transcriptional regulation. J Cell Physiol. 2019;234:1111-29.

3. Zhang Y, Sowers JR, Ren J. Targeting autophagy in obesity: from pathophysiology to management. Nat Rev Endocrinol. 2018;14(6):356-76.

4. Gadde KM, Martin CK, Berthoud HR, Heymsfield SB. Obesity: Pathophysiology and Management. J Am Coll Cardiol. 2018;71(1):69-84.

5. Kotchen TA. Obesity-related hypertension: epidemiology, pathophysiology, and clinical management. Am J Hypertens. 2010;23(11):1170-8.

6. Baleta A, Mitchell F. Country in Focus: Diabetes and obesity in South Africa. Lancet Diabetes Endocrinol. 2014;2(9):687-8.

7. Gurevich-Panigrahi T, Panigrahi S, Wiechec E, Los M. Obesity: pathophysiology and clinical management. Curr Med Chem. 2009;16(4):506-21.

8. Obesity prevalence worldwide - Adults: World Obesity Federation; [Available from: https://www.worldobesitydata.org/map/overview-adults.

9. Moseti D, Regassa A, Kim WK. Molecular Regulation of Adipogenesis and Potential Anti-Adipogenic Bioactive Molecules. Int J Mol Sci. 2016;17(1).

10. Nae S, Bordeianu I, Stancioiu AT, Antohi N. Human adipose-derived stem cells: definition, isolation, tissue-engineering applications. Rom J Morphol Embryol. 2013;54(4):919-24.

11. Janderova L, McNeil M, Murrell AN, Mynatt RL, Smith SR. Human mesenchymal stem cells as an in vitro model for human adipogenesis. Obes Res. 2003;11(1):65-74.

12. Kobolak J, Dinnyes A, Memic A, Khademhosseini A, Mobasheri A. Mesenchymal stem cells: Identification, phenotypic characterization, biological properties and potential for regenerative medicine through biomaterial micro-engineering of their niche. Methods. 2016;99(15):62-8.

13. Zakrzewski W, Dobrzynski M, Szymonowicz M, Rybak Z. Stem cells: past, present, and future. Stem Cell Res Ther. 2019;10(1):68.

14. Thomson JA, Itskovitz-Eldor J, Shapiro SS, Waknitz MA, Swiergiel JJ, Marshall VS, et al. Embryonic stem cell lines derived from human blastocysts. Science. 1998;282(5391):1145-7.

15. Itskovitz-Eldor J. 20th Anniversary of Isolation of Human Embryonic Stem Cells: A Personal Perspective. Stem Cell Reports. 2018;10(5):1439-41.

16. Jung KW. Perspectives on human stem cell research. J Cell Physiol. 2009;220(3):535-7.

17. Mummery CL. Perspectives on the Use of Human Induced Pluripotent Stem Cell-Derived Cardiomyocytes in Biomedical Research. Stem Cell Reports. 2018;11(6):1306-11.

18. Bieback K, Brinkmann I. Mesenchymal stromal cells from human perinatal tissues: From biology to cell therapy. World J Stem Cells. 2010;2(4):81-92.

19. Kobolak J, Dinnyes A, Memic A, Khademhosseini A, Mobasheri A. Mesenchymal stem cells: Identification, phenotypic characterization, biological properties and potential for regenerative medicine through biomaterial micro-engineering of their niche. Methods. 2015.

20. Marquez-Curtis LA, Janowska-Wieczorek A, McGann LE, Elliott JA. Mesenchymal stromal cells derived from various tissues: Biological, clinical and cryopreservation aspects. Cryobiology. 2015;71(2):181-97.

21. Friedenstein AJ, Piatetzky S, II, Petrakova KV. Osteogenesis in transplants of bone marrow cells. J Embryol Exp Morphol. 1966;16(3):381-90.

22. Zolocinska A. The expression of marker genes during the differentiation of mesenchymal stromal cells. Adv Clin Exp Med. 2018;27(5):717-23.

23. Xu L, Liu Y, Sun Y, Wang B, Xiong Y, Lin W, et al. Tissue source determines the differentiation potentials of mesenchymal stem cells: a comparative study of human mesenchymal stem cells from bone marrow and adipose tissue. Stem Cell Res Ther. 2017;8(1):275.

24. Hoogduijn MJ, Dor FJ. Mesenchymal stem cells: are we ready for clinical application in transplantation and tissue regeneration? Front Immunol. 2013;4:144.

25. Davies JE, Walker JT, Keating A. Concise Review: Wharton's Jelly: The Rich, but Enigmatic, Source of Mesenchymal Stromal Cells. Stem Cells Transl Med. 2017;6(7):1620-30.

26. Hassan G, Kasem I, Soukkarieh C, Aljamali M. A Simple Method to Isolate and Expand Human Umbilical Cord Derived Mesenchymal Stem Cells: Using Explant Method and Umbilical Cord Blood Serum. Int J Stem Cells. 2017;10(2):184-92.

27. Li Y, Charif N, Mainard D, Bensoussan D, Stoltz JF, de Isla N. Donor's age dependent proliferation decrease of human bone marrow mesenchymal stem cells is linked to diminished clonogenicity. Biomed Mater Eng. 2014;24(1 Suppl):47-52.

28. Orbay H, Tobita M, Mizuno H. Mesenchymal stem cells isolated from adipose and other tissues: basic biological properties and clinical applications. Stem Cells Int. 2012;2012:461718.

29. Nagamura-Inoue T, He H. Umbilical cord-derived mesenchymal stem cells: Their advantages and potential clinical utility. World J Stem Cells. 2014;6(2):195-202.

30. Baer PC. Adipose-derived mesenchymal stromal/stem cells: An update on their phenotype in vivo and in vitro. World J Stem Cells. 2014;6(3):256-65.

31. Strem BM, Hicok KC, Zhu M, Wulur I, Alfonso Z, Schreiber RE, et al. Multipotential differentiation of adipose tissue-derived stem cells. Keio J Med. 2005;54(3):132-41.

32. Kalaszczynska I, Ferdyn K. Wharton's jelly derived mesenchymal stem cells: future of regenerative medicine? Recent findings and clinical significance. Biomed Res Int. 2015;2015:430847.

33. Dominici M, Le Blanc K, Mueller I, Slaper-Cortenbach I, Marini F, Krause D, et al. Minimal criteria for defining multipotent mesenchymal stromal cells. The International Society for Cellular Therapy position statement. Cytotherapy. 2006;8(4):315-7.

34. Cristancho AG, Lazar MA. Forming functional fat: a growing understanding of adipocyte differentiation. Nat Rev Mol Cell Biol. 2011;12(11):722-34.

35. Sarjeant K, Stephens JM. Adipogenesis. Cold Spring Harb Perspect Biol. 2012;4(9):a008417.

36. Park A, Kim WK, Bae KH. Distinction of white, beige and brown adipocytes derived from mesenchymal stem cells. World J Stem Cells. 2014;6(1):33-42.

37. Ali AT, Hochfeld WE, Myburgh R, Pepper MS. Adipocyte and adipogenesis. Eur J Cell Biol. 2013;92(6-7):229-36.

38. Kuryszko J, Slawuta P, Sapikowski G. Secretory function of adipose tissue. Pol J Vet Sci. 2016;19(2):441-6.

39. Kokai LE, Marra K, Rubin JP. Adipose stem cells: biology and clinical applications for tissue repair and regeneration. Transl Res. 2014;163(4):399-408.

40. Ikeda K, Maretich P, Kajimura S. The Common and Distinct Features of Brown and Beige Adipocytes. Trends Endocrinol Metab. 2018;29(3):191-200.

41. Fedorenko A, Lishko PV, Kirichok Y. Mechanism of fatty-acid-dependent UCP1 uncoupling in brown fat mitochondria. Cell. 2012;151(2):400-13.

42. Wu J, Bostrom P, Sparks LM, Ye L, Choi JH, Giang AH, et al. Beige adipocytes are a distinct type of thermogenic fat cell in mouse and human. Cell. 2012;150(2):366-76.

43. Peirce V, Carobbio S, Vidal-Puig A. The different shades of fat. Nature. 2014;510(7503):76-83.

44. Seale P, Conroe HM, Estall J, Kajimura S, Frontini A, Ishibashi J, et al. Prdm16 determines the thermogenic program of subcutaneous white adipose tissue in mice. J Clin Invest. 2011;121(1):96-105.

45. Ramakrishnan VM, Boyd NL. The Adipose Stromal Vascular Fraction as a Complex Cellular Source for Tissue Engineering Applications. Tissue Eng Part B Rev. 2018;24(4):289-99.

46. Bourin P, Bunnell BA, Casteilla L, Dominici M, Katz AJ, March KL, et al. Stromal cells from the adipose tissue-derived stromal vascular fraction and culture expanded adipose tissue-derived stromal/stem cells: a joint statement of the International Federation for Adipose Therapeutics and Science (IFATS) and the International Society for Cellular Therapy (ISCT). Cytotherapy. 2013;15(6):641-8.

47. Zuk PA, Zhu M, Mizuno H, Huang J, Futrell JW, Katz AJ, et al. Multilineage cells from human adipose tissue: implications for cell-based therapies. Tissue Eng. 2001;7(2):211-28.

48. Watson ND, R.; Kedar, R.; Mehindru, A.; Mehindru, A.; Borlogan, M. Discarded Wharton's Jelly of the Human Umbilical Cord: A Viable Source for Mesenchymal Stem Cells Cytotherapy. 2015;17(1):14.

49. Batsali AK, Kastrinaki MC, Papadaki HA, Pontikoglou C. Mesenchymal stem cells derived from Wharton's Jelly of the umbilical cord: biological properties

and emerging clinical applications. Curr Stem Cell Res Ther. 2013;8(2):144-55.

50.   McElreavey KD, Irvine AI, Ennis KT, McLean WH. Isolation, culture and characterisation of fibroblast-like cells derived from the Wharton's jelly portion of human umbilical cord. Biochem Soc Trans. 1991;19(1):29S.

51.   Ishige I, Nagamura-Inoue T, Honda MJ, Harnprasopwat R, Kido M, Sugimoto M, et al. Comparison of mesenchymal stem cells derived from arterial, venous, and Wharton's jelly explants of human umbilical cord. Int J Hematol. 2009;90(2):261-9.

52.   Hu L, Hu J, Zhao J, Liu J, Ouyang W, Yang C, et al. Side-by-side comparison of the biological characteristics of human umbilical cord and adipose tissue-derived mesenchymal stem cells. Biomed Res Int. 2013;2013:438243.

53.   Kim JH, Jo CH, Kim HR, Hwang YI. Comparison of Immunological Characteristics of Mesenchymal Stem Cells from the Periodontal Ligament, Umbilical Cord, and Adipose Tissue. Stem Cells Int. 2018;2018:8429042.

54.   Pierdomenico LL, P.; Latchmann, R.; Grifone, G.; Cianci, E.; Gialo, L.; Pacella, S.; Romano, M.; Vitacolonna, E.; Miscia, S. and Marchisio, M. Diabetes Mellitus During Pregnancy Interferes with the Biological Characteristics of Wharton's Jelly Mesenchymal Stem Cells. The Open Tissue Engineering and Regenerative Medicine Journal. 2011;4:103-11.

55.   Ragni E, Vigano M, Parazzi V, Montemurro T, Montelatici E, Lavazza C, et al. Adipogenic potential in human mesenchymal stem cells strictly depends on adult or foetal tissue harvest. Int J Biochem Cell Biol. 2013;45(11):2456-66.

56.   Amable PR, Teixeira MV, Carias RB, Granjeiro JM, Borojevic R. Gene expression and protein secretion during human mesenchymal cell differentiation into adipogenic cells. BMC Cell Biol. 2014;15:46.

57.   Tang QQ, Otto TC, Lane MD. Mitotic clonal expansion: a synchronous process required for adipogenesis. Proc Natl Acad Sci U S A. 2003;100(1):44-9.

58.   Cornelius P, MacDougald OA, Lane MD. Regulation of adipocyte development. Annu Rev Nutr. 1994;14:99-129.

59.   Moreno-Navarrete JaF-R, JM. Adipocyte Differentiation. In: Symonds M, editor. Adipose Tissue Biology. New York: Springer; 2012. p. 17-38.

60. Gregoire FM, Smas CM, Sul HS. Understanding adipocyte differentiation. Physiol Rev. 1998;78(3):783-809.

61. Rosen ED, Sarraf P, Troy AE, Bradwin G, Moore K, Milstone DS, et al. PPAR gamma is required for the differentiation of adipose tissue in vivo and in vitro. Mol Cell. 1999;4(4):611-7.

62. Rosen ED, Walkey CJ, Puigserver P, Spiegelman BM. Transcriptional regulation of adipogenesis. Genes Dev. 2000;14(11):1293-307.

63. Poulos SP, Dodson MV, Culver MF, Hausman GJ. The increasingly complex regulation of adipocyte differentiation. Exp Biol Med (Maywood). 2016;241(5):449-56.

64. Boney CM, Fiedorek FT, Jr., Paul SR, Gruppuso PA. Regulation of preadipocyte factor-1 gene expression during 3T3-L1 cell differentiation. Endocrinology. 1996;137(7):2923-8.

65. Garces C, Ruiz-Hidalgo MJ, Bonvini E, Goldstein J, Laborda J. Adipocyte differentiation is modulated by secreted delta-like (dlk) variants and requires the expression of membrane-associated dlk. Differentiation. 1999;64(2):103-14.

66. Hudak CS, Sul HS. Pref-1, a gatekeeper of adipogenesis. Front Endocrinol (Lausanne). 2013;4:79.

67. Smas CM, Sul HS. Characterization of Pref-1 and its inhibitory role in adipocyte differentiation. Int J Obes Relat Metab Disord. 1996;20 Suppl 3:S65-72.

68. Evans RM, Barish GD, Wang YX. PPARs and the complex journey to obesity. Nat Med. 2004;10(4):355-61.

69. Ahmadian M, Suh JM, Hah N, Liddle C, Atkins AR, Downes M, et al. PPARgamma signaling and metabolism: the good, the bad and the future. Nat Med. 2013;19(5):557-66.

70. Lefterova MI, Haakonsson AK, Lazar MA, Mandrup S. PPARgamma and the global map of adipogenesis and beyond. Trends Endocrinol Metab. 2014;25(6):293-302.

71. Janani C, Ranjitha Kumari BD. PPAR gamma gene--a review. Diabetes Metab Syndr. 2015;9(1):46-50.

72. Lefterova MI, Lazar MA. New developments in adipogenesis. Trends Endocrinol Metab. 2009;20(3):107-14.

73. Wang Q, Tang J, Jiang S, Huang Z, Song A, Hou S, et al. Inhibition of PPARgamma, adipogenesis and insulin sensitivity by MAGED1. J Endocrinol. 2018.

74. Rosen ED, MacDougald OA. Adipocyte differentiation from the inside out. Nat Rev Mol Cell Biol. 2006;7(12):885-96.

75. Lekstrom-Himes J, Xanthopoulos KG. Biological role of the CCAAT/enhancer-binding protein family of transcription factors. J Biol Chem. 1998;273(44):28545-8.

76. Tang QQ, Lane MD. Adipogenesis: from stem cell to adipocyte. Annu Rev Biochem. 2012;81:715-36.

77. Guo L, Li X, Tang QQ. Transcriptional regulation of adipocyte differentiation: a central role for CCAAT/enhancer-binding protein (C/EBP) beta. J Biol Chem. 2015;290(2):755-61.

78. Onesti S, MacNeill SA. Structure and evolutionary origins of the CMG complex. Chromosoma. 2013;122(1-2):47-53.

79. Wu Z, Wang S. Role of kruppel-like transcription factors in adipogenesis. Dev Biol. 2013;373(2):235-43.

80. Birsoy K, Chen Z, Friedman J. Transcriptional regulation of adipogenesis by KLF4. Cell Metab. 2008;7(4):339-47.

81. Oishi Y, Manabe I, Tobe K, Tsushima K, Shindo T, Fujiu K, et al. Kruppel-like transcription factor KLF5 is a key regulator of adipocyte differentiation. Cell Metab. 2005;1(1):27-39.

82. Li D, Yea S, Li S, Chen Z, Narla G, Banck M, et al. Kruppel-like factor-6 promotes preadipocyte differentiation through histone deacetylase 3-dependent repression of DLK1. J Biol Chem. 2005;280(29):26941-52.

83. Pei H, Yao Y, Yang Y, Liao K, Wu JR. Kruppel-like factor KLF9 regulates PPARgamma transactivation at the middle stage of adipogenesis. Cell Death Differ. 2011;18(2):315-27.

84. Wu J, Srinivasan SV, Neumann JC, Lingrel JB. The KLF2 transcription factor does not affect the formation of preadipocytes but inhibits their differentiation into adipocytes. Biochemistry. 2005;44(33):11098-105.

85. Zhang K, Guo W, Yang Y, Wu J. JAK2/STAT3 pathway is involved in the early stage of adipogenesis through regulating C/EBPbeta transcription. J Cell Biochem. 2011;112(2):488-97.

86. Siersbaek R, Nielsen R, Mandrup S. Transcriptional networks and chromatin remodeling controlling adipogenesis. Trends Endocrinol Metab. 2012;23(2):56-64.

87. Tong Q, Dalgin G, Xu H, Ting CN, Leiden JM, Hotamisligil GS. Function of GATA transcription factors in preadipocyte-adipocyte transition. Science. 2000;290(5489):134-8.

88. Tong Q, Tsai J, Tan G, Dalgin G, Hotamisligil GS. Interaction between GATA and the C/EBP family of transcription factors is critical in GATA-mediated suppression of adipocyte differentiation. Mol Cell Biol. 2005;25(2):706-15.

89. Moon YS, Smas CM, Lee K, Villena JA, Kim KH, Yun EJ, et al. Mice lacking paternally expressed Pref-1/Dlk1 display growth retardation and accelerated adiposity. Mol Cell Biol. 2002;22(15):5585-92.

90. Helman LJ, Sack N, Plon SE, Israel MA. The sequence of an adrenal specific human cDNA, pG2. Nucleic Acids Res. 1990;18(3):685.

91. Helman LJ, Thiele CJ, Linehan WM, Nelkin BD, Baylin SB, Israel MA. Molecular markers of neuroendocrine development and evidence of environmental regulation. Proc Natl Acad Sci U S A. 1987;84(8):2336-9.

92. Fay TN, Jacobs I, Teisner B, Poulsen O, Chapman MG, Stabile I, et al. Two fetal antigens (FA-1 and FA-2) and endometrial proteins (PP12 and PP14) isolated from amniotic fluid; preliminary observations in fetal and maternal tissues. Eur J Obstet Gynecol Reprod Biol. 1988;29(1):73-85.

93. Laborda J, Sausville EA, Hoffman T, Notario V. dlk, a putative mammalian homeotic gene differentially expressed in small cell lung carcinoma and neuroendocrine tumor cell line. J Biol Chem. 1993;268(6):3817-20.

94. Smas CM, Sul HS. Pref-1, a protein containing EGF-like repeats, inhibits adipocyte differentiation. Cell. 1993;73(4):725-34.

95. Lee YL, Helman L, Hoffman T, Laborda J. dlk, pG2 and Pref-1 mRNAs encode similar proteins belonging to the EGF-like superfamily. Identification of polymorphic variants of this RNA. Biochim Biophys Acta. 1995;1261(2):223-32.

96. Jensen CH, Krogh TN, Hojrup P, Clausen PP, Skjodt K, Larsson LI, et al. Protein structure of fetal antigen 1 (FA1). A novel circulating human epidermal-growth-factor-like protein expressed in neuroendocrine tumors and

its relation to the gene products of dlk and pG2. Eur J Biochem. 1994;225(1):83-92.

97. Smas CM, Green D, Sul HS. Structural characterization and alternate splicing of the gene encoding the preadipocyte EGF-like protein pref-1. Biochemistry. 1994;33(31):9257-65.

98. Sul HS. Minireview: Pref-1: role in adipogenesis and mesenchymal cell fate. Mol Endocrinol. 2009;23(11):1717-25.

99. Wang Y, Kim KA, Kim JH, Sul HS. Pref-1, a preadipocyte secreted factor that inhibits adipogenesis. J Nutr. 2006;136(12):2953-6.

100. Kopan R, Ilagan MX. The canonical Notch signaling pathway: unfolding the activation mechanism. Cell. 2009;137(2):216-33.

101. Smas CM, Chen L, Sul HS. Cleavage of membrane-associated pref-1 generates a soluble inhibitor of adipocyte differentiation. Mol Cell Biol. 1997;17(2):977-88.

102. Wang Y, Sul HS. Ectodomain shedding of preadipocyte factor 1 (Pref-1) by tumor necrosis factor alpha converting enzyme (TACE) and inhibition of adipocyte differentiation. Mol Cell Biol. 2006;26(14):5421-35.

103. Mei B, Zhao L, Chen L, Sul HS. Only the large soluble form of preadipocyte factor-1 (Pref-1), but not the small soluble and membrane forms, inhibits adipocyte differentiation: role of alternative splicing. Biochem J. 2002;364(Pt 1):137-44.

104. Jing K, Heo JY, Song KS, Seo KS, Park JH, Kim JS, et al. Expression regulation and function of Pref-1 during adipogenesis of human mesenchymal stem cells (MSCs). Biochim Biophys Acta. 2009;1791(8):816-26.

105. Smas CM, Chen L, Zhao L, Latasa MJ, Sul HS. Transcriptional repression of pref-1 by glucocorticoids promotes 3T3-L1 adipocyte differentiation. J Biol Chem. 1999;274(18):12632-41.

106. Bost F, Aouadi M, Caron L, Binetruy B. The role of MAPKs in adipocyte differentiation and obesity. Biochimie. 2005;87(1):51-6.

107. Gehart H, Kumpf S, Ittner A, Ricci R. MAPK signalling in cellular metabolism: stress or wellness? EMBO Rep. 2010;11(11):834-40.

108. Kim KA, Kim JH, Wang Y, Sul HS. Pref-1 (preadipocyte factor 1) activates the MEK/extracellular signal-regulated kinase pathway to inhibit adipocyte differentiation. Mol Cell Biol. 2007;27(6):2294-308.

109. Wang Y, Sul HS. Pref-1 regulates mesenchymal cell commitment and differentiation through Sox9. Cell Metab. 2009;9(3):287-302.

110. Wang Y, Zhao L, Smas C, Sul HS. Pref-1 interacts with fibronectin to inhibit adipocyte differentiation. Mol Cell Biol. 2010;30(14):3480-92.

111. Zhang H, Noohr J, Jensen CH, Petersen RK, Bachmann E, Teisner B, et al. Insulin-like growth factor-1/insulin bypasses Pref-1/FA1-mediated inhibition of adipocyte differentiation. J Biol Chem. 2003;278(23):20906-14.

112. Ruiz-Hidalgo MJ, Gubina E, Tull L, Baladron V, Laborda J. dlk modulates mitogen-activated protein kinase signaling to allow or prevent differentiation. Exp Cell Res. 2002;274(2):178-88.

113. Nueda ML, Baladron V, Sanchez-Solana B, Ballesteros MA, Laborda J. The EGF-like protein dlk1 inhibits notch signaling and potentiates adipogenesis of mesenchymal cells. J Mol Biol. 2007;367(5):1281-93.

114. Nueda ML, Gonzalez-Gomez MJ, Rodriguez-Cano MM, Monsalve EM, Diaz-Guerra MJM, Sanchez-Solana B, et al. DLK proteins modulate NOTCH signaling to influence a brown or white 3T3-L1 adipocyte fate. Sci Rep. 2018;8(1):16923.

115. Falix FA, Aronson DC, Lamers WH, Gaemers IC. Possible roles of DLK1 in the Notch pathway during development and disease. Biochim Biophys Acta. 2012;1822(6):988-95.

116. Bray SJ, Takada S, Harrison E, Shen SC, Ferguson-Smith AC. The atypical mammalian ligand Delta-like homologue 1 (Dlk1) can regulate Notch signalling in Drosophila. BMC Dev Biol. 2008;8:11.

117. Komatsu H, Chao MY, Larkins-Ford J, Corkins ME, Somers GA, Tucey T, et al. OSM-11 facilitates LIN-12 Notch signaling during Caenorhabditis elegans vulval development. PLoS Biol. 2008;6(8):e196.

Chapter 3: Isolation, Expansion and Characterisation of hMSCs

3.1 Introduction

Human derived multipotent mesenchymal stromal/stem cells (hMSCs) can be obtained from various sources, such as adipose tissue, bone marrow, embryonic tissue, skin, liver and spleen amongst many others. Bone marrow and adipose tissue are the most common sources from which hMSCs are isolated (1-6). However, in terms of avoiding ethical and moral concerns, it is easier to isolate hMSCs from tissue that is generally regarded as medical/biological waste. This would include pre-natal tissue which is discarded after birth such as the umbilical cord and umbilical cord blood as well as adipose tissue obtained from patients undergoing liposuction and abdominoplasty procedures (7). For this reason, adipose tissue and umbilical cord were the chosen tissue sources from which hMSCs were isolated in the study.

3.1.1 Isolation and characterization of adipose derived MSCs

Stromal vascular fraction (SVF) refers to the cellular fraction, excluding mature adipocytes, of adipose tissue and contains a heterogeneous population of cells including adipose-derived stromal cells (ASCs), erythrocytes, endothelial cells, lymphocytes, fibroblasts, adipose tissue-associated macrophages and others (8). hASCs are only a small sub-fraction of cells in the highly heterogeneous SVF. In order to obtain a more homogenous population of hASCs, a number of culturing and washing steps are required.

Human derived adipose mesenchymal stromal/stem cells (hASCs) were first isolated by Zuk and colleagues in 2001 (9). There is no specific single marker to identify hASCs (10). We use a panel of seven markers to phenotype the ASCs isolated. These markers include CD34, CD36, CD44, CD45, CD73, CD90 and CD105. The use of these markers are in line with the recommendations set by the ISCT and IFATS (section 2.3.1) (8).

3.1.2 Isolation and characterization of human derived Wharton's jelly MSCs

Wharton's Jelly is becoming a popular source for hMSC isolation (12). It can be defined as a gelatinous/mucous connective tissue that protects the umbilical cord vessels (12, 13). The cells isolated from the Wharton's Jelly displays similar phenotypic markers to BM-hMSCs and hASCs but also express a number of embryonic stem cell markers such as NANOG, DNMT3B and GABRB3 (1, 14, 15). As with hASCs, enzymatic digestion can be used to isolate Wharton's Jelly derived stromal/stem cells (hWJSCs) but the cells can also be isolated by means of explant. Both methods result in the successful isolation of hMSCs with the same morphological and phenotypic characteristics (16-19). For this study, the explant method was chosen as it is the simplest and most economically efficient (17).

3.2 Techniques

Flow cytometry was the main technique used in this chapter, mainly for the phenotypic characterization of isolated cells. Flow cytometry can be described as a technique used to analyse physical characteristics of particles, mostly cells, as they flow in suspension past a light source (20, 21). Size, granularity and fluorescent features of cells which have been stained with dyes or fluorescent probes are some of the parameters which can be analysed using flow cytometry (21, 22). A flow cytometer is comprised of four important components: (i) a fluidics system which aligns the cells to flow past a light source in single file by means of hydrodynamic focussing, (ii) an optical system which is responsible for exciting the fluorescent markers and capturing the emitted signal, (iii) an electronic component that converts the captured light signals into electronic pulses and lastly (iv) a computer for analysing the data (21).

The underlying principle behind this powerful technique is the scattering of light and detection of fluorescence emitted by individual cells. Light scatter is a non-fluorescence signal generated from laser light scattering once it hits the particle to be analysed. Light scatter can be used to measure parameters such as cell size and granularity. There are two types of light scatter i.e. forward and side scatter. Traditionally, forward scatter was seen as an indicator of relative cell size, while side

scatter was viewed as a sensitive indicator to distinguish cells according to their morphological complexity. However, current views are that both side and forward scatter are indicators for cell size (23). However, side scatter remains a more sensitive indicator of cellular complexity. On the other hand, intensity of fluorescence signal detected is a measure of the amount of fluorescence probe bound to a single cell (20, 21). The signals detected are then converted to a data point which can be visualized on a one parameter or a two parameter plot. A typical one parameter plot (histogram) displays the fluorescence intensity of the signal detected on the X-axis. The counts on the y-axis represent the maximum number of events captured in the channel that accumulated the most events (Figure 3.1 C). The area under the histogram peak(s) represents the total number of events acquired. Two parameter plots measure one parameter on each axis. A two-parameter plot can be divided into four quadrants displaying measurements of cell populations that are positive for both parameters, negative for both parameters, or positive for only one of the parameters. (Figure 3.2) (21).
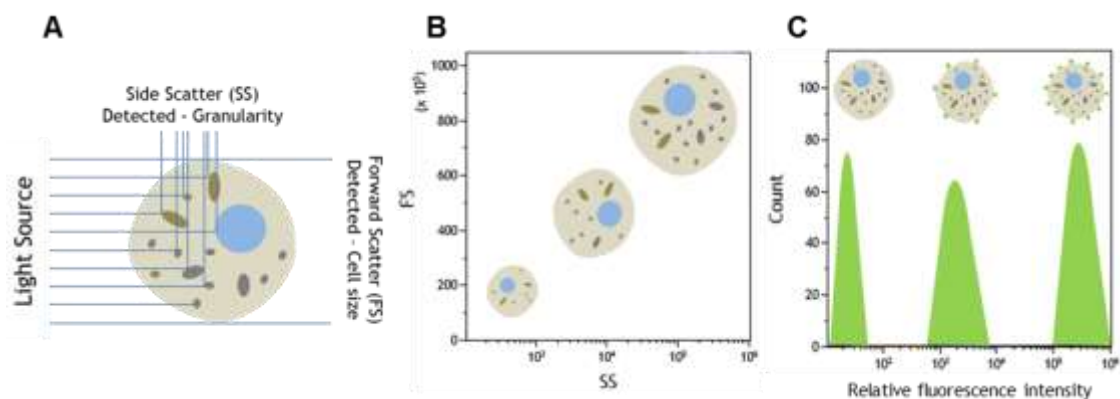
Figure 3.1: Schematic illustration of how flow cytometry makes use of scattered light and fluorescence to measure different parameters. A. Schematic representation of a cell moving through a flow cytometer. Side scatter is generally a measure of cell complexity/granularity while forward scatter is used for relative cell size determination. **B.** A plot measuring two parameters – forward scatter on Y-axis and side scatter on X-axis. C. A plot measuring one parameter (relative fluorescence intensity). When cells are stained with a fluorescent probe such as an antibody conjugated to a fluorescent marker, the more antibodies bound to the cell the greater the fluorescent signal emitted will be (signal shifts to the right).
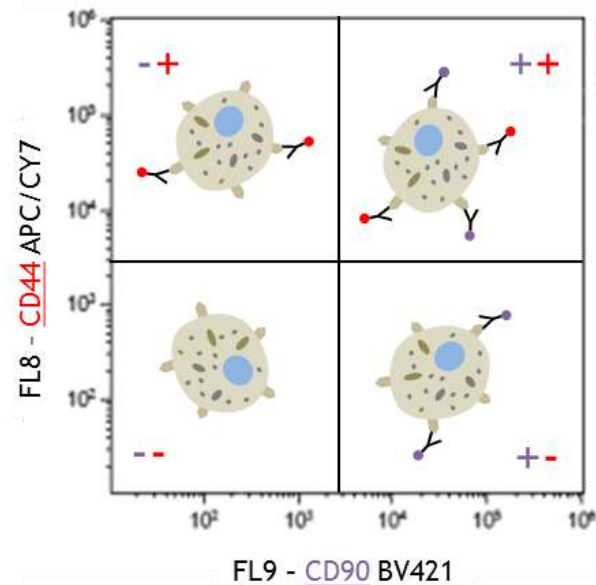
Figure 3.2: Two parameter plot interpretation. A two parameter plot can be divided into four quadrants, each quadrant displaying a different combination of the two parameters being measured. **--** = CD90-/CD44-; **-+** = CD90-/CD44+; **++** = CD90+/CD44+; **+-** = CD90+/CD44-

An important factor to be considered when more than one parameter is being measured simultaneously, such as the detection of two cell surface markers as shown in Figure 3.2, is the selection of appropriate fluorescent probes which will not interfere with one another. Fluorescent compounds are excited at specific wavelengths and emit a fluorescent signal at a longer wavelength, a concept known as stokes shift (21). It is therefore essential to ensure that the instrument being used has a laser capable of exciting the fluorophore at the correct wavelength as well as equipped with the correct detectors to capture the emitted signal. For example, two fluorescent compounds with very similar/overlapping excitation and emission spectra cannot be placed together as it will be very difficult to distinguish between the two signals. However, when there is only a small degree of spectral overlap, compensation can be used to remove signal that has "spilled over" into unwanted channels (24). Compensation can be defined as the process of removing signal from all detectors with exception to the detector where the signal is captured with maximum efficiency (optimal detection filter) (25).

Another essential factor to consider when performing flow cytometry is the use of controls – set up controls, specificity controls and biological controls. Set up controls are used to ensure that the instrument is set up correctly, specificity controls are

used to distinguish between non-specific and specific binding and biological controls are used to determine the difference between experimental conditions (26).

In this study the following controls were implemented for the phenotyping of the cells: Flow cytometer alignment verification fluorophores (Flow-Check™ Pro; Beckman Coulter, Miami, USA) were used as a set up control to verify laser alignment and ensure fluidic stability. Unstained cells were a second form of set up control as they were used to set up the regions in which the negative signals should appear. It is important to note that the use of unstained cells does not control for non-specific binding of monoclonal antibodies. And lastly, untreated cells (referred to as non-induced cells) were used as biological controls.

3.3 Methods

3.3.1 Sample Collection

Mesenchymal stromal/stem cells (MSCs) were isolated from two tissue sources – adipose tissue and umbilical cord. Written informed consent was obtained from all volunteers prior to sample collection (Annex C). Adipose tissue samples were collected by medical practitioners from patients undergoing liposuction and abdominoplasty procedures at Netcare Unitas Hospital, Pretoria. Umbilical cord samples were collected from volunteer mothers during term deliveries by gynaecologists based at Netcare Femina Hospital, Pretoria. Ethics approval for this study was obtained from the Research Ethics Committee of the Faculty of Health Sciences, University of Pretoria (protocol number 206/2016) as well as from Netcare Research Operations Committee (approval number UNIV-2016-0042).

3.3.1.1 Patient selection criteria

In order to be considered for the study, patients had to give their written informed consent for the collection and use of their tissue samples. In addition, only patients with a negative HIV status were considered.

3.3.1.2 Sample naming

Each participant's sample was assigned a specific code in order to keep the patients identity anonymous. The samples were coded as follows: "A" denotes adipose tissue sample while "C" denotes umbilical cord sample, the letter representing the

tissue source was then followed by the date the sample was collected and processed, in the format DDMMYY. If more than one sample was collected and processed on the same day, a number representing the sample was placed after the date. An example of a sample code thus looks like A141117-01. The code indicates an adipose sample (A) collected on the 14th of November 2017 (141117) and it was the first of multiple samples isolated that day (-01).

3.3.2 Human derived mesenchymal stromal/stem cell isolation

3.3.2.1 Isolation of adipose derived stromal/stem cells

The cells were isolated using previously described methods, with slight modifications (9, 27) (Figure 3.3). The lipoaspirate samples were placed in sterile 50 mL Falcon® centrifuge tubes (Falcon® by Corning, NY, USA). Solid tissue sections were finely diced before being transferred into the falcon tubes. Falcon® tubes were filled with 25 mL of adipose tissue to which 25 mL Phosphate Buffered Saline (PBS, pH 7.4, GIBCO by Invitrogen™, Grand Island, NY, USA) supplemented with 2% (v/v) penicillin (10,000 Units/ml)-streptomycin (10,000 µg/ml) (Pen/Strep) (GIBCO by Life Technologies™, Grand Island, NY, USA) was added. Samples were then centrifuged twice at 1160 x g for 3 min in order to remove excess oil before enzymatic digestion. A 0.1% (w/v) Collagenase Type I (GIBCO by Invitrogen™, Grand Island, NY, USA) solution (0.1 g in 100 mL PBS + 2% Pen/Step) was used for the enzymatic digestion of the tissue. Samples were incubated with the 0.1% Collagenase Type I solution at 37^{0}C for approximately 45 min in a rotating incubator, with time being adjusted if needed in order to obtain full digestion of the sample. Following digestion, the samples were centrifuged at 783 x g for 5 min in order to obtain the stromal vascular fraction (SVF). Falcon® tubes were then vigorously shaken until the cell pellets were disrupted and the centrifugation step (783 x g for 5 min) repeated. A 70 µm Falcon® cell strainer (Falcon® by Corning, NY, USA) was used to remove any undigested pieces of tissue. Complete growth media consisting of DMEM (DMEM 1X + GlutaMAX™-I, GIBCO by Life Technologies™, Grand Island, NY, USA) supplemented with 10% (v/v) fetal bovine serum (FBS) (GIBCO by Invitrogen™, Grand Island, NY, USA) and 2% Pen/Strep was used to neutralize the enzymatic activity of the collagenase. The 50 mL Falcon® tubes were topped up with PBS + 2% Pen/Strep and centrifuged at 300 x g for 5 min. The cell pellet was then re-suspended in VersaLyse™ Lysing Solution (Beckman Coulter, Miami, USA) for 10

min at room temperature in order to lyse any red blood cells present. Thereafter, the 50 mL Falcon® tubes were once again topped up with PBS + 2% Pen/Strep and the centrifugation step repeated (300 x g for 5 min) two more times. If red blood cell contamination persisted in the resulting cell pellet, the VersaLyse[TM] Lysing Solution step was repeated. The cell pellet, known as the stromal vascular fraction (SVF), was re-suspended in complete growth media and once again passed through a 70 µm Falcon® cell strainer. The cells were then counted on a Gallios (10 colour, 3 laser configuration) flow cytometer (Beckman Coulter, Miami, USA). In order to perform the cell count, 100 µL of cell suspension was stained with 2 µL of Vybrant® DyeCycle[TM] (VDC) Ruby (Life Technologies[TM], New York, USA) followed by the addition of 100 µL of Flow-Count™ Fluorosphores (Beckman Coulter, Miami, USA). Vybrant® DyeCycle[TM] Ruby is a cell membrane-permeable DNA stain that allows for the exclusion of non-nucleated cells (i.e. red blood cells) in the cell count. After absolute cell count was determined, cells were plated in 75 cm^2 flasks (Greiner Bio-One, Frickenhausen, Germany) at a density of 50 000 cells/cm^2. The cells were then incubated at 37^{0}C, 5% CO_2 for a period of 72 hours before washing off any non-adherent cells with complete growth media, resulting in an adherent heterogeneous cell population containing hASCs.
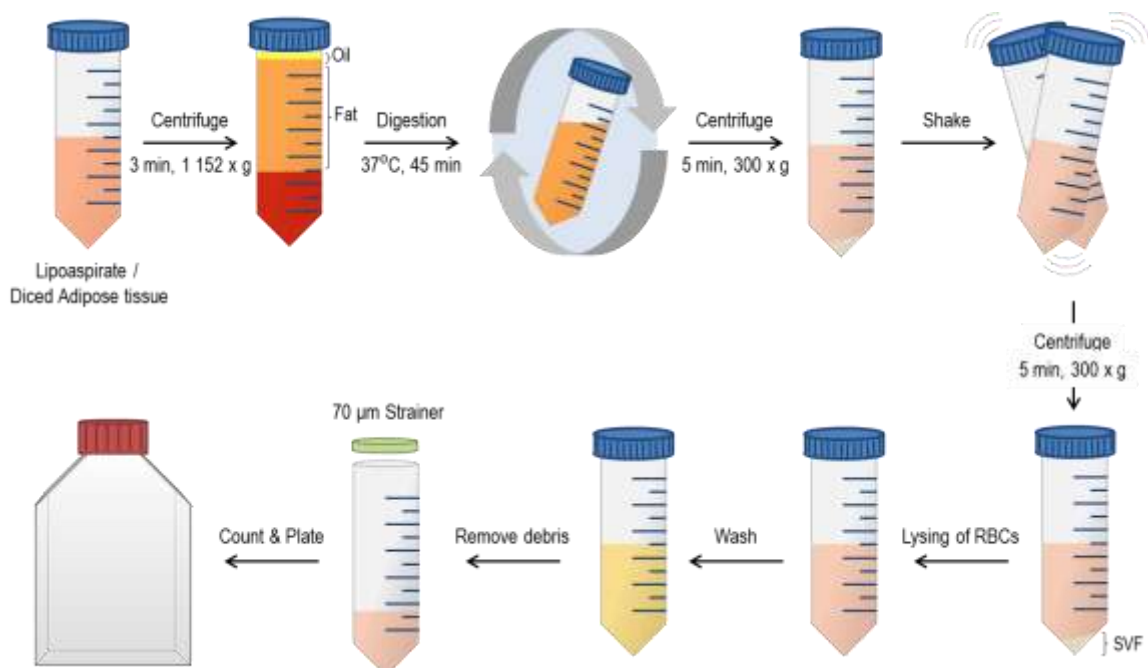
Figure 3.3: Schematic illustration of the isolation of adipose derived mesenchymal stromal/stem cells. Adipose derived stromal cells were isolated from adipose tissue samples through enzymatic digestion with collagenase.

Multiple washing steps were required in order to remove oil and contaminating red blood cells. Finally, the SVF was plated and cells maintained in complete DMEM incubated at 37^0C, 5% CO_2. SVF: stromal vascular fraction.

3.3.2.1.1 Flow cytometry setup, data acquisition and analysis

The Flow-Count[TM] fluorospheres can be detected in channels FL1, FL2, FL3 or FL4 as the fluorospheres contains a dye with a broad fluorescence emission range, ranging from 525 nm to 700 nm when excited at 488 nm. A one parameter (Count vs FL3 [Excitation: 488nm; Emission: 620/30 BP]) plot was created in order to visualise the Flow-Count[TM] fluorospheres ("BEADS" region; Figure 3.4 A). A second one parameter (FS Lin vs Time) plot was created and gated on region "BEADS" in order to identify intact fluorospheres which can be seen within the "CAL" region (Figure 3.4 B). The events which are displayed above the "CAL" region represent clumps of fluorospheres and the events displayed below the "CAL" region represent fluorospheres that disintegrated. Thus the "CAL" region only contains single intact fluorospheres. Lastly, a two parameter (SS Log vs FL7 [Excitation: 638nm; Emission: 725/20 BP]) plot was used to visualise the stained SVF cells, and a region ("Nucleated cells") created to identify cells which stained positive for VDC Ruby (Figure 3.4 C). The events excluded from the "Nucleated cells" region includes the fluorospheres which appear in red, non-nucleated fragments which appear to the left of the "Nucleated cells" region as well as cell clumps which appear to the top right of the "Nucleated cells" region. The absolute cell count was then determined using equation 1. Data analysis was performed with Kaluza Flow Cytometry Analysis Software (Version 2.1.1; Beckman Coulter, Miami, USA).

Equation 1: Absolute Cell Count

$$\text{Absolute Cell Count} = \left(\frac{\text{Number of Events in Region of interest (Nucleated Cells)}}{\text{Number of Events in the CAL region}} \times \text{CAL factor} \right)$$

"CAL factor" refers to the concentration (beads/µl) added to the sample. This information is obtained from a product information leaflet supplied with each batch of Flow Count[TM] Fluorospheres used.

Equation 2: Total Cells Harvested

$$\text{Total cells harvested} = \text{Absolute cell count} \times \text{Volume of cell suspension}$$
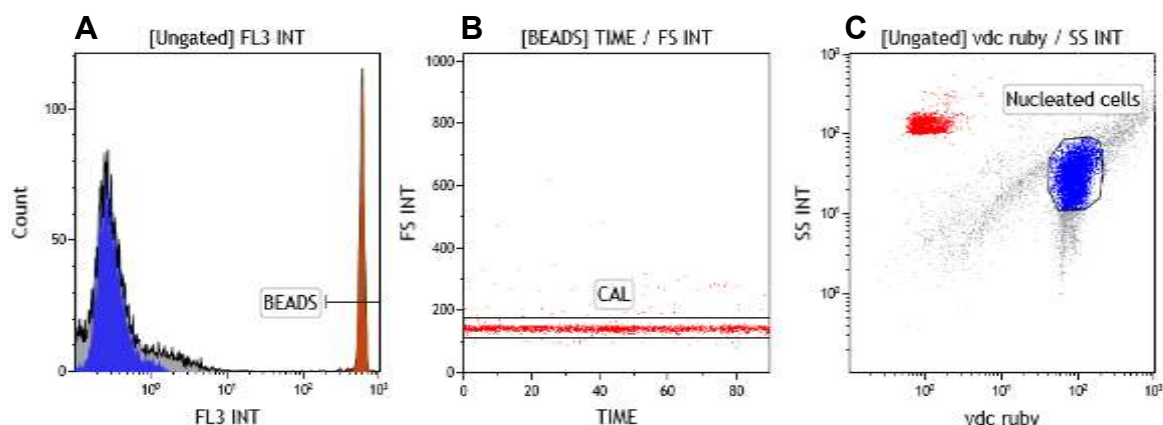
Figure 3.4: Flow cytometry gating strategy used to identify the number of nucleated cells in the SVF. Once the SVF has been obtained, a cell count was performed using Flow-Count[TM] fluorospheres (detected in FL3) and VDC Ruby (detected in FL7). Red represents Flow-Count™ fluorospheres and the blue represents the nucleated cells (VDC Ruby positive) within the stained SVF. **A:** One parameter (FL3) plot used to identify all Flow-Count beads; **B:** two-parameter plot to identify single, intact Flow-Count fluorospheres and to monitor the flow rate of Flow-Count beads during acquisition period. Flow rate should be constant throughout acquisition period; **C:** to identify and select nucleated cells

3.3.2.2 Isolation of Wharton's Jelly derived stromal/stem cells

Wharton's jelly derived MSCs (WJSCs) were isolated from umbilical cords, roughly 10 cm in length, by means of the explant method (Figure 3.5). Samples were collected in 50 mL Falcon® tubes containing complete growth medium and processed within 2 hours of collection. The cord pieces were first rinsed with PBS to remove as much blood contamination as possible. The cord was then cut lengthwise and incisions made to loosen up the tissue and expose the Wharton's Jelly to the surface of the culture dish. In order to decrease blood contamination, as much as possible of the veins/arteries within the umbilical cord were removed. The cord pieces were then placed facing down in a petri dish, complete growth media was added, and the petri dish placed in an incubator at 37^0C, 5% CO_2. Approximately 72 hours later the media was changed to remove any non-adherent cells.

Figure 3.5: Isolation of MSCs from Umbilical Cord. A. Umbilical cord samples roughly 10 cm in length were cut lengthwise and incisions made to expose the Wharton's Jelly to the surface of the cell culture dish. **B.** Veins/arteries removed from the umbilical cord.

3.3.3 Culturing and expansion of cells

Cells were cultured in complete growth medium and maintained in a 37^0C/5% CO_2 incubator. Cells were dissociated and re-plated (passaged) once they reached 90 – 100 % confluence until sufficient cell numbers ($\approx$10 x 10^6 cells) were obtained in order to plate for the various experiments detailed in Chapters 4 & 5.

3.3.3.1 Sample preparation

Once cells reached 90 – 100 % confluence, they were passaged by the addition of 0.25% trypsin-EDTA (1X, GIBCO by Life Technologies™, Grand Island, NY, USA) for 7 – 10 min at 37^0C. The enzymatic activity of the trypsin-EDTA solution was then neutralized by adding an equal volume of complete growth medium. Cells were centrifuged at 300 x g for 5 min and re-suspended in complete growth medium. Cells counts were obtained either by using the Trypan Blue exclusion assay or by flow cytometry. For the Trypan Blue exclusion assay, 20 µL of the cell suspension was stained with 20 µL Trypan Blue (Sigma, Missouri, USA) and cells counted using a haemocytometer (Figure 3.6). Total cell count was obtained by using equation 3 listed below.
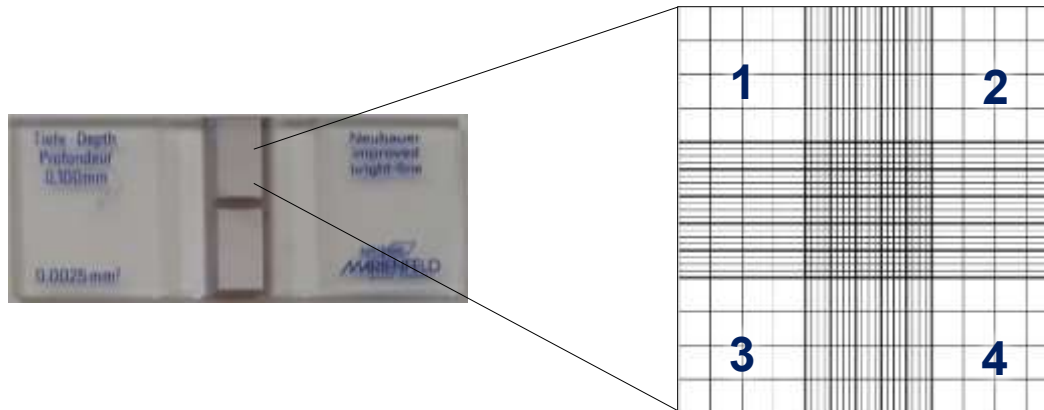
Figure 3.6: Haemocytometer and counting grid. Cells were stained with Trypan Blue and counted using a haemocytometer. Only the cells in chambers 1 – 4 were counted.

Equation 3: Manual cell count using Trypan Blue exclusion assay

$$Cells\ per\ mL = \frac{Nr.\ of\ cells\ counted\ in\ the\ 4\ chambers}{4} \times Dillution\ Factor \times 10^4$$

For cell counts using flow cytometry, a flow cytometry tube containing 50 μL or 100 μL of cell suspension and an equivalent volume of Flow-Count^{TM} fluorosphore beads was prepared. In order to determine the percentage of viable cells, 5 μL of 7-Aminoactinomycin D (7AAD) (ready-to-use solution; Beckman Coulter, Miami, USA), a DNA binding dye, was used. 7AAD is a non-membrane permeable dye that is only able to cross damaged cell membranes. Cells which stained negative for 7AAD are considered viable as it is an indication that the cell membranes are still intact. Cell count was then determined using equation 1 & 2 and cells re-plated at a density of 5 x 10^3 cells per cm^2.

3.3.3.2 Flow cytometry setup, data acquisition and analysis

The plots generated to obtain a cell counts were similar to the setup described in section 3.3.2.1.1, with the exception of using the FL1 instead of the FL3 channel to visualize the Flow-Count™ fluorospheres. As mentioned earlier in section 3.3.2.1.1, the multispectral fluorospheres can be detected in FL1, FL2, FL3 or FL4. The Flow-Count^{TM} fluorospheres were visualised on a two parameter (Count vs FL1 [Excitation: 488nm; Emission: 425/40 BP]) plot and a region "Beads" placed to identify the Flow-Count™ fluorospheres (Figure 3.7 A). Another two parameter plot

(FS Lin vs Time) was generated, gated on "Beads", and was used to identify intact Flow-Count[TM] fluorospheres within the "CAL" region (Figure 3.7 B). In order to visualise the entire cell population, excluding the fluorospheres, a Boolean gating strategy was used (A = NOT [Beads]) and a FS Lin vs SS Log plot was generated (Figure 3.7 C). This was imported as the size of the Flow-Count[TM] beads and ASCs overlapped and were therefore detected in the same particle cluster when visualized using a FS Lin vs SS Log two-parameter histogram. The Boolean gate (A) was applied post-acquisition. Lastly, in order to visualise the viable cells, a FS Lin vs FL4 Log (Excitation 488nm; Emission 695/30 BP) was generated (Figure 3.7 D). Cell count was then determined using equation 1 & 2. Data was acquired for a minimum of 1×10^4 events or for 2 min in case of low cell numbers. Data was acquired and analysed using Kaluza Flow Cytometry Analysis Software.
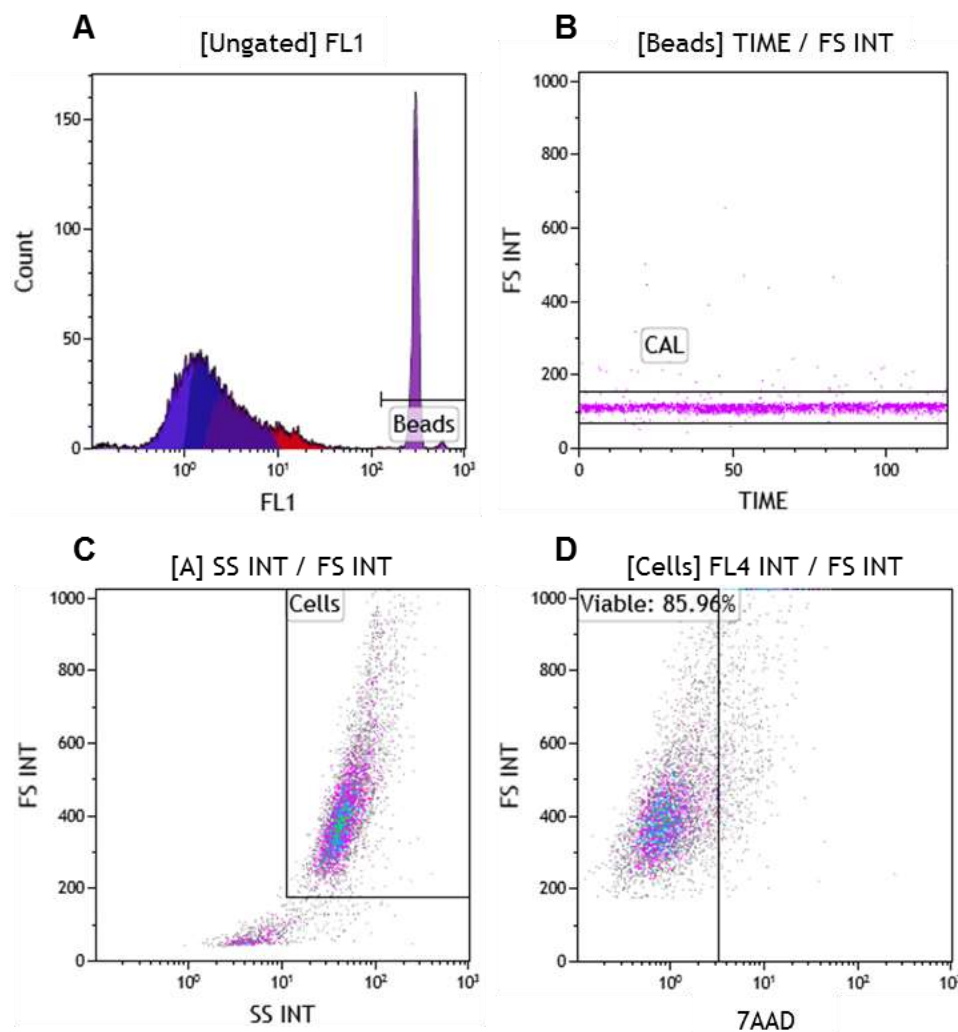
Figure 3.7: Flow cytometry gating strategy for cell counting. Once cell cultures were confluent, the cells were dissociated and re-plated. In order to obtain a cell count via flow cytometry, a flow cytometry tube was prepared with

Flow-Count^{TM} Fluorospheres (FL1; A & B) and 7-AAD (FL4; D) in order to determine viability. D: Indicates the population of viable, hMSCs ("Cells").

3.3.4 Phenotypic characterisation

Cells were induced to undergo adipogenic differentiation over a 21 day time period (details on the adipogenic differentiation can be found in Chapter 4, Section 4.3.1). Not induced cells were cultured and maintained in parallel to the induced cells to serve as controls.

Phenotypic characterisation of both non-induced and induced cells was performed by means of flow cytometry which took place at various time points during the 21 day induction period i.e. day 0, 1, 3, 7, 14 and 21. A seven colour flow cytometry panel was used to phenotypically characterize the cells. The panel comprised of the following markers: CD34 PE-CY7, CD36 APC, CD44 APC-Cy7, CD45 KO, CD73 FITC, CD90 BV421 and CD105 PE (Table 3.1). A more complete table containing additional detail can be found in Annexure A.

Table 3.1: Human MSC 7-Colour Phenotype Panel and Antibody Details

Marker	Pos / Neg	Fluorochrome	Supplier
CD 34	+/-	PE CY7	Beckman Coulter
CD 36	+	APC	Thermo Fisher Scientific
CD 44	+	APC-Cy7	Biolegend
CD 45	-	Krome Orange	Becton Dickinson
CD 73	+	FITC	eBiosciences
CD 90	+	BV421	Becton Dickinson
CD 105	+	PE	Thermo Fisher Scientific

The Pos/Neg column indicates the expected expression profiles for both hASCs and hWJSCs, respectively.

3.3.4.1 Sample preparation

Phenotyping was performed using a 100 µL aliquot of the cell suspension to which the monoclonal antibodies listed in Table 3.1 were added. Antibody and cell suspension mixture were briefly mixed and incubated for 15 min in the dark before being analysed on a Gallios flow cytometer. Data was acquired using Kaluza Flow Cytometry Data Analysis software.

3.3.4.3 Statistical analysis

A non-parametric Kruskall-Wallis test was used to compare the means between the different time points over the different experimental conditions. The significance level was set to $\alpha = 0.05$ and a p-value < 0.05 were considered statistically significant.

3.4 Results & Discussion

When isolating hMSCs for *in vitro* culturing, the resulting population of cells acquired is very heterogeneous (10, 28, 29). In addition, when isolating hMSCs from different sources, the cells may show differences in their cell surface marker expression profile and differentiation potential (10, 30).

For the purpose of this study, the respective phenotypic profiles of hASCs and hWJSCs were assessed using a seven colour flow cytometry panel (Table 3.1). The phenotype of the cells was assessed at various time points within a 21 day culture period using a series of one and two parameter plots. Individual marker expression was assessed with one parameter overlay plots (Figure 3.8), whereas co-expression was assessed using a number of two parameter plots (Figure 3.10) and two parameter overlay plots (Figure 3.11).

For the analysis of individual marker expression, all acquired events were first visualised on a forward scatter (area; FS Lin) versus side scatter (SS Log) plot. A region "Cells" was created which excluded any cell debris (Figure 3.8 A). A series of one parameter (Count vs Relative fluorescence intensity) overlay plots were used to show the shifts in expression profiles of stained cells compared to unstained cells. The grey peaks (Figure 3.8) represent the signal obtained from the unstained cells, a phenomenon known as autofluorescence. Autofluorescence refers to the natural ability of the cells to emit fluorescence due to intracellular compounds and/or organelles that emit low level of endogenous fluorescence when excited by a light source. Examples of endogenous fluorophores include riboflavins, flavin coenzymes and flavoproteins attached to mitochondria (31). Once excited, this inherent low level fluorescence is picked up by the various detectors in the flow cytometer with varying degree of efficiency. The blue peaks on the other hand represent the signal obtained from the cells that were stained with the monoclonal antibodies listed in Table 3.1. A shift to the right on the Y-axis is interpreted as an increase in relative fluorescence

intensity i.e. a positive signal, whereas no shift on the Y-axis would be interpreted as a negative signal i.e. cannot detect protein of interest. Ideally, a good separation between the unstained and stained peaks is desired for positive markers, as seen in Figure 3.8 D and F. When looking at negative markers (Figure 3.8 H), both the unstained and stained peaks should appear over one another with no observable shift in the stained sample. A small shift along the Y-axis was observed in the CD45 overlay plot which may be due to non-specific antibody binding or fluorescence spill over from neighbouring channels which cannot be compensated for (Figure 3.8 H).
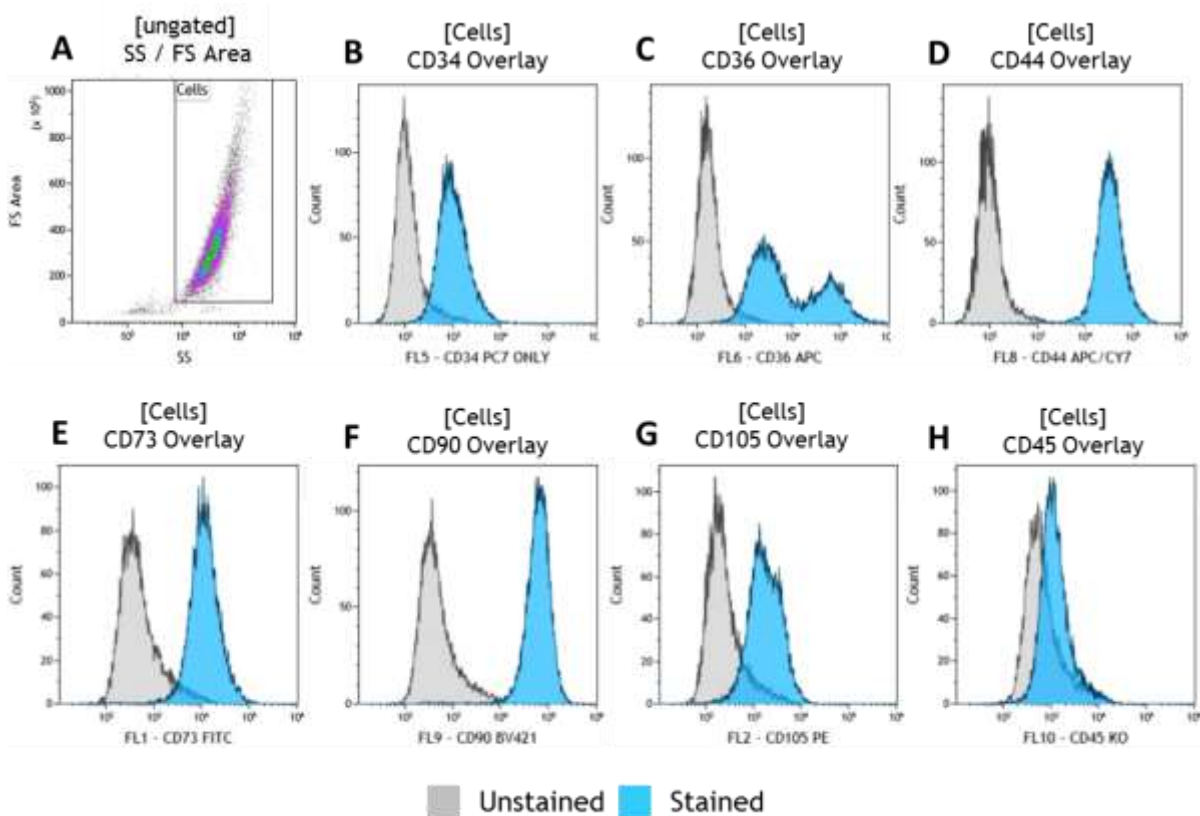
Figure 3.8: One parameter overlay plots depicting the difference between stained and unstained samples. A. Two parameter (forward scatter versus side scatter) plot displaying acquired hASCs. Gate "Cells" was used to exclude cell debris and displays the cells which are to be further analysed in plots B to H. B – H. One parameter (count versus relative fluorescence intensity) overlay plots which have been gated on region "Cells". These plots display the data acquired for the unstained cells (grey) which was overlaid with the corresponding data acquired for the stained cells (blue). A shift to the right on the Y-axis displays an increase in relative fluorescence intensity i.e. a positive signal. No or a minor shift on the Y-axis would be interpreted as a negative signal i.e. cannot detect protein of interest.

As for the analysis of simultaneous marker expression, all acquired events were first displayed on a forward scatter (cell size) height (FS Lin) versus forward scatter area (FS Lin). A region "MSCs, excluding clumps" was created in order to be able to analyse intact single MSCs only i.e. excluding any cell debris or clumps (Figure 3.10 A). As illustrated and explained by Figure 3.9 below, the events appearing below the "MSCs, excluding clumps" region represents cell clumps while the events on the bottom left of the region represent cellular debris (Figure 3.10 A).
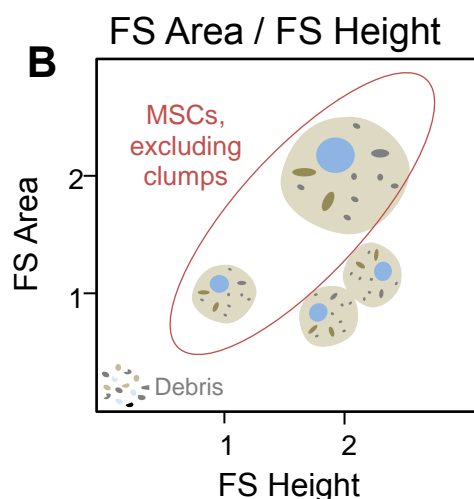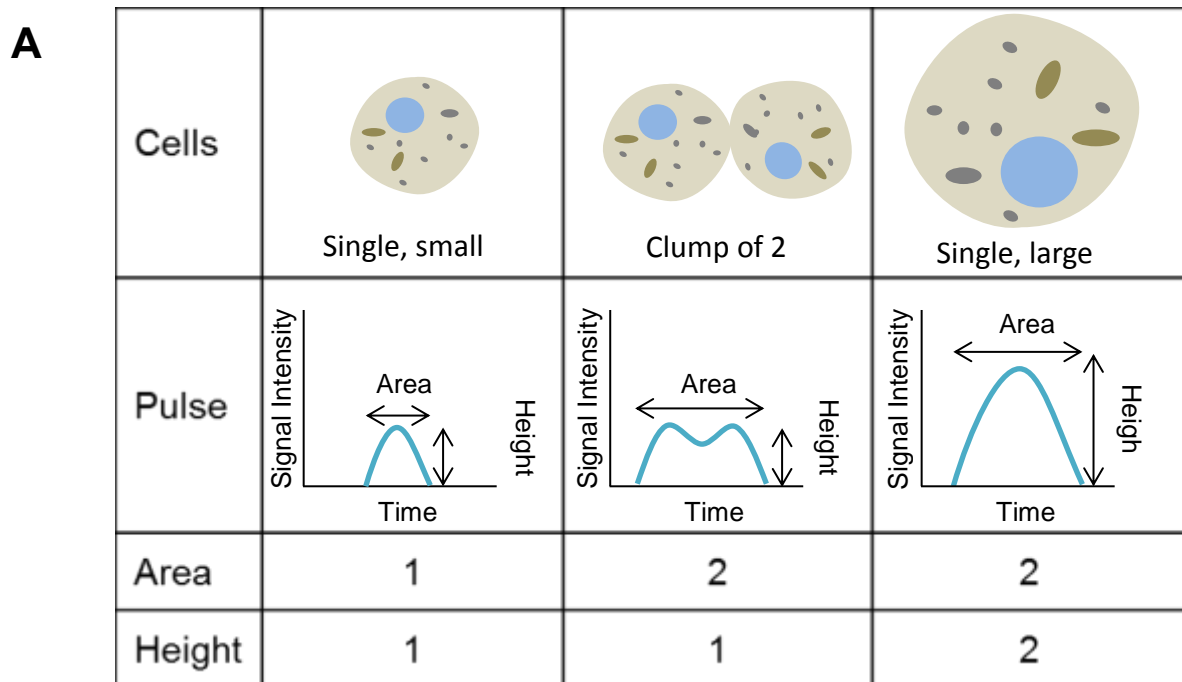
Figure 3.9: Schematic representation of how forward scatter light can be used to differentiate between single cells and clumps. As the cells in "A" pass through the flow cytometer a pulse is generated. The pulses generated can then be mapped by plotting the respective pulse heights vs pulse area (area under pulse; B).

The single-cell cell population was then displayed on a forward scatter (area; FS Lin) versus side scatter (SS Log) plot (Figure 3.10 B). The remainder of the flow cytometry two parameter plots were then gated on single, intact cells in order to determine the percentage of cells which display the MSC phenotype (Figure 3.10 C-J). Unstained cells, which only emit natural autofluorescence, were used to set up the regions in which the positive (CD44, CD73, CD90, CD105) or negative cell population (CD45) should appear (Figure 3.10 C-F). Quadrants were set based on the majority of the population (densest on the density plot) as a guide to discriminate between negative and positive staining. Some of the events were allowed to overflow in the "X++" region (Figure 3.10 C-F). This overflow is contributed to a small fraction of cells with especially high levels of autofluorescence levels. However, these events should not be viewed as true positive events. Interestingly, for reasons unknown to us, the autofluorescence tail disappeared as soon as monoclonal antibodies were added to the cells (Figure 3.11).

Plots G-J (Figure 3.10) display the signal obtained from the cells which were stained for CD34, CD36, CD44, CD45, CD73 and CD105, using the monoclonal antibodies listed in Table 3.1. A sequential gating strategy was used to determine the percentage of cells which display the MSC phenotype (CD90+, CD44+, CD105+, CD73+, CD36+, CD34 +/- and CD45-). Plot G is gated on region "MSCs". Quadrant "CD44+/CD90+" displays all cells that stain positively for CD90 and CD44. Plot H was then gated on quadrant "CD44+/CD90+", therefore all cells appearing in quadrant "CD73+/CD105+" stained positive for CD90, CD44, CD73 and CD105. Plot I is gated on quadrant "CD73+/CD105+". Thus, all cells in region "CD45-/CD90+ Cells" represent cells that are positive for CD90, CD44, CD73, CD105 and negative for CD45. Further explanation pertaining to region "CD45-/CD90+ Cells" is provided below. Lastly, plot J is gated on region "CD45-/CD90+ Cells". Consequently, quadrant "CD36+/CD34+" represents cells which display the following phenotype: CD90+/ CD44+/ CD73+/ CD105+/ CD45-/ CD34+/ CD36+. The two populations observed in this plot are representative of a CD36 dim (left) and CD36 bright (right) population.
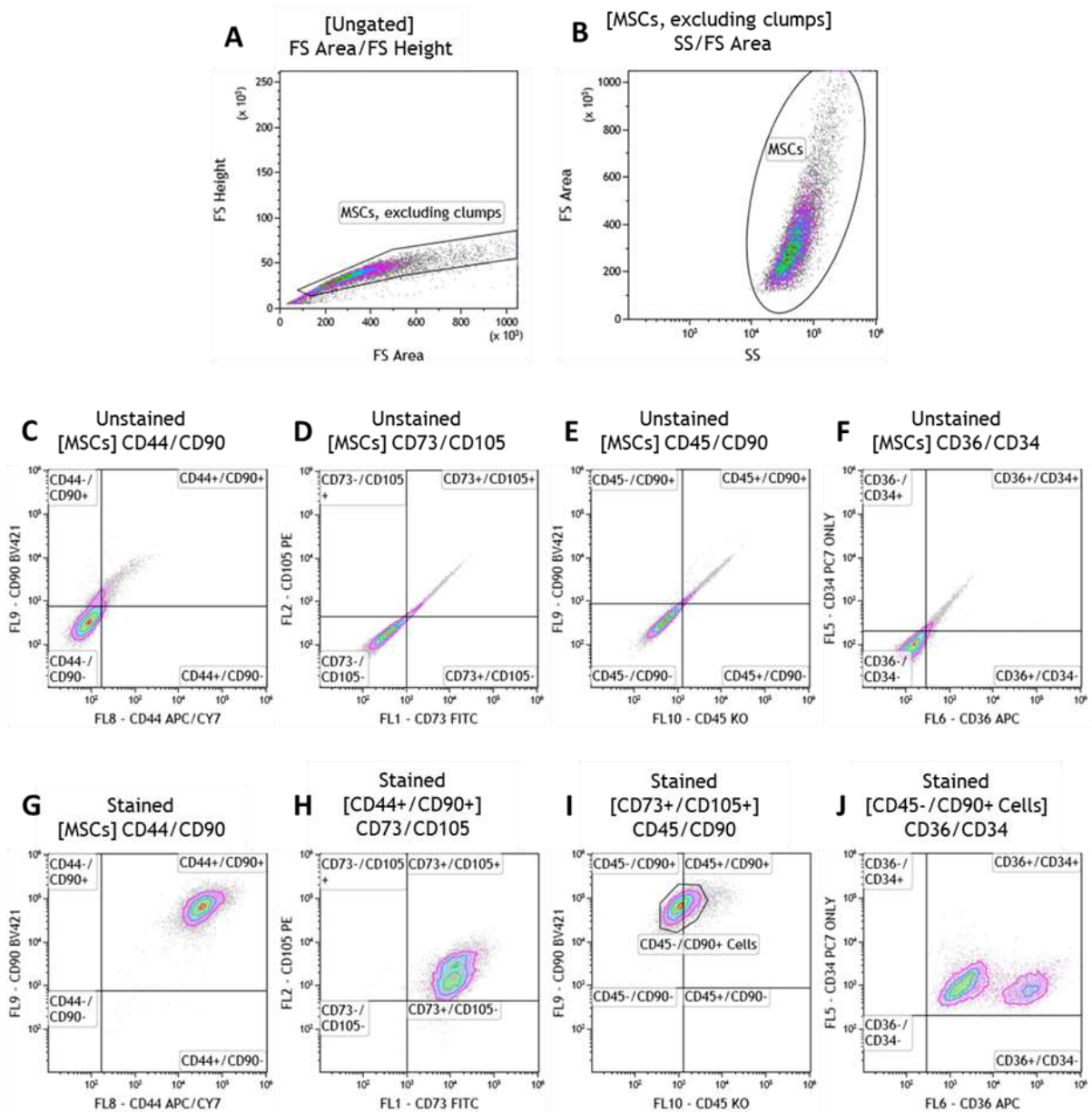
Figure 3.10: Two parameter plots depicting gating strategy used to analyse the phenotypic profile of hMSCs. A. Two parameter plot displaying all acquired events with region "MSCs, excluding clumps" created to exclude any cell debris or clumps. **B.** A two parameter plot displaying the cell population containing only single cells in region "MSCs". **C – F.** A set of two parameter plots displaying the signal detected from unstained cells. These plots are gated on region "MSCs" and are used to determine where the negative events will appear. **G – J.** A set of two parameter plots displaying the signal detected from cells that were stained for CD34, CD36, CD44, CD45, CD73 and CD105, using monoclonal antibodies. **G.** Plot G is gated on region "MSCs" displaying CD44+/CD90+ events **H.** Plot H is gated on quadrant "CD44+/CD90+", displaying CD90+/ CD44+/ CD73+/ CD105+ events. **I.** Plot I is gated on quadrant "CD73+/CD105+", displaying CD90+/ CD44+/ CD73+/ CD105+/ CD45- events. **J.**

Plot J is gated on region "CD45-/CD90+ Cells", displaying CD90+/ CD44+/ CD73+/ CD105+/ CD45-/ CD34+/ CD36+ events.
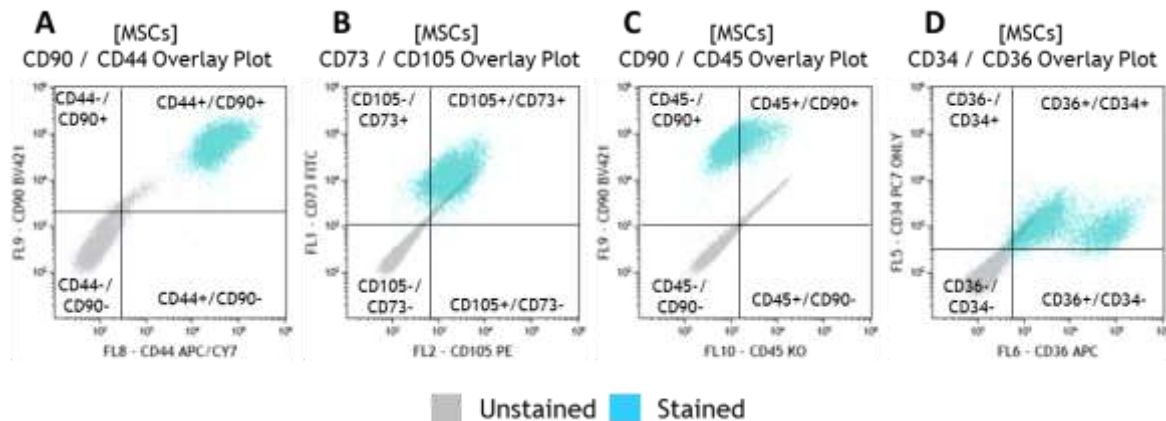
Figure 3.11: Overlay of two parameter plots depicting the difference between stained and unstained samples. A – D. Two parameter overlay plots displaying the shift observed when comparing unstained cells to stained cells. A shift upwards or to the right is representative of increased fluorescence detected and is thus interpreted as a positive signal. Blue events indicate samples stained with panel of monoclonal antibodies. Grey evens indicates unstained samples (negative staining) **A.** Two parameter plot displaying the CD90+/CD44+ population in blue. **B.** Two parameter plot displaying CD73+/ CD105+ population in blue. **C.** Two parameter plot displaying CD90+/CD45- population in blue. **D.** Two parameter plot displaying CD34+/CD36+ population in blue. (Quadrants were drawn in as software does not allow the addition of quadrants on overlay plots).

By comparing the unstained and stained cells, the overlay plots allow for a good visualisation and understanding of the data. Figure 3.8 B-G clearly shows that the cells being analysed (A150817-01 P3F0) are displaying a positive stain for markers CD34, CD36, CD44, CD73, CD90 and CD105 as the stained population (blue) shifts to the right along the Y-axis. Whereas for CD45, there is practically no shift and is therefore interpreted as a negative marker. The small shift that is observed in the overlay plot of CD45 (Figure 3.8 H) is most likely a non-specific shift caused by non-specific binding of antibodies or as a result of minor spill over from other fluorochromes used in the panel. Colour compensation adjustments aid in the removal of most, but in certain situations not all, of the interference signal from other channels. In this scenario, compensation efforts were unsuccessful in removing the nonspecific shift observed for CD45. The non-specific shift can also be seen in Figure 3.10 I and Figure 3.11 C, the shift seems more pronounced in these two

parameter plots. This is attributed to the increased sensitivity gained when using two-parameter plots. It is generally accepted that two-parameter plots are more sensitive and thus a more accurate representation of data sets.

In order to confirm that the CD45 expression was truly negative and not due to a technical artefact, hACSs were stained with a second panel of antibodies. When first designing multi-colour flow cytometry panels, it is common practice to assign bright fluorophores to weakly expressed markers and weaker fluorophores to highly expressed markers (31). However, the level of marker expression is not always known at the time the panel is set up. In this instance, the antibody used for CD90 detection was conjugated to a bright fluorophore, BV421. The antibody is thus detected in the FL9 channel, right next to the channel which is being used for CD45 detection (FL10), whose antibody is conjugated to Krome Orange. We thus have a highly expressed marker attached to a bright fluorochrome being detected right next to a weakly/not expressed marker. By rearranging the panel (which was not part of this study but was done at the end of the study) and placing a weaker fluorochrome in the FL9 detector, the nonspecific shift that was previously observed disappears. However, the phenotype data presented herein was obtained using the previous version of the phenotype panel. The new panel was introduced into our laboratory after experiments to assess the phenotypic characteristics of hASCs and hWJSCs in this study were completed. The brighter BV421 fluorochrome is now used for CD73 detection which is not expressed as abundantly as CD90, and CD90 is now detected with an antibody conjugated to a weaker fluorochrome, FITC. The minor shift observed with the previous staining panel (used in this study) disappeared, confirming that the shift observed in this study was caused by spill over from the FL9 channel which we were unable to compensate for (Figure 3.12).
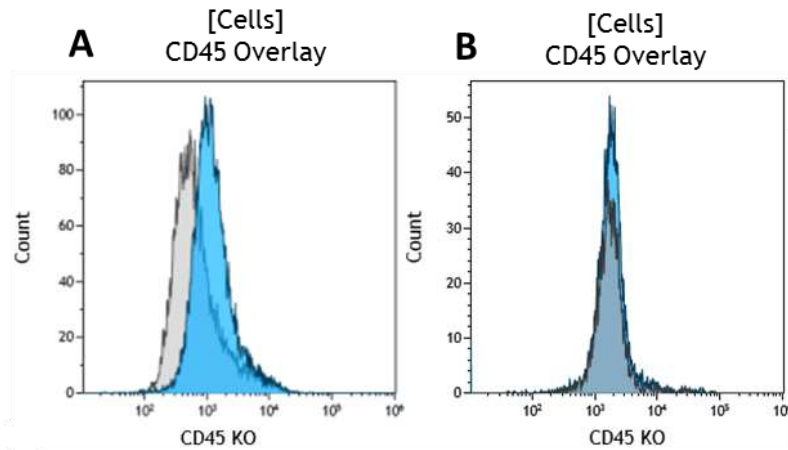
Figure 3.12: One parameter overlay plots depicting the difference between stained and unstained samples for CD45 using two different phenotype panels. Two parameter (count versus relative fluorescence intensity) plots displaying the data acquired for the unstained cells (grey) which was overlaid with the corresponding data acquired for the stained cells (blue). **A.** One parameter overlay plot for CD45 prior to modifications to the seven colour phenotype panel (contained CD90 BV421). **B.** One parameter overlay plot for CD45 after adjustments were made to the seven colour phenotype panel (CD90 changed to FITC).

Overall, the hASCs and hWJSCs displayed similar phenotypic profiles. Both cell types highly expressed CD44 and CD90. Lower levels of expression were observed for markers CD73, CD105 and CD34. The general phenotype of the cells analysed can be described as CD34, CD36, CD44, CD73, CD90 and CD105 positive and CD45 negative. The percentage hASCs and hWJSCs which adhere to the above mentioned phenotype can be found in Table 3.2 and 3.3 respectively.

Table 3.2: Percentage of hASCs that display CD34+/ CD36+/ CD44+/ CD75+/ CD90+/ CD105+/ CD45− phenotype

Time Point	A100317 P3F0		A150817-01 P3F0		A100717 P4F0		Mean ± SEM (n = 3)	
	Non-Induced	Induced	Non-Induced	Induced	Non-Induced	Induced	Non-Induced	Induced
Day 0	76.37	—	85.12	—	89.24	—	83.58±3.79	—
Day 1	77.14	80.22	91.16	89.86	91.92	91.45	86.74±4.81	87.18±3.51
Day 3	89.08	85.58	82.38	86.17	81.29	92.16	84.25±2.44	87.97±2.10
Day 7	80.66	82.48	81.02	84.84	84.56	85.65	82.08±1.25	84.32±0.95
Day 14	51.68	65.43	69.48	60.32	73.83	82.32	65.00±6.77	69.36±6.65
Day 21	43.04	49.02	61.35	59.06	79.81	74.01	61.40±10.62	60.70±7.26

Table 3.3: Percentage of hWJSCs that display CD34+/ CD36+/ CD44+/ CD75+/ CD90+/ CD105+/ CD45- phenotype

Time Point	C221116-01 P6F0		C221116-03 P7F0		C290817 P5F1		Mean ± SEM (n = 3)	
	Non-Induced	Induced	Non-Induced	Induced	Non-Induced	Induced	Non-Induced	Induced
Day 0	82.05	—	88.46	—	85.39	—	85.30±1.85	—
Day 1	86.81	89.90	84.36	82.18	85.07	89.37	85.41±0.73	87.15±2.49
Day 3	51.04	72.63	64.61	66.48	84.86	87.01	66.84±9.83	75.38±6.08
Day 7	74.77	58.47	63.80	61.77	79.62	85.88	72.73±4.68	68.71±8.64
Day 14	74.59	29.09	76.26	40.34	41.45	75.11	64.10±11.33	48.18±13.85
Day 21	NA*	NA*	80.81	4.37	47.03	41.67	63.92±13.79	26.37±18.65

NA* - Was unable to collect data for this time point

Interestingly, we observed no loss of CD34 expression in this study (Table 3.4 and 3.5). The CD34 marker was originally considered a negative marker, but it is now viewed as a variable marker during phenotypic characterisation of MSCs (10, 11). When isolating SVF, it is known that 60 – 80% of the cells are generally CD34 positive, but with extended time in culture its expression is known to decrease (8, 10, 11, 32). This may be attributed to *in vitro* culturing factors such as culture medium and cell density plated (32). In Table 3.4 and 3.5 indicate the percentage of hASCs and hWJSCs that have lost/do not express CD34. All 3 of the hASC cultures, non-induced and induced, maintained their CD34 expression throughout the 21 days in spite of the fact that the cells were already at P3 (two cultures) and P4 (one culture). As for the hWJSCs, two of the hWJSC cultures lost a considerable amount of CD34 on days 14 and 21 (Table 3.5).

Table 3.4: Percentage of hASCs that display CD34−/ CD36+/ CD44+/ CD75+/ CD90+/ CD105+/ CD45− phenotype

Time Point	A100317 P3F0		A150817-01 P3F0		A100717 P4F0		Mean ± SEM n=3	
	Non-Induced	Induced	Non-Induced	Induced	Non-Induced	Induced	Non-Induced	Induced
Day 0	3.50	—	0.07	—	0.26	—	1.28±1.11	—
Day 1	0.03	0.88	0.50	2.01	0.02	0.00	0.18±0.16	0.96±0.58
Day 3	0.25	0.19	0.68	1.34	0.04	0.24	0.32±0.19	0.59±0.37
Day 7	0.97	3.27	2.05	1.58	0.31	0.05	1.11±0.51	1.63±0.93
Day 14	0.17	7.43	1.58	16.27	1.94	2.25	0.94±0.54	8.65±4.09
Day 21	3.59	4.38	3.00	3.04	1.21	6.12	2.60±0.72	4.51±0.89

Table 3.5: Percentage of hWJSCs that display CD34-/ CD36+/ CD44+/ CD75+/ CD90+/ CD105+/ CD45- phenotype

Time Point	C221116-01 P6F0 Non-Induced	C221116-01 P6F0 Induced	C221116-03 P7F0 Non-Induced	C221116-03 P7F0 Induced	C290817 P5F1 Non-Induced	C290817 P5F1 Induced	Mean ± SEM n=3 Non-Induced	Mean ± SEM n=3 Induced
Day 0	0.65	—	1.61	—	1.34	—	1.20±0.28	—
Day 1	0.77	0.13	0.27	3.08	4.68	1.16	1.91±1.40	1.46±0.86
Day 3	17.96	2.03	0.65	5.84	3.52	1.61	7.38±5.35	3.16±1.35
Day 7	0.23	1.08	2.00	7.24	7.67	2.40	3.30±2.24	3.57±1.87
Day 14	0.32	0.04	0.88	49.46	40.09	11.71	13.76±13.16	20.40±14.91
Day 21	NA	NA	5.96	42.67	21.89	3.40	13.92±6.50	23.04±19.63

NA* - Was unable to collect data for this time point

With the exception of CD34 expression, majority of the hASCs expressed the hMSC markers in culture over time. At day 0, the mean percentage of cells which adhered to the CD34+/CD36+/CD44+/CD73+/CD90+/CD105+/CD45- phenotype was 83.58% ± 3.79% which decreased slightly over the 21-day culture period to a mean percentage of 61.40% ± 10.62 % for the non-induced hASCs and 60.70% ± 7.26% for the induced hASCs, respectively (Figure. 3.13). The general decrease observed in the percentage of cells which adhere to the hMSC phenotype over time in culture, may be attributed to the loss of markers CD73 and CD105 over time. However, since weak expression was observed for these markers, combined with the fact that they are being detected with weak fluorochromes, it may be resulting in an underestimation of cells which are positive for these markers. The observation that the percentages observed for CD34+/ CD36+/ CD44+/ CD75+/ CD90+/ CD105+/ CD45- and CD34-/ CD36+/ CD44+/ CD75+/ CD90+/ CD105+/ CD45- reported at each time point for the respective cultures do not add up to 100% are also likely due to the underestimation of the CD73 and CD105 expression levels. It is possible that the cell surface expression of certain surface proteins, such as CD73 and CD105 change in an *in vitro* environment. Thus, it is possible that the number of CD73 and CD105 epitopes on the cells decrease with increase time in culture, resulting in a decrease in the median fluorescence intensity for these two markers, consequently shifting into the negative region. The adjusted monoclonal antibody panel currently in use in our laboratory is likely to rectify this phenomenon, preventing the likely underestimation of total cells which adhere to the MSC phenotype reported in this

study. Alternatively, the observed decrease in number of non-induced cells which adhere to the MSC phenotype, especially the decrease observed for the non-induced cells, may be attributed to the *in vitro* culturing environment (33). It is important to note that these cells were cultured *in vitro* for an extensive period of time before being used for the experimental work herein described. In order to obtain sufficient cell numbers to perform the experiments, the cells underwent at least three to four rounds of trypsinisation and re-platting, and an additional ten to fourteen days to reach confluence before adipogenic differentiation could be initiated. Non-induced cells were cultured under the same conditions throughout the induction period, resulting in these cells to be in culture for an additional 1 to 21 days. When the last set of cells (day 21 time point) were analysed, these cells have already been cultured for almost two months. The cultures were not trypsinized and re-plated during the 21-day induction period, resulting in the non-induced cultures, especially the day 14 and day 21 cultures to be over confluent.

Higher levels of inter culture variability is observed on days 14 and 21 but the mean percentage of cells that adhere to the MSC phenotype seems relatively consistent between the not induced and induced cells. No significant differences were found between the phenotypes of non-induced and induced cells.
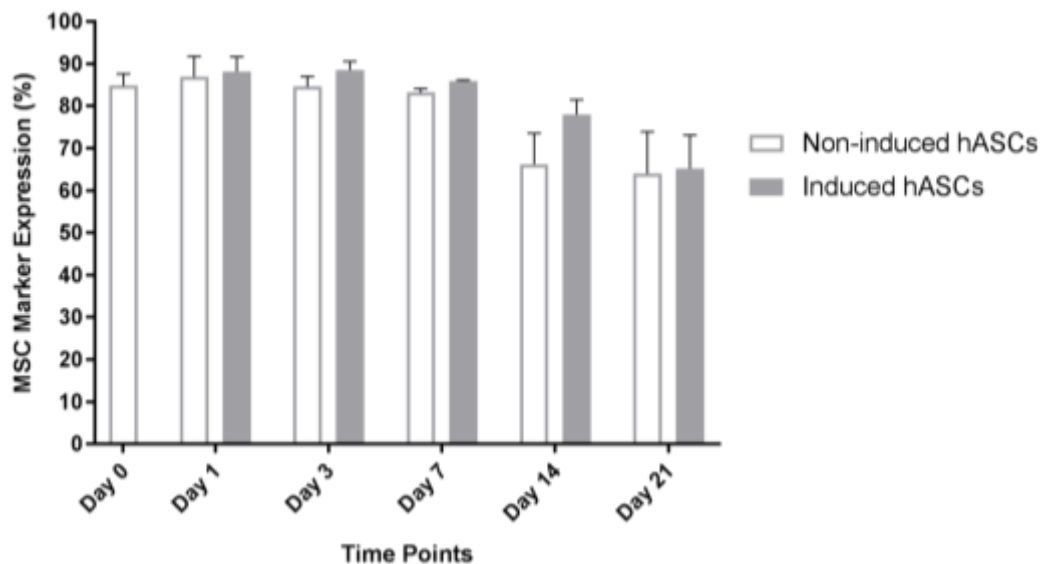
Figure 3.13: Phenotype of non-induced hASCs versus induced hASCs over a period of 21 days. The phenotype of three hASC cultures was assessed over a 21 day culture period at days 0, 1, 3, 7, 14 and 21. Both non-induced (control) and induced cells were analysed. Graph represents the percentage of cells

which displayed a CD34+/ CD36+/ CD44+/ CD73+/ CD90+/ CD105+/ CD45−
phenotype. Error bars are representative of the standard error of mean (SEM).

With regards to the hWJSCs, despite the slight fluctuations in CD34 expression in two of the cultures, majority of the cells expressed the hMSC markers (Figure 3.14). The high level of variation displayed in Figure 3.14 for day 3 not induced, day 14 (not induced and induced) and 21 (not induced and induced) is due to the loss of CD34 expression in some of the cultures at those time points (Table 3.5). The graph only displays the percentage of cells that are CD34+/ CD36+/ CD44+/ CD73+/ CD90+/ CD105+/ CD45−.
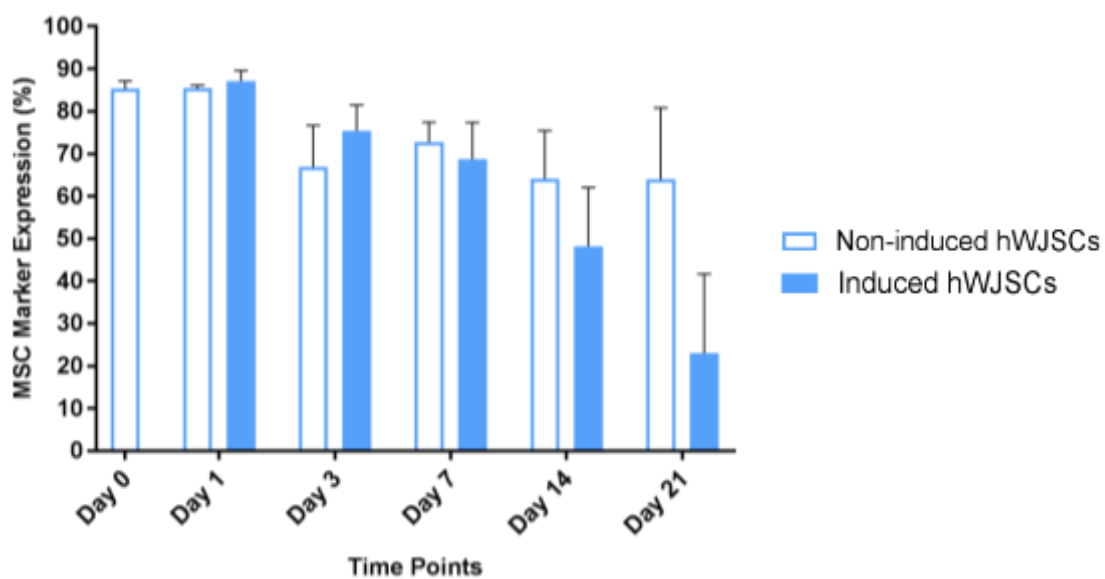
Figure 3.14: Phenotype of non-induced hWJSCs vs induced hWJSCs over a period of 21 days. The phenotype of three hWJSC cultures was assessed over a 21 day period at days 0, 1, 3, 7, 14 and 21. Both non-induced (control) and induced cells were analysed. Error bars are representative of the standard error of mean (SEM).Graph represents the percentage of cells which displayed a CD34+/ CD36+/ CD44+/ CD73+/ CD90+/ CD105+/ CD45− phenotype.

However, if CD34 is excluded (Figure 3.14), the variability observed at those time points is decreased with exception to day 14 induced. The high level of variance observed at this time point is due to one of the three cultures displaying a very low percentage of cells which adhere to the hMSC phenotype (Table 3.2 & 3.5). Given the fact that these cells are being maintained in adipogenic differentiation medium, it is not surprising that fewer of these cells adhere to the hMSC phenotype. As the cells differentiate, the amount and type of cell surface markers they express most likely changes.
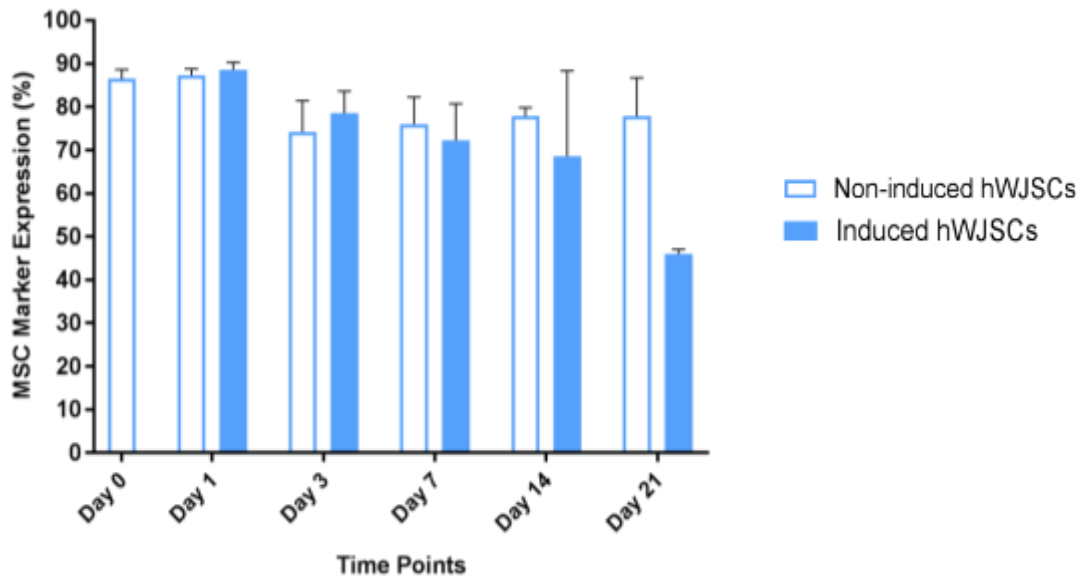
Figure 3.15: Phenotype of non-induced hWJSCs vs induced hWJSCs, excluding CD34 expression, over a period of 21 days. The phenotype of three hWJSC cultures was assessed over a 21 day period at days 0, 1, 3, 7, 14 and 21. Both non-induced (control) and induced cells were analysed. Error bars are representative of the standard error of mean (SEM).Graph represents the percentage of cells which displayed a CD36+/ CD44+/ CD73+/ CD90+/ CD105+/ CD45− phenotype.

Another observation made, was the fact that hASCs could be split into two populations, namely a population of cells which stains brightly positive for CD36 and a population which stains dimly positive for CD36 (Figure 3.16). This is in line with what has been reported by Durandt and colleagues (34). Interestingly, the two CD36 populations were only observed in hASCs. The hWJSCs were more uniform in their CD36 expression and only consisted of one population that dimly expressed CD36 (Figure 3.16).

The percentage of CD36 dim and CD36 bright cells was quantified (Figure 3.17 and Figure 3.18) in order to determine whether any changes could be observed within the two CD36 populations during the 21 day adipogenic differentiation period. A two parameter side scatter (SS Log) versus FL6 (Excitation 638nm; Emission 660/20 BP) plot was generated. The plot was gated on cells shown in Figure 3.10J, quadrant "CD34+/CD36+". These were cells that displayed the MSC phenotype i.e. CD34+/ CD36+/ CD44+/ CD73+/ CD90+/ CD73+/ CD105+/ CD45-. Given the observation made above, region "CD36 Dim" was set according to where the hWJSC CD36 dim

positive population appears on the SS Log vs FL6 plot (Figure 3.16 B). Region "CD36 Bright" was made to the right of the "CD36 Dim" region (Figure 3.16 A).
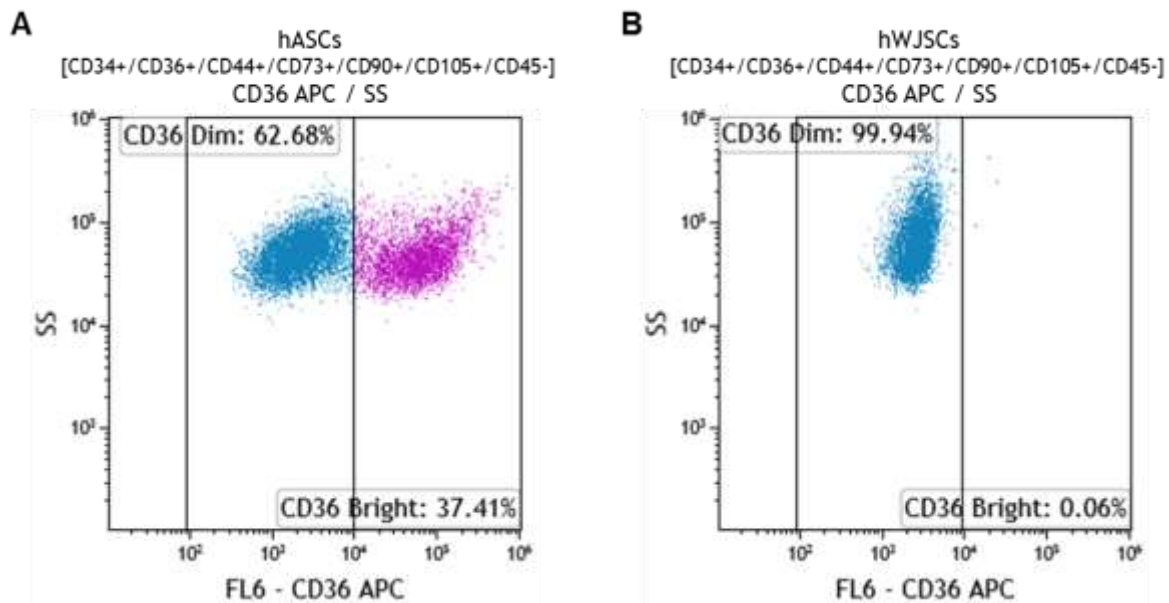
Figure 3.16: Comparison of CD36 expression in hASCs and hWJSCs. Two parameter (SS Log vs FL6 – CD36 APC) plots gated on the "CD34+/CD36+" population displayed in Figure 3.12J which represents cells that are CD34+/ CD36+/ CD44+/ CD73+/ CD90+/ CD105+/ CD45-. **A.** Two parameter plot displaying the CD36 immunophenotype profile of hASCs shows two distinct populations – CD36 bright expression and CD36 dim expression. **B.** A two parameter plot displaying the CD36 immunophenotype profile of the hWJSCs only shows one population of cells which are dimly CD36 positive.

Throughout the 21 day adipogenic differentiation period, the percentage of CD36 dim and CD36 bright non-induced hASCs remained relatively consistent (Figure 3.17 A and Table 3.1). However, when looking at the induced hASCs, a gradual decrease in CD36 dim positive hASCs was observed over the 21-day induction period, while a gradual increase in CD36 bright positive hASCs was observed (Figure 3.17 B and Table 3.1). At the end of the 21 day induction period, the majority of induced hASCs in culture displayed a CD36 bright phenotype (Figure 3.17 B and Table 3.1). This observation correlates with previous findings made in our laboratory (34). Durandt and colleagues showed that induced hASCs display an increase in CD36 expression during adipogenic differentiation *in vitro* which precedes lipid accumulation (34).
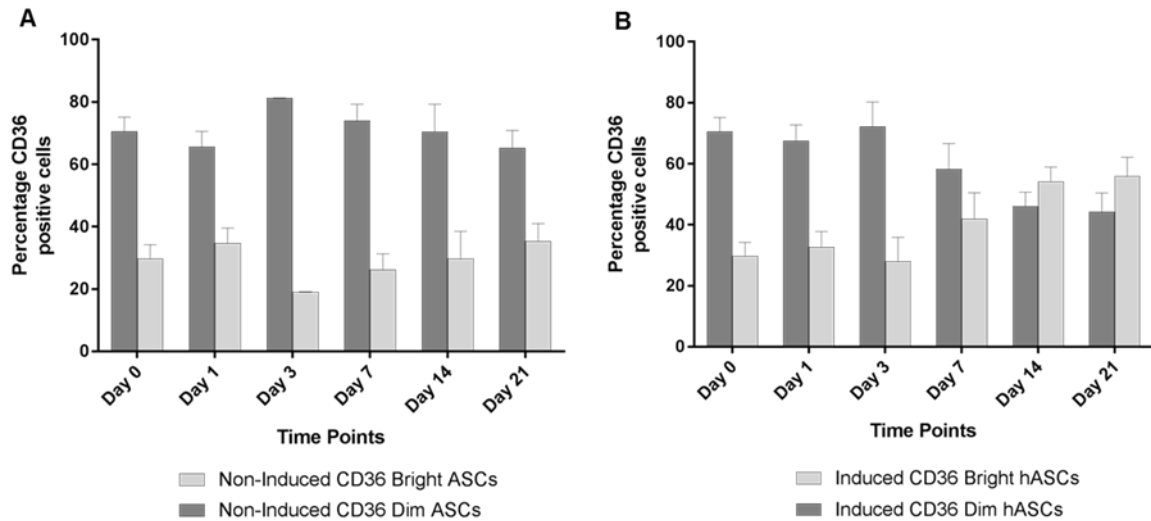
Figure 3.17: Proportion of CD36 dim positive and CD36 bright positive hASCs. A. Mean percentage of CD36 dim positive and CD36 bright positive non-induced hASCs present during the 21 day culture period. **B.** Mean percentage of CD36 dim positive and CD36 bright positive induced hASCs present during the 21 day culture period. Error bars represent the standard error of the mean (SEM). N = 3

The hWJSCs on the other hand did not show any signs of CD36 protein upregulation throughout the 21 day adipogenic differentiation period (Figure 3.18 and Table 3.2). A single CD36 dim positive population was observed in both non-induced and induced hWJSCs throughout the 21-day induction period (Figure 3.18 A & B).
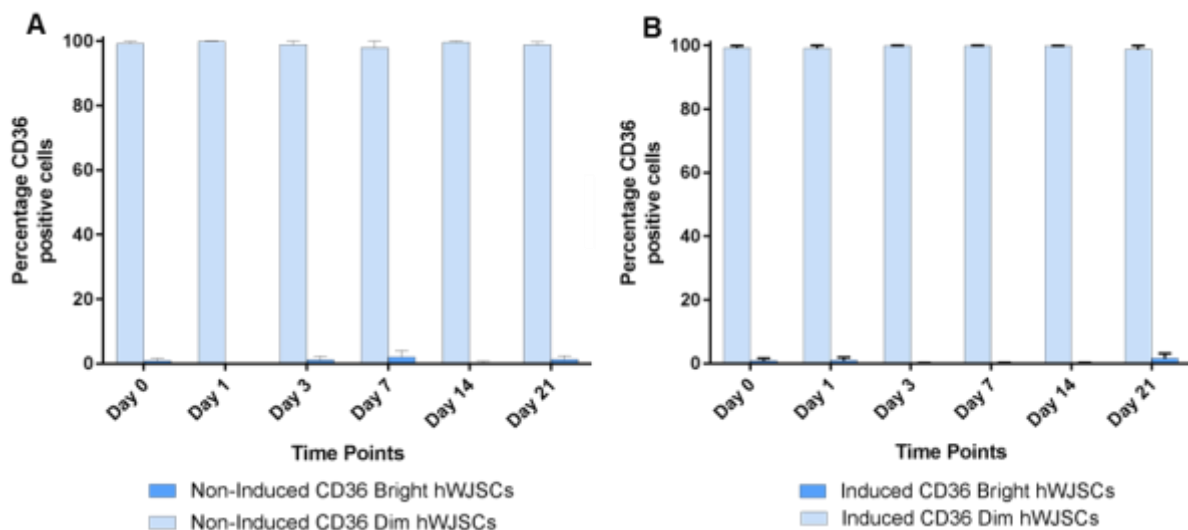
Figure 3.18: Proportion of CD36 dim positive and CD36 bright positive hWJSCs. A. Mean percentage of CD36 dim positive and CD36 bright positive non-induced hWJSCs present during the 21 day culture period. **B.** Mean percentage of CD36 dim positive and CD36 bright positive non-induced hWJSCs

present during the 21 day culture period. Error bars represent the standard error of the mean (SEM). N = 3

The observation that CD36 protein expression is upregulated in induced hASCs (Figure 3.17 and Table 3.6) but not in induced hWJSCs (Figure 3.18 and Table 3.7) is interesting given the fact that CD36 is a fatty acid translocase essential for internalisation of lipids during adipogenesis (34, 35). The lack of CD36 upregulation in induced hWJSCs may thus be an important element of the phenotype acquired by induced hWJSCs at the end of the 21 day induction period i.e. it indicates that the cells are unable to express the adipocyte phenotype (Discussed in Chapter 4).

Table 3.6: Mean percentage of hASCs displaying a CD36 dim positive subpopulation and CD36 bright positive population

Time points	Non-induced		Induced	
	CD 36 Dim	CD 36 Bright	CD 36 Dim	CD 36 Bright
Day 0	70.54 ± 4.57	29.67 ± 4.51	70.54 ± 4.57	29.67 ± 4.51
Day 1	65.57 ± 5.01	34.64 ± 4.94	67.56 ± 5.20	32.70 ± 5.08
Day 3	81.23 ± 0.08	19.04 ± 0.10	72.23 ± 7.97	27.97 ± 7.92
Day 7	74.03 ± 5.20	26.15 ± 5.15	58.25 ± 8.40	41.99 ± 8.47
Day 14	70.51 ± 8.74	29.75 ± 8.73	46.00 ± 4.67	54.22 ± 4.71
Day 21	65.22 ± 5.62	35.31 ± 5.72	44.24 ± 6.15	56.00 ± 6.07

The values displayed in the table are the mean percentages ± the standard error of the mean (SEM). (n = 3).

Table 3.7: Mean percentage of hWJSCs displaying a CD36 dim positive subpopulation and CD36 bright positive population

Time points	Non-induced		Induced	
	CD 36 Dim	CD 36 Bright	CD 36 Dim	CD 36 Bright
Day 0	99.22 ± 0.72	0.84 ± 0.77	99.22 ± 0.72	0.84 ± 0.77
Day 1	99.89 ± 0.11	0.13 ± 0.13	99.11 ± 0.89	0.97 ± 0.97
Day 3	98.92 ± 1.07	1.15 ± 1.45	99.91 ± 0.09	0.11 ± 0.11
Day 7	98.04 ± 1.96	2.05 ± 2.05	99.85 ± 0.15	0.15 ± 0.15
Day 14	99.63 ± 0.33	0.42 ± 0.38	99.83 ± 0.11	0.18 ± 0.11
Day 21	98.82 ± 0.99	1.31 ± 1.12	98.79 ± 1.15	1.61 ± 1.55

The values displayed in the table are the mean percentages ± the standard error of the mean (SEM). (n = 3).

3.5 Conclusions

In both the hASC and hWJSC cell cultures, majority of the cells analysed displayed the following phenotype: CD34+/CD36+/CD44+/CD73+/CD90+/CD105+/CD45-. The expression profile of the different cluster of differentiation markers is in line with the requirements set out by the ISCT and IFATS. Overall, it can be concluded that the hMSCs isolated from adipose tissue and Wharton's Jelly adhere to the hMSC phenotype and have similar phenotypes under both not induced and induced conditions (Table 3.4 and Table 3.5). No statistical significant differences were found between the different cell types, time points or conditions. The only observable phenotypic difference between the two cell types was the presence of two CD36 populations (CD36 dim positive and CD36 bright positive) in the hASCs which is not seen in the hWJSC cultures (Figure 3.16). When investigating the two CD36 populations further, it was noted that the CD36 bright population present in induced hASCs gradually increased over time (Figure 3.17 B) whereas the induced hWJSCs only displayed a CD36 dim population which appeared to remain static (no increase) throughout the 21 day induction period (Figure 3.18 B).

3.6 References

1.	Orbay H, Tobita M, Mizuno H. Mesenchymal stem cells isolated from adipose and other tissues: basic biological properties and clinical applications. Stem Cells Int. 2012;2012:461718.

2.	Hoogduijn MJ, Crop MJ, Peeters AM, Van Osch GJ, Balk AH, Ijzermans JN, et al. Human heart, spleen, and perirenal fat-derived mesenchymal stem cells have immunomodulatory capacities. Stem Cells Dev. 2007;16(4):597-604.

3.	Li Y, Charif N, Mainard D, Bensoussan D, Stoltz JF, de Isla N. Donor's age dependent proliferation decrease of human bone marrow mesenchymal stem cells is linked to diminished clonogenicity. Biomed Mater Eng. 2014;24(1 Suppl):47-52.

4.	Marquez-Curtis LA, Janowska-Wieczorek A, McGann LE, Elliott JA. Mesenchymal stromal cells derived from various tissues: Biological, clinical and cryopreservation aspects. Cryobiology. 2015;71(2):181-97.

5.	Xu L, Liu Y, Sun Y, Wang B, Xiong Y, Lin W, et al. Tissue source determines the differentiation potentials of mesenchymal stem cells: a comparative study

of human mesenchymal stem cells from bone marrow and adipose tissue. Stem Cell Res Ther. 2017;8(1):275.

6. Zolocinska A. The expression of marker genes during the differentiation of mesenchymal stromal cells. Adv Clin Exp Med. 2018;27(5):717-23.

7. Watson N, Divers R, Kedar R, Mehindru A, Mehindru A, Borlongan MC, et al. Discarded Wharton jelly of the human umbilical cord: a viable source for mesenchymal stromal cells. Cytotherapy. 2015;17(1):18-24.

8. Bourin P, Bunnell BA, Casteilla L, Dominici M, Katz AJ, March KL, et al. Stromal cells from the adipose tissue-derived stromal vascular fraction and culture expanded adipose tissue-derived stromal/stem cells: a joint statement of the International Federation for Adipose Therapeutics and Science (IFATS) and the International Society for Cellular Therapy (ISCT). Cytotherapy. 2013;15(6):641-8.

9. Zuk PA, Zhu M, Mizuno H, Huang J, Futrell JW, Katz AJ, et al. Multilineage cells from human adipose tissue: implications for cell-based therapies. Tissue Eng. 2001;7(2):211-28.

10. Baer PC. Adipose-derived mesenchymal stromal/stem cells: An update on their phenotype in vivo and in vitro. World J Stem Cells. 2014;6(3):256-65.

11. Lin CS, Ning H, Lin G, Lue TF. Is CD34 truly a negative marker for mesenchymal stromal cells? Cytotherapy. 2012;14(10):1159-63.

12. Davies JE, Walker JT, Keating A. Concise Review: Wharton's Jelly: The Rich, but Enigmatic, Source of Mesenchymal Stromal Cells. Stem Cells Transl Med. 2017;6(7):1620-30.

13. Watson ND, R.; Kedar, R.; Mehindru, A.; Mehindru, A.; Borlogan, M. Discarded Wharton's Jelly of the Human Umbilical Cord: A Viable Source for Mesenchymal Stem Cells Cytotherapy. 2015;17(1):14.

14. Kalaszczynska I, Ferdyn K. Wharton's jelly derived mesenchymal stem cells: future of regenerative medicine? Recent findings and clinical significance. Biomed Res Int. 2015;2015:430847.

15. Nagamura-Inoue T, He H. Umbilical cord-derived mesenchymal stem cells: Their advantages and potential clinical utility. World J Stem Cells. 2014;6(2):195-202.

16. Margossian T, Reppel L, Makdissy N, Stoltz JF, Bensoussan D, Huselstein C. Mesenchymal stem cells derived from Wharton's jelly: comparative phenotype

analysis between tissue and in vitro expansion. Biomed Mater Eng. 2012;22(4):243-54.

17. Hassan G, Kasem I, Soukkarieh C, Aljamali M. A Simple Method to Isolate and Expand Human Umbilical Cord Derived Mesenchymal Stem Cells: Using Explant Method and Umbilical Cord Blood Serum. Int J Stem Cells. 2017;10(2):184-92.

18. Wang HS, Hung SC, Peng ST, Huang CC, Wei HM, Guo YJ, et al. Mesenchymal stem cells in the Wharton's jelly of the human umbilical cord. Stem Cells. 2004;22(7):1330-7.

19. Mori Y, Ohshimo J, Shimazu T, He H, Takahashi A, Yamamoto Y, et al. Improved explant method to isolate umbilical cord-derived mesenchymal stem cells and their immunosuppressive properties. Tissue Eng Part C Methods. 2015;21(4):367-72.

20. Macey MG. Flow cytometry: principles and clinical applications. Med Lab Sci. 1988;45(2):165-73.

21. Adan A, Alizada G, Kiraz Y, Baran Y, Nalbant A. Flow cytometry: basic principles and applications. Crit Rev Biotechnol. 2017;37(2):163-76.

22. Wilkerson MJ. Principles and applications of flow cytometry and cell sorting in companion animal medicine. Vet Clin North Am Small Anim Pract. 2012;42(1):53-71.

23. Ohnuma K, Yomo T, Asashima M, Kaneko K. Sorting of cells of the same size, shape, and cell cycle stage for a single cell level assay without staining. BMC Cell Biol. 2006;7:25.

24. Szaloki G, Goda K. Compensation in multicolor flow cytometry. Cytometry A. 2015;87(11):982-5.

25. Roederer M. Compensation in flow cytometry. Curr Protoc Cytom. 2002;Chapter 1:Unit 1 14.

26. Maecker HT, Trotter J. Flow cytometry controls, instrument setup, and the determination of positivity. Cytometry A. 2006;69(9):1037-42.

27. Pu LL, Coleman SR, Cui X, Ferguson RE, Jr., Vasconez HC. Autologous fat grafts harvested and refined by the Coleman technique: a comparative study. Plast Reconstr Surg. 2008;122(3):932-7.

28. Phinney DG. Functional heterogeneity of mesenchymal stem cells: implications for cell therapy. J Cell Biochem. 2012;113(9):2806-12.

29. Han ZC, Du WJ, Han ZB, Liang L. New insights into the heterogeneity and functional diversity of human mesenchymal stem cells. Biomed Mater Eng. 2017;28(s1):S29-S45.

30. Jansen BJ, Gilissen C, Roelofs H, Schaap-Oziemlak A, Veltman JA, Raymakers RA, et al. Functional differences between mesenchymal stem cell populations are reflected by their transcriptome. Stem Cells Dev. 2010;19(4):481-90.

31. Njemini R, Onyema OO, Renmans W, Bautmans I, De Waele M, Mets T. Shortcomings in the application of multicolour flow cytometry in lymphocyte subsets enumeration. Scand J Immunol. 2014;79(2):75-89.

32. Viswanathan C, Kulkarni R, Bopardikar A, Ramdasi S. Significance of CD34 Negative Hematopoietic Stem Cells and CD34 Positive Mesenchymal Stem Cells - A Valuable Dimension to the Current Understanding. Curr Stem Cell Res Ther. 2017;12(6):476-83.

33. Yang YK, Ogando CR, Wang See C, Chang TY, Barabino GA. Changes in phenotype and differentiation potential of human mesenchymal stem cells aging in vitro. Stem Cell Res Ther. 2018;9(1):131.

34. Durandt C, van Vollenstee FA, Dessels C, Kallmeyer K, de Villiers D, Murdoch C, et al. Novel flow cytometric approach for the detection of adipocyte subpopulations during adipogenesis. J Lipid Res. 2016;57(4):729-42.

35. Christiaens V, Van Hul M, Lijnen HR, Scroyen I. CD36 promotes adipocyte differentiation and adipogenesis. Biochim Biophys Acta. 2012;1820(7):949-56.

Chapter 4:   Adipogenic Differentiation

4.1 Introduction

As mentioned in the introduction (Chapter 2), a better understanding of the process of adipose tissue formation may aid in finding sustainable solutions towards combating obesity as well as contribute to advances in regenerative medicine with regard to fat grafting (1-3). MSCs, such as hASCs, can be used as an *in vitro* model to study the complex process of fat cell formation known as adipogenesis (4). The majority of studies investigating the adipogenic differentiation process of hASCs have been done using murine cell lines, such as 3T3-L1, 3T3-F442A and C3H10T1/2 (5, 6). For the purpose of this study, the focus will be on hMSCs isolated from adipose tissue (hASCs) and umbilical cord-derived Wharton's jelly (hWJSCs).

4.1.1 Adipogenesis

Adipogenesis is the biological process that leads to the formation and maturation of adipocytes (Figure 4.1) (7, 8). *In vitro,* commitment to the adipogenic lineage is achieved by means of an adipogenic differentiation cocktail consisting of dexamethasone, IBMX, indomethacin and insulin. These chemicals provide the necessary signals to downregulate inhibitors of adipogenesis such as Pref-1 and Wnt10a while upregulating the expression of promoters of adipogenesis such as C/EBPs and PPARγ (9). Once committed, the cells undergo mitotic clonal expansion, brought about by PPARγ and C/EBPα (10). During this time cells undergo two rounds of cell division (11). This is a fundamental step in adipocyte differentiation as a number of adipogenesis related genes will be activated (12). This is followed by terminal differentiation. In this final stage of adipogenesis, pre-adipocytes acquire all the morphological features and characteristics of mature adipocytes. Genes involved in lipid biosynthesis, storage, metabolism and transport will be upregulated (5).

| ASCs | Pre-adipocyte | Immature Adipocyte | Mature Adipocyte |

Commitment	Clonal expansion	Increasing lipid accumulation and insulin sensitivity	
↑ Pref-1	↑ C/EBPβ	↑ C/EBPα ↑ PPARγ	↑ AdipoQ ↑ FABP4 ↑ LEP ↑ PLIN
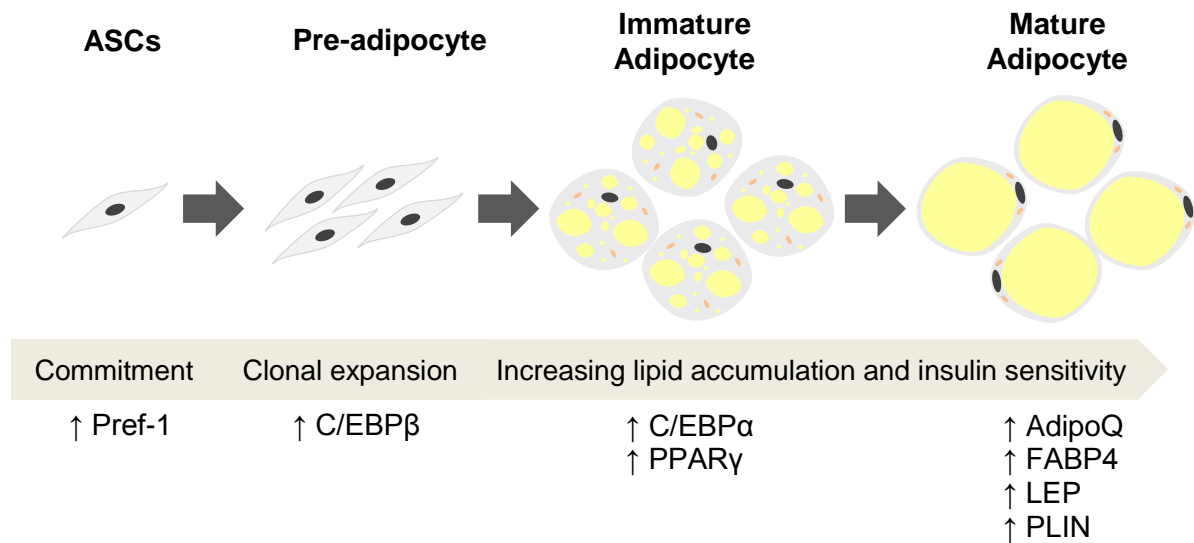
Figure 4.1: Morphological and genetic changes during adipogenic differentiation. Adipogenesis can be divided into three stages: commitment, clonal expansion and terminal differentiation. Pref-1 expression is increased when cells commit to the adipogenic lineage and become pre-adipocytes. Once committed the cells undergo mitotic clonal expansion which in is part mediated by C/EBPβ. C/EBPβ is also responsible for the activation of PPARγ the main regulator of adipogenesis along with C/EBPα. Activation of these two pro-adipogenic genes results in the expression of adipocyte specific genes. Pref-1, Pre-adipocyte factor 1; C/EBP, CAAT/enhancer binding protein; PPARγ, Peroxisome proliferator-activated receptor gamma; AdipoQ, Adiponectin; FABP4, Fatty acid binding protein 4; LEP, Leptin; Plin, Perilipin. Image was adapted from Ms Carla Dessels MSc dissertation.

4.2 Techniques

The adipogenic differentiation potential of hASCs and hWJSCs was assessed by means of fluorescence microscopy, flow cytometry and RT-qPCR. The basic principles of these techniques are described below.

4.2.1 Fluorescence microscopy

Fluorescence microscopy can be used to visualise the morphology of cells, the structure of different tissues and the localization of organelles and proteins within a cell (13, 14). The ability to magnify and visualise a sample is combined with the ability to excite and emit fluorescence by means of a filter cube. The emitted fluorescent signal and the location thereof is then visualized and captured by a

camera. As with flow cytometry (discussed in Chapter 3, section 3.2), fluorescence microscopy makes use of the principles of fluorescence which are important to keep in mind, especially when staining specimens with more than one fluorescent marker. To briefly recapitulate, fluorescence involves the excitation/absorption of light by a fluorophore followed by the emission of light at a longer wavelength (14). Therefore, in order to properly separate the signal detected by the different fluorescent compounds used to stain the specimen, the emission spectra of these fluorescent markers should be distinct with minimal overlap.

The advantage of using fluorescence microscopy lies in the ability to visualise the presence and location of components within a cell. The last-mentioned feature allowed us to visualize the formation and size of intracellular lipid droplets formed during adipocyte differentiation. In this study, fluorescence microscopy was used as a qualitative technique to assess adipogenic differentiation of hASCs and hWJSCs. However, fluorescence microscopy can be subjective. The limited number of cells in the microscopic field may lead to an under- or over-estimation of the proportion of cells with the feature of interest, intracellular lipid droplet accumulation in our case. In addition, bleaching (loss of fluorescence) of the fluorescent compounds may occur when specimens are viewed under the microscope for a long time, which may affect the accuracy of the results (15).

4.2.2 Flow cytometry

The basic principles of flow cytometry have been discussed in Chapter 3. In short, the technique is based on capturing fluorescent signals from individual cells as they flow in single file past a light source, usually a laser (16, 17). One of the advantages of flow cytometry is the ability to analyse a larger number of individual cells in a relatively short period of time. In this study, flow cytometry was used to obtain a more quantitative measurement of adipogenic differentiation by quantifying the percentage of cells with higher intracellular lipid levels as a result of intracellular lipid droplets accumulation.

4.2.3 Reverse transcription – quantitative PCR

Reverse transcription – quantitative PCR (RT-qPCR) was used to analyse the expression of *PPARG*, *Pref-1* and *Sox9*. *PPARG* was selected due to it being the

main positive regulator of adipogenesis whereas *Sox9* was selected as it is thought to be involved in the mechanism by which *Pref-1* inhibits adipogenesis (18). Only the expression of *PPARG* will be discussed in this chapter as it encodes an essential transcription factor in adipogenesis (discussed in section 4.1.2). The expression of suggested early regulators of adipogenesis *Pref-1* and *Sox9,* will be discussed in the following chapter (Chapter 5). RT-qPCR combines reverse transcription, PCR amplification and fluorescence to investigate gene expression. First, RNA is used as a template for complementary DNA (cDNA) synthesis using reverse transcription enzymes. The cDNA is then used as product for the amplification reaction. The amount of template increases exponentially with every amplification cycle, which is monitored using fluorescence. In this study, SYBR green was used to monitor amplification. SYBR green is a double stranded DNA (dsDNA) intercalating dye that binds to the minor grooves of DNA. Initially the dye emits very low levels of fluorescence that exponentially increase as the cDNA is amplified and the amount of dsDNA increases (19-21). The point at which the signal exceeds the background signal is called the threshold cycle (C_T) or crossing point (Cp). The more initial target template available, the fewer cycles will be required in order to cross the threshold (21, 22). Eventually the signal will cease to increase and a plateau phase will be reached due to the exhaustion of primers and dNTP's available for incorporation.

Using this method, gene expression can be quantified in two ways – absolute or relative quantification. Absolute quantification makes use of a set of standards at different concentrations where the initial copy number of the target gene is known. These standards are used to make a standard curve to which the Cp value of the sample in question is compared to. Relative quantification on the other hand does not require the use of standard curves. Gene expression is calculated relative to a reference gene, calibrator and an untreated or time 0 sample using mathematical equations illustrated in Equation 4 (21, 22). In this study, relative quantification was used to report the difference in gene expression between controls (non-induced) and treated (induced) samples. The most often used method to calculate relative gene expression is the delta delta Ct method i.e. $2^{-\Delta\Delta CT}$. However, this method assumes a qPCR efficiency of 100%, which is not necessarily always true. Rao and colleagues (23) have shown that this method can be improved by using the amplification efficiency (E) of each gene of interest, altering the formula to: $E^{-\Delta\Delta CT}$ (Equation 5).

The amplification efficiency is determined with the aid of a standard curve. For the purpose of this study, the modified delta delta CT method ($E^{-\Delta\Delta CT}$) was used to calculate the relative gene expression of *PPARG, Sox9 and Pref-1* in control (non-induced) and treated (induced) hASCs and hWJSCs. With regard to the control genes, three reference genes were used: *YWHAZ, PPIA* and *TBP*. These genes were chosen based on previous work conducted in our laboratory by Dr Chrisna Durandt and Ms Carla Dessels as well as literature that considers these genes to be appropriate reference genes for our application (24, 25).

Equation 4: Calculating ΔΔCt

Step 1: Calculate the difference between the target and reference gene for the induced (treated) group (Δct):

    Equation 4.1:
$$\Delta CT = (CT \text{ target gene} - CT \text{ Reference gene}) \text{ Induced}$$

Step 2: Calculate the difference between the target and reference gene for the non-induced (control) group (ΔCT):

    Equation 4.2:
$$\Delta CT = (CT \text{ Target gene} - CT \text{ Reference gene}) \text{ Non-induced}$$

Step 3: Calculate the difference between the two groups (ΔΔCT):

    Equation 4.3:
$$\Delta\Delta CT = (\Delta CT) \text{ Induced} - (\Delta CT) \text{ Non-induced}$$

Equation 5: Modified ΔΔCt

$$E\text{-}\Delta\Delta CT$$

4.3 Methods

4.3.1 Adipogenic differentiation

Cells were seeded at a density of 5 x 10^3 cells per cm^2 and cultured in complete growth medium until reaching 80 - 90% confluence. The cells were then induced by replacing the complete growth media with adipogenic induction medium. Adipogenic induction medium consists of complete growth media supplemented with 1 µM dexamethasone (Sigma-Aldrich, Merck, Missouri, USA), 0.5 mM 3-iosbutyl-methylxanthine (Sigma-Aldrich, Merck, Missouri, USA), 200 µM indomethacin (Sigma-Aldrich, Merck, Missouri, USA) and 10 µg/ml insulin (human recombinant Zinc, GIBCO by Life Technologies™, Grand Island, NY, USA). As a control, non-induced cells were cultured in parallel to induced cells (Figure 4.2). Both non-induced and induced cells were maintained for 21 days with the respective medium replacement twice a week. Throughout the induction period, adipogenic differentiation was monitored using the various assays described below. Adipogenic differentiation was assessed at days 0, 1, 3, 7, 14 and 21 using fluorescence microscopy, flow cytometry and RT-qPCR.
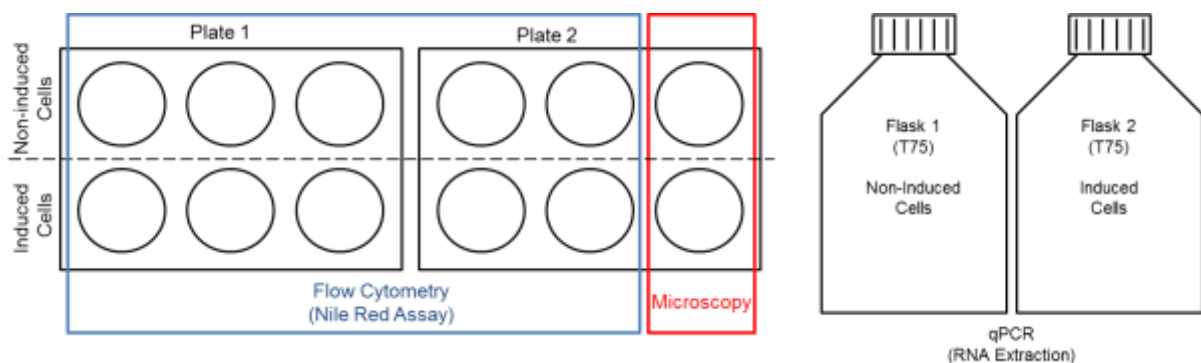
Figure 4.2: Experimental layout for adipogenic quantification. Adipogenic differentiation capacity was assessed by fluorescence microscopy, flow cytometry and RT-qPCR. For the flow cytometric Nile Red assay and fluorescence microscopy, two six well plates were plated per time point. Five wells per condition were used for the Nile Red assay and one well per condition was used for microscopy. For qPCR experiments, the cells were plated in T75 flasks for RNA extraction. Once again, non-induced cells were maintained in parallel to induced cells.

4.3.2 Fluorescence Microscopy

Cells were cultured in 6 well plates as shown in Figure 4.2. Both non-induced and induced cells were simultaneously stained with two stains – VDC Violet which is a nuclear specific dye binding to double-stranded DNA and Nile Red (Sigma-Aldrich, Merck, Missouri, USA), a lipophilic dye with high affinity for neutral lipids. Cells were then incubated for 20 min at 37^0C/5%CO_2. Prior to imaging, the culture medium was removed and cells were rinsed three times with PBS in order to remove any excess unbound dye, after which two milliliters (2 mL) of PBS were added to the wells.

Both non-induced and induced cells were visualized and representative images captured with a 20x magnification objective lens using an AxioVert A1 inverted fluorescence microscope (Carl Zeiss, Gottingen, Germany) equipped with an AxioCam Cm1 camera (Carl Zeiss, Gottingen, Germany). Images were captured using ZEN 2.3 blue edition software (Carl Zeiss, Gottingen, Germany). Images were enhanced only by adjusting contrast and brightness.

4.3.3 Nile Red Assay – Flow Cytometry

Cells were dislodged from the surface of culture flasks by adding 0.5 mL 0.25% trypsin-EDTA for 7 – 10 min at 37^0C. The enzymatic activity of the trypsin-EDTA solution was then neutralized by adding an equal volume of complete growth medium after it was visually confirmed that all the cells dislodged and were in suspension. Cells were then transferred to a 15 mL Falcon® tube and the volume topped up to 8 mL with complete growth medium. At each time point, a 1 mL aliquot of non-induced and induced cells were transferred to a flow cytometry tube, and simultaneously stained with Nile Red (20 ng/mL final concentration) and VDC Violet (2.5 µM final concentration). The cells were then incubated in the dark for 15 min before the sample was analysed on a Gallios flow cytometer.

4.3.4 Viability

The percentage of viable cells (after sample preparation) at each time point was also determined by staining an aliquot of the cell suspension with 5 µL of 7AAD (DNA binding dye). The 7AAD dye is a non-membrane permeable dye that is only able to cross damaged cell membranes. Cells, which stained negative for 7AAD, are

considered viable, as it is an indication that the cell membranes are still intact and thus preventing 7AAD to cross the cell membrane and bind to the DNA. Data was analysed using Kaluza Flow Cytometry Analysis Software.

4.3.4.1 Flow cytometry setup, data acquisition and analysis

All acquired events were first visualised on a forward scatter (FS Lin) versus side scatter (SS Log) plot (Figure 4.3 A). A region "Cells" was created which excludes any cell debris (bottom left). Next, a two parameter (FS Lin vs 7AAD / FL4 Log (Excitation 488nm; Emission 695/30 BP)) plot was generated in order to view viable cells ("Viable") i.e. 7AAD negative events (Figure 4.3 B).
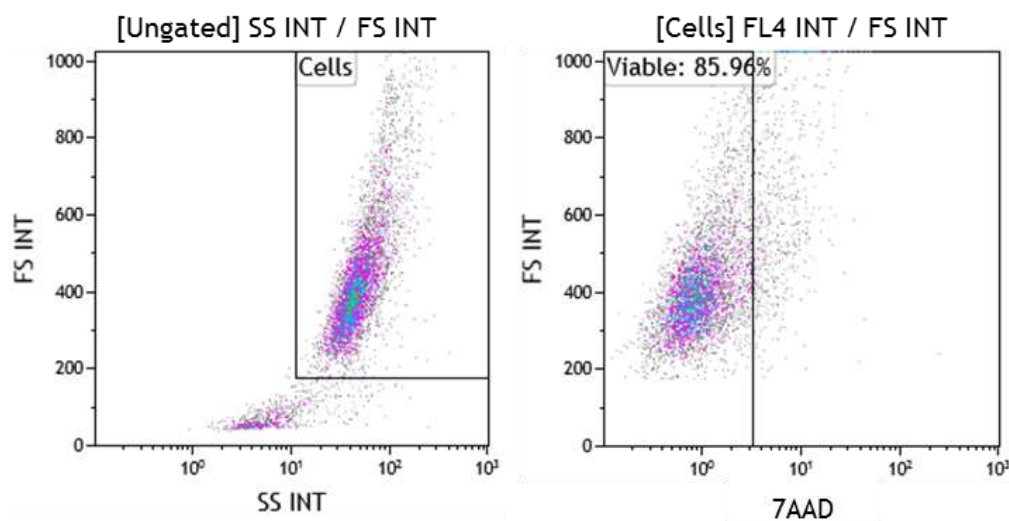
Figure 4.3: Flow cytometry gating strategy to determine percentage of viable cells. A. Plot displaying intact MSCs (i.e. hASCs or hWJSCs) within region "Cells". B. Plot gated on intact hMSCs and used to determine percentage viability (7-AAD negative; "Viable" region).

4.3.5 RNA Extraction

Cells were dislodged as described before in Chapter 3, section 3.3.3.1 using 3 mL 0.25% trypsin-EDTA for 7 – 10 min at 37^{0}C. Once dislodged, the enzymatic activity of the trypsin-EDTA solution was neutralized by adding an equal volume of complete growth medium to the culture flask. Cells were transferred to a 15 mL Falcon® tube and topped up with PBS after which the cells were centrifuged at 300 x g for 5 min. The wash step was repeated an additional two times in order to remove any phenol red within the medium that could interfere with RNA extraction.

4.3.5.1 Procedure:

Total RNA was extracted using the RNeasy Mini kit (Qiagen, Hilden, Germany), according to the manufacturer's instructions with slight modifications. Briefly, cell pellets were re-suspended in 1 mL PBS and centrifuged at 300 x g for 5 min and supernatant discarded. The cell pellet was re-suspended in 350 µL RLT buffer and vortexed for 1 minute. Thereafter, 350 µL of 70% ethanol was added and the sample vortexed for 1 minute. The resulting 700 µL was then transferred to an RNeasy spin column placed within a 2 mL collection tube and centrifuged for 15 sec at 8 000 x g. The flow through was discarded and 700 µL RW1 buffer added to the column. The centrifugation step was repeated, 15 sec at 8 000 x g. The flow through was once again discarded and 500 µL RPE buffer was added to the column and centrifuged for another 15 sec at 300 x g. This step was repeated but with a centrifugation step of 2 min at 300 x g. The collection tube was discarded and the column placed in a new collection tube and centrifuged for 1 min at max speed, after which the column was transferred to a 1.5 mL Eppendorf tube®. RNAse free water (40 µL) was added to the column after which the column was centrifuged for 1 min at 8 000 x g in order to elute the RNA from the column. The eluted RNA was then placed back into the column and the centrifugation step repeated in order to increase the RNA concentration.

4.3.6 cDNA Synthesis

The cDNA was synthesised using the SensiFast™ cDNA synthesis kit (Bioline, London, England) according to the manufacturer's instructions. The cDNA synthesis reaction was set up in a total volume of 20 µL. The 20 µL comprised of 4 µL 5x TransAmp buffer, 1 µL reverse transcriptase, 1 µg of RNA and variable amount of nuclease free water to make up the final volume (Table 4.1). In addition, a no reverse template control reaction was also set up which excluded the reverse transcriptase (Table 4.1). The samples were then transferred to a thermal cycler and the following program was used: 10 min at 25ºC for priming, 15 min at 42ºC for reverse transcription and lastly, 5 min at 85ºC for reverse transcription inactivation.

Table 4.1: Complete reaction conditions for cDNA synthesis

Reagent	cDNA Synthesis Reaction (µL)	NRT Control Reaction (µL)
5x TransAmp Buffer	4	4
Reverse Transcriptase	1	0
RNA (1 µg)*	Variable	Variable
Nuclease free H$_2$O	Variable	Variable
Final reaction volume	20 µL	20 µL

* The volume of RNA used for each sample varied so that every reaction contained only 1 µg of RNA

4.3.7 Reverse Transcription – quantitative Polymerase Chain Reaction (RT-qPCR)

RT-qPCR was performed on a LightCycler 480 II instrument (Roche, Basel, Switzerland) which was programmed as follows: denaturation at 95°C for 5 min, 45 cycles of amplification at 95°C for 30 seconds, 62°C for 30 seconds, 72°C for 30 seconds. After amplification, a melt curve was performed at 95°C for 30 seconds, 40°C for 30 seconds, and ramped at 0.11°C/seconds. A final reaction volume of 10 µL was used. The 10 µL amplification reaction contained LightCycler® 480 SYBR Green I Master Mix (Roche, Basel, Switzerland), 400 nM of each primer (IDT, Coralville, IA, USA) and template (Table 4.2). A cDNA template concentration of 20 ng/µL was used. Primer sequences for *PPARG* and reference genes can be found in Table 4.3.

Table 4.2: Complete reaction conditions for RT-qPCR

Reagents	Stock	Quantity 1 x Reaction	Volume (µL) 1 x Reaction
dH$_2$O	-	-	2.2
SYBR Green Master Mix	2 x	1 x	5
F Primer	10 µM	400 nM	0.4
R Primer	10 µM	400 nM	0.4
cDNA (20 ng/µL)	-	-	2
Total Volume	-	-	10

Gene	Forward Sequence 3' to 5'	Reverse Sequence 3' to 5'
PPARG	CGTGGATCTCTCCGTAAT	TGGATCTGTTCTTGTGAATG
PPIA	CCGAAACGCCGAATATAA	GGACTGTTCTTCACTCTTG
TBP	GAGTTAAGAGTGTTGATGTAGG	CCTGGGACTGGAAAGTAA
YWHAZ	TGACATTGGGTAGCATTAAC	GCACCTGACAAATAGAAAGA

4.3.7.1 Data analysis

Relative gene expression was calculated using the comparative C_T method with slight modification (Equation 5). Instead of assuming amplification efficiency (E) of 2, the amplification efficiency of each gene analysed was determined by making use of a standard curve. Relative fold-increase (RFI) in gene expression (ΔC_T) is reported as an increase in gene expression relative to three reference genes as well as relative to the not induced cells ($\Delta\Delta C_T$). Reference genes refer to genes that are stably expressed in the cell/tissue of interest independent of experimental conditions.

4.3.7.2 Statistical analysis

A non-parametric Mann-Whitney test was used to compare the means between the different time points. The significance level was set to $\alpha = 0.05$ and a p-value < 0.05 were considered statistically significant. The degree of association between PPARG expression and Nile red positive staining events was tested using Spearman correlation and linear regression analysis was used to determine whether the relationship between the two variables was linear.

4.4 Results & Discussion

Adipogenesis is complex process in which adipocyte precursors differentiate into lipid laden adipocytes (7, 8). *In vitro*, the adipogenic pathway can be investigated by making use of cell lines such as the 3T3-L1 mouse cell line or by means of primary cells such as mesenchymal stromal cells (4). *In vitro* adipogenic differentiation can be induced using adipogenic differentiation medium that contains compounds such as insulin, dexamethasone and isobutylmethylxanthine (IBMX), known to activate adipogenesis-associated genes. Dexamethasone and IBMX are able to increase C/EBPβ and C/EBPδ expression which lead to PPARγ activation, while insulin activates SREBP1c (26).

In this study, four hASC primary cultures from independent donors and four hWJSC primary cultures from independent donors were induced to undergo adipogenesis over a 21-day culture period. Adipogenic differentiation potential and cell viability were monitored on days 0, 1, 3, 7, 14 and 21. Cell viability was determined by flow cytometry. An average of 87.78% ± 2.41% of hASCs analysed was viable while an average of 88.59% ± 3.25% of hWJSCs were viable.

With regard to adipogenic differentiation potential, fluorescence microscopy was used to visualize the accumulation of lipid droplets (Figure 4.4). Images were captured from three individual fluorescence channels and converted into an overlay image (Figure 4.4). The first image was captured using Filter Set 49 (Excitation G 365 nm; Emission BP 445/50 nm) to visualize nuclei stained with VDC Violet (Figure 4.4 A). Due to the ability of Nile Red to shift its emission spectrum depending on the lipophilic environment, two different fluorescent channels were used to visualize lipid droplet formation after staining with Nile Red (Figure 4.4 A&B). The second image was acquired using Filter Set 9 (Excitation BP 450-490 nm; Emission LP 515 nm) to visualize yellow-green fluorescence (Figure 4.4 B) and a third single channel image was captured using Filter Set 00 (Excitation BP 530-585 nm; Emission LP 615 nm) to visualize deep-red fluorescence emission (Figure 4.4 C), respectively.
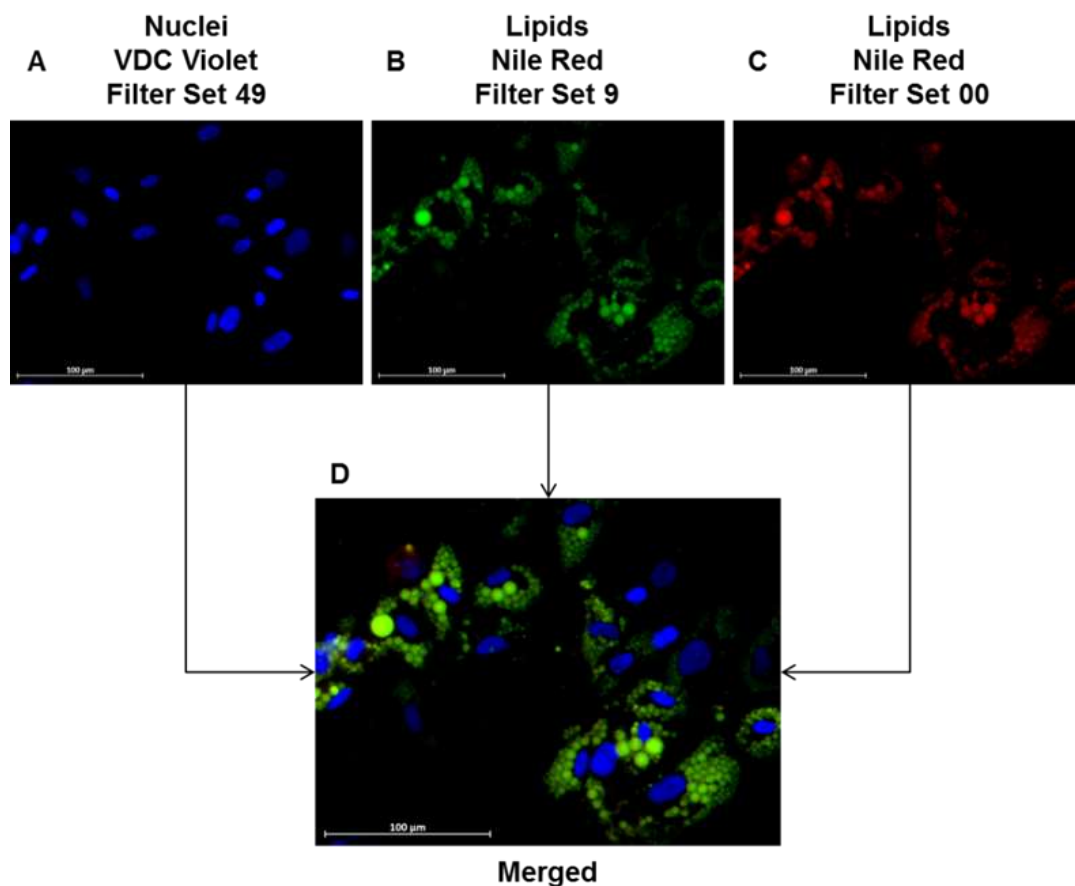
Figure 4.4: Fluorescence Microscopy Imaging. Cells were simultaneously stained with two dyes – Nile Red which is a lipophilic dye staining intracellular lipid droplets that can be detected in two channels (yellow green & red) and VDC Violet a nuclear stain detected in the blue channel. **A.** Nuclei stained with VDC Violet were detected using the blue channel (Filter set 49). **B.** Intracellular neutral lipid droplets stained with Nile Red and were detected using yellow-green channel (Filter Set 9). **C.** Lipids visualized with Nile Red using the deep red detection channel (Filter Set 00) which is mainly used for the detection of phospholipids. D: All three images (A, B and C) merged.

Fluorescence microscopy images revealed that hASCs accumulate intracellular lipids faster than hWJSCs. Lipid droplet formation in hASCs was visible from day 3 (Figure 4.5) whereas hWJSCs lipid accumulation only starts to become clearly visible around day 14 (Figure 4.6). Another difference observed was the percentage of cells in a given culture that differentiated into adipocytes. Very few hWJSCs displayed intracellular lipid accumulation (Figure 4.6 E & F), while a noticeably larger number of hASCs were able to differentiate into adipocytes (Figure 4.5 E & F). Throughout the 21-day induction period, none of the cells acquired the typical white adipocyte phenotype of a unilocular lipid droplet; this is however not uncommon for

adipogenic differentiation *in vitro* and has been observed by several other investigators (9, 27). It is important to note that the absence of a unilocular lipid droplet does not mean that the cells were unsuccessful in obtaining the mature adipocyte phenotype. There are several differences between the *in vitro* and *in vivo* environment such as the lack of an extracellular matrix that could result in the cells appearing morphologically different (9, 28)*.* However, future experiments should consider confirming that the hASCs differentiated into white or beige adipocytes by verifying Myf5 and UCP1 gene expression levels. White adipocytes should be negative for Myf5 and UCP1 whereas beige adipocytes are also Myf5 negative but express UCP1. Given the fact that multilocular beige and brown adipocytes require more than the induction stimulants provided in the adipogenic differentiation cocktail to which the cells were exposed, it is unlikely that the hASCs differentiated into these adipocytes. Brown and beige adipocyte differentiation requires additional stimulation such as cold exposure and PPARγ ligands (29).

Overall, at the end of the 21-day induction period it was clear that hASCs exhibit a greater adipogenic differentiation potential in comparison to hWJSCs. This was also reflected by the flow cytometry data (Figure 4.10).
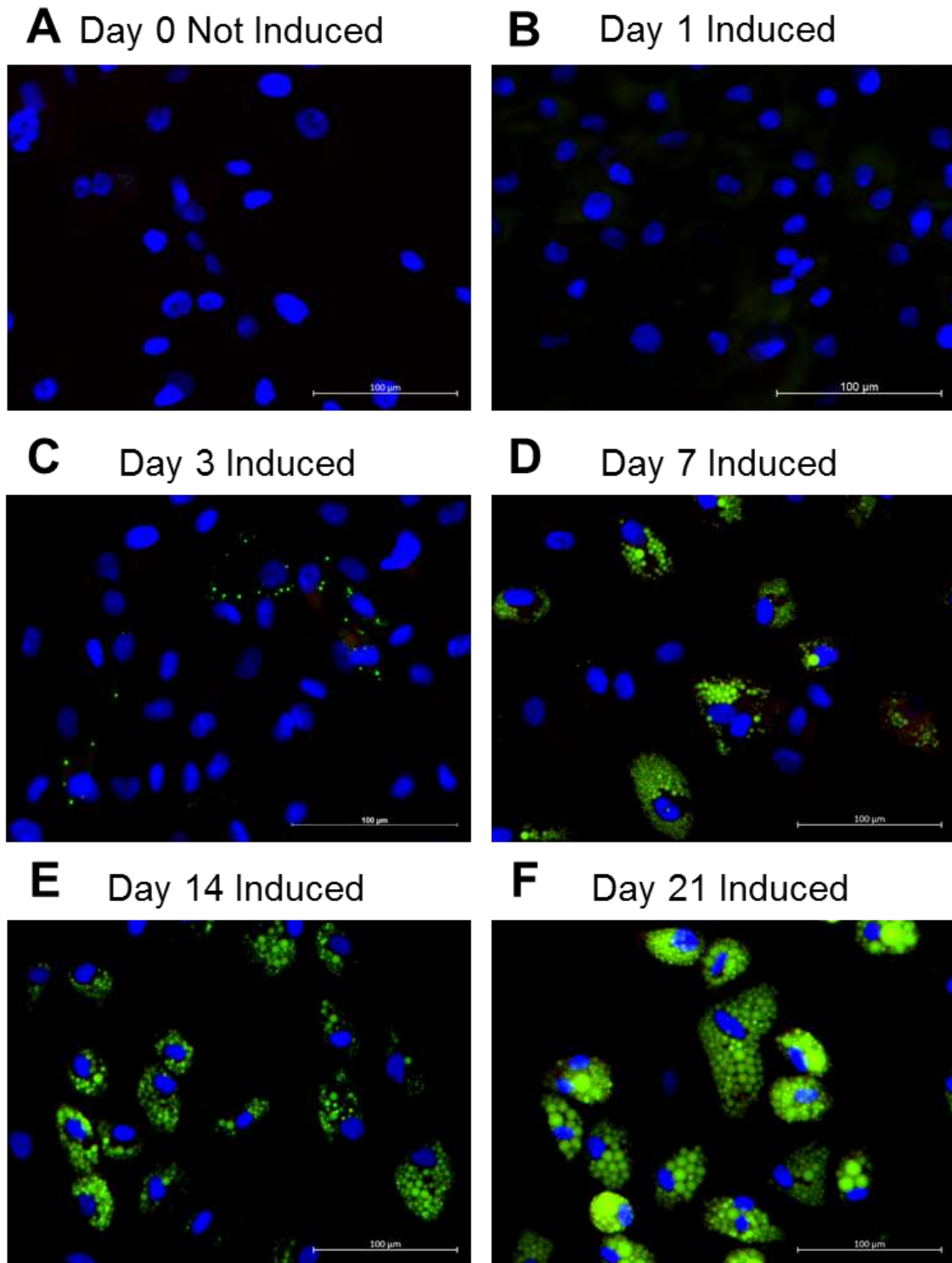
Figure 4.5: Representative fluorescence microscopy images of adipogenic differentiation of hASCs monitored over a period of 21 days. hASCs were induced to undergo adipogenesis for a period of 21 days. Images were captured on days 0, 1, 3, 7, 14 and 21. Cells were stained with a nuclear stain, VDC Violet, which is shown in blue and Nile Red, a lipophilic dye, shown in green. Scale bars: 100 µm. Magnification: 20x.
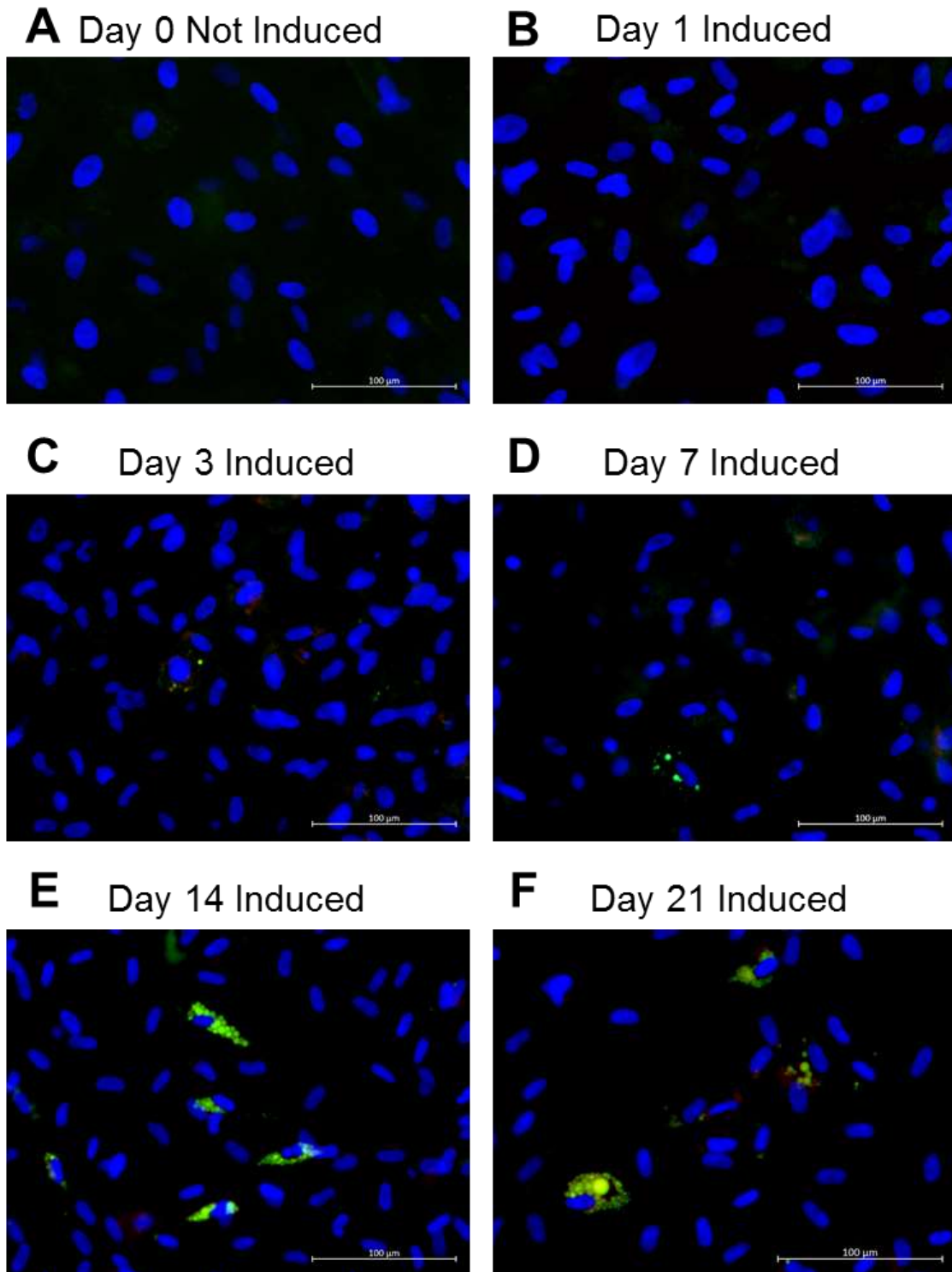
Figure 4.6: Representative fluorescence microscopy images of adipogenic differentiation of hWJSCs monitored over a period of 21 days. The hWJSCs were induced to undergo adipogenesis for a period of 21 days. Images were captured on days 0, 1, 3, 7, 14 and 21. Cells were stained with a nuclear stain, VDC Violet, which is shown in blue and Nile Red, a lipophilic dye, shown in green. Scale bars: 100 μm. Magnification: 20x.

With regard to the non-induced cells that were maintained in parallel to the induced cells as controls, no lipid droplet formation was visible at any time point (Figure 4.7 and Figure 4.8)
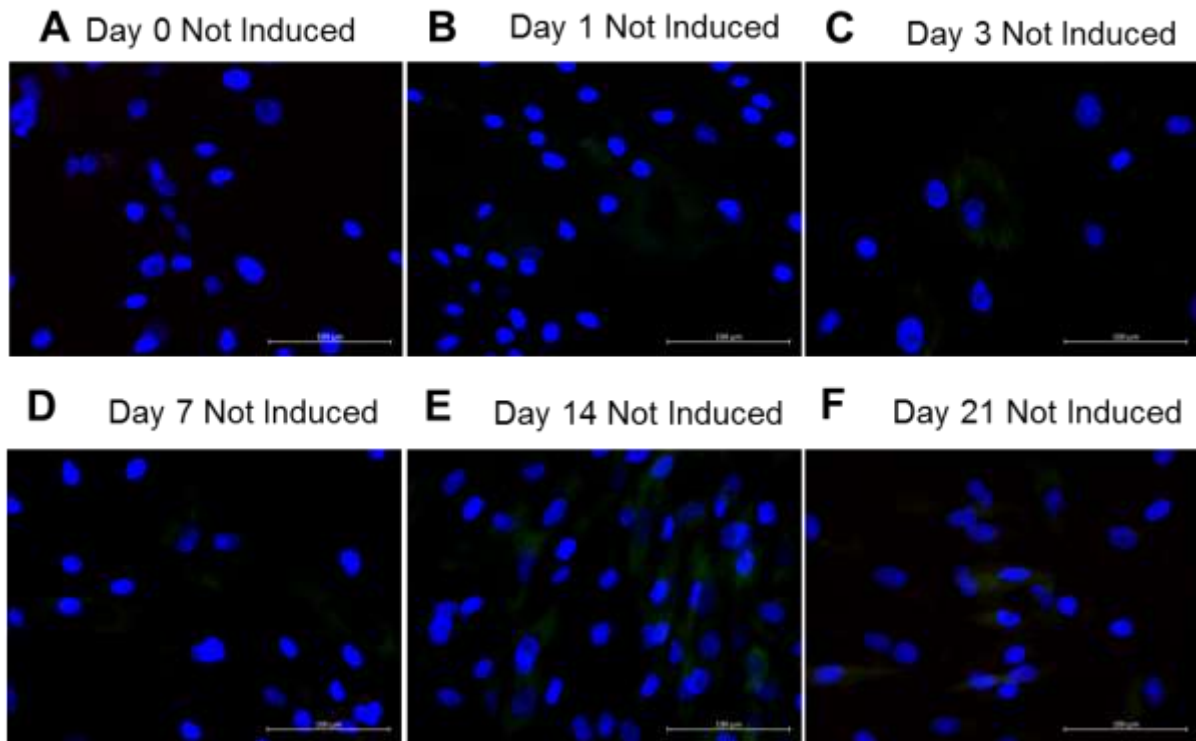
Figure 4.7: Representative fluorescence microscopy images of non-induced hASCs over a culture period of 21 days. The hASCs not exposed to adipogenic differentiation culture medium served as undifferentiated controls. Cells were cultured for a period of 21 days. Images were captured on days 0, 1, 3, 7, 14 and 21. Cells were stained with a nuclear stain, VDC Violet, which is shown in blue and Nile Red, a lipophilic dye. Scale bars: 100 µm. Magnification: 20x.
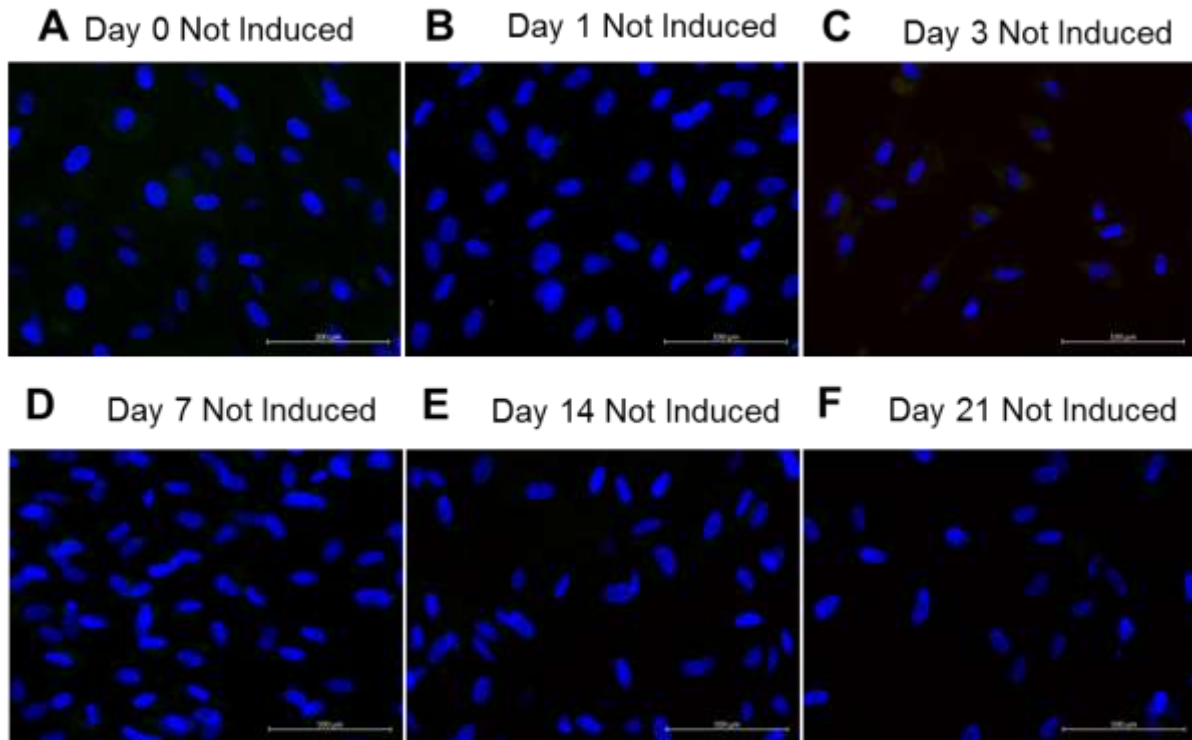
Figure 4.8: Representative fluorescence microscopy images of non-induced hWJSCs over a period of 21 days. The hWJSCs, not exposed to adipogenic differentiation culture medium served as undifferentiated controls. Cells were cultured for a period of 21 days. Cells were stained with a nuclear stain, VDC Violet, which is shown in blue and Nile Red, a lipophilic dye. Scale bars: 100 µm. Magnification: 20x.

In order to obtain more quantitative results to support and confirm the qualitative observations made using fluorescence microscopy, the proportion of cells that underwent adipogenic differentiation were quantified using a Nile red-based flow cytometric assay. Adipogenesis is associated with intracellular accumulation of lipid droplets which can be quantified through Nile Red staining (27, 30) which stains neutral lipids with high affinity. The lipid core that accumulates intracellularly in droplets during adipocyte differentiation consists mainly of neutral lipids, such as cholesterol esters and triacylglycerol (31). Increased Nile red-positive hASCs therefore indicate an increase in the number of differentiating / differentiated cells.

However, adipocytes are fragile cells that can easily shed their lipid droplets when handled harshly. Therefore, in order to exclude any free-floating lipid droplets that may have been shed during sample preparation, cells were co-stained with a nuclear stain VDC Violet. Only nucleated cells that simultaneously stained positive for Nile

Red and VDC Violet were quantified as differentiated cells. In order to do so, the following gating strategy was followed: Firstly, a one parameter (count vs VDC Violet / FL9 [Excitation 405nm; Emission 450/40 BP]) plot was created to visualise VDC Violet positive events i.e. nucleated cells (Figure 4.9 A and D). A two parameter (FS Lin vs SS Log) plot, gated on VDC Violet positive events, was then used to visualise the nucleated cells being analysed ("Total cells" region) (Figure 4.9 B and E). Lastly, a two parameter (FS Lin vs Nile Red / FL2 [Excitation: 488nm; Emission 575/30 BP]) plot was created, gated on region "Total cells" in order to quantify the Nile Red positive nucleated cells. The "NR+ cells" region was set using the non-induced cells (Figure 4.9 C) as a set up control. As seen in Figure 4.99 E and F, the Nile Red-positive differentiated cells / adipocytes shift to the right along the Y-axis of both graphs. In Figure 4.9 E, the SS Log shift is contributed to the increasing complexity of the cells caused by the accumulation of intracellular lipid droplets. In Figure 4.99 F, the Nile Red shift displays the Nile Red positive events i.e. differentiated cells/adipocytes.
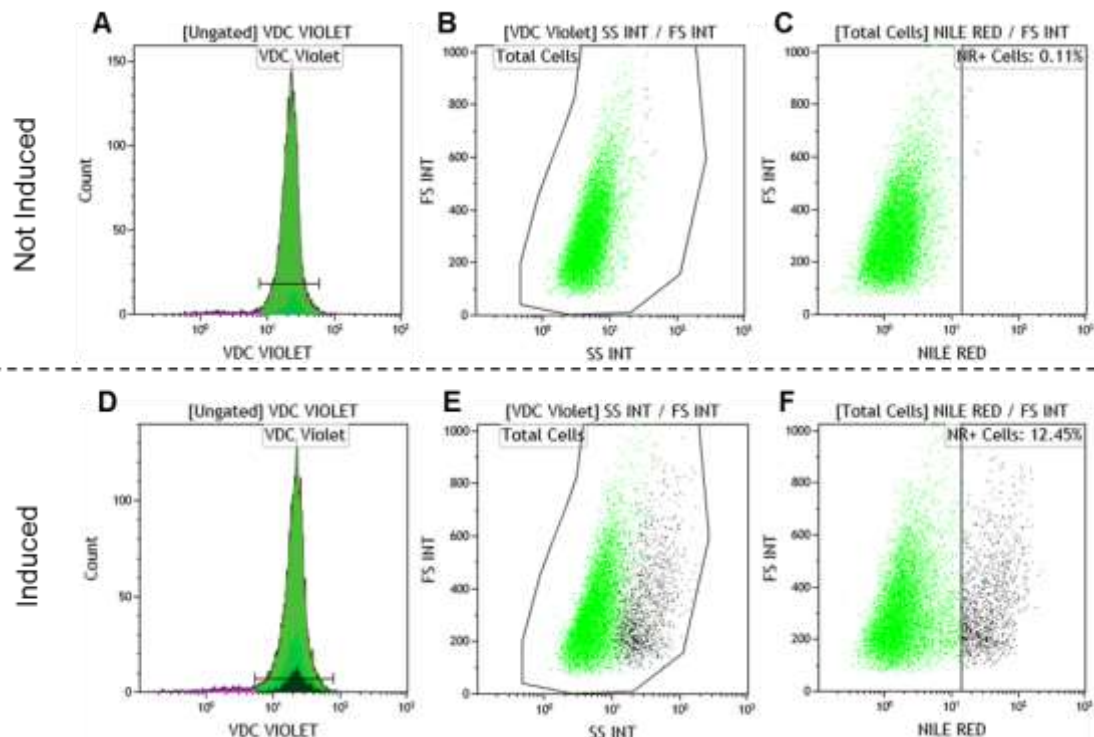
Figure 4.9: Flow cytometry set up for Nile Red Assay. **A - C.** Non-induced cells. **D - F.** Induced cells. **A & D.** VDC Violet positive events (nucleated cells) are visualised. **B & E.** Intact nucleated cells are visualised in region "Total Cells". **C & F**. Cells that contain intracellular lipids are detected in region "NR+

Cells". The events shown in black represent cells with increased intracellular lipid levels i.e. differentiated cells.

At day 21, 28.50% ± 2.91% of the hASCs were able to undergo adipocyte differentiation, while only 2.91% ± 2.72% of hWJSCs were able to undergo adipogenic differentiation after 21 days. These findings are in line with what has previously been reported in literature. Several studies reported less efficient adipogenic differentiation in hWJSCs compared to hASCs (32-35).

The mean percentage of Nile Red positive events for the non-induced cells was 1.31% ± 0.11% for the hASCs and 0.44% ± 0.05% for the hWJSCs. Statistically significant increase in hASCs that stain positive with Nile Red was observed at days 7 (10.07% ± 3.19; p = 0.0286), 14 (24.08% ± 4.02%; p = 0.0286) and 21 (28.50% ± 2.72%; p = 0.0286) when compared to day 0 non-induced cells (0.81% ± 0.26) (Figure 4.10). Comparing induced cells with non-induced cells (day 0 = 0.81% ± 0.26; day 1 = 1.18% ± 0.27%; day 3 = 0.71% ± 0.40%; day 7 = 1.30% ± 0.17%; day 14 = 1.73% ± 0.46%; day 21 = 2.12% ± 0.44%) at each time point , statistical significance was observed at days 7 (p = 0.0286), 14 (p = 0.0286) and 21 (p = 0.0286) (Figure 4.10). With regards to the hWJSC cultures, the only statistical significant increase was observed for induced cells at day 14 (3.90% ± 1.92%; p = 0.0286) when compared to day 0 (0.18% ± 0.05%) (Figure 4.11). The lack of statistical significance for this data set at day 21 (6.09% ± 2.72%) is most likely due to the high intra-culture variability observed at this specific time point (Figure 4.11). Lastly, the proportion of cells that underwent adipogenic differentiation differed significantly on days 7 (p = 0.0286), 14 (p = 0.0286) and 21 (p = 0.0286) when the induced hASCs and hWJSCs cultures were compared to one another (Figure 4.12).

It was noted that there is variability in the adipogenic differentiation potential between cultures. Not all hASC and hWJSC cultures showed the same adipogenic differentiation potential (Figure 4.12). The intra culture variability observed may be due to intra-donor variability. A number of patient-specific factors have been identified which may affect hASC differentiation and proliferation, such as age, body mass index (BMI), diabetes mellitus and exposure to radiotherapy (36-38). With regard to the hWJSCs, the intra culture variability was not as noticeable as seen with

the hASCs. This is likely to be due to the inability of these cells to optimally undergo adipogenic differentiation.
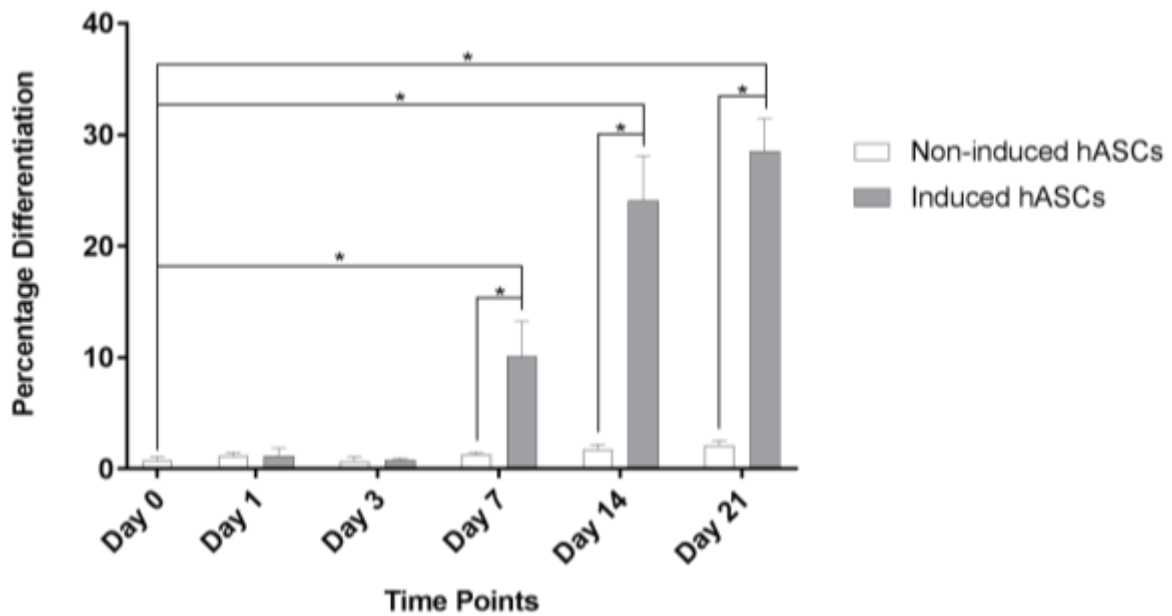
Figure 4.10: Adipogenic differentiation of hASCs. Mean ± SEM percentage of cells that stained positive for Nile Red. Statistical significance between points is displayed with an asterisk. * P < 0.05
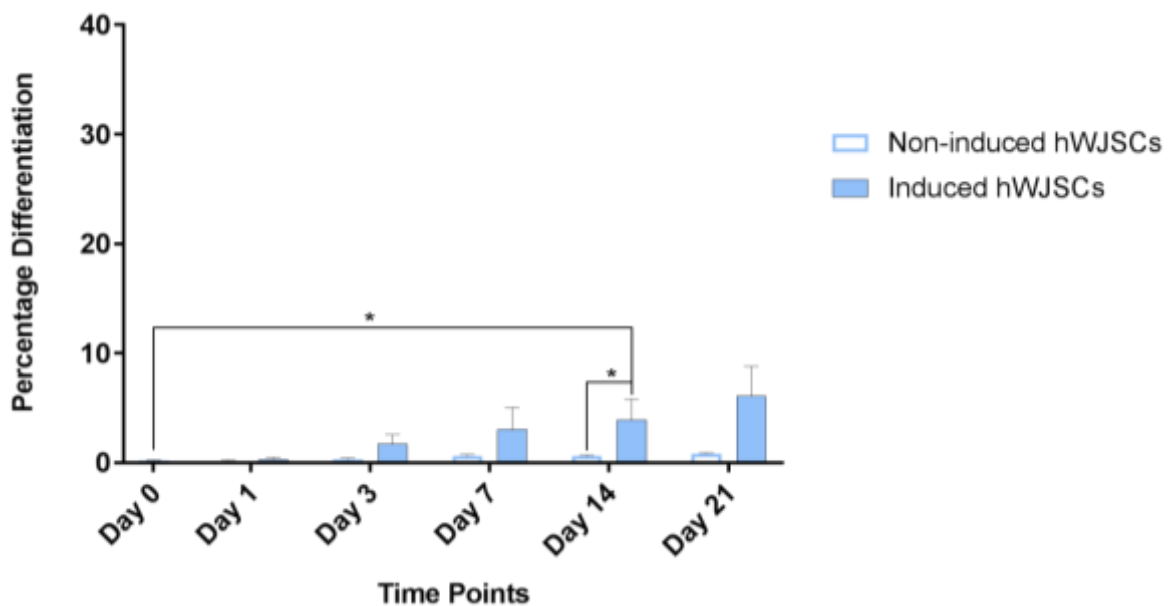
Figure 4.11: Adipogenic differentiation of hWJSCs. Mean ± SEM percentage of cells that stained positive for Nile Red. Statistical significance between points is displayed with an asterisk. The scaling of the y-axis was kept the same as used in Figure 3.10 as this clearly illustrate the different levels of adipogenic differentiation observed in the two different cells type. * P <0.05
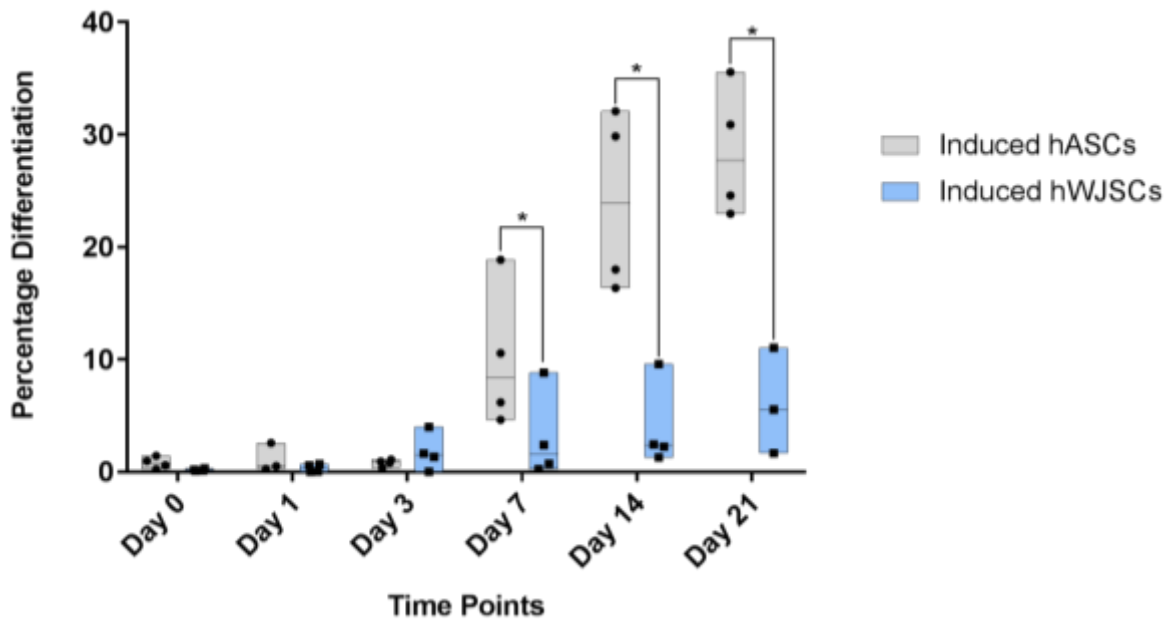
Figure 4.12: Minimum/maximum floating bar graph representing the percentage differentiation in hASCs vs hWJSCs. Percentage of cells that stained positive for Nile Red is displayed. Each dot or square within the floating bars represents a different culture. The horizontal lines within the bars represent the population median. Four independent hASC and hWJSC cultures were included in the study. Statistical significance between the two cell types at the various time points are displayed with an asterisk. *P <0.05

As mentioned before, *PPARG* is a key regulator of adipogenesis (5) and was used in this study to determine up-regulation of adipogenic associated genes. The focus of this study was on Pref-1, which has been suggested to be an early regulator of adipogenic differentiation. In this chapter, adipogenic differentiation of hASCs and hWJSCs was introduced and discussed. For this reason, only the gene expression results of the master regulator, PPARG, is discussed in this chapter. Early regulators, including Pref1 and Sox9, will be discussed in Chapter 5. Both hASC and hWJSC induced cells showed higher levels of *PPARG* gene expression when normalized to non-induced day 0 cells (Table 4.4). This confirms that the induction medium used provided the necessary signals for both cell types (hASCs and hWJSCs) to undergo adipogenesis.

However, a high degree of variability was observed between data points at the different time points (Table 4.4 and Figure 4.13). The primer used to detect *PPARG* expression is capable of detecting both *PPARG* isoforms. Isoform 1 is commonly expressed in most cell types whereas isoform 2 is adipose tissue specific (39).

Future experiments should include a primer of higher specificity for the detection of isoform 2, whose expression is of greater significance when investigating adipogenesis. Being able to detect both isoforms may have contributed to the variability observed in the results.

Interestingly, a very high relative fold increase in *PPARG* was observed at Day 7 in hWJSC cultures 1 and 2 (Table 4.5). The hWJSC culture 2 also showed very high *PPARG* expression at day 14 (Table 4.5). We suspected that high levels of *PPARG* potentially coincide with an increase in Nile red staining i.e. an increase in the number of cells undergoing adipogenesis. Thus, we decided to compare the relative *PPARG* expression to Nile red staining as shown in Table 4.5 and Table 4.6. We also investigated the relationship (correlation) between intracellular lipid accumulation and *PPARG* gene expression levels (Figure 4.17). In hASCs, we saw a good correlation (Spearman r = 0.7) between intracellular lipid accumulation (Nile Red positive) and *PPARG* gene expression levels (Figure 4.16 A). This relationship was linear (Spearman correlation = 1.0; linear regression r^2 = 0.999) between Day 3 and Day 14 (Figure 4.16 B). The correlation between lipid accumulation and *PPARG* expression was less convincing (Spearman correlation = 0.4) in the hWJSCs (Figure 4.16 C). Due to the variability observed it would be important to repeat these experiments in the future to prove the validity of these findings. Unfortunately, due to time and reagent constraints this was not possible in this study. Increasing the sample size from n=3 to perhaps n=5 would also allow for a more accurate representation of *PPARG* expression data in the two cell types. No statistical significance was observed for this data set. This was likely to be due to the variance observed.

Table 4.4: PPARG expression in hASCs and hWJSCs.

Time Point	hASCs				hWJSCs			
	1	2	3	Mean ± SEM	1	2	3	Mean ± SEM
Day 1	1.34	1.67	1.82	1.61±0.14	1.47	7.09	0.90	3.15±1.98
Day 3	6.96	2.52	0.99	3.49±1.79	5.19	7.98	0.40	4.52±2.21
Day 7	5.69	6.42	4.52	5.43±0.55	35.72	87.03	0.87	41.20±25.02
Day 14	17.12	5.49	4.02	8.87±4.14	2.02	1007.89	NA*	504.96±502.93
Day 21	9.75	2.15	2.25	4.71±2.52	5.04	0.00	1.31	2.12±1.51

*NA – Could not synthesize cDNA for this sample due insufficient RNA. Results are expressed as fold increase relative to non-induced cells
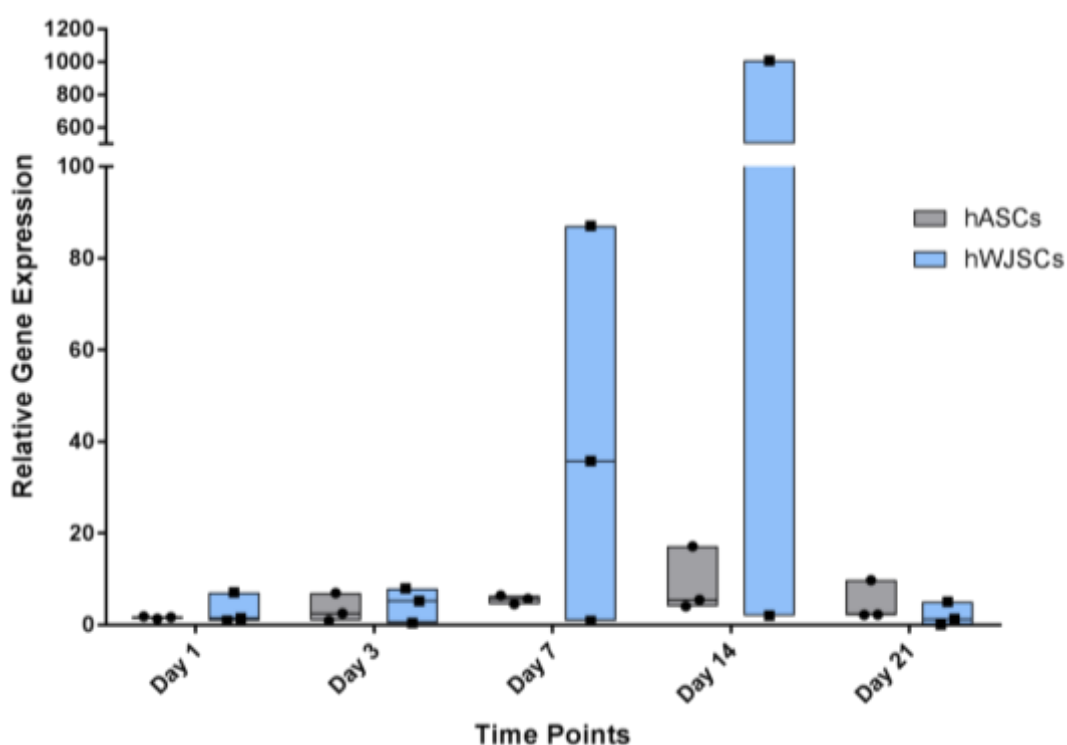
Figure 4.13: Relative mRNA expression of *PPARG* in hASCs and hWJSCs. *PPARG* expression relative to non-induced cells at each time point is displayed. Each dot (hWJSCs) or square (hASCs) within the floating bars represents a different culture. The horizontal lines within the bars represent the median. Three independent hASC and hWJSC cultures were included in the study.

Table 4.5: Relative PPARG mRNA expression in comparison to percentage of Nile red positive events at each time point for hASCs

	1		2		3		Mean ± SEM	
	PPARG	**NR**	**PPARG**	**NR**	**PPARG**	**NR**	**PPARG**	**NR**
Day 1	1.34	0.26	1.67	0.53	1.82	NA*	1.61±0.14	1.12±0.73
Day 3	6.96	0.38	2.52	1.10	0.99	0.79	3.49±1.79	0.80±0.15
Day 7	5.69	10.56	6.42	18.88	4.52	4.64	5.43±0.55	10.07±3.19
Day 14	17.12	29.85	5.49	32.09	4.02	18.01	8.87±4.14	24.08±4.02
Day 21	9.75	30.90	2.15	35.57	2.25	25.54	4.71±2.52	28.50±2.91

*NA – Data could not be collected. PPARG results are expressed as fold increase relative to non-induced cells

Table 4.6: Relative PPARG mRNA expression in comparison to percentage of Nile red positive events at each time point for hWJSCs

	1		2		3		Mean ± SEM	
	PPARG	**NR**	**PPARG**	**NR**	**PPARG**	**NR**	**PPARG**	**NR**
Day 1	1.47	0.02	7.09	0.03	0.90	0.57	3.15±1.98	0.33±0.18
Day 3	5.19	4.00	7.98	0.02	0.40	1.34	4.52±2.21	1.75±0.83
Day 7	35.72	8.83	87.03	0.24	0.87	0.72	41.20±25.02	3.05±1.98
Day 14	2.02	9.59	1007.89	1.29	NA*	2.26	504.96±502.93	3.90±1.92
Day 21	5.04	NA *	0.00	1.67	1.31	5.55	2.12±1.51	6.09±2.72

*NA – Data could not be collected. PPARG results are expressed as fold increase relative to non-induced cells
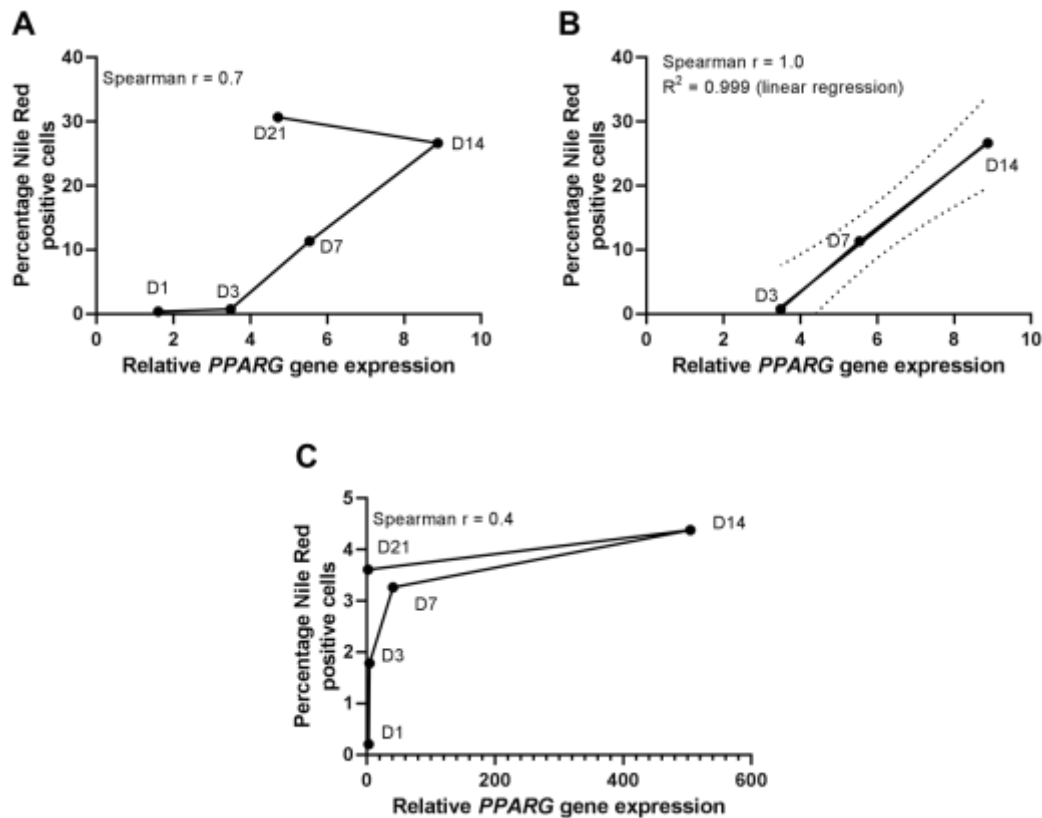
Figure 4.14: Degree of association between PPARG expression and Nile red positive staining events. A. Spearman correlation was used to test the degree of correlation between PPARG expression and Nile Red positive cells in hASCs. **B.** Based on the results obtained in A, linear regression was used to determine whether there is a linear relationship between days 3, 7 and 14. **C.** Spearman correlation was used to test the degree of correlation between PPARG expression and Nile Red positive cells in hWJSCs.

4.5 Conclusion

Our data confirms that hASCs have a greater adipogenic differentiation potential when compared to hWJSCs. These findings are in line with what has been previously stated in literature (32-35). Fluorescence microscopy images show that hASCs start to accumulate lipid droplets earlier than hWJSCs (Figure 4.5 and Figure 4.6). By the end of the 21 day adipogenic differentiation period, a significantly greater proportion of hASCs differentiate into adipocytes (Figure 4.12). At Day 21, a mean differentiation of 28.50% ± 2.91% was observed for hASCs whereas only 2.91% ± 2.72% of hWJSCs showed adipogenic differentiation (Figure 4.10 and Figure 4.11). It is important to note that both cells types were seeded at the same density and

treated under the same conditions. Lastly, gene expression analysis shows upregulation of *PPARG*, a key regulator of adipogenesis in both cell types. A good correlation was observed between intracellular lipid accumulation and *PPARG* gene expression in hASCs (Figure 4.14 A&B), but not in hWJSCs (Figure 4.14 C). The reason for the lack of adipocyte differentiation observed in hWJSCs despite *PPARG* upregulation is currently unknown and requires further investigation.

The exact reason for the poor adipogenic differentiation observed for hWJSCs are not clear, but it is possible that it is linked to the CD36 expression results presented in Chapter 3. In Chapter 3 we showed that CD36 expression is not upregulated in hWJSCs during adipogenic differentiation. It is known that CD36 expression is important during adipogenesis as it plays a role in the internalization of lipids (40).

4.6 References

1. Moseti D, Regassa A, Kim WK. Molecular Regulation of Adipogenesis and Potential Anti-Adipogenic Bioactive Molecules. Int J Mol Sci. 2016;17(1).

2. Nae S, Bordeianu I, Stancioiu AT, Antohi N. Human adipose-derived stem cells: definition, isolation, tissue-engineering applications. Rom J Morphol Embryol. 2013;54(4):919-24.

3. Zhang Y, Sowers JR, Ren J. Targeting autophagy in obesity: from pathophysiology to management. Nat Rev Endocrinol. 2018;14(6):356-76.

4. Janderova L, McNeil M, Murrell AN, Mynatt RL, Smith SR. Human mesenchymal stem cells as an in vitro model for human adipogenesis. Obes Res. 2003;11(1):65-74.

5. Mota de Sa P, Richard AJ, Hang H, Stephens JM. Transcriptional Regulation of Adipogenesis. Compr Physiol. 2017;7(2):635-74.

6. Ruiz-Ojeda FJ, Ruperez AI, Gomez-Llorente C, Gil A, Aguilera CM. Cell Models and Their Application for Studying Adipogenic Differentiation in Relation to Obesity: A Review. Int J Mol Sci. 2016;17(7).

7. Sarjeant K, Stephens JM. Adipogenesis. Cold Spring Harb Perspect Biol. 2012;4(9):a008417.

8. Ali AT, Hochfeld WE, Myburgh R, Pepper MS. Adipocyte and adipogenesis. Eur J Cell Biol. 2013;92(6-7):229-36.

9.   Lynes MD, Tseng YH. Deciphering adipose tissue heterogeneity. Ann N Y Acad Sci. 2018;1411(1):5-20.

10.   Rosen ED, Walkey CJ, Puigserver P, Spiegelman BM. Transcriptional regulation of adipogenesis. Genes Dev. 2000;14(11):1293-307.

11.   Tang QQ, Lane MD. Adipogenesis: from stem cell to adipocyte. Annu Rev Biochem. 2012;81:715-36.

12.   Cornelius P, MacDougald OA, Lane MD. Regulation of adipocyte development. Annu Rev Nutr. 1994;14:99-129.

13.   Yuste R. Fluorescence microscopy today. Nat Methods. 2005;2(12):902-4.

14.   Sanderson MJ, Smith I, Parker I, Bootman MD. Fluorescence microscopy. Cold Spring Harb Protoc. 2014;2014(10):pdb top071795.

15.   Ryding S. Flow Cytometry vs. Fluorescence Microscopy News-Medical.Net2018 [updated 20 November 2018. Available from: https://www.news-medical.net/life-sciences/Flow-Cytometry-vs-Fluorescence-Microscopy.aspx#.

16.   Macey MG. Flow cytometry: principles and clinical applications. Med Lab Sci. 1988;45(2):165-73.

17.   Adan A, Alizada G, Kiraz Y, Baran Y, Nalbant A. Flow cytometry: basic principles and applications. Crit Rev Biotechnol. 2017;37(2):163-76.

18.   Wang Y, Sul HS. Pref-1 regulates mesenchymal cell commitment and differentiation through Sox9. Cell Metab. 2009;9(3):287-302.

19.   Valasek MA, Repa JJ. The power of real-time PCR. Adv Physiol Educ. 2005;29(3):151-9.

20.   Cao H, Shockey JM. Comparison of TaqMan and SYBR Green qPCR methods for quantitative gene expression in tung tree tissues. J Agric Food Chem. 2012;60(50):12296-303.

21.   VanGuilder HD, Vrana KE, Freeman WM. Twenty-five years of quantitative PCR for gene expression analysis. Biotechniques. 2008;44(5):619-26.

22.   Arya M, Shergill IS, Williamson M, Gommersall L, Arya N, Patel HR. Basic principles of real-time quantitative PCR. Expert Rev Mol Diagn. 2005;5(2):209-19.

23.   Rao X, Huang X, Zhou Z, Lin X. An improvement of the 2^(-delta delta CT) method for quantitative real-time polymerase chain reaction data analysis. Biostat Bioinforma Biomath. 2013;3(3):71-85.

24. Fink T, Lund P, Pilgaard L, Rasmussen JG, Duroux M, Zachar V. Instability of standard PCR reference genes in adipose-derived stem cells during propagation, differentiation and hypoxic exposure. BMC Mol Biol. 2008;9(1):98.

25. Li X, Yang Q, Bai J, Xuan Y, Wang Y. Identification of appropriate reference genes for human mesenchymal stem cell analysis by quantitative real-time PCR. Biotechnol Lett. 2015;37(1):67-73.

26. Sugimoto R, Ishibashi-Ohgo N, Atsuji K, Miwa Y, Iwata O, Nakashima A, et al. Euglena extract suppresses adipocyte-differentiation in human adipose-derived stem cells. PLoS One. 2018;13(2):e0192404.

27. Durandt C, van Vollenstee FA, Dessels C, Kallmeyer K, de Villiers D, Murdoch C, et al. Novel flow cytometric approach for the detection of adipocyte subpopulations during adipogenesis. J Lipid Res. 2016;57(4):729-42.

28. Zhang S, Wang Y, Cui L, Deng Y, Xu S, Yu J, et al. Morphologically and Functionally Distinct Lipid Droplet Subpopulations. Sci Rep. 2016;6:29539.

29. Ikeda K, Maretich P, Kajimura S. The Common and Distinct Features of Brown and Beige Adipocytes. Trends Endocrinol Metab. 2018;29(3):191-200.

30. Aldridge A, Kouroupis D, Churchman S, English A, Ingham E, Jones E. Assay validation for the assessment of adipogenesis of multipotential stromal cells--a direct comparison of four different methods. Cytotherapy. 2013;15(1):89-101.

31. Thiam AR, Beller M. The why, when and how of lipid droplet diversity. J Cell Sci. 2017;130(2):315-24.

32. Bieback K, Brinkmann I. Mesenchymal stromal cells from human perinatal tissues: From biology to cell therapy. World J Stem Cells. 2010;2(4):81-92.

33. Amable PR, Teixeira MV, Carias RB, Granjeiro JM, Borojevic R. Protein synthesis and secretion in human mesenchymal cells derived from bone marrow, adipose tissue and Wharton's jelly. Stem Cell Res Ther. 2014;5(2):53.

34. Ragni E, Vigano M, Parazzi V, Montemurro T, Montelatici E, Lavazza C, et al. Adipogenic potential in human mesenchymal stem cells strictly depends on adult or foetal tissue harvest. Int J Biochem Cell Biol. 2013;45(11):2456-66.

35. Fong CY, Subramanian A, Biswas A, Bongso A. Freezing of Fresh Wharton's Jelly From Human Umbilical Cords Yields High Post-Thaw Mesenchymal

Stem Cell Numbers for Cell-Based Therapies. J Cell Biochem. 2016;117(4):815-27.

36.   Varghese J, Griffin M, Mosahebi A, Butler P. Systematic review of patient factors affecting adipose stem cell viability and function: implications for regenerative therapy. Stem Cell Res Ther. 2017;8(1):45.

37.   Kirkland JL, Hollenberg CH, Gillon WS. Age, anatomic site, and the replication and differentiation of adipocyte precursors. Am J Physiol. 1990;258(2 Pt 1):C206-10.

38.   Pachon-Pena G, Serena C, Ejarque M, Petriz J, Duran X, Oliva-Olivera W, et al. Obesity Determines the Immunophenotypic Profile and Functional Characteristics of Human Mesenchymal Stem Cells From Adipose Tissue. Stem Cells Transl Med. 2016;5(4):464-75.

39.   Janani C, Ranjitha Kumari BD. PPAR gamma gene--a review. Diabetes Metab Syndr. 2015;9(1):46-50.

40.   Christiaens V, Van Hul M, Lijnen HR, Scroyen I. CD36 promotes adipocyte differentiation and adipogenesis. Biochim Biophys Acta. 2012;1820(7):949-56.

Chapter 5: Pref-1 Expression in hASCs and hWJSCs

5.1 Introduction

In 1993, Smas and Sul investigated novel regulators of adipogenesis using the mouse 3T3-L1 pre-adipocyte cell line and identified pre-adipocyte factor 1 (*Pref-1*) as a potential inhibitor of adipogenesis (1). High levels of *Pref-1* mRNA were found in pre-adipocytes, but were undetectable in mature adipocytes (1). Smas and Sul also reported that the sustained expression of the Pref-1 protein was able to inhibit adipogenesis. Since then, several investigators have investigated the role of Pref-1 in adipogenesis (2-8). Outcomes of some of these studies have been discussed in Chapter 2. The main consensus among investigators is that sustained high levels of Pref-1 expression are able to inhibit adipogenesis.

However, most work regarding the role of Pref-1 in adipogenesis has been conducted in murine models (2, 7, 9-12). More studies using cells of human origin are required in order to determine with confidence whether the findings of the murine-based studies are directly translatable to the human setting. The aim of this project was therefore to investigate adipogenesis using MSCs isolated from two sources (adipose tissue and umbilical cord-derived Wharton's jelly) and to determine if Pref-1 protein expression levels contribute to the difference in adipogenic potential of these two MSC sources. WJSCs have previously been shown to have poor adipogenic differentiation capacity (Reviewed in Chapter 2). In addition, previously generated gene expression data from our laboratory (results unpublished; study performed by Ms Karlien Kallmeyer, MSc student) suggested that *Pref-1* is expressed at higher levels in hWJSCs than in hASCs. The adipogenic differentiation potential and Pref-1 protein expression in hWJSCs was thus compared to that of hASCs which readily undergo adipogenic differentiation. *Pref-1* gene expression was also investigated to confirm and supplement the data generated by Ms Karlien Kallmeyer.

5.1.1 Pref-1 protein

During embryonic development, Pref-1 can be detected in a number of organs such as liver, ovaries, pancreas, tongue, placenta and pituitary glands (1, 13, 14). However, in adults the expression becomes restricted mainly to adipose tissue, adrenal glands, pancreas and peripheral blood (13, 15-18). In adipose tissue, pre-adipocytes, but not mature adipocytes, are the cells which are known to express high levels of Pref-1 (1, 19, 20).

The Pref-1 protein is a transmembrane protein expressed on the cell surface which is cleaved by tumour necrosis factor alpha converting enzyme (TACE) to gives rise to 25 kDa and 50 kDa soluble forms of the protein. Only the 50 kDa soluble protein has been shown to be biologically active and plays a role in the inhibition of adipogenesis (6, 21). (Protein structure and cleavage is reviewed in more detail in Chapter 2.) Several studies have suggest that the 50 kDa soluble Pref-1 protein acts as an inhibitor of adipogenesis by maintaining cells in a pre-adipocyte state (19, 20). The exact mechanism by which Pref-1 inhibits adipogenesis has not yet been fully elucidated (Reviewed in Chapter 2).

5.1.2 Link between Pref-1, Sox9 and adipogenesis

It has been suggested in literature that Pref-1 is capable of inhibiting adipogenesis through its interaction with Sex-Determining Region Box 9 (Sox9) (8). Sox9 is more commonly known for its role in chondrogenesis and osteogenesis (8). Studies have suggested that Pref-1 activates the expression of Sox9 during adipogenesis through the MEK/ERK pathway (19, 22). Once expressed, the Sox9 transcription factor binds to the promoter regions of *C/EBPβ* and *C/EBPδ* (8, 20), which prevents the activation of the two key pro-adipogenic factors, *PPARγ* and *C/EBPα*, resulting in inhibition of adipocyte differentiation (20). A more recent study showed that Sox9 inhibits adipogenesis through the activation of myeloid ectropic insertion site 1 (Meis1) which is also able to bind to the promoter regions of *C/EBPβ* and *C/EBPδ* preventing them from activating *C/EBPα* and *PPARγ* (23).

5.2 Techniques

In order to investigate the expression of Pref-1 in hASCs and hWJSCs, a number of techniques were employed.

5.2.1 Flow Cytometry

Flow cytometry was used to detect Pref-1 on the cell surface of hASCs and WJSCs. The basic principles of the technique were discussed in detail in Chapter 3, section 3.2.

5.2.2 Enzyme-linked immunosorbent assay

As mentioned in Chapter 2, the Pref-1 protein is capable of being cleaved from the cell surface by TACE resulting in the release of the active 50 kDa form of the protein into solution (19-21). Enzyme-linked immunosorbent assay (ELISA) allows for the detection and quantification of peptides, antibodies and hormones in solution (24). Thus, a sandwiched ELISA was performed using conditioned medium in an attempt to quantify soluble Pref-1 protein. Condition medium refers to culture medium in which the MSCs were cultured. The technique makes use of a 96-well plate in which the surface is coated with an antibody (capture antibody) that is capable of binding to the molecule of interest (Figure 5.1, steps 1 and 2). A second antibody (detection antibody) conjugated to biotin, is then added (Figure 5.1, step 3). The detection antibody also binds to the molecule of interest, but at a different epitope (Figure 5.1, step 3). An enzyme such as horse radish peroxidase (HRP) conjugated to streptavidin is then added to the wells (Figure 5.1, step 4). Biotin and streptavidin bind to each other with high affinity. A substrate solution, usually consisting of a 1:1 mixture of H_2O_2 and tetramethylbenzidine, is then added which results in a colorimetric reaction (Figure 5.1, step 5). The intensity of the colour is directly proportional to the amount of target molecule, Pref-1 protein in this study, present in the condition medium.
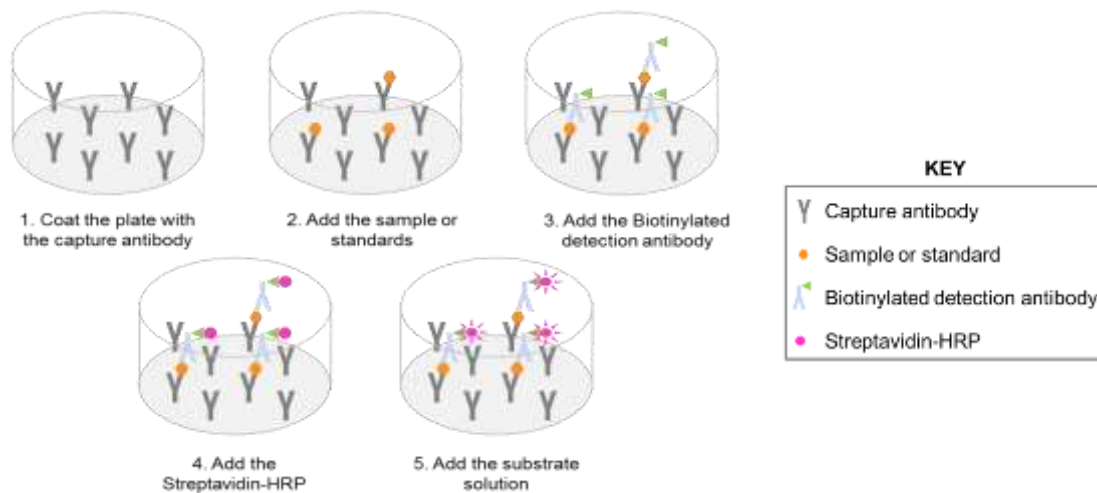
Figure 5.1: Illustration of the basic principles of a sandwiched ELISA assay.

5.2.3 Western Blot

Western blot was used to detect total Pref-1 protein (intracellular and membrane bound) as well as cleaved protein in conditioned media (Figure 5.2). This technique makes use of sodium dodecyl sulfate polyacrylamide gel electrophoresis (SDS-PAGE) to separate proteins, solely on their size. Protein structure and charge do not play a role as the SDS denatures the protein and gives it a negative charge. Once an electric current is applied, large proteins migrate slowly through the polyacrylamide gel while small proteins migrate faster. The proteins are then transferred from the gel to a nitrocellulose or polyvinylidene difluoride (PVDF) membrane by means of electro-blotting. This step renders the proteins accessible to antibodies. However, before the membrane can be stained with antibody, a blocking solution is required to prevent any interaction between the membrane and antibody. This interaction would result in non-specific binding of the antibody to the membrane. Bovine serum albumin or non-fat dry milk can be used to block the membrane. The proteins present within the blocking agents will bind to any open spaces on the membrane which do not already contain protein from the sample. Once the membrane has been successfully blocked, the detection antibody (primary antibody) can be added. Next, a secondary antibody (capture antibody) conjugated to an enzyme, such as horse radish peroxidase (HRP), which is capable of reacting with a substrate such as luminol, is used. When the chemiluminescent substrate is oxidised by HRP, light is emitted. The emitted light is then captured by a camera.
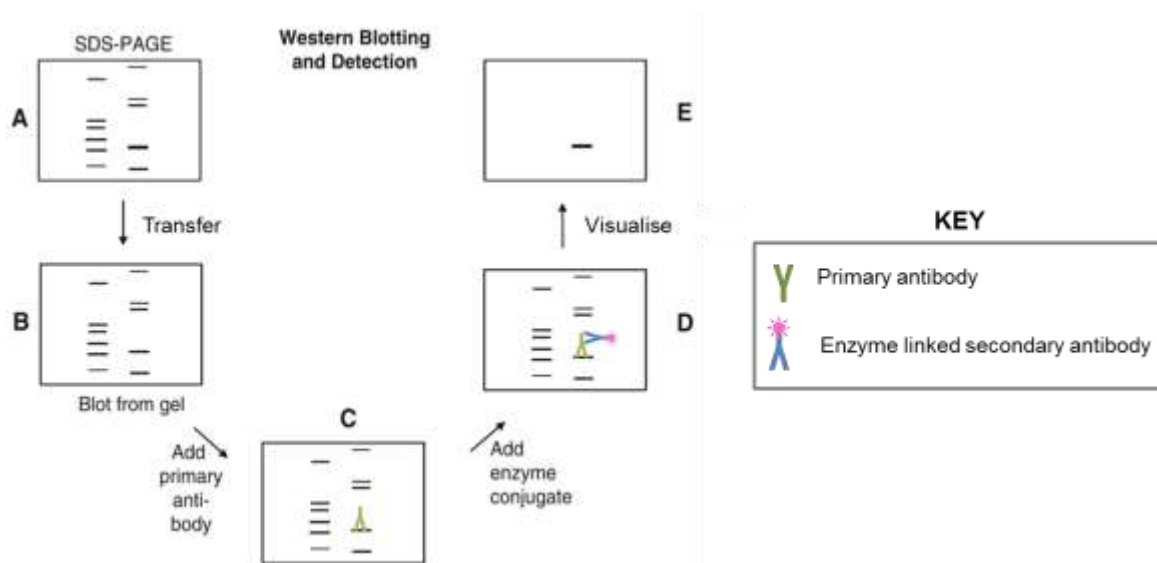
Figure 5.2: Illustration of the western blot procedure. A. Proteins are first run on an SDS-PAGE gel which separates proteins based on size. **B.** Proteins are then transferred onto a membrane. **C.** Membrane is incubated with primary antibody. **D.** Membrane is incubated with secondary antibody. **E.** Addition of substrate and visualisation. Image was adapted from Kurien and Scofield 2015 (25).

5.2.4 Reverse Transcription – quantitative Polymerase Chain Reaction (RT-qPCR)

RT-qPCR was used to investigate *Pref-1* mRNA expression levels in conjunction with *Sox9*. This technique combines reverse transcription, PCR amplification and fluorescence to investigate gene expression. The basic principles of RT-qPCR were discussed in detail in Chapter 4, section 4.2.

5.2.5 Immunohistochemistry (IHC)

All previous methods mention above investigated Pref-1 expression *in vitro.* In order to determine whether Pref-1 was present *in vivo*, immunohistochemistry was performed on adipose tissue and umbilical cord samples. Immunohistochemistry is a technique which combines aspects of immunology, chemistry and histology for the detection of antigens in tissue sections (26). Briefly, the method relies on the binding of antibodies to an antigen of interest (Pref-1 in the case of this study) in order to determine the presence and location of the specific antigen in a tissue sample. Tissue samples are first fixed in order to crosslink the proteins. Formalin is commonly used for this purpose. The fixed sample is then embedded in paraffin

before sectioning. Tissue samples are finely sliced (3 – 5 µm) with the aid of a microtome before staining (27, 28). Haematoxylin and eosin (H&E) is a common staining combination used for histological analysis of tissue sections. Haematoxylin stains DNA a dark blue or purple colour while eosin stains cytoplasmic components and collagen pink. In addition, a labelled antibody conjugated to a substrate such as peroxidase or alkaline phosphatase can be used in combination with H&E to stain a specific protein. The protein of interest is visualized by adding an enzyme substrate that results in a colorimetric change. Peroxidase and 3,3'-diamino-azobenzadine (DAB) is a common substrate/enzyme combination used in immunohistochemistry and was also used in this study. The oxidized DAB forms a brown pigment which precipitates out of solution at the location of the antibody (29). The section can then be visualised under a microscope (Figure 5.3).
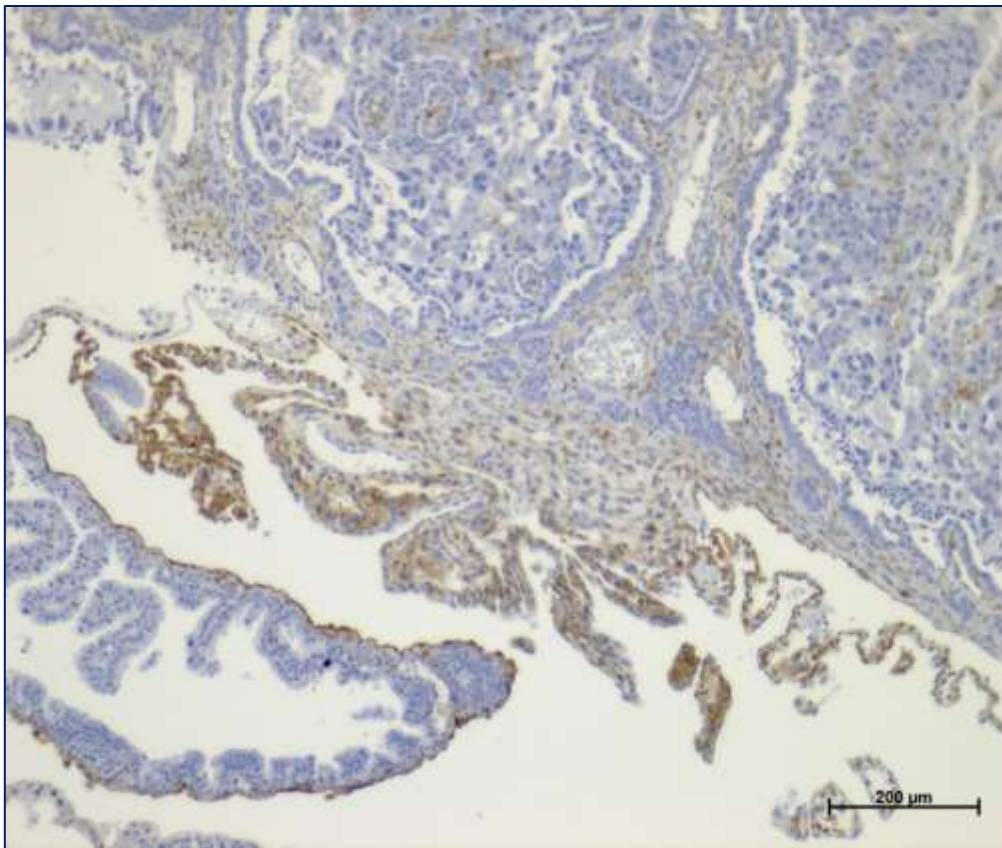
Figure 5.3: Immunohistochemistry image of mouse placenta. A section of mouse placenta was stained with a Pref-1 monoclonal antibody (primary) and a peroxidase labelled secondary antibody to visualize the Pref-1 staining. The brown areas indicate positive cytoplasmic Pref-1 staining. Counter stained with haematoxylin.

5.3 Methods

5.3.1 Pref-1 cell surface protein detection using flow cytometry

At each time point (day 0, 1, 3, 7, 14 and 21) the cells were dislodged by the addition of 0.25% trypsin-EDTA for 7 – 10 min at 37ºC, 5% CO_2. The enzymatic activity of the trypsin-EDTA solution was neutralized by adding an equal volume of complete growth medium to the wells. Cells were centrifuged at 300 x g for 5 min and re-suspended in 1 mL of complete growth medium. The cell suspension obtained was split into two flow cytometry tubes, one tube containing 1 µL of Mouse IgG1, kappa monoclonal [15-6E10A7] – isotype control (Abcam, Cambridge, UK; ab170190) antibody – and the second containing 1µL of Anti-DLK antibody [3A10] (Abcam, Cambridge, UK; ab119930). Cells were incubated overnight at 4ºC before the secondary antibody (Goat Anti-Mouse IgG H&L; Alexa-Fluor® 488 labelled; Abcam, Cambridge, UK; ab150113) was added. The cells were incubated for an additional 2 hours at 4ºC in the dark after the secondary antibody was added. An antibody wash was then performed by adding 2 mL of PBS supplemented with 1% Human Serum Albumin (HSA) (Sigma-Aldrich, Merck, Missouri, USA) and centrifuging at 300 x g for 5 min. This step was repeated twice before re-suspending the cells in 500 µL PBS + 1% HSA. For hWJSCs, 1 µL of VDC Ruby was added to the cells before analysis in order to distinguish cells from debris as it was observed that the hWJSC cultures have more debris in the sample than hASCs. Cells were then acquired on a BD FACS Aria Fusion cell sorter (BD Biosciences, USA) and the data sets were analysed using Kaluza flow cytometry data analysis software (Version 3.1).

5.3.2 Pref-1 detection - ELISA

An ELISA was used to determine the level of Pref-1 protein in culture media. A human Pref-1/DLK1/FA1 DuoSet ELISA (DY1144-05 and DY008) kit was purchased from R&D Systems (Minnesota, USA). The assay was performed according to the manufacturer's instructions. Briefly, a 96-well microplate was coated with Pref-1 capture antibody (4 µg/mL) and incubated overnight. The following day, the wells were washed three times with the supplied washing buffer (0.05% Tween® 20 in PBS, pH 7.2-7.4) after which the plate wells were blocked for 2 hours using the supplied reagent diluent (1% BSA in PBS, pH 7.2-7.4, 0.22 µm filtered). The washing

step was repeated before 100 µL of each sample (in duplicate) and standard (in duplicate) were added to the plate. Samples were incubated for 2 hours at room temperature and the washing step was repeated. Streptavidin-HRP (100 µL) was added to each well, followed by incubation for 20 min in the dark. The wells were washed again as described earlier. The substrate solution (100 µL) was added to the wells and the plate once again incubated for 20 min in the dark. Finally, 50 µL of a 2 N H2SO4 solution, referred to as the stop solution in the product insert, was added to each well. Thorough mixing of the well content was ensured by lightly tapping the plate for a few seconds. Optical density was measured using a microplate reader (PowerWave$_x$, A.D.P. South Africa, Roodepoort, South Africa) with wavelength correction. A dual reading was obtained at 540 nm and 570 nm. The values obtained for all the duplicate samples were averaged and normalised to the blank.

5.3.3 Western Blot

5.3.3.1 Sample preparation

At each time point, the conditioned medium was transferred to a 15 mL Falcon® tube. The cells were then dislodged by the addition of 0.25% trypsin-EDTA for 7 – 10 min at 37ºC, 5% CO_2. After incubation, the enzymatic activity of the trypsin-EDTA solution was neutralized by adding an equal volume of complete growth medium to the wells. The dislodged cell suspension was transferred to a second 15 mL Falcon® tube. Cells were centrifuged at 300 x g for 5 min and the supernatant discarded. Cell pellets were stored at −20ºC until samples were further processed.

5.3.3.2 Lysis

Radio-immunoprecipitation assay (RIPA) buffer was used to lyse the cells before protein quantification. Cell pellets were allowed to thaw on ice before 100 µL RIPA buffer was added. Cell pellets were incubated in the lysis buffer for 45 min on ice and vortexed every 10 min to aid the lysis process. After incubation, the lysate was centrifuged at 14 000 x g for 10 min. The supernatant was then carefully transferred to a new Eppendorf® tube, leaving behind any insoluble material which was discarded. Stored cell supernatants obtained from the cells used in the experiments described in section 5.3.1 were prepared in the same manner.

5.3.3.3 Protein Quantification Procedure

The protein concentrations of the samples were determined using a Pierce™ BCA Protein Assay (Thermo Fisher Scientific, Massachusetts, USA) according to the manufacturer's instructions. First, the samples (cell lysate or conditioned media) were centrifuged at 10 000 x g for 5 min. The samples (10 µL of cell lysates or 25 µL conditioned media) and standards (volume equal to that of sample being loaded) were loaded in duplicate into the wells of a 96-well plate. The BCA working reagent (50:1, reagent A:B) was added to each well (200 µL). The plate was sealed and allowed to incubate for 30 min at 37°C before the absorbance was read on an iMark™ Microplate Reader (Bio-Rad, California, USA). Next, in order to prepare the samples for loading onto the western blot gel, loading buffer was added to each sample and the control. The samples were boiled for 5 min at 95°C and stored at 4°C until further use.

5.3.3.4 Western Blot Procedure

Western blot was carried out on both cell lysate and conditioned medium. Equal amounts of protein were loaded into each lane of the pre-cast Any KD™ Mini-PROTEAN® TGX™ gels (Bio-Rad, California, USA). The gels were run at 100 V for 45-50 min after which the proteins were transferred onto a PVDF Membrane (Bio-Rad, California, USA) using a Trans-Blot® Turbo™ (Bio-Rad, California, USA) transfer machine. The membrane was blocked by submerging it in a 5% (w/v) milk solution made by dissolving 1g of skim milk powder (Sigma-Aldrich, Merck, Missouri, USA) in 20 mL PBS. The membrane was blocked for 1 hour at room temperature, on an UltraRocker Rocking Platform (Bio-Rad, California, USA). The blocking solution was removed and the primary antibody (Anti-DLK antibody [3A10] (Abcam, Cambridge, UK, ab119930)) was added. Before addition, the primary antibody was diluted 1:1000 in blocking solution and allowed to incubate overnight at 4°C on the UltraRocker Rocking Platform. The following day, the primary antibody was removed and the membrane washed five times with PBS supplemented with 0.1% Tween® 20 (Sigma-Aldrich, Merck, Missouri, USA). The secondary antibody (goat anti-mouse) was diluted 1:5000 in 5% milk powder solution before addition. The membrane was incubated with the secondary antibody for an hour at room temperature on the UltraRocker Rocking Platform. PBS with no supplementation was then used to wash

the membrane thrice before adding the Clarity™ Western ECL Substrate (Bio-Rad, California, USA) as per manufacturer's instructions. The membrane was incubated with the Clarity™ Western ECL Substrate for 5 min before visualization.

5.3.4 Reverse Transcription - qPCR

This chapter will focus on the RT-qPCR results obtained for *Pref-1* and *Sox9.* RT-qPCR was performed in the same manner as described in Chapter 4, section 4.3.7. However, the template concentration used for *Pref-1* mRNA detection was 62.5 ng/µL, instead of the cDNA template concentration of 20 ng/µL used for all the other genes of interest. The cDNA concentration was increased for *Pref-1*, because of the low levels of detection observed for *Pref-1* during optimization experiments performed by Dr C Durandt, in a separate, unrelated study. Please note that the template concentration used for the reference genes analysed on the same plate as the *Pref-1* samples was also increased to 62.5 ng/µL.

Primer sequences and accession numbers and can be found in Appendix A, section A6 and A7. Reference genes used are also listed in Appendix A, Table A.15.

5.3.4.1 RNA Extraction

Total RNA extraction from hASCs and hWJSCs was performed as described in Chapter 4, section 4.3.5.

5.3.4.2 cDNA Synthesis

The cDNA synthesis was performed in the same manner as described in Chapter 4, section 4.3.6.

5.3.4.3 Data analysis

Data was analysed in the same manner as described in Chapter 4, section 4.3.7.1.

5.3.4.4 Statistical significance

Statistical significance was determined in the same manner as described in Chapter 4, section 4.3.7.2.

5.3.5 Immunohistochemistry

Immunohistochemistry (IHC) was performed by a collaborator, Mrs Marlene van Heerden, from the department of Oral Pathology and Oral Biology at the University of Pretoria.

5.3.5.1 Samples

Solid adipose tissue and umbilical cord samples were collected from both humans and mice. Pancreas, ovaries, placenta and adrenal glands were also collected from mice and served as control tissue.

5.3.5.2 Human Specimen Collection

Details regarding the collection of human specimens can be found in Chapter 3, section 3.3.1.

5.3.5.2.1 Murine Specimen Collection

With regard to murine tissue, 10 adipose tissue and 5 umbilical cord samples were collected from CD1 mice by a trained veterinary technician (Ms Ilse Janse van Rensburg) at the University of Pretoria's Onderstepoort campus. Additional organs/tissues, such as the pancreas, adrenal glands, ovaries and placenta, were harvested from the mice. All animals were euthanized prior to tissue harvesting and carcasses disposed according to the University of Pretoria's Biomedical Research Centre (UPBRC) regulations. Euthanasia was done by a qualified veterinarian/veterinary technologist/laboratory animal technologist by means of sodium pentobarbital overdose. Ethics approval was obtained from the University of Pretoria Animal Ethics Committee (protocol number: H0012-17).

5.3.5.2.2 Naming of samples

Mouse samples were labelled with a code in order to identify and track them. Coding happened in a similar manner to what was used for humans. An example of a code would be M_AT141117-01. The "M" indicated that the tissue was harvested from a mouse. Next, the tissue type was assigned as "AT" for adipose tissue, "UC" for umbilical cord, "O" for ovaries, "P" for pancreas, "PL" for placenta and "AD" for adrenal glands. This was followed by the date the sample was collected. Lastly, if more than one sample was collected on the same day, a number representing the sample was placed after the date ("-01" as illustrated in the example above).

5.3.5.3 Animal Housing and Care

Animals were housed at the Conventional Rodent Unit of the University of Pretoria's Biomedical Research Centre (UPBRC) at Onderstepoort, Faculty of Veterinary Sciences. Animals were housed in autoclaved conventional Type II cages. Autoclaved wood shavings were used as bedding and changed once a week. Animals were provided with autoclaved wooden sticks for chewing as well as paper tissues, toilet roll inners and egg containers for enrichment. Room temperature for the animals was maintained between 21-24 °C. Relative humidity in the rooms was maintained between 40% - 60%, and a 12-hour dark/light cycle implemented. The animals were allowed free access to EPOL rodent pellets and were supplied with reverse osmosis water *ad libitum.* Male mice were housed two animals per cage, and were separated if fighting occurred.

5.3.5.4 Immunohistochemistry Procedure

The IHC was performed on 3 µm sections cut from formalin fixed paraffin embedded (FFPE) tissue samples and baked overnight at 58°C. The sections were dewaxed in xylene and hydrated with distilled water. Endogenous peroxidase was quenched by incubating the slides in an aqueous 3% hydrogen peroxide solution for 5 min at 37°C followed by 5 min washes in distilled water and PBS at room temperature. Thereafter background staining was quenched with Novolink Protein Block (Leica Biosystems, Newcastle Upon Tyne, UK) for 20 min at room temperature followed by two washes in fresh PBS for 5 min each. The sections were covered with a 1:1000 dilution of polyclonal anti DLK1 antibody (Abcam, Cambridge, UK, ab21682, Anti-DLK-1 antibody), covered with a coverslip and incubated at room temperature for 2 hours. This was followed by two washes in fresh PBS buffer, 5 min per wash. Detection of the antibody was performed using the Ventana OptiView Detection kit (760-700, Ventana Medical Systems, USA) as follows: the slides were incubated in OptiView HQ Universal Linker for 30 min at room temperature, rinsed in two fresh PBS solutions followed by incubation with OptiView HRP Multimer for 30 min at room temperature. Thereafter the slides were rinsed in two changes of fresh PBS and treated with Dako EnVision FLEX DAB+ Chromogen to visualise the protein. The sections were counterstained in haematoxylin, dehydrated in graded alcohol solutions, cleared in xylene and mounted with DPX mountant for microscopy.

Negative controls were performed by substituting the primary antibody with PBS on duplicate slides.

5.4 Results & Discussion

This study was built on the hypothesis that Pref-1, a known inhibitor of adipogenesis, might be responsible for the reduced adipogenic differentiation capacity observed in hWJSCs (Reviewed in Chapter 4). A number of techniques were therefore used to determine the level of Pref-1 expression in hASCs and hWJSCs.

5.4.1. Pref-1 protein detection using flow cytometry

Since Pref-1 is a transmembrane protein, flow cytometry was the chosen technique to investigate Pref-1 expression on the cell surfaces of hASCs (n = 4) and hWJSCs (n = 4). The cells were first visualized using a forward scatter (area; FS Lin) versus side scatter (SS Log) plot. A region "Cells" was created which excluded cell debris (Figure 5.4 A and C). A second two-parameter [FS Lin; area versus Pref-1-Alexa Fluor 488 (excitation 488 nm; emission 530/30] plot gated on region "Cells" was used to determine the number of Pref-1 positive events acquired (Figure 5.4 D). The region "Pref-1 +" was set according to negative staining observed for the majority of the cells. The Pref-1 isotype control gave rise to some positive results that were randomly distributed in the "Pref-1" positive region (Figure 5.4 B). An isotype control is a specificity control used in flow cytometry to distinguish between non-specific and specific binding of the monoclonal antibody (see Chapter 3, section 3.2). The isotype antibody lacks specificity to the target antigen but is of the same immunoglobulin class and type as the detection antibody. Any signal detected by the isotype antibody is thus due to antibody that non-specifically attaches to the cells, consequently generating a non-specific signal. In order to determine the true amount of signal detected, the percentage of events acquired using the isotype antibody (which should be almost negligible) must be deducted from the percentage of events acquired using the specific detection antibody.
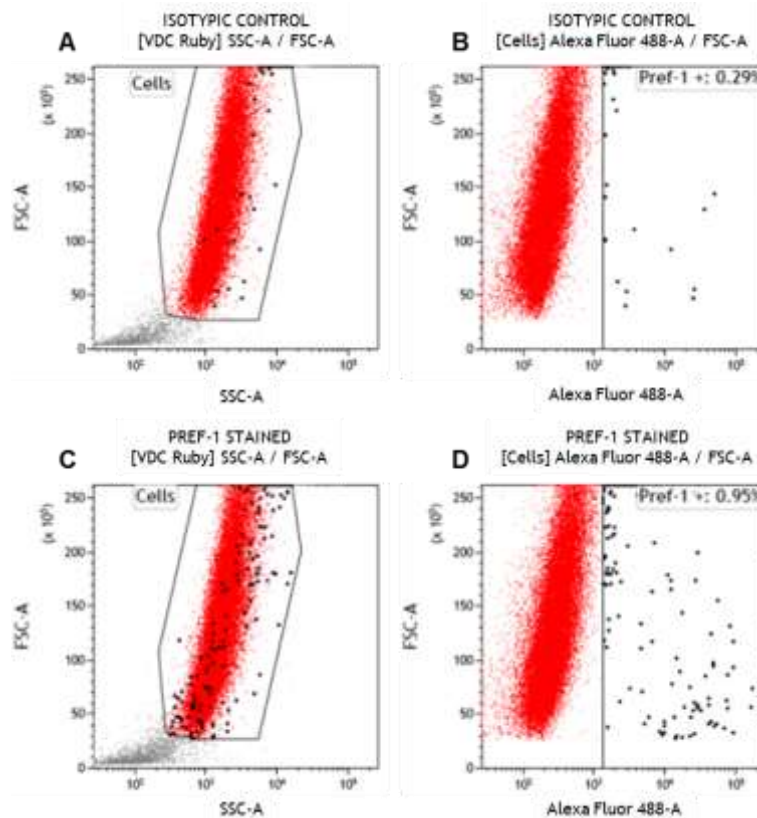
Figure 5.4: Two parameter plots displaying the gating strategy used to determine the percentage of cells that express Pref-1 in hASCs. A. A two parameter (FS Lin; area vs SS Log) plot displaying all acquired events for cells stained with isotype antibody. Region "Cells" was created in order to gate out any cellular debris. **B.** A two parameter (FS Lin; area vs Pref-1) plot, gated on region "Cells", displaying the percentage of non-specific events acquired in the Pref-1 positive regions after staining with the isotypic control. The rare-event display setting was used for this region to allow for improved visualization of the Pref-1-positive rare events. **C.** A two parameter (FS Lin; area vs SS Log) plot displaying all acquired events for cells stained with the Pref-1 detection antibody. Region "Cells" was created in order to gate out any cellular debris. **D.** A two parameter (FS Lin; area vs Pref-1) plot, gated on region "Cells", displaying the percentage of Pref-1 positive events acquired after staining with the Pref-1 monoclonal antibody. The rare-event display setting was used for this region to allow for improved visualization of the Pref-1-positive rare events.

A slight modification was made for the detection of Pref-1 in hWJSCs. Cells were first stained with VDC Ruby as there was more debris (non-nucleated particles) present in these cultures (Figure 5.5). The subsequent forward scatter (area; FS Lin) versus side scatter (SS Log) plot was gated on nucleated events which are shown by the region marked "VDC Ruby" (Figure 5.5 A and D). Other than that, the sample

preparation for hASCs and hWJSCs was the same. The reason for the higher levels of debris present in the hWJSCs sample suspension is not known and needs further investigation.
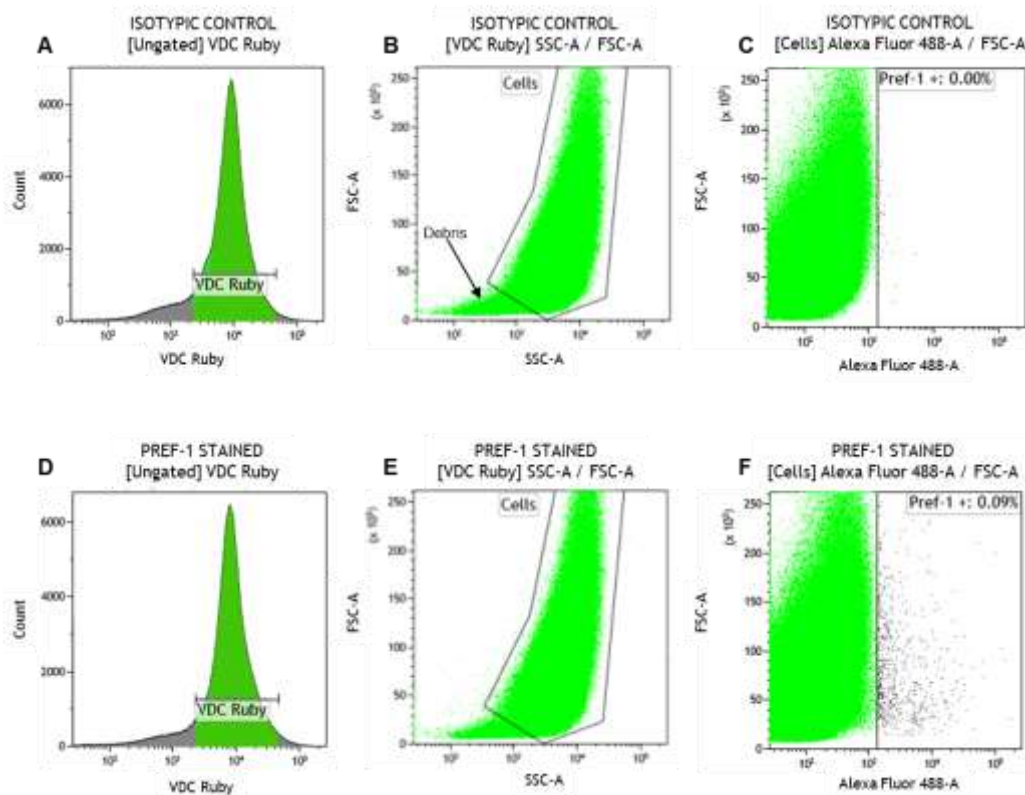
Figure 5.5: Two parameter plots displaying the gating strategy used to determine the percentage of cells that express Pref-1 in hWJSCs. A — C: Cells stained with isotype control antibody. **D — F:** Cells stained with Pref-1 detection antibody. **A & D:** A one parameter plot displaying the cells stained with VDC Ruby. A region "VDC Ruby" was created to identify the nucleated cells. **B & E:** A two parameter (FS Lin; area vs SS Log) plot, which has been gated on region "VDC Ruby", displays all VDC Ruby positive (nucleated cell) events. Region "Cells" was created to exclude any cellular debris. Cellular debris is pointed out with black arrow **C:** A two parameter (FS Lin; area vs Pref1) plot, gated on region "Cells", displaying the percentage of non-specific events acquired. **F:** A two parameter (FS Lin; area vs Pref1) plot, gated on region "Cells", displaying the percentage of Pref-1 positive events acquired.

The data obtained revealed low levels of Pref-1 expression on both cell types. Representative images of the data obtained can be seen in Figure 5.6.
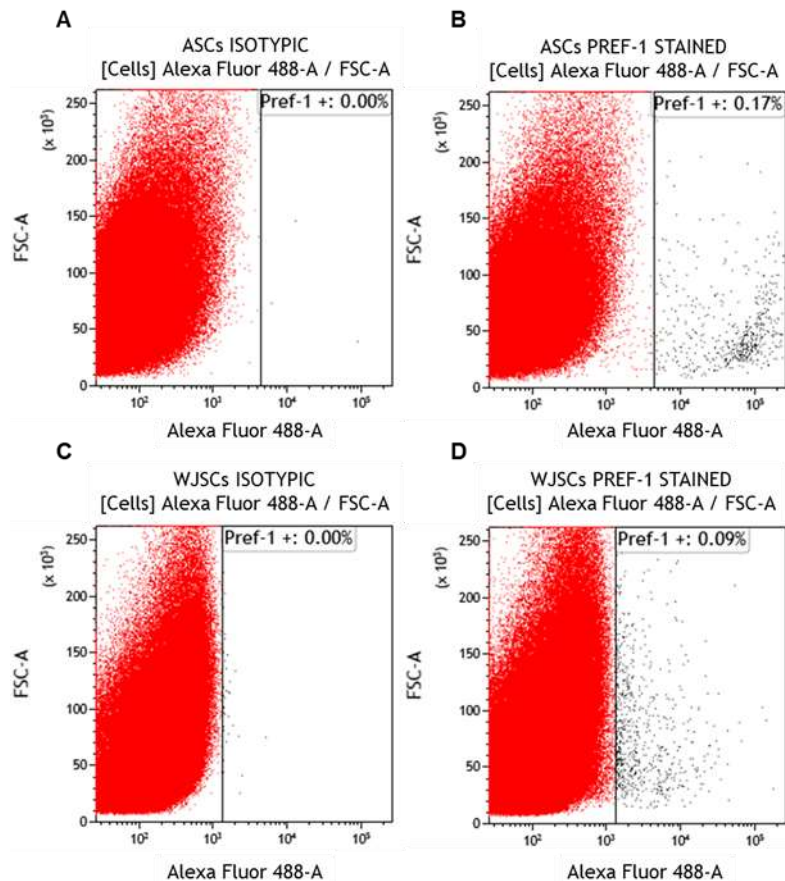
Figure 5.6: Representative images of Pref-1 flow cytometry data obtained for hASCs and hWJSCs. A. Two parameter (FS Lin; area vs Pref1) plot displaying hASCs stained with isotypic control antibody. **B.** Two parameter (FS Lin; area vs Pref1) plot displaying hASCs stained with the Pref-1 detection antibody. **C.** Two parameter (FS Lin vs Pref-1) plot displaying hWJSCs stained with isotype control antibody. **D.** Two parameter (FS Lin vs Pref-1) plot displaying hWJSCs stained with the Pref-1 detection antibody. (Detailed gating strategy explained in Figure 5.4 and Figure 5.5).

The mean percentage of cells staining positively for Pref-1 on their surface was 0.09% ± 0.04% and 0.05% ± 0.01% for non-induced hASCs and induced hASCs, respectively. The mean percentage of Pref-1 detected on the cell surface was 0.05% ± 0.02% and 0.21% ± 0.12% for non-induced hWJSCs and induced hWJSCs respectively. However, as shown in Figure 5.7 & Figure 5.8, the mean of the data is skewed at several time points by one data point. Statistical tests to identify outliers could not be performed due to the small sample size. It is worth noting that these apparent "outliers" are not representative of a single culture i.e. this was a different culture at every time point.
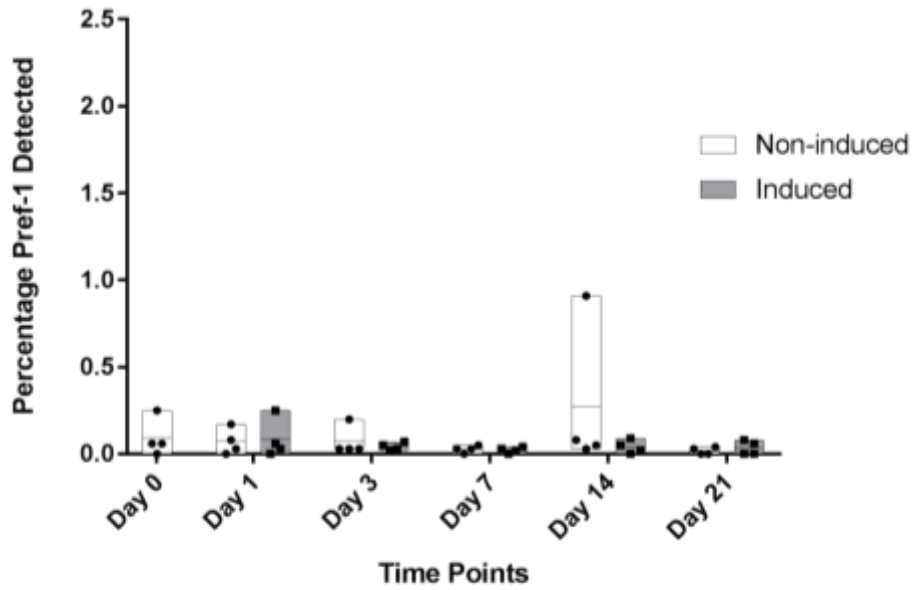
Figure 5.7: Min to max floating bar graph representing the percentage hASCs that expressed Pref-1 on the cell surface. Four hASC cultures were assessed at various time points (days 0, 1, 3, 7, 14 and 21) over a 21-day culture period. Both non-induced (control) and induced cells were analysed. The symbols represent the different cultures (n=4) at each time point. The line in the middle of the floating bar represents the mean whereas the top and bottom of the floating bar represents the maximum and minimum value.
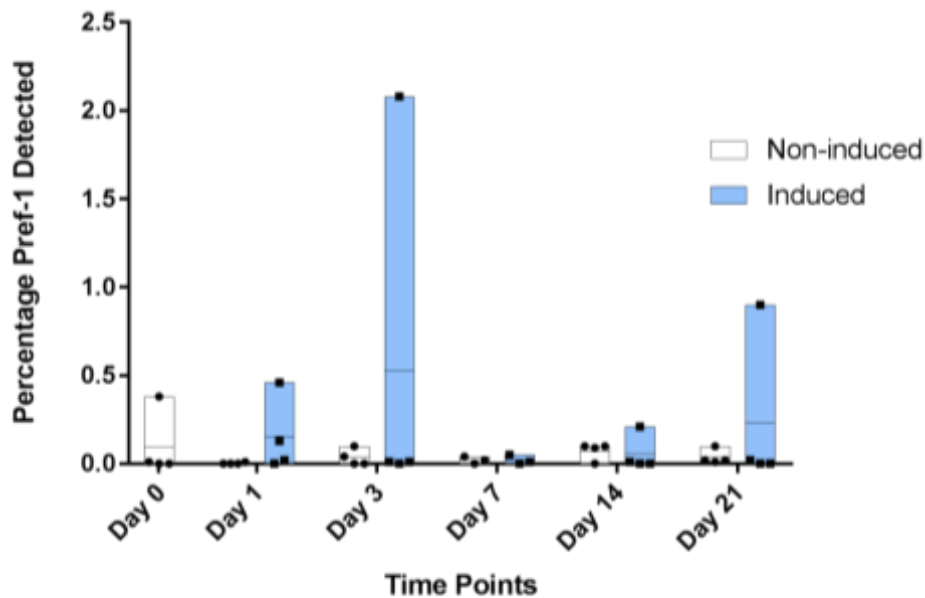
Figure 5.8: Min to max floating bar graph representing the percentage hWJSCs that expressed Pref-1 on the cell surface. Four hWJSC cultures were assessed at various time points (days 0, 1, 3, 7, 14 and 21) over a 21-day adipogenic induction period. Both non-induced (control) and induced cells were analysed. The symbols represent the different cultures (n=4) at each time point. The line in the middle of the floating bar represents the mean whereas the top

and bottom of the floating bar represents the maximum and minimum values, respectively.

As a result of the skewedness of the Pref-1 expression data at several time points, in order to make more sense of the data, the medians were plotted (Figure 5.9 and Figure 5.10). Considering the medians, it appears that the hASCs have a higher and more consistent level of Pref-1 protein expression on their surface when compared to hWJSCs. This was irrespective of the culture conditions i.e. non-induced or induced. In general, the data suggests that hASCs exhibit higher levels of membrane bound Pref-1 over the 21-day culturing period. However, as mentioned the data is highly skewed at certain time points, which impacts on the accuracy of the data and therefore the data must be interpreted with caution. Additional experiments in follow up studies would be important to confirm the trends observed in this study.

It is well described that the soluble form of Pref-1 is responsible for the inhibition of adipogenesis (5). The observation that the hWJSCs displaying less Pref-1 protein on their surface raises the question of whether Pref-1 is cleaved from the cell surface of hWJSCs and therefore would be present in higher concentrations in the culture supernatant.
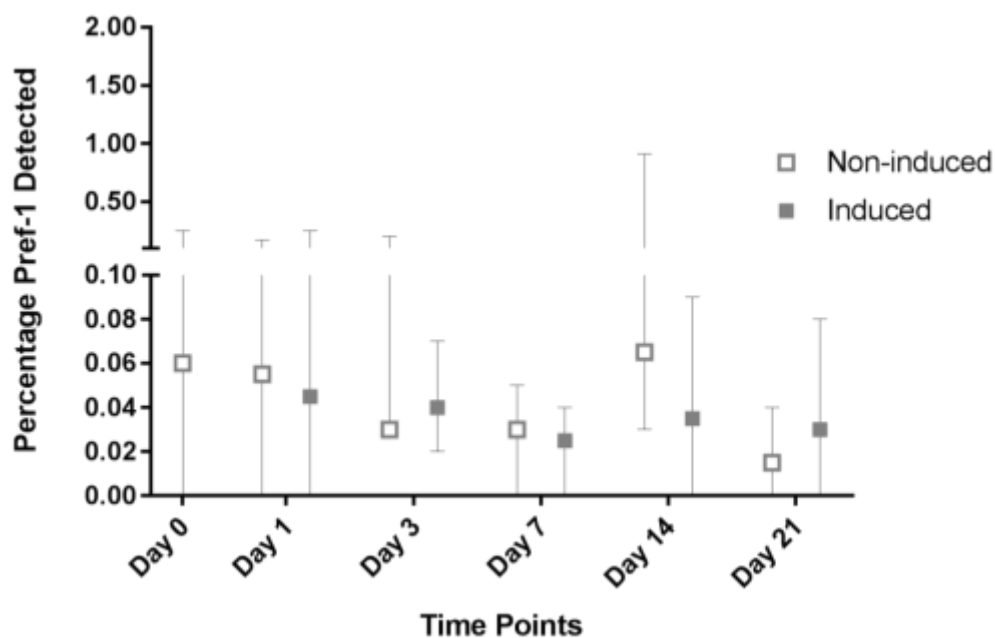
Figure 5.9: Bar graph representing the median percentage with range of hASCs that expressed Pref-1 on the cell surface. Four hASC cultures were assessed over a 21-day culture period at days 0, 1, 3, 7, 14 and 21 for Pref-1 expression. Both non-induced (control) and induced cells were analysed. Graph

represents the median percentage of cells which displayed Pref-1 on their cell surface.
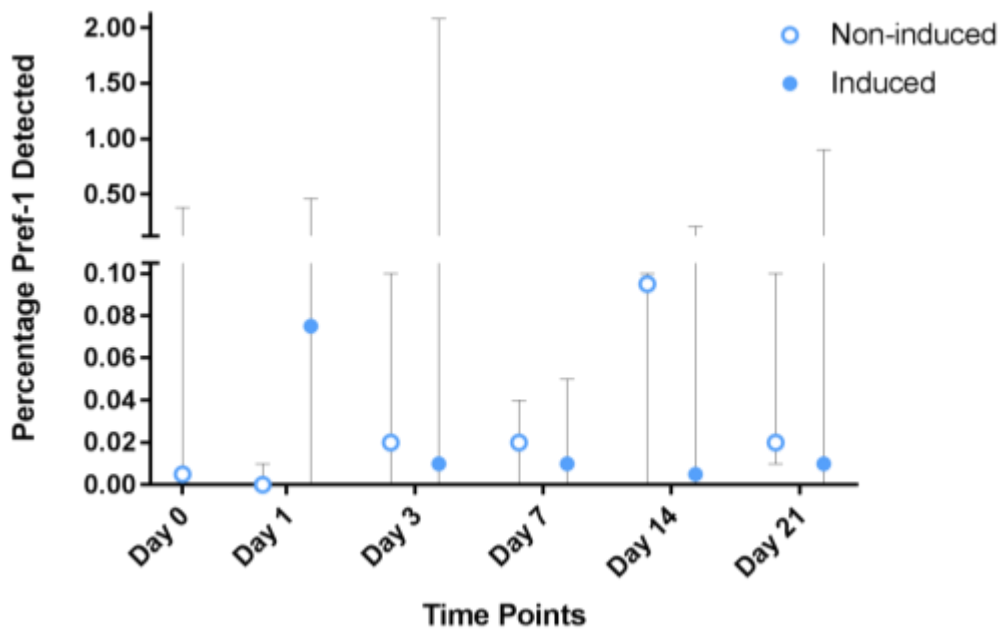
Figure 5.10: Bar graph representing the median percentage with range of hWJSCs that expressed Pref-1 on the cell surface. Four hWJSC cultures were assessed over a 21-day culture period at days 0, 1, 3, 7, 14 and 21 for Pref-1 expression. Both non-induced (control) and induced cells were analysed. Graph represents the median percentage of cells which displayed Pref-1 on their cell surface.

5.4.2. Pref-1 protein detection using ELISA

In order to test the above-mentioned hypothesis (higher concentrations of Pref-1 in the culture supernatant), an ELISA was performed to quantify the soluble Pref-1 in conditioned media. However, we were unable to detect soluble Pref-1 using an ELISA (Figure 5.11 and Table 5.1). Peripheral blood plasma was used as a positive control and Pref-1 was successfully detected. Peripheral blood was used as literature has suggested that Pref-1 is detectable in peripheral blood (collected for a study done by Catherine Wickham, MSc student; Ethics number: 204/2016) (30, 31). The standards and controls experiment worked successfully, indicating that the assay was performed successfully and that no Pref-1 was detected in the culture supernatant. It is possible that the concentration of Pref-1 in the culture supernatant is lower than the detection limit of the ELISA used. The lower limit of detection of the ELISA is unfortunately not reported by the manufacturers and is thus unknown.
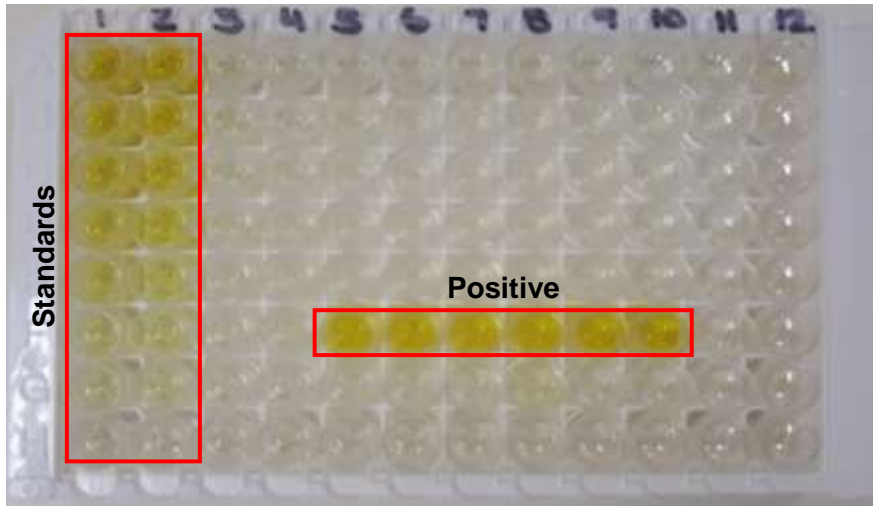
Figure 5.11: Representative image of ELISA plate. An ELISA was used to detect soluble Pref-1 in conditioned media. A standard curve ranging from 0 pg/mL to 6000 pg/mL was used – indicated in the "standards" block. Plasma obtained from peripheral blood was used as a positive control – indicated in the "positive control" block. Three different peripheral blood plasma samples were run on the plate shown above. All samples were run in duplicate.
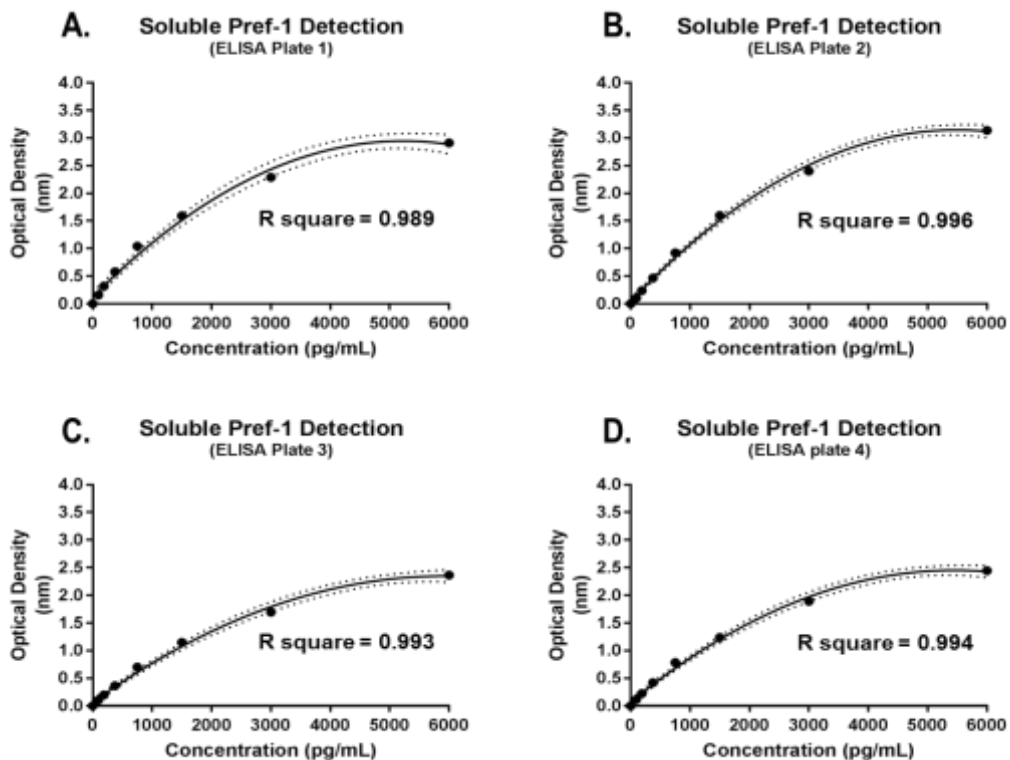
Figure 5.12: Standard curves generated for ELISAs. Four ELISA were performed. Standard curves were generated for each ELISA plate with GraphPad Prism statistical software using a second order polynomial (quadratic) model. Solid lines represent the standard curve while dotted lines represent the 95% confidence interval.

Table 5.1: ELISA results obtained for controls and samples

Sample	OD (nm)	SEM	Interpolated (pg/mL)
Positive control 1	0.196	0.017	144.297
Positive control 2	0.271	0.009	233.784
Positive control 3	1.012	0.013	1 211.376
Positive control 4	0.534	0.012	557.701
Average of samples	- 0.008[*]	0.001	Not detectable

Positive controls refer to peripheral blood plasma samples. [*]Average of samples represents the mean reading obtained for all samples analysed, this includes hASCs and hWJSCs since Pref-1 was not detected in any of the samples analysed (same OD readings for all the samples) Standard Error of the Mean.

5.4.3. Pref-1 protein detection using Western Blot

As we were unable to detect soluble Pref-1 using an ELISA, it was decided to use western blot to confirm the absence/presence of the protein in cell lysates and culture supernatants. Western blot is known to detect low levels of proteins present in the test sample (25). A Western blot was performed on cell lysates (hASCs n=1; hWJSCs n=1) as well as conditioned medium (hASCs n=1; hWJSCs n=1) obtained from hASCs and hWJSCs. Prior to performing the Western blot, the protein concentration of the test samples and control samples (peripheral blood plasma) were first quantified using the Pierce™ BCA Protein Assay (Table 5.2, Table 5.3 and Table 5.4). Once the protein concentrations were known, an equal concentration of protein (25 µg) was loaded onto each lane of the gel. A positive control (peripheral blood plasma) and ladder were included in every Western blot gel.

The four peripheral blood samples (i.e. positive controls) could not be analysed on the same gel as the test samples as there was only one lane available on the gels for a control sample. Therefore, we first determined the most appropriate control sample to use with the test samples by performing a Western blot using only the four positive control samples. Based on the western blot results obtained (Figure 5.13), control 2 was selected as the preferred control sample for subsequent Western blot experiments. Even though control 2 did not have the highest Pref-1 concentration according to the ELISA results, it did give the best results in the Western blot assay.

The reasons for the discrepancy between the ELISA and Western results are not completely known. However it is important to note that two different Pref-1 monoclonal antibodies were used in the respective assays. No information is provided by the manufacturers of the ELISA kit with regards to the detection antibody. The Pref-1 monoclonal antibody used in the Western blot assay was able to detect both soluble forms of Pref-1 i.e. 25 kDa and 50 kDa (Figure 5.14). The epitope to which the antibodies bind to is not mentioned in the product datasheet. There is however information provided on the immunogen used to generate the monoclonal antibody used for Western blot and flow cytometry (same antibody used for both applications). The immunogen spans a large area of the protein; it corresponds to amino acids 174 to 349 of the total 385 amino acids.

Table 5.2: Protein quantification results obtained for cell lysates

Samples	Concentration (ng/µL) Mean ± SEM	
	hASCs	hWJSCs
Day 0 Non-induced	3 054.50 ± 17.32	14 492.11 ± 141.69
Day 1 Non-induced	4 717.70 ± 86.63	13 767.87 ± 330.63
Day 1 Induced	4 094.00 ± 51.98	10 335.59 ± 267.65
Day 3 Non-induced	5 116.20 ± 34.64	20 081.37 ± 220.42
Day 3 Induced	4 579.10 ± 51.98	11 264.51 ± 283.40
Day 7 Non-induced	3 314.30 ± 69.30	20 002.65 ± 78.72
Day 7 Induced	2 898.50 ± 138.60	8 761.15 ± 15.75
Day 14 Non-induced	9 031.70 ± 34.65	11 280.25 ± 47.23
Day 14 Induced	10 400.50 ± 15.59	7 659.04 ± 15.75
Day 21 Non-induced	8 338.70 ± 69.30	30 409.70 ± 188.93
Day 21 Induced	7 247.20 ± 51.98	13 090.86 ± 125.96

Protein concentrations were measured in duplicate. The table displays the average concentration obtained for each sample ± the standard error of the mean (SEM) for the technical replicates. (N=1)

Table 5.3: Protein quantification results obtained for conditioned medium

Samples	Concentration (ng/µL) Mean ± SEM	
	hASCs	hWJSCs
Day 0 Non-induced	5 731.11 ± 360.60	4 152.63 ± 6.82
Day 1 Non-induced	4 574.46 ± 88.45	4 935.07 ± 13.60
Day 1 Induced	5 370.51 ± 27.22	4 935.07 ± 13.60
Day 3 Non-induced	5 105.16 ± 61.24	4 383.96 ± 20.41
Day 3 Induced	5 499.78 ± 102.06	5139.18 ± 81.64
Day 7 Non-induced	5 016.16 ± 61.24	4 057.37 ± 47.62
Day 7 Induced	4 567.66 ± 81.64	5 288.87 ± 54.43
Day 14 Non-induced	4 894.24 ± 68.04	4 771.78 ± 13.60
Day 14 Induced	5 492.98 ± 54.43	4 826.21 ± 108.86
Day 21 Non-induced	5 043.93 ± 81.64	4 622.09 ± 27.22
Day 21 Induced	4 867.03 ± 95.25	5 200.42 ± 102.06

Protein concentrations were measured in duplicate. The table displays the average concentration obtained for each sample ± the standard error of the mean (SEM) for the technical replicates. (N=1)

Table 5.4: Protein quantification results obtained for the controls

Samples	Concentration (ng/µL) Mean ± SEM
Positive control 1	22 879.76 ± 978.44
Positive control 2	25 965.61 ± 2 829.95
Positive control 3	33 763.03 ± 481.70
Positive control 4	31 836.25 ± 722.54
Negative control	4 430.15 ± 263.97

Protein concentrations were measured in duplicate. The table displays the average concentration obtained for each sample ± the standard error of the mean (SEM), all technical replicates included in calculation. Negative control refers to complete growth media which has not come into contact with cells.
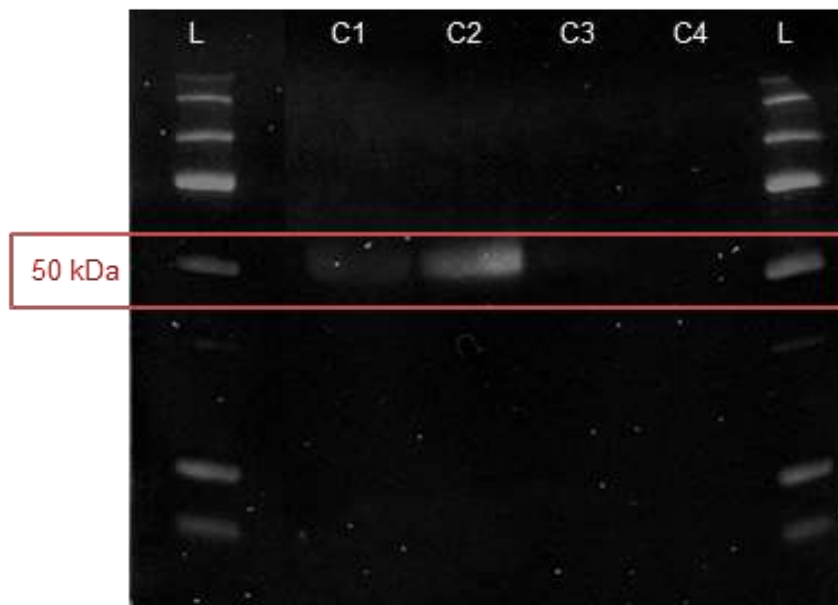
Figure 5.13: Western blot results for the control samples. The four controls used in the ELISA assay were assessed by Western blot in order to determine which would be the best control for further western blot experiments. L represents the lanes containing the ladder (Precision Plus Protein™ All Blue Prestained Protein Standard ladder); C1 to C4 represents peripheral blood plasma controls 1 to 4.

The western blot performed on the cell lysates obtained from hASCs and hWJSCs resulted in no Pref-1 protein detection (Figure 5.14). After 1 min of exposure, the 50 kDa Pref-1 protein was clearly visible in the control sample. After 30 min, there was still no Pref-1 protein detected in the samples. Given that the protein was detected in the control sample, at the correct molecular weight, this indicated that the assay was performed successfully. Detecting both soluble forms of the Pref-1 protein (control samples) gave us further confidence that the protein being detected by the antibody was indeed Pref-1 (Figure 5.14). However, the 25 kDa soluble protein only appeared after the 30 min exposure time suggesting that it is present in very low abundance. The amount present may be on the minimal detection limit margin of the assay. This may be the reason why the 25 kDa was detected (visible) in some Western blots (Figure 5.14), while not detected (no visible bands) in other Western blots (Figure 5.13; Figure 5.14).
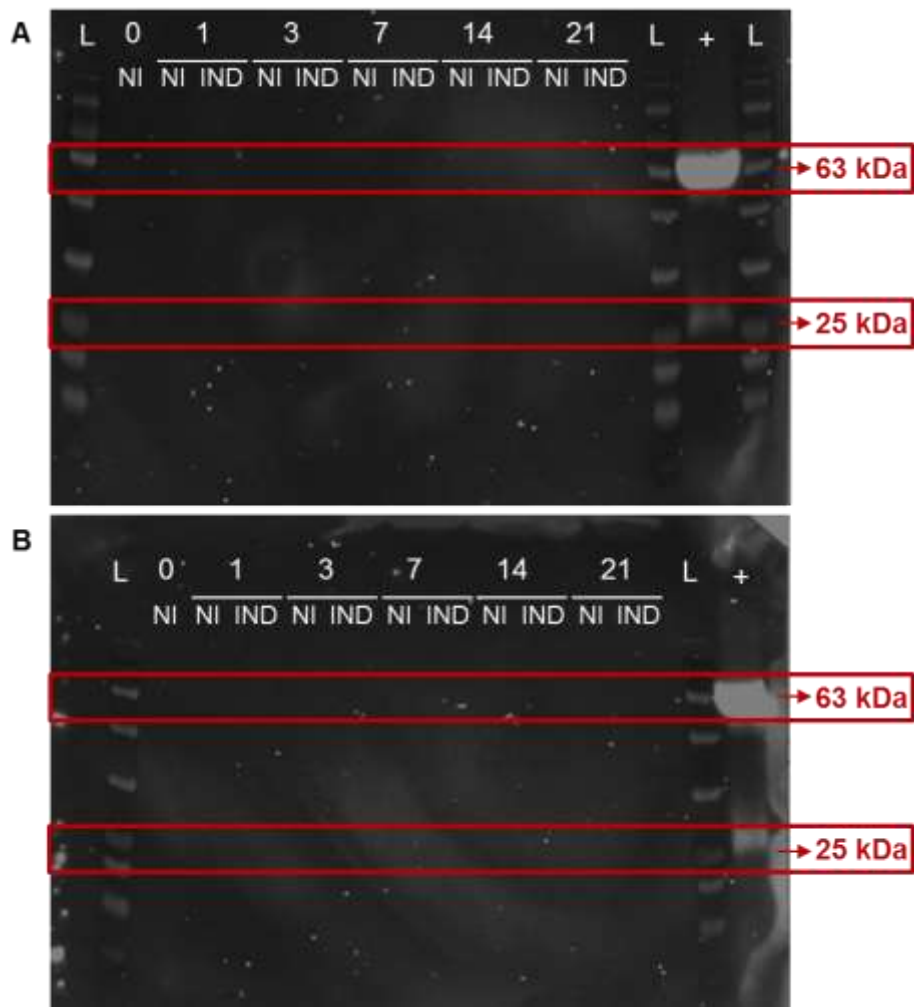
Figure 5.14: Western blot results for cell lysates. A. Western blot results obtained from hASC cell lysates. **B.** Western blot results obtained from hWJSC cell lysates. Numbers indicate the respective time points. "NI" indicates non-induced; "IND" indicates induced. Positive control lane marked with a "+". Peripheral blood plasma was used as a positive control. Lane containing the ladder (BLUelf Prestained Protein Ladder) is marked with an "L". Exposure time: 30 min.

The Western blot assay was also performed using conditioned culture medium. Once again, after 1 min of exposure, the 50 kDa Pref-1 protein could be detected in the control sample, but not in the experimental samples. However, after 30 min exposure we were able to detect a positive signal in all the samples (Figure 5.15). The protein detected was between 48 and 63 kDa which corresponds to the predicted size of the active soluble form of the Pref-1 protein. The Pref-1 protein size is known to range between 50 kDa and 60 kDa due to post translational modifications such as N-linked glycosylation (19).

The long exposure time and faintness of the signal detected does however suggest very low levels of Pref-1 present in the samples. Also, the amount of protein detected does not seem to change over the time periods nor does it seem to change with culturing conditions i.e. non-induced or induced. Detecting small differences between samples and sample types was challenging, due to the faintness of the signal detected. However, the signal obtained from the hWJSCs conditioned medium seems to show slightly higher levels of Pref-1 (Figure 5.15 B). This observation can however not be claimed with certainty. One would need to quantify the amount of protein present in each band. This was unfortunately not possible due to the faintness of the bands (higher protein concentration would be required) and the lack of an appropriate reference protein to which the data could be normalised. In order to be confident in the observation made more sensitive detection methods such as mass spectrometry (32, 33) should be considered in future experiments.
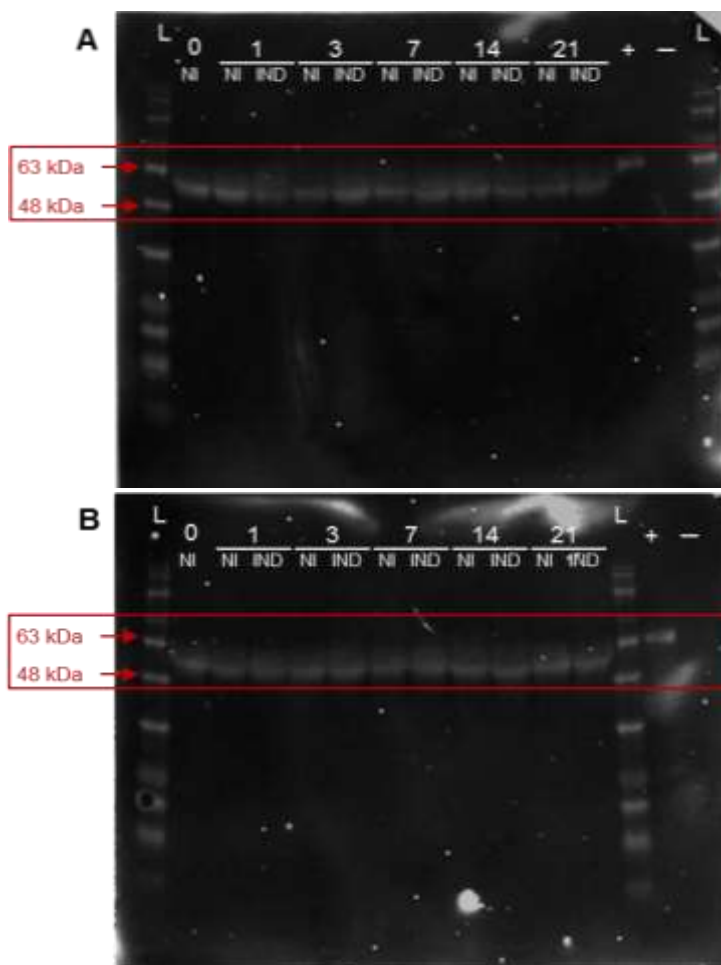
Figure 5.15: Western blot results for conditioned medium. A. Western blot results obtained from hASC conditioned medium. **B.** Western blot results obtained from hWJSC conditioned medium. Numbers indicate the respective time points. "NI" indicates non-induced; "IND" indicates induced. Positive control (peripheral blood plasma) lane is marked with a "+" and negative control lane (growth media) is marked with a "−". Lane containing the ladder (BLUelf Prestained Protein Ladder) is marked with an "L". Exposure time: 30 min.

A negative control (complete growth medium) was also included during the Western blot analysis. Since complete growth medium is supplemented with 10% FBS which is protein rich, it was important to ensure that the positive signal detected came from proteins released by the hMSCs and not the FBS. No signal was detected with the negative control (complete growth medium), indicating that the Pref-1 signal detected was hASC- and hWJSC-associated Pref-1 which was released into the culture supernatant (Figure 5.15, lane marked "−").

With regard to the positive control (peripheral blood plasma), it was noted that the band detected was of a higher molecular weight compared to what we observed in a previous experiment (Figure 5.13 and Figure 5.14). This is the same positive control (control 2) used in the two experiments (Figure 5.13 and Figure 5.14). The only difference between the control samples was that fresh controls were prepared from frozen stock samples, before performing the Western blot on the conditioned medium (Figure 5.15). This means that the new sample aliquot had been frozen for a slightly longer period of time. In addition, during the preparation, a different loading buffer had to be used. Whether these factors could have impacted the protein is unknown. However, the protein detected was still within the size specifications for Pref-1.

5.4.4. Detection of Pref-1 gene expression levels using RT-qPCR

Pref-1 and *Sox9* mRNA expression levels were investigated using RNA extracted from hASCs and hWJSCs respectively at various time points during adipogenic differentiation (Table 5.5, Figure 5.16, Table 5.6 and Figure 5.17). *Sox9* was included as literature suggested that Pref-1 exerts an inhibitory role in adipogenesis through the upregulation of *Sox9* which in turn prevents the upregulation of *C/EBPβ*, is required for the upregulation of *PPARγ* and *C/EBPα* (8, 23).

Table 5.5: Relative gene expression levels of *Pref-1* in hASCs and hWJSCs

Time Point	hASCs				hWJSCs			
	1	2	3	Mean ± SEM	1	2	3	Mean ± SEM
Day 1	2.80	1.35	0.64	1.60±0.64	10.15	1.63	5.01	5.60±2.48
Day 3	2.34	2.25	0.34	1.64±0.65	2.34	0.83	18.17	7.11±5.58
Day 7	1.04	0.98	0.04	0.69±0.32	1.68	0.49	28.80	10.32±9.24
Day 14	0.23	0.50	0.14	0.29±0.11	0.93	NA*	6.37	3.65±2.72
Day 21	1.19	0.67	0.39	0.75±0.23	18.22	2.47	0.26	6.98±5.66

* NA – Could not synthesize cDNA for this sample due insufficient RNA. Results were normalised to three reference genes (*PPIA, TBP* and *YWHAZ)* and are expressed as fold increase ± standard error of mean (SEM) relative to the non-induced control at each time point.
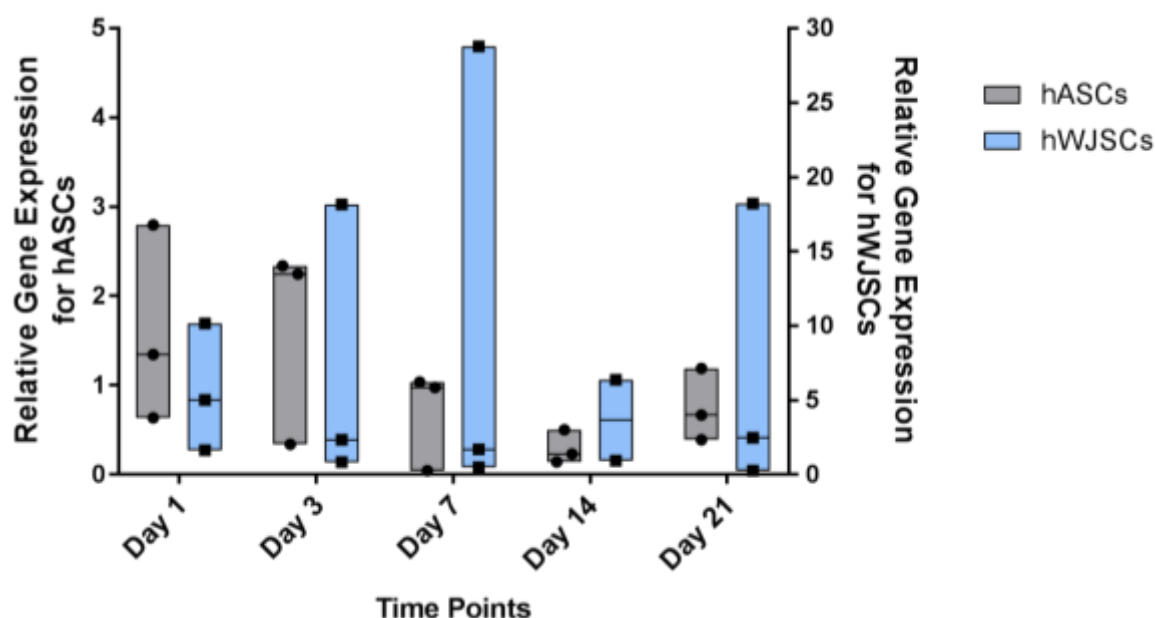
Figure 5.16: Minimum/maximum floating bar graph representing *Pref-1* mRNA expression in hASCs and hWJSCs. *Pref-1* expression relative to non-induced cells at each time point. Each square (hWJSCs) or dot (hASCs) within the floating bars represents a different culture. The horizontal lines within the bars represent the median. Three independent hASC and hWJSC cultures were included in the study. The Y-axis on the left represents the relative gene expression for hASCs (grey bars), while the Y-axis on the right represents the relative gene expression for hWJSCs (blue bars).

The data suggest that there is more *Pref-1* mRNA present in the hWJSCs compared to hASCs (Table 5.5). However, a large degree of variability was also observed for the qPCR data. In most cases, the data was skewed by a single data point at each

time point and this was not from a single culture that showed higher levels of expression throughout the experimental period. Therefore, as done previously, in order to obtain a clearer representation of the data, another graph was generated displaying the medians. Looking at the medians (Figure 5.17), the data continues to suggest that there are higher levels of *Pref-1* expression in hWJSCs. However, it is not possible to make confident conclusions from the data presented due to the limited number of biological repeats analysed and the wide range of variability observed in performing the assay. However, when the results obtained in this study were combined with the results obtained in a previous study, which also compared Pref-1 mRNA expression between hWJSCs and hASCs, hWJSCs remained the cell type with higher levels of Pref-1 expression.
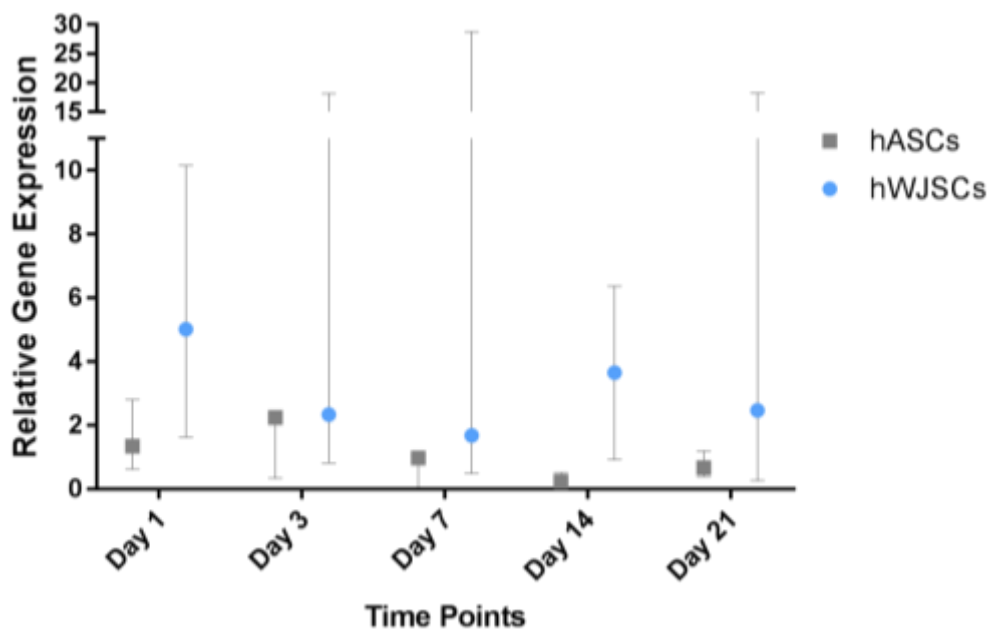
Figure 5.17: Bar graph representing the median percentage with range of Pref-1 mRNA detected in hASCs and hWJSCs. *Pref-1* expression relative to non-induced cells. Three independent hASC and hWJSC cultures were included in the study.

Table 5.6: Relative gene expression levels of *Sox9* in hASCs and hWJSCs.

Time Point	hASCs				hWJSCs			
	1	2	3	Mean ± SEM	1	2	3	Mean ± SEM
Day 1	1.54	0.49	1.05	1.03±0.31	0.52	0.48	0.62	0.54±0.04
Day 3	2.86	0.44	1.36	1.55±0.70	0.29	0.37	0.58	0.41±0.09
Day 7	2.06	0.82	1.50	1.40±0.36	0.23	0.16	0.00	0.13±0.07
Day 14	3.30	0.80	1.53	1.88±0.74	0.10	NA*	0.66	0.38±0.28
Day 21	1.90	0.46	0.98	1.11±0.42	0.12	0.08	13.62	4.61±4.51

*NA – Could not synthesize cDNA for this sample due insufficient RNA. Results were normalised to three reference genes (*PPIA, TBP* and *YWHAZ)* and are expressed as fold increase ± standard error of mean (SEM) relative to non-induced cells.

Literature suggests that Pref-1 expression results in the up regulation of *Sox9* (19, 22)*.* However, our results did not reflect higher levels of *Sox9* mRNA in hWJSCs (Table 5.6 and Figure 5.18). Instead, higher levels of *Sox9* expression were expressed in hASCs. There was one data point in the hWJSCs that displayed very high levels of *Sox9* at day 21. This is most likely a technical error; perhaps an incorrect amount of cDNA was added to the reaction. Ideally, this data point should be repeated but due to time constraints this was not done. Lastly, no statistical significance was observed in this data set.
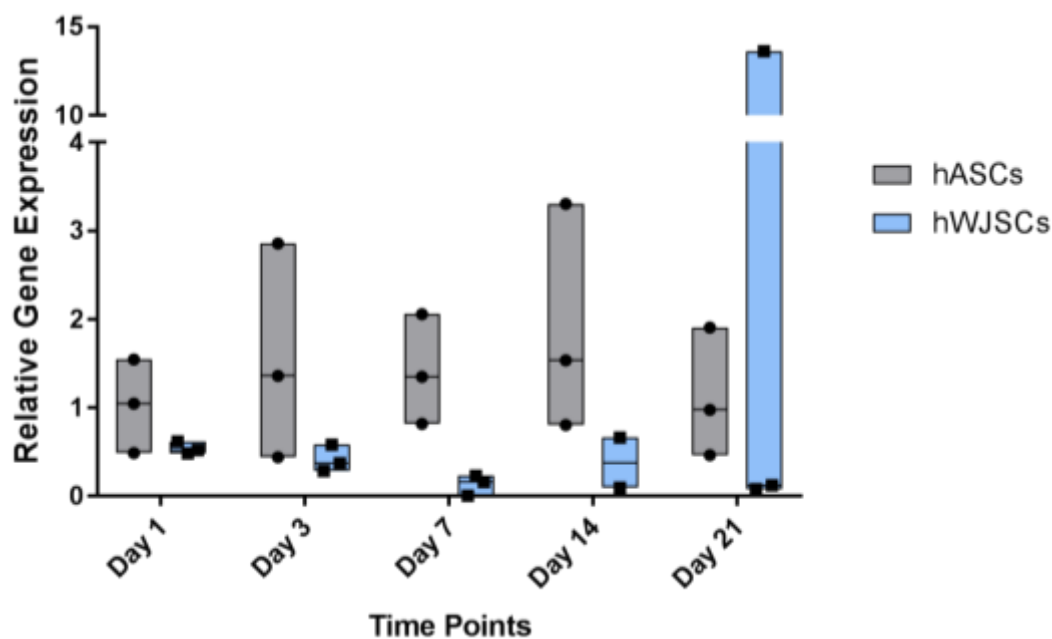
Figure 5.18: Minimum/maximum floating bar graph representing *Sox9* mRNA expression in hASCs and hWJSCs. *Sox9* expression relative non-induced cells at each time point. Each square (hWJSCs) or dot (hASCs) within the

floating bars represents a different culture. The horizontal lines within the bars represent the median. Three independent hASC and hWJSC cultures were included in the study.
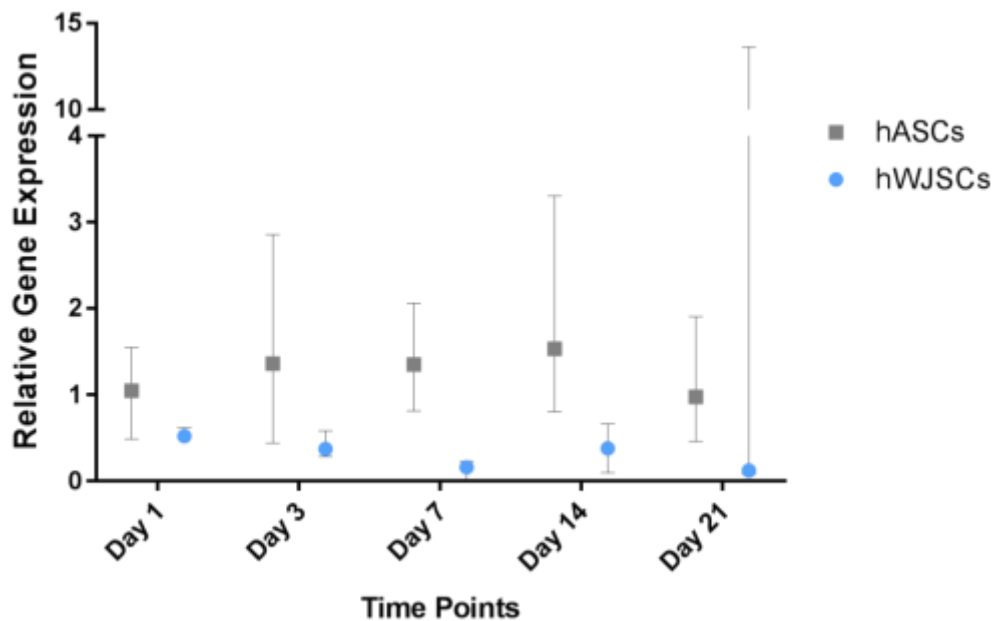
Figure 5.19: Bar graph representing the median percentage with range of *Sox9* mRNA detected in hASCs and hWJSCs. *Sox9* expression relative to non-induced cells at each time point. Three independent hASC and hWJSC cultures were included in the study.

5.4.5. *In vivo* Pref-1 protein detection using immunohistochemistry

The expression of Pref-1 was also investigated in vivo. Immunohistochemistry was used to investigate the expression of Pref-1 protein in adipose tissue and umbilical cord tissue sections - the sources from which the hMSCs used were isolated.

As mentioned before, most studies that have investigated the role of Pref-1 in adipogenesis have been performed using murine cell lines or experimental animal models (1, 6, 19). A goat anti-mouse Pref-1 antibody, that cross reacts with human tissue, was used for immunohistochemistry staining. Murine tissue, in which Pref-1 is known to be expressed (13, 34) was collected to be used as positive controls and to test the performance of the antibody. This included the ovaries, placenta, pancreas and adrenal glands. The tissue was collected and delivered to Mrs Marlene van Heerden from the department of Oral Pathology and Oral Biology, who performed the sample processing and immunohistochemistry staining. Dr Tsholofelo Kungoane,

an oral pathologist and senior lecturer at the department of Oral Pathology and Oral Biology, assisted with the interpretation of the results. The immunohistochemical staining of the tissues was done in the presence of a negative control. The negative control in this case was tissue stained with secondary antibody only. Positive staining was observed in all murine tissue sections collected as positive controls, with the exception of the pancreas, providing confirmation that the antibody selected was working. From the tissues collected, the ovaries were selected as the best positive control tissue (Figure 5.20).
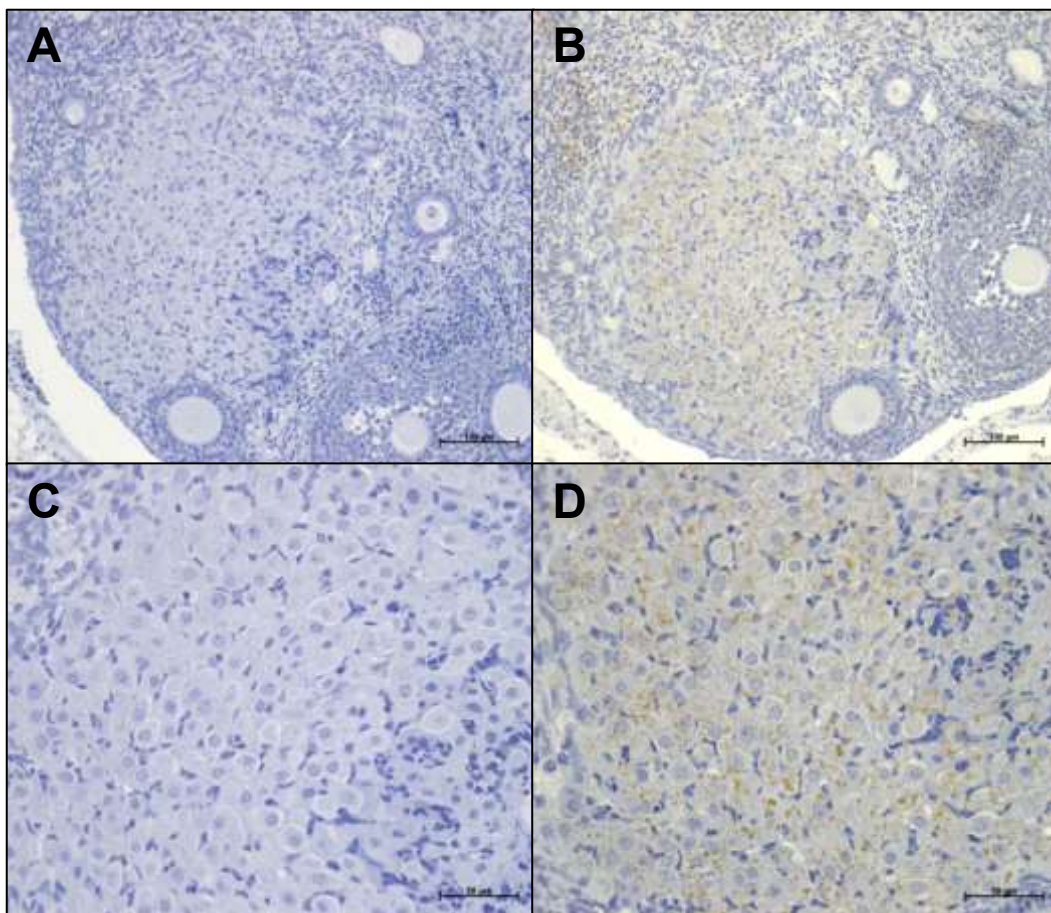
Figure 5.20: Immunohistochemistry images illustrating Pref-1 staining in mouse ovary tissue. Mouse ovaries were used as positive control tissue for Pref-1 staining. Dark blue staining indicates nuclei acid staining; brown staining indicates the presence of Pref-1. **A.** Negative control, section of ovary stained with secondary antibody only. Magnification 20x. **B.** Pref-1 stained section of the ovary displaying granular cytoplasmic staining in follicular cells. Magnification 20x. **C.** Negative control section of ovary stained with secondary antibody only. Magnification 40x. **D.** Pref-1 stained section of the ovary displaying granular cytoplasmic staining in follicular cells. Magnification 40x.

The blood vessels found within the tissue sections can also serve as internal positive controls as it has been shown that Pref-1 can be detected in the endothelial cells and pericytes around blood vessels (35). In the adipose sections we observed some faint Pref-1 positive staining around blood vessels (Figure 5.21 B and D). This positive staining is not present in the negative control stained tissue and therefore is considered to be true, positive staining (Figure 5.21 A and C). The negative controls are tissue sections stained with only the secondary antibody. Besides the staining around the blood vessels, no other Pref-1 positive staining could be detected in the adipose tissue sections. Staining of the umbilical cord sections also revealed positive Pref-1 staining around the blood vessels (Figure 5.23 B, D and F). The Wharton's Jelly also showed a noticeable level of Pref-1 staining. The positively stained cells are most likely hWJSCs.
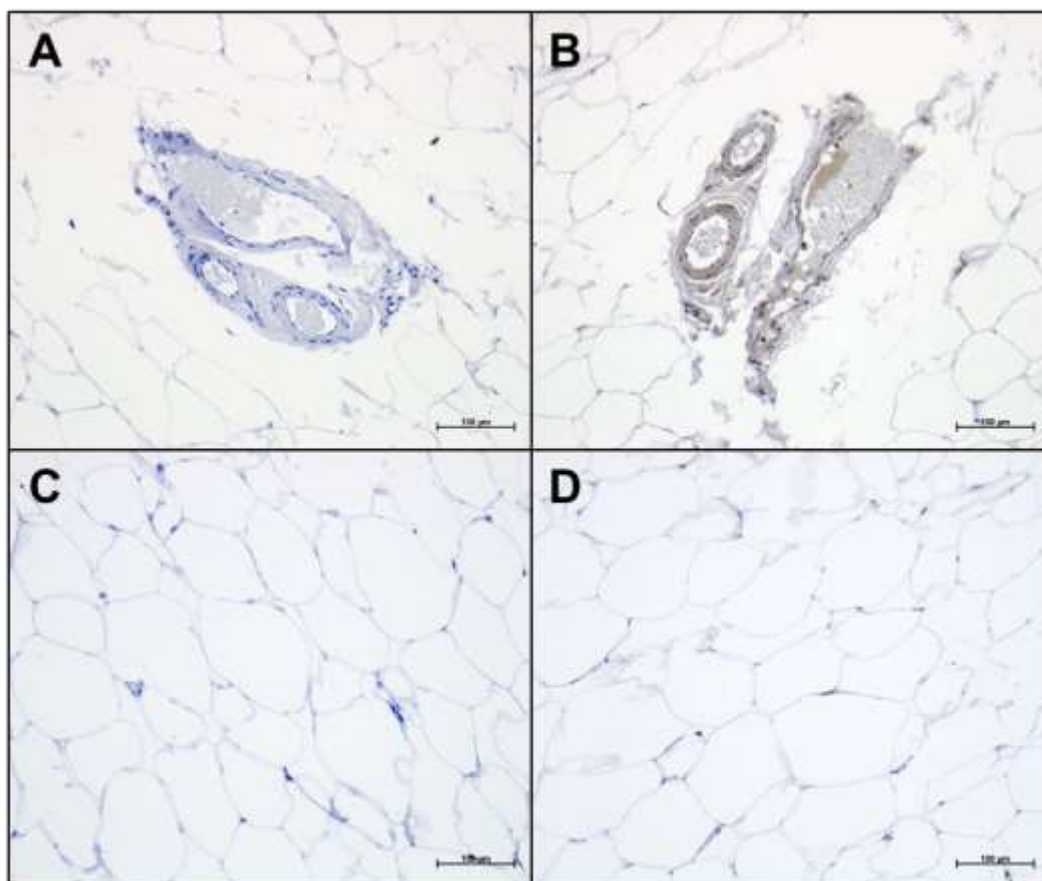
Figure 5.21: Immunohistochemistry images illustrating Pref-1 staining in human adipose tissue sections. A. Negative control adipose tissue section with blood vessels. Magnification 40x. **B.** Adipose tissue section displaying cytoplasmic Pref-1 staining of endothelial cells lining the blood vessels. Staining intensity = 2. Magnification 40x. **C.** Negative control adipose tissue

section with blood vessels. Magnification 20x. **D.** Adipose tissue section displaying cytoplasmic Pref-1 staining of endothelial cells lining the blood vessels. Magnification 20x. V, Blood vessel.
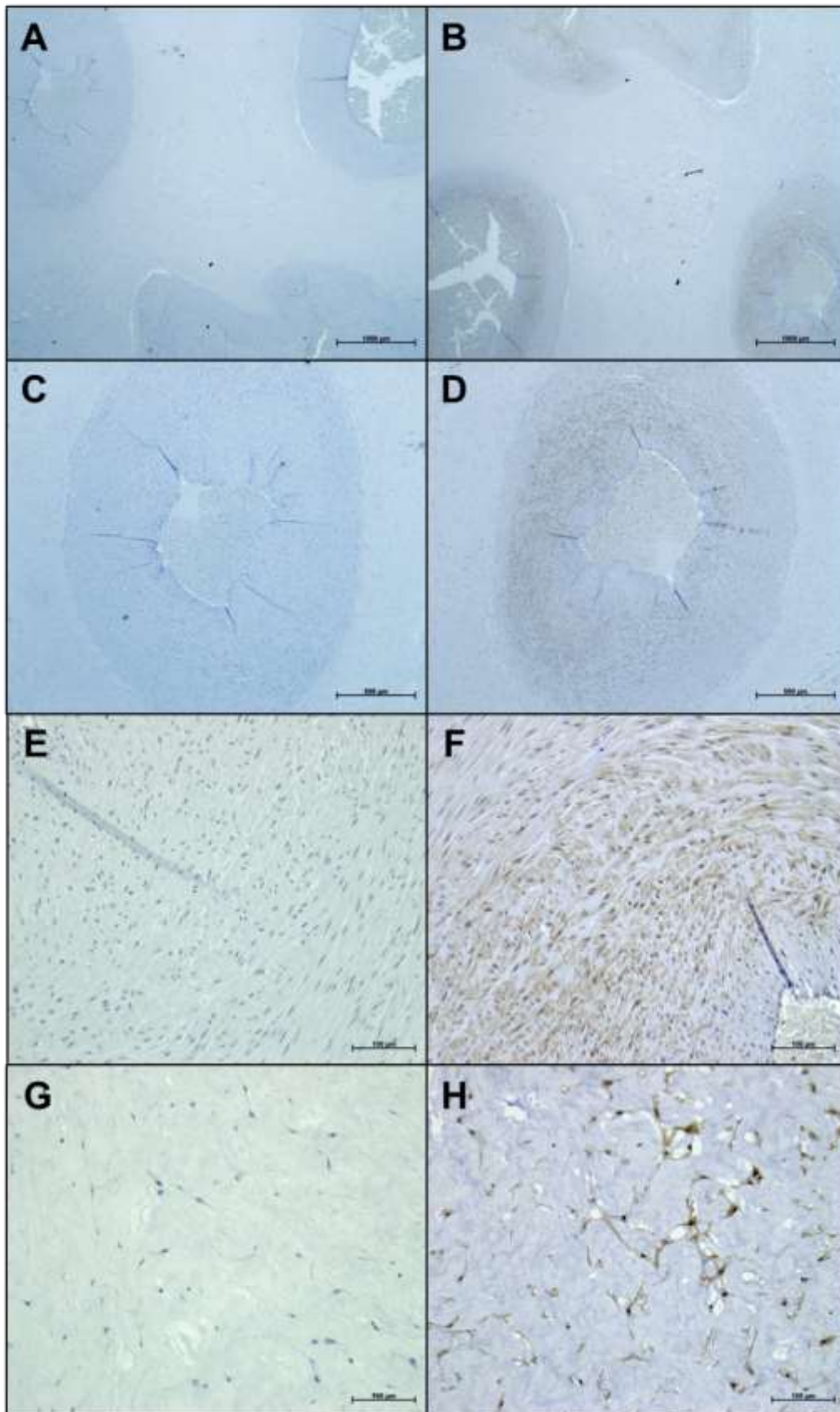
Figure 5.22: Immunohistochemistry images illustrating Pref-1 staining in human umbilical cord sections. A. Negative control, cross section of umbilical cord. Magnification 2.5x. **B.** Positive control, cross section of umbilical cord displaying cytoplasmic Pref-1 staining in smooth muscle cells of the blood vessels and stromal cells in the Wharton's jelly. Magnification 2.5x. **C.** Negative control, blood vessel. Magnification 5x. **D.** Positive control, umbilical cord section displaying granular cytoplasmic Pref-1 staining in stromal cells within the Wharton's Jelly. Magnification 5x. **E.** Negative control, Wharton's jelly. Magnification 5x. **F.** Positive control, umbilical artery displaying cytoplasmic Pref-1 staining in smooth muscle cells. Magnification 5x. **G.** Negative control, umbilical vein. Magnification 20x. **H.** Positive control, displaying positive cytoplasmic Pref-1 staining in the smooth muscle cells. Magnification 20x. **I.** Negative control, Wharton's Jelly. Magnification 20x. **J.** Positive control displaying granular cytoplasmic Pref-1 staining in stromal cells within the Wharton's. Magnification 20x. Brown staining indicates Pref-1 protein detection.

In summary, the immunohistochemistry images demonstrated the presence of Pref-1 around blood vessels in both tissues. However, the umbilical cord displayed additional Pref-1 staining in stromal cells of the Wharton's jelly.

5.5 Conclusions

The hWJSCs were included in this study based on several reports that these cells poorly differentiate into adipocytes. Previous findings (in a study performed by Karlien Kallmeyer – MSc student) in our group (data unpublished) showed higher levels of Pref-1 gene expression in hWJSCs compared to hASCs. One of the hypotheses in this study was therefore that Pref-1 protein expression would be higher in hWJSCs than hASCs. Several *in vitro* techniques were used in an attempt to confirm the presence of Pref-1 protein on the surface of hWJSCs, but none of these techniques provided conclusive results. Immunohistochemistry showed Pref-1 staining in human umbilical cord and adipose tissue sections in vascular smooth muscle cells and also in Warton's jelly stroma. How this related to our *in vitro* observations is not clear.

The *in vitro* data was not convincing and needs further investigation. The main challenge encountered was the low level of Pref-1 protein expression observed in the assays used. Many studies which have investigated Pref-1's role in adipogenesis

have done so in murine models or genetically modified cell lines in which the cells were modified to either overexpress or supress Pref-1 gene expression (1, 13, 21). This study was an attempt to determine physiological Pref-1 expression levels during in vitro adipogenic differentiation of two types of hMSCs.

Flow cytometry data revealed very low levels of Pref-1 protein expression on the cell surface of both cell types with hASCs displaying slightly higher levels than hWJSCs under both non-induced and induced culturing conditions (Figure 5.9 and Figure 5.10). However, since it is the soluble form of Pref-1 that is known to inhibit adipogenesis (5), it was hypothesised that most of the protein is most likely to be found in its cleaved form in the culture supernatant / conditioned media. This would explain the low levels of Pref-1 detected by flow cytometry.

Therefore, an ELISA assay was performed on condition medium in a second series of experiments in an attempt to detect the soluble form of Pref-1. However, no detectable levels of soluble Pref-1 were observed for either cell type using the ELISA (Table 5.1). The ELISA may not have been sensitive enough to detect the low levels of Pref-1 protein present in the samples. Flow cytometry is a much more sensitive technique which is capable of analysing a single cell/particle at a time and it was used to demonstrate that there was less than 1% (expressed as % of total cells) Pref-1 protein present in the samples analysed. It is likely that these low levels of Pref-1 are below the ELISAs lower detection limit.

A Western blot performed on cell lysates was also unable to detect Pref-1 protein. Both the 25 kDa and 50 kDa forms of the protein were detectable Figure 5.14 in the positive control (Figure 5.14). Low levels of Pref-1 were however detected when the Western blot assay was repeated using conditioned medium (Figure 5.15). The faintness of the bands observed makes it difficult for any clear conclusions to be made with regards to which cell (hASC or hWJSC) secreted the most Pref-1. Visually it seems that the bands obtained from the hWJSC conditioned medium may be slighter brighter when compared to the bands observed when hASC conditioned medium was used. However, we acknowledge that a visual assessment is very subjective and alternative, more specific methods should be considered in future experiments to quantify these bands.

We also investigated *Pref-1* gene expression levels during adipogenic differentiation. The qPCR data indicated higher levels of *Pref-1* expression in hWJSCs (Figure 5.17). Given the fact that *Sox9* purportedly increases with *Pref-1* expression in order to inhibit adipogenesis (19, 22) it was decided to look at *Sox9* expression too. Interestingly, even though the hWJSCs display higher levels of *Pref-1*, it is the hASCs that displayed higher levels of *Sox9*. These results are not aligned with what has been reported in literature (8). Wang and colleagues found that *Sox9* was up-regulated in mouse embryonic fibroblasts as well as 3T3-L1 and C3H10T1/2 cells when Pref-1 expression was induced (8). The authors were however looking at protein expression within a short time period. In this study mRNA expression was investigated over a number of days. It is however known that there is not necessarily a correlation between mRNA and protein expression (36, 37). It may still be possible that there are higher levels of the Sox9 protein present in hWJSC cultures. This was not investigated.

Overall, the findings made in this study do not conclusively implicate Pref-1 in the poor adipogenic differentiation capacity of hWJSCs (Figure 4.9). There are a number of adipogenic differentiation regulators. Pref-1 is only one of the many identified inhibitors. Other inhibitors of adipogenesis include Krüppel-like factor (KLF) 2 and 7, Wnt-10b, Wnt-5, C/EBPγ and C/EBPζ, to name just a few (38-40). Differentiation pathways are governed by an intricate network of genes and their interactions. It is unlikely that a single gene/protein is responsible for the poor adipogenic differentiation capacity observed in hWJSCs. Given the fact that we saw upregulation of PPARG in combination with poor differentiation suggests that downstream regulators of adipogenesis are also implicated, which prevent the hWJSCs from obtaining the full adipocyte phenotype.

5.6 References

1.   Smas CM, Sul HS. Pref-1, a protein containing EGF-like repeats, inhibits adipocyte differentiation. Cell. 1993;73(4):725-34.

2.   Garces C, Ruiz-Hidalgo MJ, Bonvini E, Goldstein J, Laborda J. Adipocyte differentiation is modulated by secreted delta-like (dlk) variants and requires the expression of membrane-associated dlk. Differentiation. 1999;64(2):103-14.

3.   Jing K, Heo JY, Song KS, Seo KS, Park JH, Kim JS, et al. Expression regulation and function of Pref-1 during adipogenesis of human mesenchymal stem cells (MSCs). Biochim Biophys Acta. 2009;1791(8):816-26.

4.   Kim KA, Kim JH, Wang Y, Sul HS. Pref-1 (preadipocyte factor 1) activates the MEK/extracellular signal-regulated kinase pathway to inhibit adipocyte differentiation. Mol Cell Biol. 2007;27(6):2294-308.

5.   Mei B, Zhao L, Chen L, Sul HS. Only the large soluble form of preadipocyte factor-1 (Pref-1), but not the small soluble and membrane forms, inhibits adipocyte differentiation: role of alternative splicing. Biochem J. 2002;364(Pt 1):137-44.

6.   Smas CM, Chen L, Sul HS. Cleavage of membrane-associated pref-1 generates a soluble inhibitor of adipocyte differentiation. Mol Cell Biol. 1997;17(2):977-88.

7.   Traustadottir GA, Kosmina R, Sheikh SP, Jensen CH, Andersen DC. Preadipocytes proliferate and differentiate under the guidance of Delta-like 1 homolog (DLK1). Adipocyte. 2013;2(4):272-5.

8.   Wang Y, Sul HS. Pref-1 regulates mesenchymal cell commitment and differentiation through Sox9. Cell Metab. 2009;9(3):287-302.

9.   Nueda ML, Baladron V, Sanchez-Solana B, Ballesteros MA, Laborda J. The EGF-like protein dlk1 inhibits notch signaling and potentiates adipogenesis of mesenchymal cells. J Mol Biol. 2007;367(5):1281-93.

10.   Karagianni M, Brinkmann I, Kinzebach S, Grassl M, Weiss C, Bugert P, et al. A comparative analysis of the adipogenic potential in human mesenchymal stromal cells from cord blood and other sources. Cytotherapy. 2013;15(1):76-88.

11. Zhang X, Hirai M, Cantero S, Ciubotariu R, Dobrila L, Hirsh A, et al. Isolation and characterization of mesenchymal stem cells from human umbilical cord blood: reevaluation of critical factors for successful isolation and high ability to proliferate and differentiate to chondrocytes as compared to mesenchymal stem cells from bone marrow and adipose tissue. J Cell Biochem. 2011;112(4):1206-18.

12. Boney CM, Fiedorek FT, Jr., Paul SR, Gruppuso PA. Regulation of preadipocyte factor-1 gene expression during 3T3-L1 cell differentiation. Endocrinology. 1996;137(7):2923-8.

13. Wang Y, Kim KA, Kim JH, Sul HS. Pref-1, a preadipocyte secreted factor that inhibits adipogenesis. J Nutr. 2006;136(12):2953-6.

14. Bachmann E, Krogh TN, Hojrup P, Skjodt K, Teisner B. Mouse fetal antigen 1 (mFA1), the circulating gene product of mdlk, pref-1 and SCP-1: isolation, characterization and biology. J Reprod Fertil. 1996;107(2):279-85.

15. de Zegher F, Diaz M, Sebastiani G, Martin-Ancel A, Sanchez-Infantes D, Lopez-Bermejo A, et al. Abundance of circulating preadipocyte factor 1 in early life. Diabetes Care. 2012;35(4):848-9.

16. Floridon C, Jensen CH, Thorsen P, Nielsen O, Sunde L, Westergaard JG, et al. Does fetal antigen 1 (FA1) identify cells with regenerative, endocrine and neuroendocrine potentials? A study of FA1 in embryonic, fetal, and placental tissue and in maternal circulation. Differentiation. 2000;66(1):49-59.

17. Carlsson C, Tornehave D, Lindberg K, Galante P, Billestrup N, Michelsen B, et al. Growth hormone and prolactin stimulate the expression of rat preadipocyte factor-1/delta-like protein in pancreatic islets: molecular cloning and expression pattern during development and growth of the endocrine pancreas. Endocrinology. 1997;138(9):3940-8.

18. Halder SK, Takemori H, Hatano O, Nonaka Y, Wada A, Okamoto M. Cloning of a membrane-spanning protein with epidermal growth factor-like repeat motifs from adrenal glomerulosa cells. Endocrinology. 1998;139(7):3316-28.

19. Sul HS. Minireview: Pref-1: role in adipogenesis and mesenchymal cell fate. Mol Endocrinol. 2009;23(11):1717-25.

20. Hudak CS, Sul HS. Pref-1, a gatekeeper of adipogenesis. Front Endocrinol (Lausanne). 2013;4:79.

21. Wang Y, Sul HS. Ectodomain shedding of preadipocyte factor 1 (Pref-1) by tumor necrosis factor alpha converting enzyme (TACE) and inhibition of adipocyte differentiation. Mol Cell Biol. 2006;26(14):5421-35.

22. Moon Y, Lee S, Park B, Park H. Distinct hypoxic regulation of preadipocyte factor-1 (Pref-1) in preadipocytes and mature adipocytes. Biochim Biophys Acta. 2018;1865(2):334-42.

23. Gulyaeva O, Nguyen H, Sambeat A, Heydari K, Sul HS. Sox9-Meis1 Inactivation Is Required for Adipogenesis, Advancing Pref-1(+) to PDGFRalpha(+) Cells. Cell Rep. 2018;25(4):1002-17 e4.

24. Aydin S. A short history, principles, and types of ELISA, and our laboratory experience with peptide/protein analyses using ELISA. Peptides. 2015;72:4-15.

25. Kurien BT, Scofield RH. Western blotting: an introduction. Methods Mol Biol. 2015;1312:17-30.

26. Ramos-Vara JA. Technical aspects of immunohistochemistry. Vet Pathol. 2005;42(4):405-26.

27. Duraiyan J, Govindarajan R, Kaliyappan K, Palanisamy M. Applications of immunohistochemistry. J Pharm Bioallied Sci. 2012;4(Suppl 2):S307-9.

28. Cartun RWT, C. R. and Dabbs, D. J. Techniques of Immunohistochemistry: Principles, Pitfalls, and Standardization. In: Dabbs DJ, editor. Diagnostic Immunohistochemistry: Theranostic and Genomic Applications. Fith ed. Philadelphia, PA: Elsevier; 2019. p. 1-46.

29. Mescher AL. Histology & Its Methods of Study. In: Weitz MaK, B., editor. Junqueira's Basic Histology Text and Atlas. Thirteenth ed: McGraw-Hill Medical; 2013. p. 1-17.

30. Faje AT, Fazeli PK, Katzman D, Miller KK, Breggia A, Rosen CJ, et al. Inhibition of Pref-1 (preadipocyte factor 1) by oestradiol in adolescent girls with anorexia nervosa is associated with improvement in lumbar bone mineral density. Clin Endocrinol (Oxf). 2013;79(3):326-32.

31. Lee SH, Rhee M, Yang HK, Ha HS, Lee JH, Kwon HS, et al. Serum preadipocyte factor 1 concentrations and risk of developing diabetes: a nested case-control study. Diabet Med. 2016;33(5):631-8.

32. Du R, Zhu L, Gan J, Wang Y, Qiao L, Liu B. Ultrasensitive Detection of Low-Abundance Protein Biomarkers by Mass Spectrometry Signal Amplification Assay. Anal Chem. 2016;88(13):6767-72.

33. Finehout EJ, Lee KH. An introduction to mass spectrometry applications in biological research. Biochem Mol Biol Educ. 2004;32(2):93-100.

34. Su AI, Wiltshire T, Batalov S, Lapp H, Ching KA, Block D, et al. A gene atlas of the mouse and human protein-encoding transcriptomes. Proc Natl Acad Sci U S A. 2004;101(16):6062-7.

35. Zwierzina ME, Ejaz A, Bitsche M, Blumer MJ, Mitterberger MC, Mattesich M, et al. Characterization of DLK1(PREF1)+/CD34+ cells in vascular stroma of human white adipose tissue. Stem Cell Res. 2015;15(2):403-18.

36. Lundberg E, Fagerberg L, Klevebring D, Matic I, Geiger T, Cox J, et al. Defining the transcriptome and proteome in three functionally different human cell lines. Mol Syst Biol. 2010;6:450.

37. Wilhelm M, Schlegl J, Hahne H, Gholami AM, Lieberenz M, Savitski MM, et al. Mass-spectrometry-based draft of the human proteome. Nature. 2014;509(7502):582-7.

38. Rosen ED, MacDougald OA. Adipocyte differentiation from the inside out. Nat Rev Mol Cell Biol. 2006;7(12):885-96.

39. Rosen ED, Walkey CJ, Puigserver P, Spiegelman BM. Transcriptional regulation of adipogenesis. Genes Dev. 2000;14(11):1293-307.

40. Sarjeant K, Stephens JM. Adipogenesis. Cold Spring Harb Perspect Biol. 2012;4(9):a008417.

Chapter 6:   Conclusions

The potential use of hMSCs in tissue engineering and regenerative medicine has been extensively explored over the last few years (1-10). In addition, the ability of these multipotent cells to differentiate into various cell types, including adipocytes, allows investigators to use these cells as a model to study cellular processes such as adipogenesis. MSCs can be isolated from most adult tissues and several studies suggest that MSCs isolated from different sources differ in their differentiation potential, cytokine secretion profile and matrix remodelling properties (11). Thus, it is important to fully understand the characteristics and capabilities of MSCs isolated from different sources before they can be considered for therapeutic purposes. The study described in this dissertation focus on the ability of hASCs and hWJSCs to differentiate into adipocytes *in vitro*. (12). A better understanding of the molecular and cellular regulators involved in adipogenesis will potentially lead to the development of treatment strategies that would target these molecular and/or cellular candidates identified in these studies. Improved treatment strategies might consequently assist in improved treatments for obesity and its associated comorbidities.

Several studies, including work performed in our laboratory, have shown that hWJSCs have poor adipogenic differentiation potential (1, 13, 14). This study attempts to develop a better understanding of early regulators that suppress adipogenic differentiation in hMSCs and by so doing, to potentially understand the poor adipogenic differentiation capacity of hWJSCs. Previous data generated in our laboratory by Ms Karlien Kallmeyer (unpublished) suggested that Pref-1, a protein that has been considered as an inhibitor of adipogenesis since its discovery, may be responsible for suppressing adipogenic differentiation of hWJSCs; however, her study only examined levels of expression of Pref-1 mRNA. In order to investigate this hypothesis, both hWJSCs and hASCs were induced to undergo adipogenic differentiation for 21 days. During the differentiation period, Pref-1 expression was measured at both mRNA and protein levels. This study is novel in that we investigated physiological Pref-1 expression levels during adipogenesis as opposed to the majority of studies where Pref-1 expression was either genetically induced or

suppressed in cells or murine models (15-19). hASCs served as the control cell type to investigate adipogenic differentiation in hWJSCs since the former readily differentiate into adipocytes. The hypothesis was that higher levels of Pref-1 protein expression would be detected in hWJSCs cultures compared to hASCs, indirectly suggesting that Pref-1 may play a role in preventing WJSCs to undergo adipogenic differentiation.

Isolated hWJSCs and hASCs were cultured and induced to undergo adipogenic differentiation over a period of 21 days. Throughout the differentiation period, the cells were monitored and data collected on days 0, 1, 3, 7, 14 and 21 post adipogenic induction. Firstly, the phenotype of the two different cell types was assessed in order to determine whether they adhere to the ISCT (20) and IFATS (21) Guidelines. The data obtained confirmed that both isolated cell types adhered to the guidelines and do in fact display similar phenotypic characteristics under both non-induced and induced conditions (Table 3.4 and Table 4.5)). The majority of the cells analysed display the following immunophenotype: CD34+/ CD36+/ CD44+/ CD73+/ CD90+/ CD105+/ CD45-. The only observable phenotypic difference between the two cell types was the presence of two CD36 populations (CD36 dim positive and CD36 bright positive) in the hASCs which was not seen in the hWJSC cultures (Figure 3.16). The hWJSCs only possessed a CD36 dim positive population. During adipogenic differentiation of hASCs, the proportion of CD36 bright cells gradually increased (Figure 3.17) over the 21-day differentiation period. CD36 is a fatty acid translocase which has been shown to play an essential role in adipocyte differentiation by binding long chain fatty acids and aiding their transport into cells (22).

With regard to the adipogenic differentiation capacity of hWJSCs, our data confirms what has previously been stated in literature (1, 11, 13, 14). The hWJSCs displayed very poor adipogenic differentiation capacity in comparison to hASCs. This was reflected by the fluorescent microscopy data (Figure 4.5 and Figure 4.6) as well as the Nile red flow cytometry data (Figure 4.12). The fluorescent microscopy images show that hASCs accumulate lipid droplets earlier than hWJSCs during the differentiation process and by the end of the differentiation period there were a greater number of terminally differentiated adipocytes present in the induced hASC

cultures. The Nile red flow cytometry data provides a more quantitative measure of differentiation. By the end of the 21-day differentiation period, a mean differentiation of 28.50% ± 2.91% was observed for hASCs whereas only 2.91% ± 2.72% of hWJSCs showed adipogenic differentiation (Figure 4.10 and Figure 4.11). Lastly, adipogenic differentiation was also compared by looking at the expression of PPARG, the main regulator of adipogenesis (23-25), using RT-qPCR. Gene expression data showed upregulation of *PPARG* in both cell types (Figure 4.13). The meaning of the lack of adipogenic differentiation in hWJSCs despite *PPARG* up regulation is not clear and needs further investigation. One could hypothesize that factors beyond *PPARG* expression are inhibiting the differentiation process in the hWJSCs.

Pref-1 and Sox9 gene expression were also studied using RT-qPCR. Higher levels of Pref-1 mRNA were observed in hWJSCs even though this was not statistically significant when compared to hASC Pref-1 mRNA expression levels (Table 5.5). Sox9 expression was investigated as literature suggested that Sox9 increases with Pref-1 expression in order to inhibit adipogenesis (26, 27). However, this was not the case in our study. Even though hWJSCs showed higher levels of Pref-1 mRNA, hASCs had higher levels of Sox9 mRNA (Table 5.6). Given the fact that mRNA and protein levels do not necessarily correlate (28, 29), it may still be possible that there are higher levels of Sox9 protein in the hWJSCs; this was not investigated.

Pref-1 protein expression was also investigated. Flow cytometry data revealed that hASCs to have higher levels of Pref-1 protein present on the cell surface (Figure 5.9 and Figure 5.10) even though the number of cells expressing the protein constituted a very small percentage of the cells: Pref-1 expression was observed in less than 1% of the cells analysed. As mentioned before, flow cytometry is a very sensitive technique which allows for the accurate detection of rare events. Using this technique, one can analyse a single cell at a time and identify cells of interest present at low frequency within a heterogeneous population based on specific characteristics, such as Pref-1 cell surface expression. However, it must be noted that the hWJSCs data was skewed by a large degree of variability observed in the Pref-1 protein expression. Once again, no statistical significance could be shown.

The low level of protein detected by flow cytometry was attributed to the cleavage of the protein from the cell surface; whether this is the case will need to be confirmed.

As a result, the focus of the remaining experiments turned towards the detection of the 50 kDa soluble form of the protein. An ELISA was performed on conditioned medium. The ELISA was however unable to detect Pref-1 protein in either cell type (Table 5.1). A Western blot performed on cell lysates was also unable to detect Pref-1 protein (Figure 5.14). However, the 50 kDa form of the protein were consistently detectable (Figure 5.13) in the positive control (peripheral blood plasma). The Western blot was also performed on cell extracts and conditioned media. Faint Pref-1 bands were detected in conditioned media from both cell types after prolonged exposure of blots - 30 min (Figure 5.15). Visually it seems that the bands obtained from the hWJSC conditioned media were slightly brighter, suggesting more Pref-1 protein present. However, this cannot be stated with confidence. Pref-1 protein was not detected in cell extracts, confirming the very low levels detected by flow cytometry. The only conclusion that can be made with certainty was that the active form of the protein is released by both cell types.

The data obtained from the immunohistochemical staining of human derived adipose tissue and umbilical cord shows that Pref-1 is present around blood vessels in both tissues (Figure 5.21 and Figure 5.22). The umbilical cord does however display additional Pref-1 staining in the Wharton's jelly (Figure 5.22 J). Whether the presence of Pref-1 in the hWJSC micro-environment plays a role in preventing its adipogenic differentiation in vitro remains to be investigated.

With regard to future studies, the lack of differentiation observed in hWJSCs despite PPARG upregulation should be further investigated. Our data suggest that mechanisms regulating the poor adipogenic differentiation observed in hWJSCs may be downstream of *PPARG* expression. It is possible that molecular regulatory elements downstream of *PPARG* are involved in preventing hWJSCs from expressing end-stage adipogenic genes, such as CD36 (Figure 3.16 and Figure 4.13). The phenotype data obtained herein suggests that CD36, a fatty acid translocase, may be a potential target for future studies. Previous work conducted in our laboratory has shown that there is an increase in CD36 expression in hASCs

which precedes lipid accumulation (30). Our data showed that hWJSCs only possess a CD36 dim population, with no upregulation of CD36 expression during the 21-day induction period (Figure 3.17 and Figure 3.18). In contrast, hASCs possess a CD36 bright population in addition to their CD36 dim population which gradually increases over time in culture when induced to undergo adipogenesis (Figure 3.17). In summary, our data suggests that mechanisms downstream of *PPARG* may be responsible for preventing adipogenesis in hWJSCs.

6.6 References

1. Bieback K, Brinkmann I. Mesenchymal stromal cells from human perinatal tissues: From biology to cell therapy. World J Stem Cells. 2010;2(4):81-92.

2. Hug K. Therapeutic perspectives of human embryonic stem cell research versus the moral status of a human embryo--does one have to be compromised for the other? Medicina (Kaunas). 2006;42(2):107-14.

3. Kobolak J, Dinnyes A, Memic A, Khademhosseini A, Mobasheri A. Mesenchymal stem cells: Identification, phenotypic characterization, biological properties and potential for regenerative medicine through biomaterial micro-engineering of their niche. Methods. 2016;99(15):62-8.

4. Nae S, Bordeianu I, Stancioiu AT, Antohi N. Human adipose-derived stem cells: definition, isolation, tissue-engineering applications. Rom J Morphol Embryol. 2013;54(4):919-24.

5. Nagamura-Inoue T, He H. Umbilical cord-derived mesenchymal stem cells: Their advantages and potential clinical utility. World J Stem Cells. 2014;6(2):195-202.

6. Nagamura-Inoue T, Mukai T. Umbilical Cord is a Rich Source of Mesenchymal Stromal Cells for Cell Therapy. Curr Stem Cell Res Ther. 2016;11(8):634-42.

7. Trounson A. New perspectives in human stem cell therapeutic research. BMC Med. 2009;7:29.

8. Varghese J, Griffin M, Mosahebi A, Butler P. Systematic review of patient factors affecting adipose stem cell viability and function: implications for regenerative therapy. Stem Cell Res Ther. 2017;8(1):45.

9. Fitzsimmons REB, Mazurek MS, Soos A, Simmons CA. Mesenchymal Stromal/Stem Cells in Regenerative Medicine and Tissue Engineering. Stem Cells Int. 2018;2018:8031718.

10. Hosseini S, Taghiyar L, Safari F, Baghaban Eslaminejad M. Regenerative Medicine Applications of Mesenchymal Stem Cells. Adv Exp Med Biol. 2018;1089:115-41.

11. Amable PR, Teixeira MV, Carias RB, Granjeiro JM, Borojevic R. Protein synthesis and secretion in human mesenchymal cells derived from bone marrow, adipose tissue and Wharton's jelly. Stem Cell Res Ther. 2014;5(2):53.

12. Janderova L, McNeil M, Murrell AN, Mynatt RL, Smith SR. Human mesenchymal stem cells as an in vitro model for human adipogenesis. Obes Res. 2003;11(1):65-74.

13. Ragni E, Vigano M, Parazzi V, Montemurro T, Montelatici E, Lavazza C, et al. Adipogenic potential in human mesenchymal stem cells strictly depends on adult or foetal tissue harvest. Int J Biochem Cell Biol. 2013;45(11):2456-66.

14. Fong CY, Subramanian A, Biswas A, Bongso A. Freezing of Fresh Wharton's Jelly From Human Umbilical Cords Yields High Post-Thaw Mesenchymal Stem Cell Numbers for Cell-Based Therapies. J Cell Biochem. 2016;117(4):815-27.

15. Smas CM, Sul HS. Pref-1, a protein containing EGF-like repeats, inhibits adipocyte differentiation. Cell. 1993;73(4):725-34.

16. Wang Y, Kim KA, Kim JH, Sul HS. Pref-1, a preadipocyte secreted factor that inhibits adipogenesis. J Nutr. 2006;136(12):2953-6.

17. Wang Y, Sul HS. Ectodomain shedding of preadipocyte factor 1 (Pref-1) by tumor necrosis factor alpha converting enzyme (TACE) and inhibition of adipocyte differentiation. Mol Cell Biol. 2006;26(14):5421-35.

18. Garces C, Ruiz-Hidalgo MJ, Bonvini E, Goldstein J, Laborda J. Adipocyte differentiation is modulated by secreted delta-like (dlk) variants and requires the expression of membrane-associated dlk. Differentiation. 1999;64(2):103-14.

19. Karagianni M, Brinkmann I, Kinzebach S, Grassl M, Weiss C, Bugert P, et al. A comparative analysis of the adipogenic potential in human mesenchymal

stromal cells from cord blood and other sources. Cytotherapy. 2013;15(1):76-88.

20. Dominici M, Le Blanc K, Mueller I, Slaper-Cortenbach I, Marini F, Krause D, et al. Minimal criteria for defining multipotent mesenchymal stromal cells. The International Society for Cellular Therapy position statement. Cytotherapy. 2006;8(4):315-7.

21. Bourin P, Bunnell BA, Casteilla L, Dominici M, Katz AJ, March KL, et al. Stromal cells from the adipose tissue-derived stromal vascular fraction and culture expanded adipose tissue-derived stromal/stem cells: a joint statement of the International Federation for Adipose Therapeutics and Science (IFATS) and the International Society for Cellular Therapy (ISCT). Cytotherapy. 2013;15(6):641-8.

22. Christiaens V, Van Hul M, Lijnen HR, Scroyen I. CD36 promotes adipocyte differentiation and adipogenesis. Biochim Biophys Acta. 2012;1820(7):949-56.

23. Mota de Sa P, Richard AJ, Hang H, Stephens JM. Transcriptional Regulation of Adipogenesis. Compr Physiol. 2017;7(2):635-74.

24. Cristancho AG, Lazar MA. Forming functional fat: a growing understanding of adipocyte differentiation. Nat Rev Mol Cell Biol. 2011;12(11):722-34.

25. Cui TT, Xing TY, Chu YK, Li H, Wang N. Genetic and epigenetic regulation of PPARgamma during adipogenesis. Yi Chuan. 2017;39(11):1066-77.

26. Moon Y, Lee S, Park B, Park H. Distinct hypoxic regulation of preadipocyte factor-1 (Pref-1) in preadipocytes and mature adipocytes. Biochim Biophys Acta. 2018;1865(2):334-42.

27. Sul HS. Minireview: Pref-1: role in adipogenesis and mesenchymal cell fate. Mol Endocrinol. 2009;23(11):1717-25.

28. Lundberg E, Fagerberg L, Klevebring D, Matic I, Geiger T, Cox J, et al. Defining the transcriptome and proteome in three functionally different human cell lines. Mol Syst Biol. 2010;6:450.

29. Wilhelm M, Schlegl J, Hahne H, Gholami AM, Lieberenz M, Savitski MM, et al. Mass-spectrometry-based draft of the human proteome. Nature. 2014;509(7502):582-7.

30. Durandt C, van Vollenstee FA, Dessels C, Kallmeyer K, de Villiers D, Murdoch C, et al. Novel flow cytometric approach for the detection of adipocyte subpopulations during adipogenesis. J Lipid Res. 2016;57(4):729-42.

Appendix A: MIQE Guidelines

A.1 Introduction

The Minimal Information for publication of Quantitative real-time PCR Experiments (MIQE) is a set of guidelines that was established to attain accurate, reliable and reproducible qPCR data amongst researchers. MIQE guidelines provide a list of essential and desirable information which should be included in any research paper that contains qPCR data (1). The establishment of these guidelines was essential due to publication of misleading, irreproducible and inconsistent results which was impacting research, drug development and disease monitoring (1, 2).

For the purpose of this study, RT-qPCR was used to determine the mRNA expression of *Pref-1, Sox9* and *PPARG*, all which are genes associated with adipogenesis. In order to have confidence and assess the quality of the results produced, the MIQE guidelines check-list was used (Annexure D).

A.2 Experimental design

Cells were seeded at a density of 5 x 10^3 cells per cm^2 in T75 flasks. The cells were maintained in complete growth medium until reaching 80 - 90% confluence. At this point, the medium was aspirated and discarded. Fresh complete growth medium was added to the cells which served as the control group – referred to as non-induced cells. For the remainder of the flasks, adipogenic induction medium was added. The cells grown in adipogenic differentiation medium were the experimental group – referred to as induced cells. Non-induced / control cells were maintained in complete growth medium in parallel with the induced cells. Adipogenic differentiation was monitored over a 21-day induction period.

Three biological replicates were used for each MSC cell type.

Table A.1: Experimental layout of flasks for RNA Extraction

Day 0	Day 1	Day 3	Day 7	Day 14	Day 21
2 x T75 Non-induced	2 x T75 Non-induced	2 x T75 Non-induced	1 x T75 Non-induced	1 x T75 Non-induced	1 x T75 Non-induced
	2 x T75 Induced	2 x T75 Induced	2 x T75 Induced	2 x T75 Induced	2 x T75 Induced

A.3 Samples

A.3.1 Description

RNA was extracted from both non-induced cells (control) and induced cells at the following time points: days 0, 1, 3, 7, 14 and 21

A.3.2 Microdissection or macrodissection

The samples were not subject to micro- or macrodissection.

A.3.3 Processing

Sample processing was performed as described in Chapter 4, section 4.3.5.

A.3.4 If frozen – how and how quickly?

Samples were not subject to freezing.

A.3.5 If fixed – how and how quickly?

Samples were not fixed.

A.3.6 Storage

RNA extraction was performed directly after cells were dislodged from the bottom of the flask using a 0.25% Trypsin/EDTA solution. Extracted RNA was stored at -80ºC until used further (cDNA synthesis).

A.4 Nucleic Acid Extraction

Total RNA extraction was performed as described in Chapter 4, section 4.3.5.1.

A.4.1 DNase or RNase treatment

No DNase or RNase treatment was performed.

A.4.2 Contamination assessment

Genomic DNA (gDNA) contamination was assessed with the use of no reverse transcription (NRT) controls generated during cDNA synthesis.
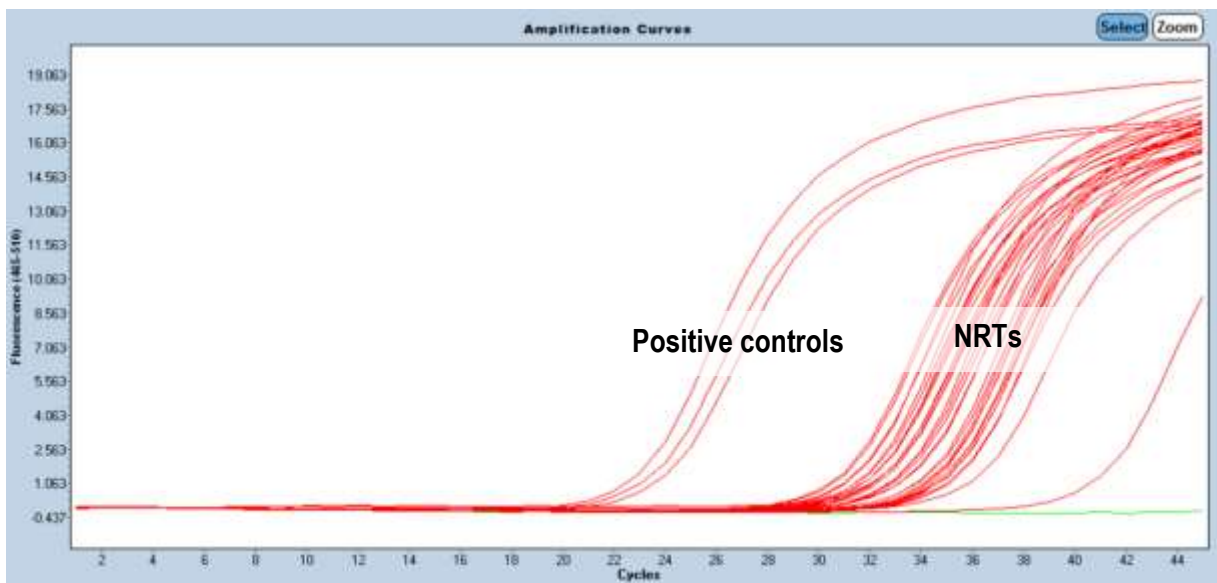
Figure A. 1: Amplification plot for NRT controls. The reference gene YWHAZ was used as a positive control with 20 ng/uL cDNA template (Mean Cp 23.19) (n = 3). Some amplification was detected in the NRT controls with mean Cp values ranging from 31 to 33.

A.4.3 Nucleic acid quantification and purity

A Nanodrop ND 1000 spectrophotometer (Thermo Fisher Scientific; Waltham, MA, USA) was used to measure the RNA concentration (ng/µL) (Table A.2 and Table A.4) and assess RNA quality (A260/A280) (Table A.3 and Table A.5). A ratio between 1.8 and 2.1 is generally accepted as pure for RNA and acceptable for use in downstream experiments (3, 4). An A260/A280 ratio outside the recommended range (1.8 to 2.1) is suggestive of contaminants in the sample. All RNA extracted and used for qPCR experiments had an A260/A280 ratio between 1.8 and 2.1.

Table A.2: RNA Concentrations obtained for RNA extracted from hASC cultures

	Concentrations (ng/µL)					
	Non- Induced			**Induced**		
	A1	**A2**	**A3**	**A1**	**A2**	**A3**
Day 0	245.40	667.80	551.40			
Day 1	296.60	892.40	648.30	361.90	1 062.30	1 170.50
Day 3	278.50	840.10	457.30	338.60	800.00	561.10
Day 7	165.80	261.30	425.80	264.00	996.10	699.40
Day 14	133.40	351.70	400.60	293.00	1 009.40	768.40
Day 21	116.60	385.10	639.90	320.80	436.40	737.80

A1 = ASC culture 1; A2 = ASC culture 2; A3 = ASC culture 3

Table A.3: RNA purity (A260/A280) values obtained for RNA extracted from hASC cultures

	A260/A280					
	Non-Induced			**Induced**		
	A1	**A2**	**A3**	**A1**	**A2**	**A3**
Day 0	2.08	2.08	2.07			
Day 1	2.06	2.09	2.09	2.03	2.08	2.07
Day 3	2.07	2.09	2.02	2.04	2.09	2.06
Day 7	2.07	2.06	2.02	2.07	2.09	2.07
Day 14	2.10	2.04	2.04	2.06	2.08	2.07
Day 21	2.03	2.04	2.09	2.03	2.03	2.09

A1 = ASC culture 1; A2 = ASC culture 2; A3 = ASC culture 3

Table A.4: RNA Concentrations obtained for RNA extracted from hWJSC cultures

	Concentrations (ng/µL)					
	Non- Induced			**Induced**		
	C1	**C2**	**C3**	**C1**	**C2**	**C3**
Day 0	1 210.10	959.10	948.10			
Day 1	1 470.80	1 158.20	643.60	1 930.80	792.20	655.80
Day 3	1 077.00	1 008.70	969.30	997.50	724.10	641.10
Day 7	654.00	448.70	359.40	1 087.60	740.90	446.70
Day 14	374.70	6.70	904.40	729.50	13.40	1131.60
Day 21	155.20	660.30	664.00	1 013.90	687.00	436.80

C1 = WJSC culture 1; C2 = WJSC culture 2; C3 = WJSC culture 3

Table A.5: RNA purity (A260/A280) values for RNA extracted from hWJSC cultures

	A260/A280					
	Non-Induced			**Induced**		
	C1	**C2**	**C3**	**C1**	**C2**	**C3**
Day 0	2.08	2.08	2.09			
Day 1	2.24	2.07	2.09	2.06	2.08	2.07
Day 3	2.08	2.09	2.10	2.08	2.09	2.09
Day 7	2.09	2.04	2.07	2.08	2.10	2.04
Day 14	2.05	1.87	2.08	2.07	1.82	2.09
Day 21	2.07	2.09	2.06	2.10	2.08	2.02

C1 = WJSC culture 1; C2 = WJSC culture 2; C3 = WJSC culture 3

A.4.4 RNA integrity

The integrity of isolated RNA was determined on a TapeStation® 2200 platform (Agilent Technologies; Santa Clara, CA, USA) using the RNA Screen Tape® (Agilent Technologies; Santa Clara, CA, USA) and sample buffer (Agilent Technologies; Santa Clara, CA, USA). A RINe value ≥ 8 is indicative of intact, high quality RNA (5). All RNA used for RT-qPCR experiments had RINe values above 8 (Table A.6 and Table A.7).

Briefly, 5 µL of sample buffer was added to 1 µL of RNA (~ 200 ng/uL) and vortexed for a minute to ensure thorough mixing. According to the manufacturer's instructions, the RNA concentration can range between 25-500 ng/µL. The sample was then transferred to a thermal cycler (Gene Amp® PCR 28 system 9700; Applied Biosystems, Life Technologies®, Thermo Fisher Scientific; Carlsbad, 29 CA, USA) where it was heated to 72ºC for 3 min and then placed on ice for 2 min. The sample was then analysed on the TapeStation® 2200.

Table A.6: RNA integrity (RIN Values) for RNA extracted from hASC samples

	Not Induced			Induced		
	A1	**A2**	**A3**	**A1**	**A2**	**A3**
Day 0	10.00	10.00	9.80			
Day 1	10.00	10.00	9.90	10.00	10.00	10.00
Day 3	10.00	10.00	9.80	10.00	10.00	10.00
Day 7	10.00	10.00	9.90	10.00	10.00	9.80
Day 14	10.00	10.00	9.90	10.00	10.00	9.50
Day 21	9.10	9.90	9.90	8.80	9.90	10.00

A1 = ASC culture 1; A2 = ASC culture 2; A3 = ASC culture 3

Table A.7: RNA integrity (RIN Values) for hWJSC samples

	Not Induced			Induced		
	A1	**A2**	**A3**	**A1**	**A2**	**A3**
Day 0	10.00	9.90	10.00			
Day 1	10.00	10.00	10.00	10.00	9.90	10.00
Day 3	10.00	10.00	10.00	10.00	10.00	10.00
Day 7	10.00	10.00	10.00	10.00	9.90	9.90
Day 14	10.00	NA	10.00	10.00	NA	9.90
Day 21	8.50	10.00	9.80	10.00	9.90	9.40

NA – Not applicable as there was no sample available

A1 = ASC culture 1; A2 = ASC culture 2; A3 = ASC culture 3
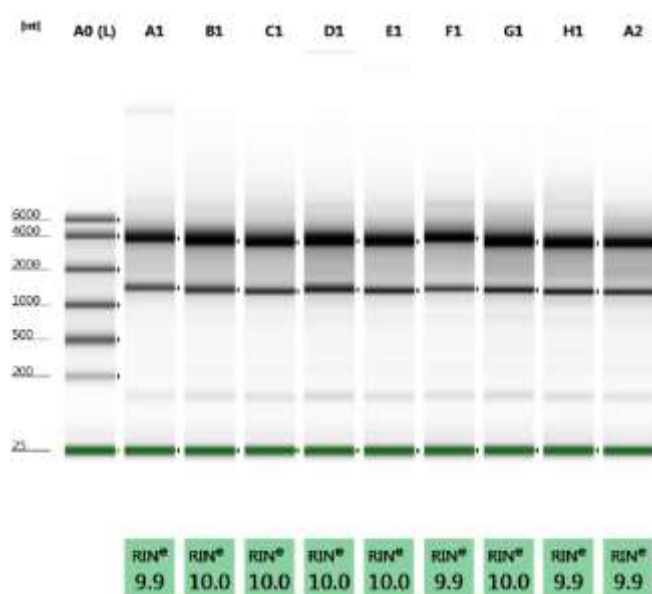
Figure A.2: Representative image of RNA integrity results obtained from TapeStation® 2200. Lane "A0" represents the ladder, remaining lanes (A1 – A2) represent the samples tested. The green blocks beneath the lanes represent the test results i.e. RIN^e values.

A.3.5 Inhibition testing:

No inhibition testing was performed.

A.5 Reverse Transcription

Reverse transcription was performed as described in Chapter 4, section 4.3.6. With regard to the reverse transcriptase enzyme, no information is given in the product leaflet except that "one unit catalyzes the incorporation of 1 nmol of dTTP into acid-soluble material in 10 min at 37^0C in 50nM Tris-HCL, pH8.6, 40nm KCl, 1mM $MnSO_4$, 1 mM DTT, and 0.5 mM [3H]TTP, using 200 µM oligo(dT)$_{12-18}$-primed poly(A)$_n$ as template."

A.5.1 cDNA Quantification & Purity Check

A Nanodrop ND 1000 spectrophotometer was used to measure the cDNA concentration (ng/µL) and quality (A260/A280). An A260/A280 ratio ~1.8 is considered pure for DNA (4). The A260/280 ratios obtained for the synthesized cDNA ranged from 1.58 to 1.81 and were deemed of good enough quality to be used for qPCR (Table A.10 and Table A.12). The slightly lower A260/280 ratios may be due to contaminants, such as phenol, within the sample.

Table A.8: cDNA Concentrations obtained for hASC cultures

	Concentrations (ng/µL)					
	Not Induced			Induced		
	A1	A2	A3	A1	A2	A3
Day 0	1154.50	1200.90	1170.70			
Day 1	1151.50	1215.40	1158.90	1365.80	1223.40	1148.10
Day 3	1172.00	1222.20	1168.70	1069.00	1197.80	1160.50
Day 7	1185.30	1210.60	1187.20	1168.20	1224.40	1140.40
Day 14	1151.10	1261.40	1138.30	959.40	1193.70	1167.40
Day 21	1150.20	1204.60	1222.20	1024.70	1160.20	1139.10

A1 = ASC culture 1; A2 = ASC culture 2; A3 = ASC culture 3

Table A.9: cDNA purity (A260/A280) values for hASC cultures

	A260/A280					
	Not Induced			Induced		
	A1	A2	A3	A1	A2	A3
Day 0	1.82	1.79	1.80			
Day 1	1.77	1.79	1.78	1.77	1.79	1.82
Day 3	1.76	1.79	1.80	1.66	1.79	1.81
Day 7	1.80	1.79	1.80	1.75	1.81	1.81
Day 14	1.76	1.79	1.81	1.58	1.79	1.80
Day 21	1.76	1.79	1.81	1.66	1.79	1.81

A1 = ASC culture 1; A2 = ASC culture 2; A3 = ASC culture 3

Table A.10: cDNA Concentrations obtained for hWJSC cultures

	Concentrations (ng/µL)					
	Not Induced			Induced		
	C1	C2	C3	C1	C2	C3
Day 0	1137.60	1150.30	1210.00			
Day 1	1171.30	1158.80	1230.80	1201.50	1199.50	1278.70
Day 3	1204.20	1163.00	1245.60	1169.70	1176.00	1262.20
Day 7	1116.90	1217.70	1241.30	1157.00	1159.90	1277.80
Day 14	1169.20	NA	1195.30	1186.70	NA	1238.50
Day 21	1193.90	1156.10	1285.00	1203.40	1144.30	1231.50

NA – Not applicable as there was no sample available

C1 = WJSC culture 1; C2 = WJSC culture 2; C3 = WJSC culture 3

Table A.11: cDNA purity (A260/A280) values for hWJSC cultures

	A260/A280					
	Not Induced			Induced		
	C1	C2	C3	C1	C2	C3
Day 0	1.80	1.80	1.81			
Day 1	1.80	1.80	1.80	1.80	1.80	1.80
Day 3	1.80	1.80	1.81	1.80	1.80	1.80
Day 7	1.80	1.80	1.80	1.81	1.81	1.79
Day 14	1.80	NA	1.81	1.80	NA	1.79
Day 21	1.80	1.80	1.80	1.81	1.82	1.80

NA – Not applicable as there was no sample available

C1 = WJSC culture 1; C2 = WJSC culture 2; C3 = WJSC culture 3

A.5.2 Quantitation cycle (Cq) values with and without reverse transcriptase (RT)

In order to save reagents, 22 stored cDNA aliquots were randomly selected (NRT 1 -11) and tested for DNA contamination. These randomly selected cDNA aliquots consisted of 11 cDNA aliquots isolated from ASCs and WJCs, respectively. The primers for reference gene *YWHAZ* were used for the amplification of the NRT controls. A cDNA concentration equivalent to that which was used for the amplification reactions was used (20 ng/uL). A positive control i.e. sample with reverse transcriptase was also amplified using the YWHAZ primers; a cDNA concentration of 20 ng/uL was also used for the positive control. The results obtained are summarized in Table A.12. Figure A.1 is a visual representation of the data in Table A.12

Table A.12: Quantitation cycle values of NRT controls

	Cq's	
Sample	hASC	hWJSC
NRT 1	31.73	35.97
NRT 2	34.91	34.00
NRT 3	31.50	33.53
NRT 4	32.11	34.24
NRT 5	34.07	34.82
NRT 6	33.50	33.44
NRT 7	34.76	36.12
NRT 8	30.88	33.60
NRT 9	32.55	36.90
NRT 10	36.17	36.61
NRT 11	34.33	36.45
Mean Cq	33.32	35.06
Positive Ctrl	23.2	

The results suggest that there is some genomic DNA contamination. However, the NRT controls amplify roughly 10 cycles after the positive control.

A.5.3 cDNA storage

The cDNA was stored at -20 ºC until used in RT-qPCR experiments.

A.6 qPCR Target Information

The accession numbers for the target genes (Pref-1, Sox9, PPARG) as well as reference genes (PPIA, TBP, YWHAZ) used are listed in Table A.13. Amplicon location and length is listed in Table A.14.

Table A.13: Accession numbers for genes of interest and reference genes

Genes of Interest		
Gene name		**Accession number**
Pre-adipocyte Factor 1	*Pref-1*	NM_001032997.1
Sex-Determining Region Y-Box 9 Protein	*Sox9*	NM_000346.3
Peroxisome proliferator-activated receptor gamma	*PPARG*	NM_138712.3
Peptidylprolyl Isomerase A	*PPIA*	NM_001300981.1
TATA binding protein	*TBP*	NM_001172085.1
Tyrosine 3-Monooxygenase/Tryptophan 5-Monooxygenase Activation Protein, Zeta	*YWHAZ*	NM_001135699.1

Table A.14: Amplicon location for genes of interest and reference genes

Gene	Amplicon Location		Amplicon Length
	Start	**Stop**	
Pref-1	1165	1257	92
Sox9	2763	2899	136
PPARG	304	428	124
PPIA	800	916	116
TBP	638	768	130
YWHAZ	2235	2361	126

A.6.1 *In* silico specificity screen

The specificity of the primers was tested *in silico* using NCBI BLAST® (Version 4.1.0). If any of the primer pairs returned any match other than the sequence of interest, they were excluded from the study.

A.6.2 Primer locations

NCBI's Primer-BLAST® was used to visualise the primer locations as seen in Figure A.3.

A.6.3 Splice variants targeted

No splice variants were targeted.

A. *Pref-1*
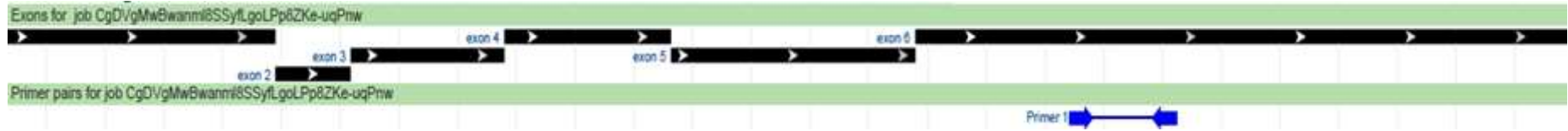
B. *Sox9*
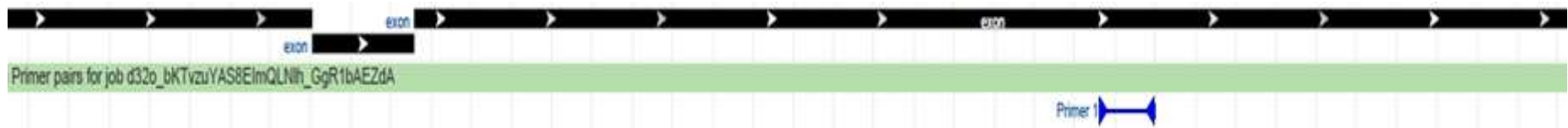
C. *PPARG*
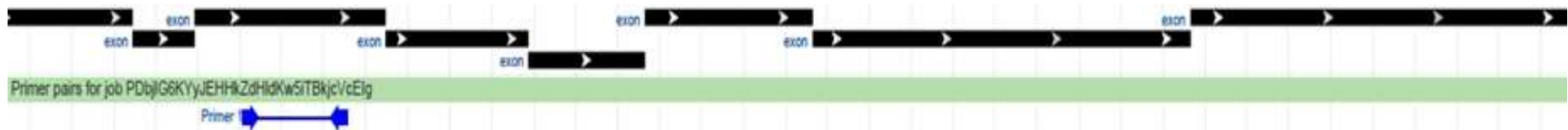
D. *TBP*
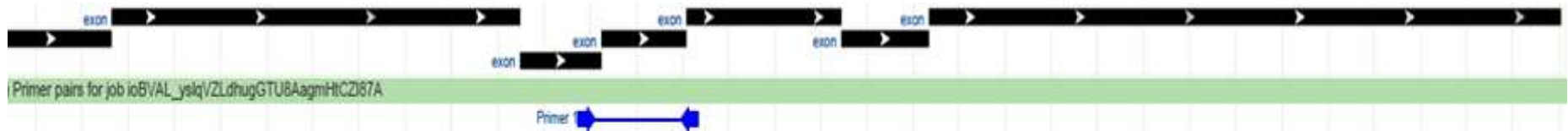
E. *PPIA*

F. *YWHAZ*
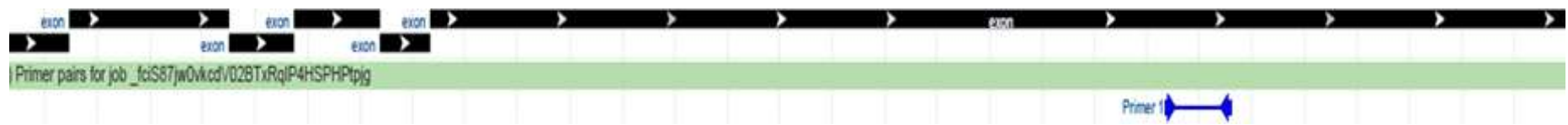
Figure A.3: Primer locations. NCBI's Primer-BLAST® tool was used to show the binding location of the primers. The black bars represent the genes exons while the blue indicates the position at which the primer binds.

A.7 qPCR Oligonucleotides

The primer sequences for the genes of interest (*Pref-1, Sox9, PPARG*) as well as reference genes (*PPIA, TBP, YWHAZ*) used can be found in Table A.15.

Table A.15: Primer sequences for genes of interest and reference genes

Gene	Forward Sequence 3' – 5'	Reverse Sequence 3' – 5'
Pref-1	ACTGTGGGTATCGTCTTCCT	AGCAGCAGGTTCTTCTTCTTC
Sox9	GCTGCTGGGAAACATTTG	CACTTATTGGCTGCTGAAAC
PPARG	CGTGGATCTCTCCGTAAT	TGGATCTGTTCTTGTGAATG
PPIA	GAGTTAAGAGTGTTGATGTAGG	CCTGGGACTGGAAAGTAA
TBP	CCGAAACGCCGAATATAA	GGACTGTTCTTCACTCTTG
YWHAZ	TGACATTGGGTAGCATTAAC	GCACCTGACAAATAGAAAGA

A.7.1 Location and identity of any modifications

No modifications were made.

A.7.2 Manufacturer of oligonucleotides

The oligonucleotides were manufactured by Integrated DNA Technologies (IDT; Coralville, IA, USA).

A.8 RT-qPCR Protocol

RT-qPCR was performed as described in Chapter 4, section 4.3.7 and Chapter 5, section 5.3.7.

A.8.1 Polymerase identity & concentration

The polymerase in the LightCycler® 480 SYBR Green I Master Mix is FastStart™ Taq DNA polymerase (Roche, Basel, Switzerland). No concentration was indicated.

A.8.2 Buffer/kit identity and manufacturer

The LightCycler® 480 SYBR Green I Master Mix (Roche, Basel, Switzerland; Catalogue number: 04887352001) was used in all RT-qPCR reactions).

A.8.3 Additives

No additives were used.

A.8.4 Manufacturer of plates/tubes and catalogue numbers

The LightCycler® 480 Multiwell Plate 96 white plates (Roche, Basel, Switzerland; Catalogue 17 number: 04729692001) were used for the qPCR assays.

A.8.5 Manufacturer of qPCR instrument

The qPCR reactions were carried out using a LightCycler 480 II instrument (Roche,Basel, Switzerland).

A.9 qPCR Validation

A.9.1 Specificity

Melt curves were used to determine the specificity of the qPCR reactions. Melt curves were performed at the end of every run in order to determine the presence of primer dimers, secondary product and contamination. The presence of contamination or secondary product would result in the presence of an additional peak before or after the melting temperature (T_m) peak. With regard to primer dimers, a small shoulder would be visible before the main T_m peak. Representative images of the melt curves obtained in this study can be found in. Figure A.4 below

A. *Pref-1*
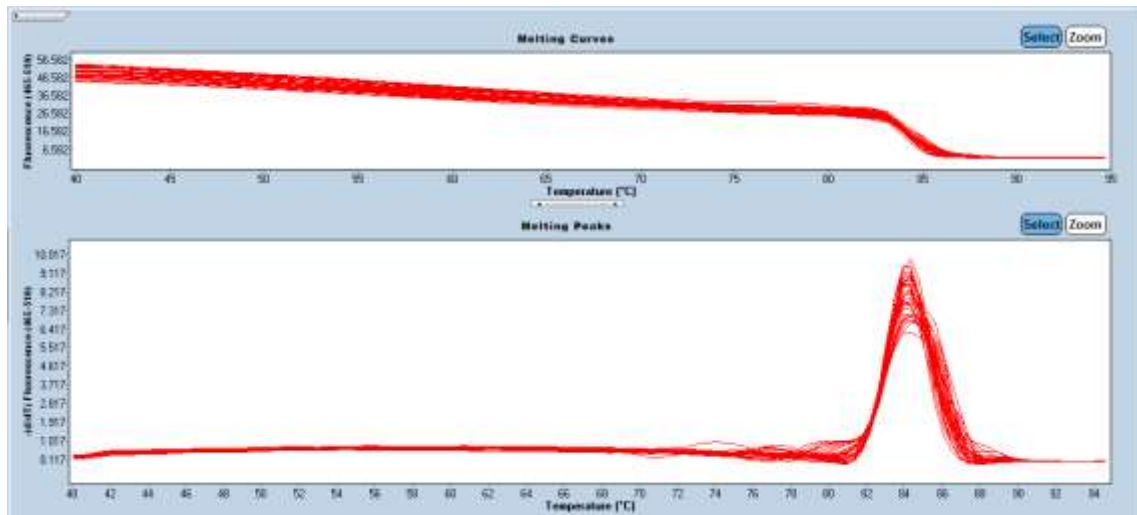
B. *Sox9*
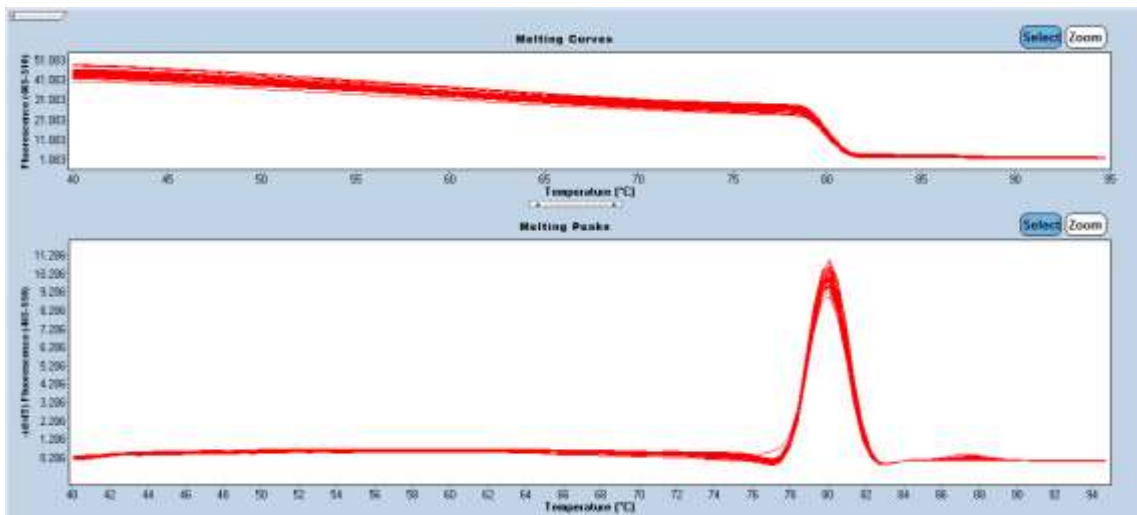
C. *PPARG*
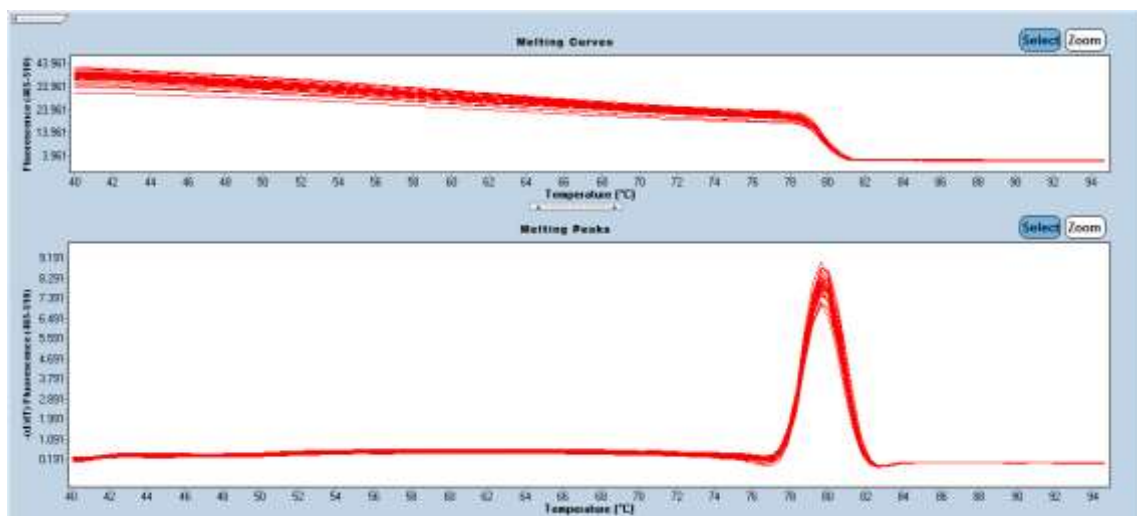
D. *PPIA*
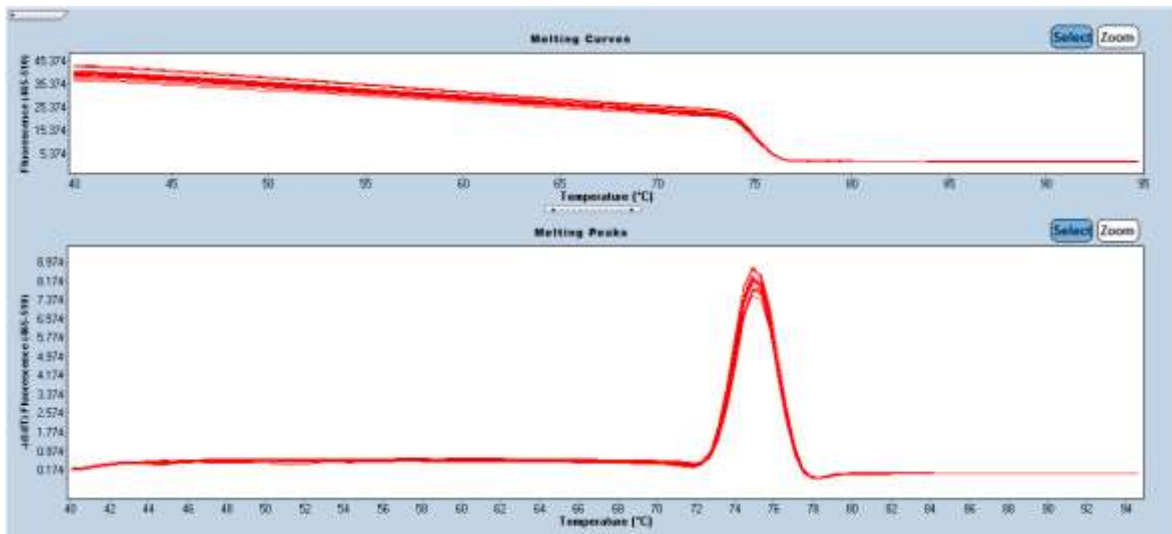
E. *TBP*
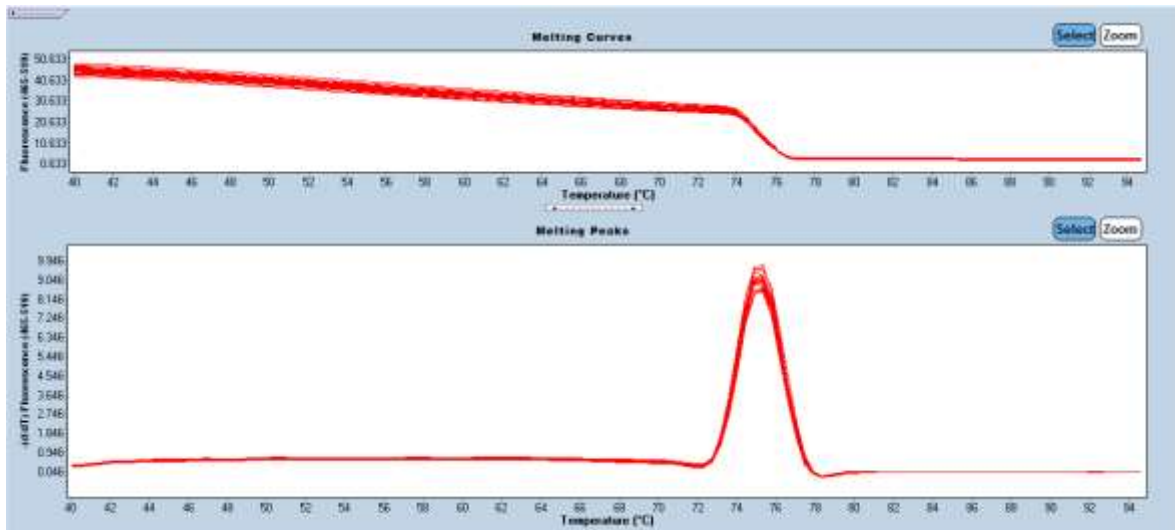
F. *YWHAZ*
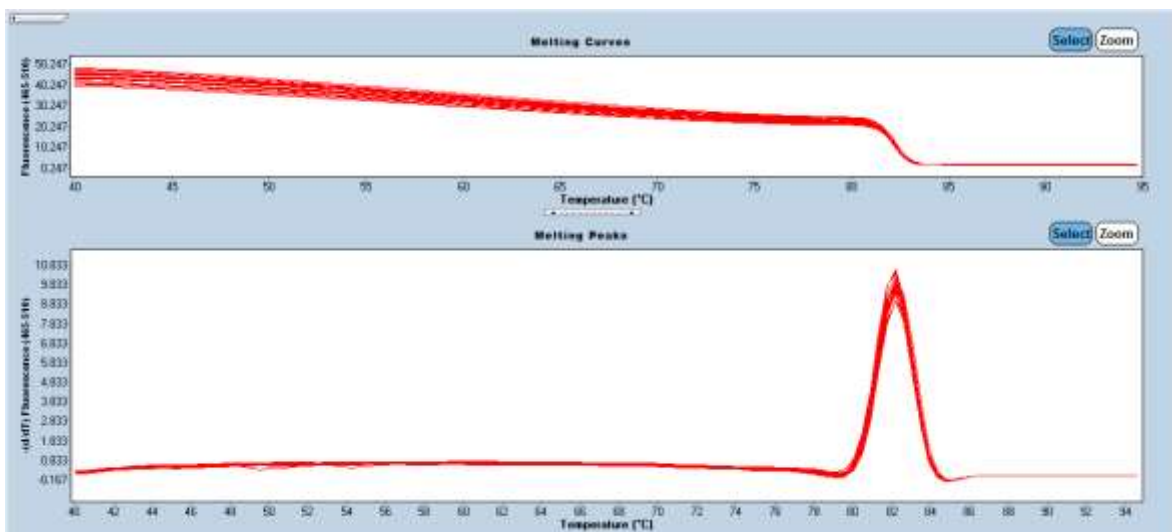
A.9.2 No template controls (NTCs)
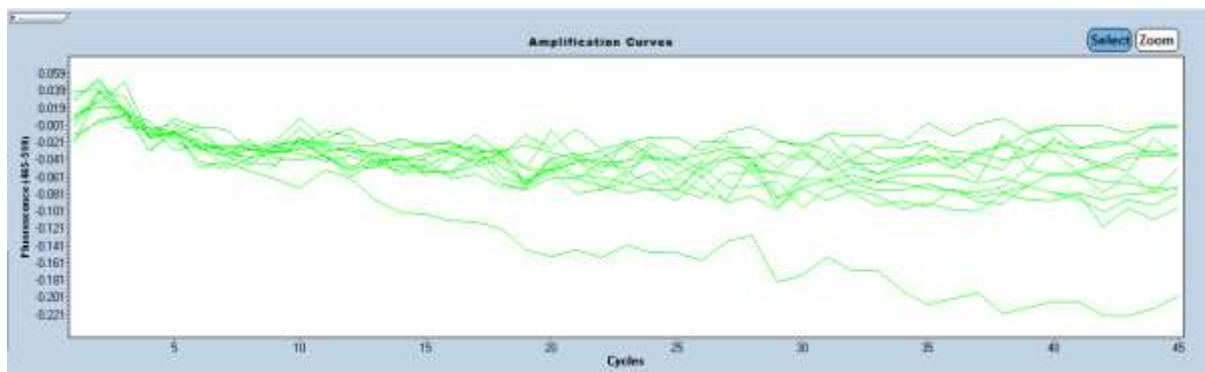
If amplification was detected in the NTCs, the assay was excluded and rerun.

A.9.3 Standard curves

The standard curves for each gene along with amplification efficiency (E), Y-intercept, slope and R^2 values are summarised in Figure A6.

A. *Pref-1*

$$Y = -3.315x + 35.25$$
$$E = 1.003$$
$$R^2 = 0.772$$

B. *Sox9*

$$Y = -3.486x + 33.64$$
$$E = 0.936$$
$$R^2 = 0.770$$

C. *PPARG*

$$Y = -3.277x + 29.19$$
$$E = 1.019$$
$$R^2 = 0.780$$

D. *PPIA*

Y = -3.478x + 25.11
E = 0.939
R² = 0.724

E.*TBP*

Y = -3.045x + 33.09
E = 1.130
R² = 0.722

F. *YWHAZ*

Y = -3.173x + 29.04
E = 1.066
R² = 0.795
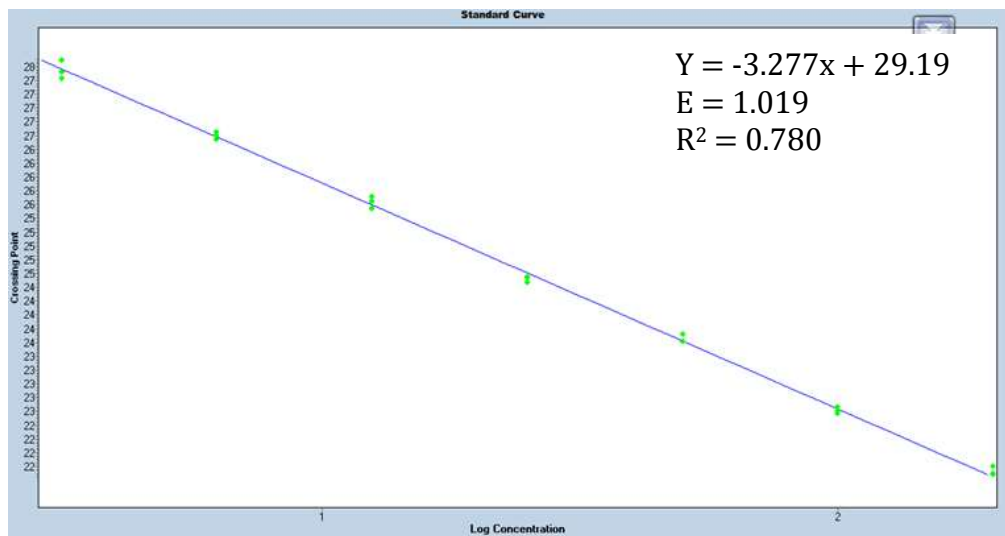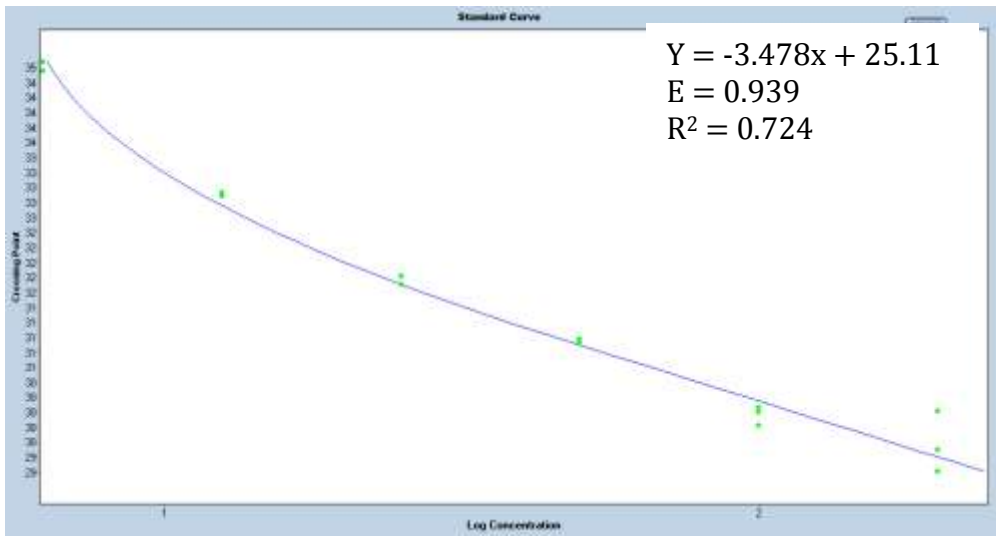
Figure A.6: Standard curves for genes of interest and reference genes. A standard curve was generated for each gene to determine the amplification efficiencies. Amplification efficiency (E) was calculated from the slope of the standard curve using the formula: $E = 10^{(-1/slope)} - 1$.

Amplification efficiencies were calculated based on the slope of the standard curves. An amplification efficiency of 1 is desired (1). It is an indication that the product to be amplified is doubling with every cycle. The amplification efficiencies obtained were within specification. Efficiencies above 1 may be attributed to contaminant carry over from either the RNA isolation step (ethanol, phenol) or cDNA synthesis (reverse transcriptase).

It is noted that the standard curve obtained for reference gene *PPIA* is not ideal as it is not linear, especially at the low concentration ranges. The standard curve should therefore be repeated in a next round of experiments. However, the results (relative gene expression) were calculated individually for each reference gene and no differences were observed between the results when compared to each other. This would suggest that the *PPIA* standard curve used in this study did not affect the end result.

A.9.4 Linear dynamic range

The cDNA concentration was measured using a Nanodrop ND 1000 spectrophotometer. The cDNA stock solution (SS) was then diluted to 100 ng/µl, except for *Pref-1* for which a concentration of 400 ng/µl was used (STD 1) and a serial dilution made to achieve the required cDNA working (WS) solution. The concentration was increased as poor amplification was achieved from *Pref-1* using the lower cDNA concentrations which impacted on generating a standard curve with an acceptable efficiency for this gene.

STD	Amount of cDNA (ng)	Concentration (ng/µL)	Dilution Setup (µL)	
			cDNA	H$_2$O
1	200.00	100.00	Variable	Variable
2	100.00	50.00	30 µL STD1	30 µL
3	50.00	25.00	30 µL STD2	30 µL
4	25.00	12.50	30 µL STD3	30 µL
5	12.50	6.25	30 µL STD4	30 µL
6	6.25	3.13	30 µL STD5	30 µL
7	3.13	1.56	30 µL STD6	30 µL

Table A.17: Standard curve set up for Pref-1

STD	Amount of cDNA (ng)	Concentration (ng/µL)	Dilution Setup (µL)	
			cDNA	H$_2$O
1	800.00	400.00	Variable	Variable
2	400.00	200.00	30 µL STD1	30 µL
3	200.00	100.00	30 µL STD2	30 µL
4	100.00	50.00	30 µL STD3	30 µL
5	50.00	25.00	30 µL STD4	30 µL
6	25.00	12.50	30 µL STD5	30 µL
7	12.50	6.25	30 µL STD6	30 µL

A.9.5 Quantitation cycle values variation at lower limit

The variation observed for the lowest concentration standard (lower limit) is shown in Table A.18.

Table A.18: Standard variation of Cq values at lower limit

Gene	Cq	Standard Deviation
Pref-1	31.71	0.15
Sox9	32.89	0.48
PPARG	27.54	0.11
PPIA	35.98	0.70
TBP	32.34	0.10
YWHAZ	27.33	0.04

A.9.6 Evidence for limit of detection

Limit of detection was not performed. Cq value < 31 was viewed as acceptable values. Cq values > 31 were viewed with less confidence and not completely trustworthy.

A.9.7 If multiplex, efficiency and LOD for each assay

Multiplexing was not performed in this study.

A.10 Data Analysis

A.10.1 qPCR analysis program

The qPCR analysis program used for data analysis was the LightCycler® Software (Version 1.5.1; Roche, Basel, Switzerland).

A.10.2 Quantitation cycle (Cq) method determination

The second derivative maximum method was used to determine the Cq values according to the LightCycler® Software and algorithms.

A.10.3 Outlier identification and disposition

Due to a small sample size of n=3, outlier tests could not be performed.

A.10.4 Results of no template controls (NTCs)

The Cq value for the NTCs were zero. If amplification was detected in the NTCs, the assay was excluded and re run. Representative image for NTC amplification plot can be seen in Figure A.5.

A.10.5 Justification of number and choice of reference genes

Three reference genes were used in this study: *TBP, PPIA* and *YWHAZ*. These genes were chosen due to previous findings in the literature (6, 7) as well as previous work performed in our laboratory by Dr Chrisna Durandt and Ms Carla Dessels in two independent studies, which suggests that the above mentioned reference genes are appropriate for use.

A.10.6 Normalisation method

The induced samples were normalised to the non-induced samples by subtracting the Cq values of the non-induced samples from the Cq of the induced samples.

A.10.7 Number of biological replicates

Three biological replicates were used for both hASCs and hWJSCs.

A.10.8 Number and stage (RT or qPCR) of technical replicates

Three wells were set up for every sample (three technical repeats) on the qPCR plate using the same sample cDNA.

A.10.9 Repeatability (intra-assay variation)

A standard deviation (SD) of 1 or less between the technical replicates was considered repeatable.

A.10.10 Statistics

Statistical analysis was performed using GraphPad Prism (GraphPad Software version 7, La Jolla California USA, www.graphpad.com). The statistical significance level was set at α=0.05. A Mann-Whitney test was used to determine significance between gene expressions observed at the different time points. If statistical significance was found, a Dunn's test was performed.

A.11 References

1.   Bustin SA, Benes V, Garson JA, Hellemans J, Huggett J, Kubista M, et al. The MIQE guidelines: minimum information for publication of quantitative real-time PCR experiments. Clin Chem. 2009;55(4):611-22.

2.   Bustin SA. Why the need for qPCR publication guidelines?--The case for MIQE. Methods. 2010;50(4):217-26.

3.   Taylor S, Wakem M, Dijkman G, Alsarraj M, Nguyen M. A practical approach to RT-qPCR-Publishing data that conform to the MIQE guidelines. Methods. 2010;50(4):S1-5.

4.   Matlock B. Assessment of Nucleic Acid Purity. 2015.

5.   Padhi BK, Singh M, Rosales M, Pelletier G, Cakmak S. A PCR-based quantitative assay for the evaluation of mRNA integrity in rat samples. Biomol Detect Quantif. 2018;15:18-23.

6.   Fink T, Lund P, Pilgaard L, Rasmussen JG, Duroux M, Zachar V. Instability of standard PCR reference genes in adipose-derived stem cells during propagation, differentiation and hypoxic exposure. BMC Mol Biol. 2008;9(1):98.

7.   Li X, Yang Q, Bai J, Xuan Y, Wang Y. Identification of appropriate reference genes for human mesenchymal stem cell analysis by quantitative real-time PCR. Biotechnol Lett. 2015;37(1):67-73.

Annexure A: Informed Consent Documents

A.1: Informed consent for umbilical cord and cord blood collection

UMBILICAL CORD AND CORD BLOOD COLLECTION

PATIENT INFORMATION LEAFLET AND INFORMED CONSENT

(Each patient must receive, read and understand this document before the start of the study)

STUDY TITLE

Main Study:

The role of Pref-1 in *in vitro* adipogenic differentiation of mesenchymal stromal/stem cells

Secondary study titles (Other studies that will also make use of the umbilical cord and cord blood donated):

1. The susceptibility of hematopoietic stem and progenitor cells to acute and latent HIV-1 infection
2. Novel approaches to conventional quality assurance parameters usually performed before freezing and after thawing cord blood units
3. Correlation of Hematopoietic stem cell transplantation quality assurance parameters with engraftment success in Multiple Myeloma patients. (Please note that a small volume of cord blood will be used in this project to study if the current methods that are used to identify haematopoietic stem cells (HSCs) are still optimal in detecting HSCs).
4. Evaluating the effects of HIV-1 infection on haematopoietic stem cell colony formation

Dear Patient/Participant: _____

INTRODUCTION

This information leaflet is to help you decide whether you would like to participate in a research project. Before agreeing to take part in the study, please make sure you understand and are comfortable with all procedures involved. Please do not hesitate to ask the investigator about anything you might be uncertain of. You should not agree to take part unless you are completely satisfied about all procedures involved.

WHAT IS THE PURPOSE OF THE STUDY?

Researchers at the University of Pretoria would like to investigate the properties of stem cells. These researchers are interested in two types of stem cells. Hematopoietic stem cells are very early (young) cells that have the potential to become any of the cells (more mature) in your bone marrow and blood. These hematopoietic stem cells can be found in the afterbirth (placenta), peripheral (circulating) blood, and bone marrow. There are more hematopoietic stem cells in cord blood than in peripheral (circulating) blood. It is important to realize that hematopoietic stem cells can only be collected from peripheral blood in sufficient numbers, after the donor was treated with a drug that will stimulate the production and release of these hematopoietic stem cells in the circulating blood. This is usually done when a donor donate hematopoietic stem cells to be used in treatment of blood-related cancers and other blood diseases. However, the higher numbers of hematopoietic cells in umbilical cord occurs naturally and is not due to any treatment received by the expecting mother. Please note that this consent form serves for the purpose of umbilical cord and umbilical cord blood collection only. Hematopoietic stem cells could potentially be used to treat patients with various kinds of diseases such as cancer, blood diseases and HIV. In order to use these cells to treat humans in the future, researchers must first study these cells in a laboratory. The research also involves improving the current techniques in the laboratory in order to detect the haematopoietic stem cells more efficiently and optimally. As mentioned, these cells are very rare and researchers also look in to ways to store these precious cells optimally as well as how to expand (increase) the cell numbers in the laboratory. Please be assured that the collection of these cells and the research will not use any unethical procedures.

Hematopoietic stem cells make up only approximately 1% of all the cells present in the umbilical cord blood. After isolation of the hematopoietic stem cells the rest of these cells are discarded, but these cells can be very useful for other research projects. For example, monocytes (one of the cell types present in the blood) can be very useful to researchers that are doing tuberculosis research and lymphocytes, especially T-lymphocytes, are very useful to researchers that are doing HIV research. Blood cells are usually mature. Therefore, the genetic make-up of these cells are often used by researchers as a reference point of how a mature cell looks like and to what extend the genetic make-up of immature (young) cells, such as hematopoietic cells, differ from the mature cells.

By signing this document you give the researchers permission to use the other cells (otherwise regarded as biological waste) in research projects. Please note that researchers are not allowed to do any research with these cells, before they received permission from the relevant ethics committees for their individual research projects.

Researchers at the University of Pretoria are also investigating the biological properties of mesenchymal stromal/stem cells. These cells are isolated from the umbilical cord tissue itself. Researchers at the University of Pretoria would like use these mesenchymal stem cells to investigate the process of fat cell maturation (adipogenesis), as obesity is becoming an increasing problem worldwide. The mesenchymal stem cells isolated from the umbilical cord can be used to investigate this maturation process. However, in order to better understand fat cell maturation, researchers must first study the behaviour and growth of the stem cells isolated from the umbilical cord, in the laboratory and/or animal models. The collection of adult stem cells does not make use of any unethical procedures.

WHEN AND HOW IS THE BLOOD AND UMBILICAL CORD COLLECTED?

There are no risks or discomfort involved with the collection of the cord or cord blood, for you or your baby. The birth of the child would still render the normal risks and discomforts associated with your normal birth procedure.

Under normal circumstances, the umbilical cord and placenta is discarded after a baby is born, since they serve no further purpose for either the mother or the baby. Researchers could however use the normally discarded blood and tissue for

research purposes. After the birth of the baby, the cord blood will be collected from the cord and a 15 cm long piece of cord will be cut and collected. The remainder of the cord will be discarded as normal. Collecting the blood does not harm the mother or the baby in any way. The collection can only take place at the time of delivery and is performed by your doctor.

WHAT WILL BE EXPECTED OF ME?

Researchers will have access to your medical information, however, all your personal information will be regarded as confidential and anonymous during the study.

Laboratory tests will be performed on the cord blood and umbilical cord samples if you wish to donate them to the study. Laboratory tests sometime require the isolation of genetic material. Genetic material is the means by which cells store information and transfer "instructions" from one generation to the next. Genetic material is stored within the cell in molecules called DNA and RNA. The information contained within the genetic material about the cell that only can be revealed if researchers perform specialized tests on the genetic material. These tests are often needed in order to completely understand the characteristics of cells. Genetic information also allows researchers to look into what effect infectious agents, such as *Mycobacterium tuberculosis* (cause tuberculosis in humans) and HIV, might have on these cells. In addition, molecular biology tests (tests that make use of DNA or RNA) are often the most sensitive tests available to detect if cells are infected with bacteria (such as *Mycobacterium tuberculosis)* and/or viruses (such as HIV). By signing this document you give researchers permission to perform these tests. Please note that as soon as the genetic material is extracted from the cells, it would receive an anonymous code to protect your identity.

By signing this document you also give the researchers permission to request your HIV status from your doctor, since it is important for the study that only HIV-negative blood is used. If your HIV status is unknown, please indicate below whether you give the researchers permission to test for HIV. If you do not wish us to know the result of your HIV test, we will not be able to include you in the study. In the case of an HIV positive result, you will be counselled by qualified medical personnel.

In some isolated cases it might however be important for the doctors or researchers involved in the study to convey medical information to medical personnel or appropriate Research Ethics committees. In such a case, you by signing this document, give permission to the investigator to release your medical records to regulatory health authorities or an appropriate Research Ethics committee. If necessary, these medical professionals will discuss the results with your doctor and everyone will act in your best interest.

HAS THE STUDY RECEIVED ETHICAL APPROVAL?

A protocol for the study was submitted to the Research Ethics Committee of the Faculty of Health Sciences at the University of Pretoria and received written approval from the committee. The study is structured in accordance with the Declaration of Helsinki, which deals with the recommendations guiding doctors in biomedical research involving humans.

WHAT ARE MY RIGHTS AS A PARTICIPANT IN THE STUDY?

Your participation in the study is entirely voluntary and you can refuse to participate or withdraw consent at any time without stating any reason. Your withdrawal will not affect your access to medical care or the quality of medical care that you or your baby will receive.

IS THERE ANY RISK OR DISCOMFORT DURING COLLECTION?

No. The cord blood is collected after your baby has been born. The collection is painless, easy, and does not involve you or your baby, and takes about 5 minutes.

IS THERE FINANCIAL GAIN / LOSS FOR MY ACCOUNT IN THE STUDY?

There will be no gain or loss for you or your baby should you participate/withdraw from the study. The research could potentially lead to future profitable treatments. Neither you nor your baby will have access to these profits. There will be no additional financial costs for you to participate in the study.

SOURCE OF ADDITIONAL INFORMATION

If at any time you have any questions about the study, please do not hesitate to contact Ms. Juanita Mellet (079-523-6401), Dr. Chrisna Durandt (084-484-5561) or Prof. Michael Pepper (012-319-2190). You are also welcome to contact the Faculty

of Health Sciences Ethics Committee at the University of Pretoria if you have any concerns or questions. Their contact details are:

The Research Ethics Office:
Tel: 012 - 354 1330 or 012 - 354 1677
Fax: 012 - 354 1367

For information regarding the collection procedure, you may contact your doctor.

CONFIDENTIALITY

Each participant's sample will be assigned a specific code and this code will be used from there on in all research studies. Certain information, including race, ethnicity, gender and medical history, may be important for scientific reasons. This information will be linked to the sample code and not to your identity. Research reports and articles in scientific journals will not include any information that may identify you.

In some isolated cases it might however be important for the doctors or researchers involved in the study to convey medical information to medical personnel or appropriate Research Ethics committees. In such a case, you by signing this document, give permission to the investigator to release your medical records to regulatory health authorities or an appropriate Research Ethics committee. If necessary, these medical professionals will discuss the results with your doctor and everyone will act in your best interest.

INFORMED CONSENT

I confirm that the person asking my consent to take part in this study has told me about the nature, process, risks, discomforts and benefits of the study.

I have received, read and understood the above written information (Information Leaflet and Informed Consent) regarding the study.

I am aware that the results of the study, including personal details, will be anonymously processed into research reports.

I am participating willingly. I have had time to ask questions and have no objection to participate in the study.

I understand that there is no penalty should I wish to discontinue with the study and my withdrawal will not affect my access to medical care or the quality of medical care I will receive.

I hereby give the researchers permission to request my HIV status from my doctor.

I hereby also give consent for genetic tests and studies to be performed on the source donated.

YES	NO

I hereby consent to donate the source indicated below to the present study (please tick appropriate box):

Umbilical Cord ……………....... ☐

Umbilical Cord Blood ………… ☐

I have received a copy of this informed consent agreement.

Participant full names (print):_____

Participant signature:_____ Date: _____

Investigator full names (print):_____

Investigator signature:_____ Date: _____

Doctor full names (print):_____

Doctor signature:_____ Date: _____

A.2: Informed consent for adipose tissue collection

PATIENT INFORMATION LEAFLET AND INFORMED CONSENT FORM

(Each patient must receive, read and understand this document before the start of the study)

STUDY TITLE

The isolation, characterisation and differentiation of mesenchymal stem cells from adipose tissue.

The mesenchymal stem/stromal cells isolated from the voluntary donated adipose (fat) tissue will be used in various studies. The current studies are listed below. The isolated cells may also be used in future studies. Permission to use the cells in future experiments/studies will be obtained from the Ethics Committee at the Faculty of Health Sciences, University of Pretoria before the cells are used.

1. Do adipose-derived stromal cells possess endocytic function?
2. The role of Pref-1 in *in vitro* adipogenic differentiation of mesenchymal stromal/stem cells (MSCs)
3. Characterization of adipose-derived stromal cell heterogeneity
4. Comparison of the effect of human platelet lysate and foetal bovine serum on adipose-derived stem cell characteristics in culture
5. Is HIV-1 able to infect mesenchymal stromal/ stem cells (MSC)?
6. Effects of reactive oxygen species on adipogenesis.
7. An assessment of the efficacy of human alternatives to fetal bovine serum for the expansion of human adipose-derived stem cells

Dear Patient/Participant: _____

INTRODUCTION

You are invited to participate in a research study that is being carried out by the Department of Immunology at the University of Pretoria. This information leaflet is to help you to decide if you would like to participate. Before you agree to take part in this study you should fully understand what is involved. If you have any questions, which are not fully explained in this leaflet, do not hesitate to ask the investigator.

You should not agree to take part unless you are completely happy about all the procedures involved. Your personal health will not be compromised at all by the procedures. These procedures have already been discussed with your doctor beforehand.

THE PURPOSE OF THE STUDY

Researchers at the University of Pretoria would like to investigate the healing properties of adult stem cells for possible future application in regenerative medicine. Regenerative medicine refers to experimental (current status) medicine where researchers try to replace, improve or restore the function of cells that do not function optimally in the body. Adult stem cells are present in various tissues in the body, including fat (adipose) tissue. These adult stem cells could potentially be used to cure patients with various kinds of injuries or diseases. In order to use these cells to cure humans in the future, researchers must first study their characteristics, behaviour, growth and interactions with other cells and/or organisms in the body. This is done by isolating these cells from the fat (adipose) tissue and perform experiments in the laboratory (tissue culture) and/or using experimental animal models.

These adult stem cells can also be used to investigate the process of fat formation. Scientists are able to mimic the formation of fat cells using adult stem cells isolated from fat (adipose) tissue. Obesity is becoming an increasing problem worldwide and in order to find solutions to combat obesity it is important to understand the biological processes involved in the formation of fat. It is also important to understand the interactions of infectious organisms, like HIV and *Mycobacterium tuberculosis* (organism that cause tuberculosis in humans), with stem cells in order to provide safe treatment options in the future. It is therefore important that researchers also investigate the interactions between these infectious organisms and stem cells by performing experiments in the laboratory as well as using experimental animal models. Investigations will be performed on cellular (intact cells) and molecular (investigating the effect on various treatments/exposures to the genetic footprint of cells) levels. For molecular studies we will need to isolate genetic material (DNA and RNA) from your cells.

Many of the experiments that researchers perform require the isolation of genetic material, also known as DNA and RNA, from cells. Genetic material contains information about the cell that only can be revealed if researchers perform specialized tests on the genetic material. These tests are often needed in order to completely understand the characteristics of cells. Genetic information also allows researchers to look into what effect infectious agents, such as *Mycobacterium tuberculosis* (cause tuberculosis in humans) and HIV, might have on these cells. In addition, molecular biology tests (tests that make use of DNA or RNA) are often the most sensitive tests available to detect if cells are infected with bacteria (such as *Mycobacterium tuberculosis)* and/or viruses (such as HIV).

No unethical procedures will be used when collecting the samples and performing the experiments.

ADIPOSE TISSUE COLLECTION

During various normal plastic surgery operations, adipose tissue (fat) will be excised (cut out) or aspirated (sucked out), and discarded. This adipose tissue, does not serve a purpose to the patient's body anymore, but could serve as a valuable source of stem cells for researchers in the field of regenerative medicine. No additional fat will be collected for the study. Only the fat that the doctor planned to aspirate/cut away during the procedures discussed with you during the consultation visits will be collected.

There will be no added risks or discomfort with the collection of the adipose tissue other than normally associated with the specific procedure the patient will experience during normal operative procedures.

CONFIDENTIALITY

Each participant's sample will be assigned a specific code and this code will be used from there on in all research studies. Certain information, including race, ethnicity, gender and medical history, may be important for scientific reasons. This information will be linked to the sample code and not to your identity. Research reports and articles in scientific journals will not include any information that may identify you.

In some isolated cases it might however be important for the doctors or researchers involved in the study to convey medical information to medical personnel or appropriate Research Ethics committees. In such a case, you by signing this document, give permission to the investigator to release your medical records to regulatory health authorities or an appropriate Research Ethics committee. If necessary, these medical professionals will discuss the results with your doctor and everyone will act in your best interest.

ETHICAL APPROVAL

The protocol involved for this study was submitted to the Research Ethics Committee. This study has received written approval from the Research Ethics Committee of the Faculty of Health Sciences at the University of Pretoria. The study is structured in accordance with the Declaration of Helsinki, which deals with the recommendations of guiding doctors in biomedical research involving humans.

You are also welcome to contact the Faculty of Health Sciences Ethics Committee at the University of Pretoria if you have any concerns or questions. Their contact details are:

The Research Ethics Office:
Tel: 012 - 354 1330 or 012 - 354 1677
Fax: 012 - 354 1367

RIGHTS OF THE PARTICIPANT

Your participation in this study is entirely voluntary and you can refuse to participate or withdraw consent at any time without stating any reason. Your withdrawal will not affect your access to medical care or the quality of medical care that you will receive. Your participation or withdrawal from the study would not affect you in any way.

FINANCIAL GAIN OR LOSS

There will be no financial gain or loss to you, should you participate or withdraw from the study. This research could potentially lead to future profitable treatments. However, you will not have access to these profits. There will be no additional financial costs for you to participate in the study.

The participant has no legal remedy and will not share in

INFORMATION AND CONTACT PERSON

If at any time you would like to find out more information or have any questions regarding the study, please do not hesitate to contact the researchers.

Dr. C. Durandt: 012 -319 2101

Prof. M.S. Pepper: 012 420 3845 or 012 420 5317

PERSONAL/MEDICAL INFORMATION

The information below may be important for scientific reasons. This information will be linked to the sample code and not to your identity.

Gender: _____

Ethnicity: _____

Date of Birth: _____

Weight: _____

Height: _____

Waist Circumference: _____

Do you smoke?   [YES]   [NO]

Are you suffering from:

Diabetes   [YES]   [NO]

Cardiovascular disease   [YES]   [NO]

Hypertension   [YES]   [NO]

INFORMED CONSENT

WHAT IS EXPECTED?

I confirm that the person asking my consent to take part in this study has told me about the nature, process, risks, discomforts and benefits of the study. I have also received, read and understood the above written information regarding the study. I am aware that the results of the study, including personal details, will be anonymously processed into research reports. I am participating willingly. I have had time to ask questions and have no objection to participate in the study. I understand that there is no penalty should I wish to discontinue with the study and my withdrawal will not affect my access to medical care or the quality of medical care I will receive.

I also understand that certain laboratory tests may require the isolation of genetic material, also known as DNA and RNA and give herewith permission that the researchers may extract RNA/DNA from cells isolated from the adipose tissue.

YES	**NO**

I hereby give the researchers permission to perform routine HIV, hepatitis B and hepatitis C tests on the adipose tissue donated. Testing for these infectious agents is important for our work as we only like to work with tissue that is negative for these infections. If the researchers detect HIV or hepatitis B or C in the sample, the codified sample details will be sent to _____, who will notify you. If you do not wish us to test your tissue for HIV or hepatitis B or hepatitis C, or if you do not wish to know the results of these tests, we will not be able to include you in the study. In the case on an HIV positive result, you will be counselled and treated by qualified medical personnel.

I have received a copy of this informed consent agreement.

YES	**NO**

Participant full names (print):_____

Participant signature:_____Date: _____

Investigator full names (print):_____

Investigator signature:_____Date:_____

Witness full names (print):_____

Witness signature:_____Date:_____

Witness full names (print):_____

Witness signature:_____Date:_____

Annexure B: Ethical Approvals

B.1 University of Pretoria's Research Ethics Committee

The Research Ethics Committee, Faculty Health Sciences, University of Pretoria complies with ICH-GCP guidelines and has US Federal wide Assurance.
- FWA 00002567, Approved dd 22 May 2002 and Expires 20 Oct 2016
- IRB 0000 2235 IORG0001762 Approved dd 22/04/2014 and Expires 22/04/2017.

UNIVERSITEIT VAN PRETORIA
UNIVERSITY OF PRETORIA
YUNIBESITHI YA PRETORIA

Faculty of Health Sciences Research Ethics Committee

30/06/2016

Approval Certificate
New Application

Ethics Reference No.: 206/2016

Title: The role of Pref-1 in in vitro adipogenic differentiation of mesenchymal stromal/stem cells.

Dear Carina da Silva

The **New Application** as supported by documents specified in your cover letter dated 27/06/2016 for your research received on the 27/06/2016, was approved by the Faculty of Health Sciences Research Ethics Committee on its quorate meeting of 29/06/2016.

Please note the following about your ethics approval:
- Ethics Approval is valid for 3 years
- Please remember to use your protocol number (**206/2016**) on any documents or correspondence with the Research Ethics Committee regarding your research.
- Please note that the Research Ethics Committee may ask further questions, seek additional information, require further modification, or monitor the conduct of your research.

Ethics approval is subject to the following:
- The ethics approval is conditional on the receipt of 6 monthly written Progress Reports, and
- The ethics approval is conditional on the research being conducted as stipulated by the details of all documents submitted to the Committee. In the event that a further need arises to change who the investigators are, the methods or any other aspect, such changes must be submitted as an Amendment for approval by the Committee.

Additional Conditions:
- Conditional approval, pending approval from Netcare Femina Clinic.

We wish you the best with your research.

Yours sincerely

Dr R Sommers; MBChB; MMed (Int); MPharMed,PhD
Deputy Chairperson of the Faculty of Health Sciences Research Ethics Committee, University of Pretoria

The Faculty of Health Sciences Research Ethics Committee complies with the SA National Act 61 of 2003 as it pertains to health research and the United States Code of Federal Regulations Title 45 and 46. This committee abides by the ethical norms and principles for research, established by the Declaration of Helsinki, the South African Medical Research Council Guidelines as well as the Guidelines for Ethical Research: Principles Structures and Processes 2004 (Department of Health).

☎ 012 356 3085   ✉ fhsethics@up.ac.za   🌐 http://www.up.ac.za/healthethics
✉ Private Bag X323, Arcadia, 0007 - Tswelopele Building, Level 4-59, Gezina, Pretoria

B.2 University of Pretoria's Animal Ethics Committee

UNIVERSITEIT VAN PRETORIA
UNIVERSITY OF PRETORIA
YUNIBESITHI YA PRETORIA

Animal Ethics Committee

PROJECT TITLE	The role of Pref-1 in in vitro adipogenic differentiation of mesenchymal stroma/stem cells
PROJECT NUMBER	H012-17
RESEARCHER/PRINCIPAL INVESTIGATOR	Carina da Silva

STUDENT NUMBER (where applicable)	u12019527
DISSERTATION/THESIS SUBMITTED FOR	MSc Medical Immunology

ANIMAL SPESIES	Mouse	
NUMBER OF ANIMALS	15	
Approval period to use animals for research/testing purposes		Sept 2017- Sept 2018
SUPERVISOR	Dr Chrisna Durandt	

Approved Phase 1: 15 animals

KINDLY NOTE:

Should there be a change in the species or number of animal/s required, or the experimental procedure/s - please submit an amendment form to the UP Animal Ethics Committee for approval before commencing with the experiment

APPROVED	Date	31 August 2017
CHAIRMAN: UP Animal Ethics Committee	Signature	

S4285-15

B.3 Netcare Research Operations Committee

Netcare Hospitals (Pty) Ltd

Tel: + 27 (0)11 301 0000
Fax: Corporate +27 (0)11 301 0499
76 Maude Street, Corner West Street, Sandton, South Africa
Private Bag X34, Benmore, 2010, South Africa
www.netcare.co.za

RESEARCH OPERATIONS COMMITTEE FINAL APPROVAL OF RESEARCH

Approval number: UNIV-2016-0042

Ms Carina C da Silva

E mail: carinacrdasilva@gmail.com

Dear Ms Da Silva

RE: THE ROLE OF PREF-1 IN IN VITRO ADIPOGENIC DIFFERENTIATION OF MESENCHYMAL STEM/STROMAL CELLS

The above-mentioned research was reviewed by the Research Operations Committee's delegated members and it is with pleasure that we inform you that your application to conduct this research at Netcare Femina Hospital, has been approved, subject to the following:

i) Research may now commence with this FINAL APPROVAL from the Netcare Research Operations Committee.

ii) All information regarding Netcare will be treated as legally privileged and confidential.

iii) Netcare's name will not be mentioned without written consent from the Netcare Research Operations Committee.

iv) All legal requirements regarding patient / participant's rights and confidentiality will be complied with.

v) The research will be conducted in compliance with the GUIDELINES FOR GOOD PRACTICE IN THE CONDUCT OF CLINICAL TRIALS IN HUMAN PARTICIPANTS IN SOUTH AFRICA (2006)

vi) Netcare must be furnished with a STATUS REPORT on the progress of the study at least annually on 30th September irrespective of the date of approval from the Netcare Research Operations Committee as well as a FINAL REPORT with reference to intention to publish and probable journals for publication, on completion of the study.

Directors: J du Plessis, S Chetty, R H Friedland, K N Gibson

Company Secretary: L Bagwandeen

Reg. No. 1966/006591/07

vii) A copy of the research report will be provided to the Netcare Research Operations Committee once it is finally approved by the relevant primary party or tertiary instilution, or once complete or if discontinued for any reason whatsoever prior to the expected completion date.

viii) Netcare has the right to implement any recommendations from the research.

ix) Netcare reserves the right to withdraw the approval for research at any time during the process, should the research prove to be detrimental to the subjects/Netcare or should the researcher not comply with the conditions of approval.

x) APPROVAL IS VALID FOR A PERIOD OF 36 MONTHS FROM DATE OF THIS LETTER OR COMPLETION OR DISCONTINUATION OF THE TRIAL, WHICHEVER IS THE FIRST.

We wish you success in your research.

Yours faithfully

3/8/2016.

Prof Dion du Plessis
Full member: Netcare Research Operations Committee & Medical Practitioner evaluating research applications as per Management and Governance Policy

Shannon Neil
Chairperson: Netcare Research Operations Committee
Netcare Hospitals (Pty) Ltd
Date: 17/8/2016

Annexure C: Additional Flow Cytometry Information

Table C.1: Human MSC 7-Colour Phenotype Panel Details

Marker	Pos/Neg	Fluorochrome	Excitation (nm)	Emission (nm)	Distributor
CD34	+ / -	Phycoerythrin/Cyanin7 (PE/Cy7)	480, 743	767	Beckman Coulter
CD36	+	Allophycocyanin (APC)	650	660	Thermo Fisher Scientific
CD44	+	Allophycocyanin /Cyanin7 (APC/Cy7)	650, 755	767	Biolegend
CD45	-	Krome Orange (KO)	398	528	Becton Dickinson
CD73	+	Fluorescein isothiocyanate (FITC)	494	518	eBiosciences
CD90	+	Brilliant Violet™ 421 (BV421)	407	421	Becton Dickinson
CD105	+	Phycoerythrin (PE)	480, 565	575	Thermo Fisher Scientific

Table C.2: Gallios Flow Cytometer Filter Configuration and Antibody Detection

Laser	Filter	PMT	Antibody Detected
488nm, 22mW	525/40	1	CD73 FITC
	575/30	2	CD105 PE
	620/30	3	NA
	695/30	4	NA
	755LP	5	CD34 PE/Cy7
638nm, 25mW	660/20	6	CD36 APC
	724/20	7	NA
	755LP	8	CD44 APC/Cy7
405nm, 40mW	450/40	9	CD90 BV421
	550/40	10	CD45 KO

NA – Not applicable, channel was not used

PMT – Photomultiplier tube

Annexure D: MIQE Checklist

A MIQE guidelines checklist was provided by Bustin *et al.* 2009 (1). The checklist provided can be found below (Figure D.1):

Table 1. MIQE checklist for authors, reviewers, and editors.

Item to check	Importance	Item to check	Importance
Experimental design		**qPCR oligonucleotides**	
Definition of experimental and control groups	E	Primer sequences	E
Number within each group	E	RTPrimerDB identification number	D
Assay carried out by the core or investigator's laboratory?	D	Probe sequences	D[d]
Acknowledgment of authors' contributions	D	Location and identity of any modifications	E
Sample		Manufacturer of oligonucleotides	D
Description	E	Purification method	D
Volume/mass of sample processed	D	**qPCR protocol**	
Microdissection or macrodissection	E	Complete reaction conditions	E
Processing procedure	E	Reaction volume and amount of cDNA/DNA	E
If frozen, how and how quickly?	E	Primer, (probe), Mg²⁺, and dNTP concentrations	E
If fixed, with what and how quickly?	E	Polymerase identity and concentration	E
Sample storage conditions and duration (especially for FFPE[b] samples)	E	Buffer/kit identity and manufacturer	E
Nucleic acid extraction		Exact chemical composition of the buffer	D
Procedure and/or instrumentation	E	Additives (SYBR Green I, DMSO, and so forth)	E
Name of kit and details of any modifications	E	Manufacturer of plates/tubes and catalog number	D
Source of additional reagents used	D	Complete thermocycling parameters	E
Details of DNase or RNase treatment	E	Reaction setup (manual/robotic)	D
Contamination assessment (DNA or RNA)	E	Manufacturer of qPCR instrument	E
Nucleic acid quantification	E	**qPCR validation**	
Instrument and method	E	Evidence of optimization (from gradients)	D
Purity (A260/A280)	D	Specificity (gel, sequence, melt, or digest)	E
Yield	D	For SYBR Green I, Cq of the NTC	E
RNA integrity: method/instrument	E	Calibration curves with slope and y intercept	E
RIN/RQI or Cq of 3′ and 5′ transcripts	E	PCR efficiency calculated from slope	E
Electrophoresis traces	D	Cls for PCR efficiency or SE	D
Inhibition testing (Cq dilutions, spike, or other)	E	r² of calibration curve	E
Reverse transcription		Linear dynamic range	E
Complete reaction conditions	E	Cq variation at LOD	E
Amount of RNA and reaction volume	E	Cls throughout range	D
Priming oligonucleotide (if using GSP) and concentration	E	Evidence for LOD	E
Reverse transcriptase and concentration	E	If multiplex, efficiency and LOD of each assay	E
Temperature and time	E	**Data analysis**	
Manufacturer of reagents and catalogue numbers	D	qPCR analysis program (source, version)	E
Cqs with and without reverse transcription	D[c]	Method of Cq determination	E
Storage conditions of cDNA	D	Outlier identification and disposition	E
qPCR target information		Results for NTCs	E
Gene symbol	E	Justification of number and choice of reference genes	E
Sequence accession number	E	Description of normalization method	E
Location of amplicon	D	Number and concordance of biological replicates	D
Amplicon length	E	Number and stage (reverse transcription or qPCR) of technical replicates	E
In silico specificity screen (BLAST, and so on)	E	Repeatability (intraassay variation)	E
Pseudogenes, retropseudogenes, or other homologs?	D	Reproducibility (interassay variation, CV)	D
Sequence alignment	D	Power analysis	D
Secondary structure analysis of amplicon	D	Statistical methods for results significance	E
Location of each primer by exon or intron (if applicable)	E	Software (source, version)	E
What splice variants are targeted?	E	Cq or raw data submission with RDML	D

[a] All essential information (E) must be submitted with the manuscript. Desirable information (D) should be submitted if available. If primers are from RTPrimerDB, information on qPCR target, oligonucleotides, protocols, and validation is available from that source.
[b] FFPE, formalin-fixed, paraffin-embedded; RIN, RNA integrity number; RQI, RNA quality indicator; GSP, gene-specific priming; dNTP, deoxynucleoside triphosphate.
[c] Assessing the absence of DNA with a no–reverse transcription assay is essential when first extracting RNA. Once the sample has been validated as DNA free, inclusion of a no–reverse transcription control is desirable but no longer essential.
[d] Disclosure of the probe sequence is highly desirable and strongly encouraged; however, because not all vendors of commercial predesigned assays provide this information, it cannot be an essential requirement. Use of such assays is discouraged.

Figure D.1: MIQE checklist. MIQE guidelines checklist provided by Bustin *et al.* 2009 (1).

References

1.   Bustin SA, Benes V, Garson JA, Hellemans J, Huggett J, Kubista M, et al. The MIQE guidelines: minimum information for publication of quantitative real-time PCR experiments. Clin Chem. 2009;55(4):611-22.